ProNGF, NGF and their receptors in tumour innervation and progression: a study in breast and thyroid cancers.

Sam Faulkner

B. Biomed Sci (Hons) (Newcastle)

A thesis submitted in fulfilment of the requirements for the degree of

Doctor of Philosophy in Molecular Biochemistry

School of Biomedical Sciences and Pharmacy

The University of Newcastle, Australia

September 2017

Declarations

TESTIMONY OF ORIGINALITY

I hereby certify that the work embodied in the thesis is my own work, conducted under normal supervision. The thesis contains no material which has been accepted, or is being examined, for the award of any other degree or diploma in any university or other tertiary institution and, to the best of my knowledge and belief, contains no material previously published or written by another person, except where due reference has been made in the text. I give consent to the final version of my thesis being made available worldwide when deposited in the University's Digital Repository, subject to the provisions of the Copyright Act 1968 and any approved embargo.

THESIS BY PUBLICATION

I hereby certify that this thesis is in the form of a series of papers. I have included as part of the thesis a written statement from each co-author, endorsed in writing by the Faculty Assistant Dean (Research Training), attesting to my contribution to any jointly authored papers.

Signature: …….. *Date: 29/09/2017*

Sam Faulkner *dd/mm/yyyy*

Acknowledgements

Firstly, I would like to thank my supervisor Professor Hubert Hondermarck for giving me the opportunity to complete my PhD under your expert supervision. Thank you for providing me with a positive environment, ongoing support as well as your friendship and humour over the last four years. Despite being one of the most challenging experiences to date, I will always look back on this time with fond memories.

I would also like to thank Doctor Severine Roselli for her expert guidance, patience and friendship during this time. I accredit a lot of the knowledge and fundamental lab skills I now possess to your careful and well thought out teachings.

To my lab partners Jay Pundavela and Sheridan Keene, thank you for your assistance, guidance and unwavering willingness to help at any given time, despite me constantly interrupting your own work. Your support was essential to the completion of this thesis and was always very much appreciated.

To my parents, Steve and Lee, I am forever thankful for the love, support and fantastic opportunities that you have both provided and continue to provide me with on a daily basis. I most certainly would not have accomplished this feat without either of you.

To my beautiful (and very patient) partner Aleisha, you have been in the passenger seat for the entirety of this journey, experienced the rollercoaster that was the PhD and despite all of this continued to love and support me (physically, emotionally and at times financially) through it all. You truly are an amazing person whose laughter could always light up even the darkest of days. I love you and cannot wait to see what the future has in store for us both.

Finally to the rest of my family and friends, I would also like to thank you for supporting me during this time and for making life the wonderful adventure and experience that it is and will hopefully continue to be for many years to come.

List of Publications Included as Part of this Thesis

Boilly B*, Faulkner S*, Jobling P, Hondermarck H: **Nerve Dependence: From Regeneration to Cancer**. *Cancer Cell*. 2017 Mar 13;31(3):342-354.

* Co-first author

Pundavela J, Roselli S, Faulkner S, Attia J, Scott RJ, Forbes JF, Bradshaw RA, Walker MM, Jobling P, Hondermarck H: **Nerve fibers Infiltrate the tumor microenvironment and are associated with nerve growth factor production and lymph node invasion in breast cancer**, *Mol Oncol.* 2015 Oct;9(8):1626-35.

Faulkner S, Roselli S, Demont Y, Pundavela J, Choquet G, Leissner P, Oldmeadow C, Attia J, Walker MM, Hondermarck H: **ProNGF is a potential diagnostic biomarker for thyroid cancer**. *Oncotarget*. 2016 May 10;7(19):28488-97.

Faulkner S, Jobling P, Rowe C, Rodriguez-Oliveira S, Roselli S, Thorne R, Oldmeadow C, Attia J, Jiang CC, Zhang XD, Walker MM, Hondermarck H: **Neurotrophin Receptors TrkA, p75^{NTR} and Sortilin are Increased and Targetable in Thyroid Cancer**. *Am J Pathol.* 2018 Jan;188(1):229-241.

List of Abbreviations

0-9

6OHDA	6-Hydroxydopamine

A

ATCC	American Type Culture Collection
AA	Amino Acid
ANOVA	Analysis of Variance
ATC	Anaplastic Thyroid Carcinoma
AGR	Anterior Gradient Protein
AUROC	Area Under the Receiver-Operating Characteristic Curve

B

BMP	Bone Morphogenetic Protein
BDNF	Brain-Derived Neurotrophic Factor

C

CSC	Cancer Stem Cell
CNS	Central Nervous System
CI	Confidence Interval
CRD	Cysteine-Rich Domain

D

DD	Death Domain
DNA	Deoxyribonucleic Acid
DAB	3,3'-Diaminobenzidine
DRG	Dorsal Root Ganglia
DCIS	Ductal Carcinoma In Situ
DMEM	Dulbecco’s Modified Eagle Medium

E

EGF	Epidermal Growth Factor
ER	Estrogen Receptor

ECM	Extracellular Matrix
ERK	Extracellular Signal-Regulated Kinase

F

FGF	Fibroblast Growth Factor
FNAB	Fine Needle Aspiration Biopsy
FCS	Foetal Calf Serum
FTC	Follicular Thyroid Carcinoma

G

GDNF	Glia-Derived Neurotrophic Factor
GAPDH	Glyceraldehyde-3-Phosphate Dehydrogenase
G-CSF	Granulocyte-Colony Stimulating Factor

H

HER2	Human Epidermal Growth Factor Receptor 2
HME	Human Mammary Epithelium

I

IgG	Immunoglobulin G
IHC	Immunohistochemistry
IR-Dye	Infrared Dye
IDC	Invasive Ductal Carcinoma
ILC	Invasive Lobular Carcinoma

J

JNK	c-Jun N-terminal Kinase

K

kDa	Kilodalton

M

MTC	Medullary Thyroid Carcinoma

mRNA	Messenger Ribonucleic Acid
MAPK	Mitogen-Activated Protein Kinase
MW	Molecular Weight

N

NGF	Nerve Growth Factor
NGFR	Nerve Growth Factor Receptor
NT	Neurotrophin
NT-3	Neurotrophin-3
NT-4/5	Neurotrophin-4/5
NTRK1	Neurotrophin Tyrosine Receptor Kinase 1
nAG	Newt Anterior Gradient
NFkB	Nuclear Factor-κB

P

$p75^{NTR}$	p75 neurotrophin receptor
PTC	Papillary Thyroid Carcinoma
PNI	Perineural Invasion
PBS	Phosphate Buffered Saline
PI3K	Phosphoinositide-3-Kinase
PLCγ	Phosphoinositide Phospholipase C Gamma
PDGF	Platelet-Derived Growth Factor
PCR	Polymerase Chain Reaction
PTR	Post-Translational Modification
proNGF	Precursor of NGF
PR	Progesterone Receptor
PGP9.5	Protein Gene Product 9.5

Q

qRT-PCR	Quantitative Reverse Transcription Polymerase Chain Reaction

R

ROC	Receiver-Operating Characteristic
RTK	Receptor Tyrosine Kinase
RAC	Rho GTPase
RNA	Ribonucleic Acid
RPMI	Roswell Park Memorial Institute Media

S

siRNA	Small/Short Interfering RNA
SHH	Sonic Hedgehog
SORT	Sortilin
SAS	Statistical Analysis System

T

TPA	Tetradecanoyl Phorbol Acetate
TCGA	The Cancer Genome Atlas
TMA	Tissue Microarray
Trk	Tropomyosin-Related Kinase
TNF	Tumour Necrosis Factor
TRAF	Tumour Necrosis Factor Receptor-Associated Factor

V

VPS10P	Vacuolar Protein Sorting 10 Protein

Table of Contents

Declarations i

Acknowledgements ii

List of Publications Included as Part of this Thesis iii

List of Abbreviations iv

Table of Contents viii

Abstract 10

CHAPTER 1 | Thesis Overview 12

1.1 Introduction 12

1.2 Aims of the study 12

1.3 Organisation of the thesis 13

CHAPTER 2 | Literature Review 15

2.1 Nerve Dependence: From Regeneration to Cancer 15

2.1.1 Preface 15

2.1.2 Publication 16

2.2 Neurotrophin family of growth factors and receptors 29

2.2.1 Nerve growth factor (NGF) 31

2.2.2 Structure and function of proNGF 31

2.2.3 Structural and functional characteristics of receptors for proNGF 32

2.2.4 $P75^{NTR}$ (p75 neurotrophin receptor) 34

2.2.5 Sortilin receptor 35

2.2.6 TrkA receptor 36

2.3 NGF, proNGF and their receptors in cancer 37

2.3.1 Breast cancer 37

2.3.2 Pancreatic cancer 40

2.3.3 Melanoma 42

2.3.4 Prostate and gastric cancer 43

CHAPTER 3 | Nerve fibers infiltrate the tumor microenvironment and are associated with nerve growth factor production and lymph node invasion in breast cancer 45

3.1 Preface 45

3.2 Publication 46

3.3 Supplemental Files 56

CHAPTER 4 | ProNGF is a potential diagnostic biomarker for thyroid cancer 59

4.1 Preface 59

4.2 Publication 60

4.3 Supplementary Files 70

CHAPTER 5 | Neurotrophin Receptors TrkA, p75^{NTR} and Sortilin are Increased and Targetable in Thyroid Cancer 71

5.1 Preface 71

5.2 Publication 72

5.3 Supplementary Files 85

CHAPTER 6 | General Discussion 89

Appendices 95

A.1 Additional publications supplemental to this thesis 95

A.2 Co-authorship declaration 129

A.3 List of prizes and awards 131

Bibliography 132

Abstract

Infiltration of the tumour microenvironment by nerve fibres, termed cancer neurogenesis, is a relatively understudied feature of human carcinogenesis. Until only recently, perineural invasion (PNI), a process by which cancer cells surround and invade nerves, was thought to be the sole interaction between both tumoural and neuronal populations. PNI has traditionally been associated with clinically advanced tumours, in which it is thought to provide an alternate route for metastasis, generally resulting in a relatively poor prognosis for the patients. Recent studies however have demonstrated that denervation can supress tumour growth and metastasis, suggesting that there is separate interplay between both cancer and neuronal cells, extending far beyond that of PNI. However, what is yet to be fully elucidated in the literature is the molecular mechanism or mediators at play, responsible for facilitating this nerve-cancer cell crosstalk. What has been hypothesised, and since proven in a handful of human cancers, is that trophic factors are released by nerves and are capable of acting on cancer or other cells encompassing the tumour microenvironment. Conversely, cancer cells release neurotrophic factors that are capable of stimulating nerve infiltration or neurogenesis of the tumour. Neurotrophins and their receptors are one such family of neurotrophic factors that are emerging targets in oncology. More specifically, NGF and its precursor protein proNGF, along with their receptors, TrkA, $p75^{NTR}$ and sortilin, have already been implicated in several human cancers, including but not limited to that of the breast, skin (melanoma) and prostate. The overarching aim of this thesis was to develop a greater understanding of the emerging importance of both nerves and neurotrophic growth factors in influencing the growth and dissemination of human cancers. More specifically, this body of work aims to elucidate the extent and role of nerve infiltration within the tumour microenvironment of breast and thyroid cancers, as well as to determine any associations with the expression and function of NGF, proNGF and their receptors, TrkA, $p75^{NTR}$ and sortilin.

In a large cohort of primary breast tumours, we detected neural infiltration using the broad neuronal marker, PGP9.5. Invasive ductal carcinomas had a higher proportion of nerves as compared with that of invasive lobular carcinomas as well

as ductal carcinomas in situ. Additionally, the secretion of NGF was detected from a series of breast cancer cell lines, within their conditioned culture media. Co-culturing breast cancer cells with that of neuronal-like cells resulted in neurite outgrowth, which was ablated with the use of an NGF blocking-antibody, highlighting its potential role in stimulating breast cancer neurogenesis.

Following this, we looked to further clarify the expression and function of both nerves and neurotrophic growth factors in thyroid cancer. ProNGF expression was analysed by immunohistochemistry in two cohorts of cancer versus benign and normal thyroid tissues. Although innervation of thyroid cancers has not been previously reported, using the neuronal marker PGP9.5 we detected nerves in primary thyroid tumours. In both cohorts, proNGF was found to be overexpressed in thyroid cancer cells, as compared with both thyroid adenomas and normal thyroid tissue. We also demonstrated that proNGF is secreted by anaplastic thyroid cancer cell lines, highlighting its potential as a diagnostic biomarker, both histologically and within that of the blood. Next we looked to define the expression of TrkA, $p75^{NTR}$ and sortilin in thyroid cancer, as well as to determine if targeting these receptors reduced features of aggressiveness. TrkA was found to be more commonly expressed in tumours, where it was found to be associated with lymph node metastasis. In addition, nerves in the tumour microenvironment were positive for TrkA. $P75^{NTR}$ was overexpressed in anaplastic thyroid cancers compared to papillary and follicular subtypes whereas sortilin was overexpressed in all histological subtypes, as compared with adenomas and normal thyroid tissue. Targeting TrkA, $p75^{NTR}$ and sortilin *in vitro* using a pair of anaplastic thyroid cancer cell lines decreased cell survival and features of metastasis (migration and invasion), thus highlighting their potential are novel therapeutic targets in this devastating subtype of thyroid disease. Taken together, the work portrayed in this thesis has provided new evidence highlighting the importance of nerve infiltration in human carcinomas of the breast and thyroid, elucidated a role for NGF as a potential regulator of neurogenesis in the breast tumour microenvironment, as well as implicated NGF, its precursor proNGF and their receptors (TrkA, $p75^{NTR}$ and sortilin) as novel targets for therapeutic intervention.

CHAPTER 1 | Thesis Overview

1.1 Introduction

To date, cancer research has primarily focussed on targeting cellular control pathways in cancer cells arising from mutations of both tumour suppressor genes and proto-oncogenes. More recently, the tumour microenvironment has been the subject of increasing investigation, as the immune and circulatory systems have drawn additional focus as alternate or supplementary means for recognising, managing and eliminating tumour growth and metastasis. However, the potential role of nerves and by association neurotrophic factors in the initiation and progression of human tumours remains understudied.

1.2 Aims of the study

The overarching aim of this thesis was to develop a greater understanding of the emerging importance of both nerves and neurotrophic growth factors in influencing the growth and dissemination of human cancers. More specifically, this body of work aims to elucidate the extent and role of nerve infiltration within the tumour microenvironment of breast and thyroid cancers, as well as to determine any associations with the expression and function of NGF, proNGF and their receptors, TrkA, $p75^{NTR}$ and sortilin.

1.3 Organisation of the thesis

At the outset, discussed here within **Chapter 1** is a **thesis overview** of the body of work contained within this thesis, in which all subsequent chapters containing published or written work are summarised.

Chapter 2 of this thesis is composed part thereof a review article entitled **"Nerve Dependence: From Regeneration to Cancer"** (published in *Cancer Cell*). This publication discusses parallels between the necessity for nerves and trophic factors in the phenomena of regeneration as well as their requirement for cancer progression. Of particular interest, the suggestion of a bidirectional communication between that of the nervous system and the tumour microenvironment, termed a nerve-cancer cell crosstalk, is highlighted as an exciting, unexploited concept that will form the framework of this thesis. The second half of Chapter 2 acts as an introduction to the neurotrophin family of growth factors and receptors. More specifically, NGF and its precursor proNGF, as well as their receptors TrkA, $p75^{NTR}$ and sortilin, are explored in regard to what is currently known about their expression and function, with respect to growth and metastasis, in a variety of human cancers.

Following on, **Chapter 3** is presented as a published article entitled, **"Nerve fibers infiltrate the tumor microenvironment and are associated with nerve growth factor production and lymph node invasion in breast cancer"** (published in *Molecular Oncology*). Whilst the expression and biological function of neurotrophins and their receptors have been explored to some extent in the breast cancer setting, the presence of nerves within the tumour microenvironment remained fragmentary. Chapter 3 focuses on clarifying the extent of nerve fibre infiltration in a large cohort of breast tumours as well as elucidating any potential role for NGF in promoting or facilitating this observation.

As a result of the data obtained for breast cancer in Chapter 3, we looked to extend this study in **Chapter 4**, to determine if the same observations apply to different tumour types, in this case thyroid cancer. This is presented as a

publication entitled **"ProNGF is a potential diagnostic biomarker for thyroid cancer"** (published in *Oncotarget*).

Chapter 5 is comprised of the publication entitled **"Neurotrophin Receptors TrkA, p75^{NTR} and Sortilin are Increased and Targetable in Thyroid Cancer"** (in final revision for *The American Journal of Pathology*). Given the striking overexpression of proNGF in thyroid tumours covered within Chapter 4 of this thesis, it was logical to explore the expression of its receptors, TrkA, p75^{NTR} and sortilin, as well as the presence of nerves, in the same cohort of thyroid tumours, as well as to determine any biological role they may play with respect to tumour growth and metastasis.

Chapter 6 is in the form of a **general discussion**, in which the findings of the publications contained within this thesis are summarised, placed into perspective, with respect to both past and present literature, and potential future directions or translational aspects for this body of work are postulated.

CHAPTER 2 | Literature Review

2.1 Nerve Dependence: From Regeneration to Cancer

2.1.1 Preface

Chapter 2 contains a review article entitled **"Nerve Dependence: From Regeneration to Cancer"** which has been published in in the journal *Cancer Cell*. This review serves as an introduction to my thesis and provides relevant background information on a comparative analysis between the role of the nervous system and derived molecules in cancer versus regeneration. Furthermore, this article postulates the extent and role of neurogenesis in the tumour microenvironment and discusses possible mechanisms and mediators at play in this phenomenon. Chapter 2 is also composed of a literature review introducing the neurotrophin family of growth factors and receptors, which have been identified as potential candidates or mediators of tumour neurogenesis. More specifically, nerve growth factor (NGF) and its precursor proNGF, along with their receptors TrkA, $p75^{NTR}$ and sortilin, are discussed in relation to their structure and function, in both the neuronal and tumoural setting.

2.1.2 Publication

CellPress

Cancer Cell
Review

Nerve Dependence: From Regeneration to Cancer

Benoni Boilly,[1,3] Sam Faulkner,[2,3] Phillip Jobling,[2] and Hubert Hondermarck[2,*]
[1]UFR de Biologie, Université de Lille, 59655 Villeneuve d'Ascq, France
[2]School of Biomedical Sciences and Pharmacy, Hunter Medical Research Institute, University of Newcastle, Callaghan, NSW 2308, Australia
[3]Co-first author
*Correspondence: hubert.hondermarck@newcastle.edu.au
http://dx.doi.org/10.1016/j.ccell.2017.02.005

Nerve dependence has long been described in animal regeneration, where the outgrowth of axons is necessary to the reconstitution of lost body parts and tissue remodeling in various species. Recent discoveries have demonstrated that denervation can suppress tumor growth and metastasis, pointing to nerve dependence in cancer. Regeneration and cancer share similarities in regard to the stimulatory role of nerves, and there are indications that the stem cell compartment is a preferred target of innervation. Thus, the neurobiology of cancer is an emerging discipline that opens new perspectives in oncology.

Introduction

Nerves are usually described as signaling structures, the function of which is primarily associated with chemical and electrical transmission. By connecting organs to the central nervous system, nerves are essential to body internal communication and proper physiological regulation. However, and less known, nerves have also been reported to play a role in various contexts of tissue development, repair, and regeneration (Kaucka and Adameyko, 2014). Nerve dependence for tissue growth was initially discovered during the 19th century in the context of salamander limb regeneration (Todd, 1823). Salamanders and newts regenerate appendages (limb and tail) after amputation, but this process does not take place if the stump is denervated. The requirement for nerves has subsequently been shown in other regenerative processes (Kumar and Brockes, 2012), including, but not limited to body and head regeneration in worms (Morgan, 1901), arm regeneration in the starfish (Huet, 1975), or fin regeneration in the fish (Geraudie and Singer, 1977). In mammals, a deficiency in digit tip regeneration also occurs following denervation (Rinkevich et al., 2014). Interestingly, the concept of nerve dependence may not be restricted to tissue regeneration, but could also be relevant to cancer progression. Landmark publications in prostate (Magnon et al., 2013) and gastric (Zhao et al., 2014) cancers have proposed the stimulating role of nerves in cancer progression as a new paradigm in oncology, by showing that the denervation of the primary tumor suppresses cancer growth and metastasis. Therefore, nerves may be as necessary to tumorigenesis as they are to regeneration. Although the phenomenon of nerve dependence in cancer has not yet been fully characterized in most tissue systems, the long-standing question in regeneration now applies to cancer: what are the molecular mechanisms of nerve dependence? The parallels between nerve dependence in regeneration and cancer are discussed here, with a particular emphasis on the latest developments regarding the molecular events involved and the potential therapeutic ramifications.

The Analogy between Regeneration and Cancer

Regeneration is a complex and fascinating biological phenomenon that can be defined as the replacement of lost body parts. This post-embryonic development occurs in many invertebrates and some vertebrate species after injury or amputation, and the cellular bases of regeneration have been nicely reviewed (King and Newmark, 2012). Regeneration is usually classified as morphallaxis versus epimorphosis. In morphallactic regeneration, such as in hydra, the remaining part of the amputated organism is profoundly remodeled to regenerate all parts of the body. In contrast, in epimorphic regeneration (Figures 1A and 1B), such as in limb regeneration, the amputated organism is not reorganized and the stump provides stem/progenitor cells that will form a bud called the blastema. From the blastema, the missing structure will be progressively reconstructed (Figure 1B). Interestingly, the blastema presents several similarities with the tumor, and parallels can be drawn between epimorphic regeneration and cancer. First, there are reciprocal interactions between epithelial and mesenchymal cells that drive blastema growth. Second, the involvement of stem cells has been demonstrated in the blastema and contributes to its development (Rinkevich et al., 2011). Third, angiogenesis (Rageh et al., 2002) and inflammation (Godwin et al., 2013) also occur in the blastema. Finally, and this will be further detailed in this review, nerves and individual axons infiltrate the blastema and are necessary to regeneration (Figure 1C); this is redolent of the recent findings in cancer showing that nerves are actively participating in tumor growth (Figure 1D). The interaction of nerves with blastema and tumor cells fuels regeneration and tumorigenesis, respectively.

Nerve Dependence in Regeneration

Limb regeneration and other epimorphic regeneration processes start with a wound epithelium covering the amputation site and, subsequently, the mesenchymal tissue beneath the wound epithelium develops into a blastema consisting of a growth zone of stem/progenitor cells (Figure 1C). Simultaneously, the wound epithelium becomes thicker and evolves into the epidermal cap. The blastema will grow and progressively differentiate to reconstitute the limb following a proximodistal pattern. Early blastema cells are considered stem cells originating from the stump (Rinkevich et al., 2011), and studies in various regenerative processes have demonstrated that the blastema is a heterogeneous collection of restricted progenitor cells (Kragl et al., 2009; Lehoczky et al., 2011; Rinkevich et al., 2011; Sandoval-Guzman

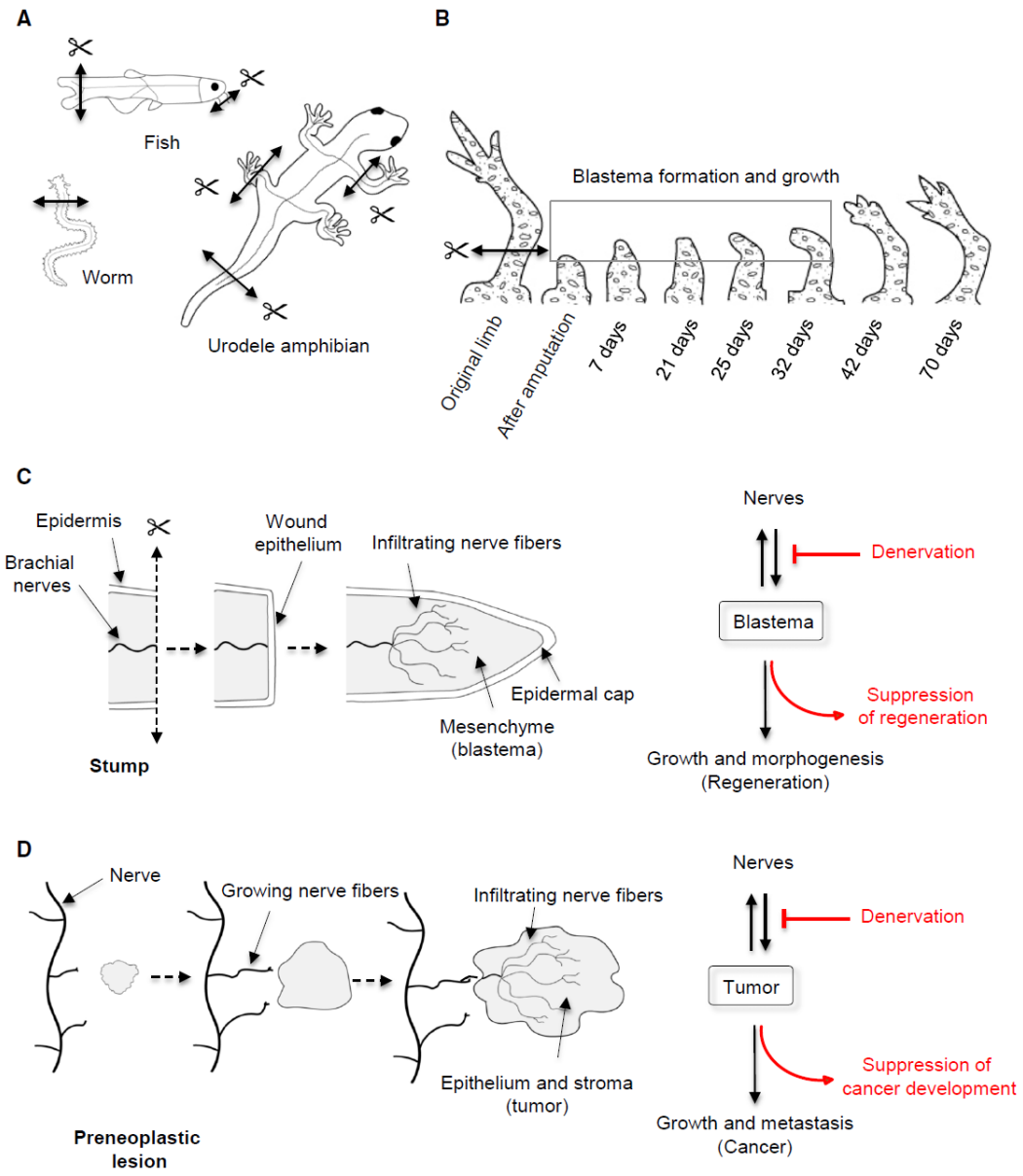

Figure 1. Nerve Dependence in Regeneration and Cancer

(A) Many examples of animal regeneration, including but not limited to body and head regeneration in annelid worms, fin and barbel regeneration in fish, and appendage (limb and tail) regeneration in Urodele amphibians are dependent on the presence of nerves.

(B) In Urodele amphibians, after a period of about 2 months post amputation, the limb is completely reconstituted and functional (redrawn from Goss, 1969). This regeneration process takes place only if the stump is innervated.

(C) After limb amputation, the epidermal cells migrate over the amputation plane and multiply to constitute the epidermal cap. Underneath, mesenchymal cells proliferate to form the blastema. Early on, growing nerve fibers infiltrate the blastema and there are reciprocal interactions between nerves and the blastema. As indicated by the red arrows, surgical denervation of the stump completely prevents regeneration (nerve dependence).

(D) In cancer, as demonstrated in prostate and gastric cancer, the innervation of the tumor participates in tumor growth and metastasis. Similarly to the blastema, there are reciprocal interactions between nerves and the tumor, and as indicated by the red arrows, the denervation of the tumor suppresses its growth and metastasis.

et al., 2014; Tu and Johnson, 2011). As the blastema grows, the progenitor cells progressively differentiate into fibroblasts, chondrocytes, endothelial and muscular cells. In addition, growing nerve fibers originating from the stump progressively invade the microenvironment of the blastema and stimulate the development of the regeneration. The ingrowth of nerve fibers

into the blastema starts during the early stage of its formation, as recently confirmed by using germline transgenic methods (Khattak et al., 2013). Nerve fibers reach out to both the mesenchyme and the epidermal cap, as shown with nerve regulation of fibroblast dedifferentiation (Satoh et al., 2010) and keratinocyte proliferation (Satoh et al., 2012). As initially discovered (Todd, 1823), surgical denervation of the limb before amputation prevents regeneration and results in healing with the formation of fibrotic scar tissues. The effect size is important, as a complete denervation of the stump results in a complete inhibition of regeneration with no blastema formation. Conversely, the deviation of nerves to the blastema increases the speed of regeneration (Singer, 1947; Geraudie and Singer, 1977), and more impressively, the deviation of nerves to a wounded area of skin is also sufficient to induce the growth of a supernumerary limb (Endo et al., 2004). In embryonic development, nerves have also been shown to drive several aspects of early organogenesis. This is illustrated with the development of the salivary gland, where innervation coordinates the interactions between the epithelium and the mesenchyme, resulting in tubulogenesis (Knox et al., 2013; Nedvetsky et al., 2014). The development of the inner ear (Kersigo and Fritzsch, 2015) and airway morphogenesis also require local innervation (Bower et al., 2014).

The method of choice for investigating nerve dependence in regeneration is the surgical denervation of the blastema by cutting afferent nerves. The prevention of blastema growth by denervation can be analyzed at various levels: morphologic (scarring versus regeneration), histologic (cell growth and differentiation), and molecular (changes in gene/protein expression). Many questions remain unanswered in regeneration, such as the reason why there is greater regeneration in salamanders and newts than many other species, or why regeneration is lost after metamorphosis in frogs for instance. Although regeneration cannot be reduced to nerve dependence, it does not occur unless nerves invade the blastema, and denervation leads to scarring. Therefore, one could speculate that the failure to regenerate may be related to insufficient nervous input and/or stem cell failure, the two events being potentially related.

Molecular Basis for Nerve Dependence in Regeneration

Despite nerve dependence in regeneration having been described for almost two centuries, the underlying molecular mechanisms remain unclear. The reason is that most of the research on this topic was published in the 1950s up to the 1970s when modern molecular approaches were not yet available. To date, most of the molecular data about nerve dependence has been obtained in limb regeneration. Neuropeptides and neurotransmitters were initially described, but most recent investigations also point to growth factors and morphogens as mediators of nerve dependence (Figure 2 and Table 1).

Early Investigations: Neuropeptides and Neurotransmitters

Initial attempts to identify the molecular mediators of nerve dependence consisted of studying spinal cord metabolism after limb amputation. In co-culture, the spinal cord from regenerating amphibians could stimulate the proliferation of blastema cells (Tomlinson et al., 1981), more than that of non-regenerating animals (Boilly and Bauduin, 1988). These results indicated the presence of an unknown proliferation factor in the nerve tissue, the production of which was increased following limb amputation. Conversely, the release of soluble proteins from the blastema, presumably neurotrophic growth factors, could stimulate neurite outgrowth from the spinal cord (Bauduin et al., 2000). The reactivity of nerve tissue to the blastema was more recently investigated at the transcriptional level (Athippozhy et al., 2014; Monaghan et al., 2009), and has confirmed that regeneration involves bidirectional interactions between nerves and blastema cells. In cancer, co-culture experiments have highlighted a similar crosstalk between neuronal and tumor cells, leading to both a stimulation of neuronal outgrowth by cancer cells and an induction of cancer cell aggressiveness by neuronal cells (Ayala et al., 2008; Deborde et al., 2016; Pundavela et al., 2015).

Importantly, the release of transferrin (Mescher et al., 1997), neuregulin (Wang et al., 2000) and the neurotransmitter substance P (Smith et al., 1995) by nerve endings in the regenerating blastema has been demonstrated, and can partially rescue the denervated blastema and support regeneration. In contrast, early investigations have shown that acetylcholine and its receptors (Drachman and Singer, 1971), as well as noradrenaline (Rathbone et al., 1980), were not involved in stimulating blastema cells. However, a recent investigation in heart regeneration has shown that cholinergic nerves are necessary to cardiomyocyte proliferation and that the pharmacological inhibition of muscarinic acetylcholine receptors can block heart regeneration (Mahmoud et al., 2015). Direct mechanical denervation impaired heart regeneration in neonatal mice and was rescued by the administration of neuregulin and nerve growth factor (NGF). These data clearly implicated cholinergic nerves and corresponding signaling pathways in heart regeneration. Therefore, in the years to come, we may witness a renewed interest for the impact of acetylcholine and its receptors in regeneration. This is comparable with the recently described involvement of cholinergic nerves in prostate (Magnon et al., 2013) and gastric (Hayakawa et al., 2017; Zhao et al., 2014) cancer, and their requirement for tumor growth and metastasis. Therefore, neurotransmitters released by nerves in the microenvironment are in the position of stimulating both regenerative and cancer cells.

Growth Factors and Morphogens

The expression of newt anterior gradient (nAG) protein, bone morphogenetic protein 2 (BMP2), and fibroblast growth factors (FGFs) has been shown to be crucial to the trophic effect of nerves in regeneration.

The protein nAG is a determinant of proximodistal position and a growth factor that binds to Prod1, a glycophosphatidylinositol-anchored membrane glycoprotein member of the three-finger protein family (Yin and Poss, 2008). nAG is expressed in Schwann cells at the nerve endings and in gland cells underlying the wound epithelium, resulting in the stimulation of blastema cell growth through Prod1 (Kumar et al., 2007). Strikingly, ectopic expression of nAG can mimic innervation and rescue the regeneration of a denervated blastema (Kumar et al., 2007). Therefore, nAG is a mediator of nerve dependence in limb regeneration. The mechanism was studied in vitro and involved nAG binding to Prod1 (Kumar et al., 2015), but the downstream signaling pathways have not yet been clarified. A recent study has indicated that there is no human ortholog for nAG (Grassme et al., 2016). However, closest human proteins consist of the anterior gradient proteins (AGRs) and, in particular, AGR2 and AGR3, which

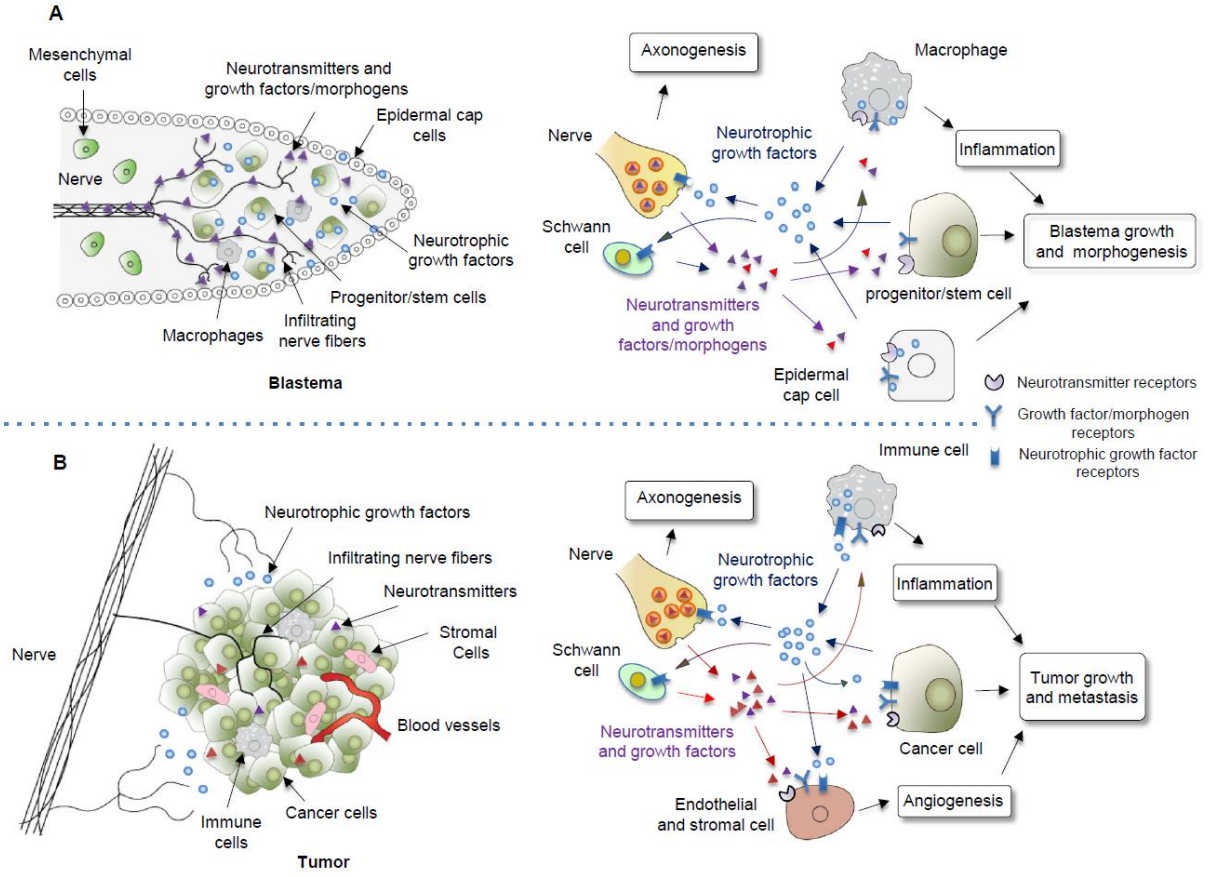

Figure 2. Molecular Mechanisms of Nerve Dependence in Regeneration Versus Cancer

(A) In regeneration, nerve infiltration (axonogenesis) in the blastema is driven by the secretion of neurotrophic growth factors (such as FGFs) by mesenchymal progenitor/stem cells and cells from the epidermal cap. Conversely, nerves (including axons and surrounding Schwann cells) liberate mitogenic growth factors (such as nAG and FGFs), morphogens (such as BMP2), and neurotransmitters (such as SP) in the microenvironment of the blastema, resulting in the stimulation of proliferation of both mesenchymal and epidermal cells. Macrophages have also been identified to be necessary to regeneration and the mechanism may involve the release of neurotrophic growth factors to stimulate axonogenesis. Together, the crosstalk between nerves and blastema cells results in the stimulation of growth and morphogenesis.

(B) In cancer, nerve infiltration (axonogenesis) in the tumor microenvironment is stimulated by the release of neurotrophic growth factors by cancer cells. Conversely, nerve endings (including axons and surrounding Schwann cells) release neurotransmitters (catecholamines and acetylcholine have mostly been described so far) that can activate the growth of both cancer and stromal cells through the stimulation of specific membrane receptors. Neurotrophic growth factors and neurotransmitters liberated in the tumor microenvironment can also activate stromal, endothelial, and immune cells, and therefore have a stimulatory impact on tumor neo-angiogenesis and inflammation. The crosstalk between nerves, and cancer/stromal cells contributes to tumor growth and metastasis.

demonstrate a significant similarity with nAG. Unlike nAG, AGR2 and AGR3 are not secreted proteins (Grassme et al., 2016), they lack a signal peptide and, as a consequence, are sequestered in the membrane of the endoplasmic reticulum. Thus, AGR proteins cannot have a growth factor activity comparable with nAG in regeneration, and whether the loss of limb regeneration in higher vertebrates is due to the evolution of nAG toward a non-secreted protein remains to be elucidated. Nevertheless, AGR proteins are also expressed in human tumors (Tsuji et al., 2015; Zhang et al., 2016b), and whether their expression is related to nerve dependence in cancer should be investigated.

FGFs and BMPs are secreted from nerves into the blastema and stimulate regeneration (Satoh et al., 2016). These factors directly act as mitogens for blastema cells (Boilly et al., 1991; Lehrberg and Gardiner, 2015). Using accessory limb or tail models, where nerve deviation to a wounded epithelium can stimulate the growth of an extra limb or tail, it was also shown that a co-operative application of BMP2 and FGF-8 could mimic the presence of nerves (Makanae et al., 2014, 2016). Inversely, the production of FGFs by blastema cells is thought to play a role in stimulating axonogenesis in the blastema (Cannata et al., 2001; Zenjari et al., 1997). Therefore, it can be postulated that FGFs and BMPs are major players in nerve dependence. In addition, BMP signaling promotes blood vessel formation in the blastema (Thorimbert et al., 2015) and could be a link between nerve infiltration and angiogenesis. The role of FGFs has also been indicated through the demonstration that FGF-8 and Sonic hedgehog (SHH) substitute for anterior-posterior tissue interactions in inducing blastema growth (Nacu et al., 2016). FGF-8

Table 1. Molecular Mediators of Nerve Dependence in Regeneration and Cancer

Regeneration	Cancer
Released by nerves to stimulate blastema cells: substance P (Smith et al., 1995) transferrin (Mescher et al., 1997) neuregulin (Wang et al., 2000; Mahmoud et al., 2015) nAG (Kumar et al., 2007) FGFs (Mullen et al., 1996; Satoh et al., 2016) BMP2 (Satoh et al., 2016) oncostatin M (Johnston et al., 2016) PDGF (Johnston et al., 2016)	Released by nerves to stimulate tumor cells: noradrenaline (Magnon et al., 2013) acetylcholine (Magnon et al., 2013; Zhao et al., 2014) Wnt (Zhao et al., 2014)
Released by blastema cells to stimulate nerve outgrowth: Wnt (Takeo et al., 2013) FGFs (Zenjari et al., 1997; Cannata et al., 2001)	Released by tumor cells to stimulate nerve outgrowth: NGF (Pundavela et al., 2014, 2015) G-CSF (Dobrenis et al., 2015) Neurturin (Wang et al., 2014)

BMP2, bone morphogenetic protein 2; FGFs, fibroblast growth factors; G-CSF, granulocyte-colony stimulating factor; nAG, newt anterior gradient; NGF, nerve growth factor; PDGF, platelet-derived growth factor.

was found to signal anterior cell position in the blastema, whereas SHH expression was associated with posterior position, and the expression of the two proteins was essential to limb regeneration in the presence of nerves (Nacu et al., 2016). The involvement of SHH is not limited to limb regeneration, as SHH is produced in murine sensory nerves to control skin cell renewal (Xiao et al., 2015) and tooth regeneration (Hardcastle et al., 1998). Importantly, SHH (Martinez et al., 2015), FGFs (Grothe et al., 2001) and BMPs (Chou et al., 2013) are expressed in mammalian nerves; they are therefore potentially transferrable as mediators of nerve dependence in cancer progression.

Other Mediators?

Immune cells could also be involved in nerve dependence in regeneration. Immune response and inflammation in the injured tissue is a prominent feature during the formation of the blastema (Mescher et al., 2016). Interestingly, macrophage infiltration in the blastema is required for limb (Godwin et al., 2013) and fin regeneration (Petrie et al., 2014). Although the mechanism is still unclear, immune cells and macrophages in particular are known to be a rich source of neurotrophic growth factors such as NGF (Garaci et al., 1999). The secretion of growth factors by macrophages has been shown to stimulate nerve regeneration (Yin et al., 2003), and macrophages could therefore contribute to nerve outgrowth into the blastema. In addition, macrophages are known to be influenced by nerves (Borovikova et al., 2000; Rosenberg et al., 2012), and they have also been linked to intestinal regeneration after irradiation (Saha et al., 2016). Here again, the parallel can be made with cancer, where immune cells and in particular tumor-associated macrophages have a crucial impact on stimulating tumor growth (Noy and Pollard, 2014).

Mammalian digit tip regeneration has provided complementary information about the molecular mechanisms of nerve dependence. A Wnt-dependent differentiation of nail progenitor cells is required for attracting nerves that promote blastema growth (Takeo et al., 2013). This study has shown that nail progenitor cells undergo Wnt-dependent differentiation, which is required for nail regeneration and also for attracting nerves that promote mesenchymal blastema growth. In addition, Schwann cell precursors have been discovered to be required for digit tip regeneration, through the secretion of paracrine factors and in particular the cytokine oncostatin M and platelet-derived growth factor AA (Johnston et al., 2016). Of note, Schwann cells are involved in limb regeneration in amphibians (Kumar et al., 2007), digit regeneration in mammals (Johnston et al., 2016), as well as cancer (Deborde et al., 2016), and they may therefore be crucial to nerve dependence in general.

Together, after neuropeptides and neurotransmitters, growth factors and morphogens, new players involved in nerve dependence in regeneration continue to be identified. Although these factors are not exclusively produced by nerves, more progress should be anticipated in the years to come, in particular to clarify and fully integrate the networks of cellular and molecular interactions involved. The cancer research community should closely watch this progress in regeneration, as it may provide insights to help better understand the molecular mechanisms of nerve dependence in cancer.

The Discovery of Nerve Dependence in Cancer

Given the similarities between blastema and tumor growth, the essential role of nerves in the formation and growth of the blastema suggests that nerve ablation in cancer may block cancer initiation and progression. However, early publications describing the impact of denervation on tumor growth (Barnbrook, 1953; Batkin et al., 1970; De Sousa Pereira, 1946) have been relatively unnoticed and nerves were considered as passive bystanders in cancer progression. Until recently, the interaction between nerves and cancer was essentially described through the process called perineural invasion, by which cancer cells surround and invade nerve trunks. Perineural invasion has been shown to be generally associated with tumor aggressiveness by providing a path for cancer cell dissemination (Amit et al., 2016), but nerves were believed to have no active role in stimulating tumor growth and metastasis. A new paradigm was proposed in two major publications, in prostate (Magnon et al., 2013) and gastric (Zhao et al., 2014) cancers, demonstrating that nerves are necessary for tumor progression and metastasis.

Similarly to regeneration, denervation experiments in vivo were at the basis of the discovery of nerve dependence in cancer. Tumor initiation and progression was analyzed after denervation and by comparison with control animals, where the organ or the tumor was not denervated. Surgical cutting of afferent nerves, or the injection of neurotoxic drugs in the organ/tumor, such as 6-hydroxydopamine (6OHDA) or botulinum toxin, has been used (Magnon et al., 2013; Zhao et al., 2014). Although these methods have potential limitations related to possible incomplete denervation or nerve regeneration, they have allowed for studying the impact of nerves in cancer progression. In

addition, the interaction between neurons and cancer cells can also be analyzed in vitro, and co-culturing these two cell types together can provide useful information about the molecular crosstalk involved (Pundavela et al., 2014).

Prostate Cancer

The fact that nerves infiltrate the microenvironment of prostate tumors and are associated with poor patient survival is recognized (Ayala et al., 2008; Olar et al., 2014), but Magnon et al. (2013) were first to clearly demonstrate the requirement of nerves in stimulating cancer progression. In various mouse models, denervation of autonomic nerves of the primary tumor resulted in a strong decrease in cancer growth and dissemination (Magnon et al., 2013). Destruction of both sympathetic (adrenergic) and parasympathetic (cholinergic) nerves, performed either surgically or pharmacologically using 6OHDA, suppressed tumor development. A kinetic analysis of autonomic nerve infiltration, coupled to a measurement of tumor size and metastasis occurrence, suggested that sympathetic nerves stimulated the early stages of cancer progression. In contrast, parasympathetic nerves were found to activate cancer cell dissemination at later stages. The effect size of denervation was important, as there was no significant tumor detected in the denervated animals over the course of a few weeks. In a clinical setting, it was also shown that the density of sympathetic and parasympathetic nerves was higher in tumors with poor clinical outcomes. The phenomenon was described for autonomic nerves, but as sensory and motor nerves were not investigated in this study, their potential involvement in prostate cancer cannot be excluded.

Gastric Cancer

Similarly to prostate cancer, denervation suppresses tumorigenesis in gastric cancer (Zhao et al., 2014). Using three separate animal models of gastric cancer, an intact vagal innervation was found critical at all stages of gastric tumorigenesis. As in prostate cancer, surgical or chemical denervation of the stomach, by vagotomy or local injection of botulinum toxin, markedly reduced tumor incidence and progression. A considerable effect size after vagotomy was observed, with tumor incidence and volume reduced by about 90%, but the survival difference of animals after 18 months was more limited, possibly due to partial regeneration of the vagus nerve in the long term. Denervation particularly affected the renewal of the stem cell compartment of gastric tumors and was also able to enhance the effect of chemotherapy and prolong survival. The authors concluded that denervation represents a feasible strategy for the control of gastric cancer, and this work was a further demonstration of the active role of nerves in tumor progression.

Other Cancers

Evidence for nerve dependence is emerging in other malignancies. In pancreatic cancer, nerves infiltrating pancreatic tumors can induce the migration of cancer cells along their axons via a mechanism involving glia-derived neurotrophic factor (GDNF) (Gil et al., 2010), and perineural invasion of nerves by cancer cells has long been described to be related to pancreatic tumor severity and pain (Demir et al., 2015). In addition, nerve infiltration in pancreatic tumors occurs early in the initial phase of tumor development (Stopczynski et al., 2014), suggesting a causative impact of nerves in tumor initiation. Furthermore, ablation of sensory neurons in a genetic model of pancreatic adenocarcinoma has been shown to slow the initiation and progression of cancer, with a significantly prolonged survival (Saloman et al., 2016). In basal cell carcinomas, a non-melanoma form of skin cancer emerging from epithelial cells, surgical ablation of cutaneous nerves in hair follicles blunts tumor formation (Peterson et al., 2015). Head and neck cancers have long been known for high levels of perineural invasion that are indicative of poor survival and cancer-associated pain (Carter et al., 1983; Soo et al., 1986), and sympathectomy decreases size and invasiveness of tongue cancer in rats (Raju et al., 2007). In colon (Liebl et al., 2013) and breast (Pundavela et al., 2015) cancers, although nerve dependence has not yet been demonstrated, nerve infiltration in the tumor microenvironment correlates with tumor aggressiveness. Primary breast tumors are infiltrated by sympathetic axons (Pundavela et al., 2015), and the sympathetic nervous system can induce a metastatic switch in breast cancer (Sloan et al., 2010). Therefore, the stimulatory role of nerves in cancer progression, initially discovered in prostate and gastric cancer, may prove to be relevant to other, if not all, types of human tumors.

Molecular Basis for Nerve Dependence in Cancer

Similarly to regeneration, nerve dependence in cancer appears to involve, on the one hand, a combination of trophic factors released by nerves toward both cancer and stromal cells. On the other hand, cancer cells release neurotrophic factors that stimulate nerve infiltration. Together, the molecular mediators of the nerve-cancer cell crosstalk fuel tumor growth and dissemination (Figure 2 and Table 1).

Nerve Stimulation of Tumor Growth

In prostate cancer, nerve dependence involves the expression of adrenergic receptors and muscarinic acetylcholine receptors by both stromal and cancer cells (Magnon et al., 2013). Impairment of β-adrenergic and muscarinic receptors could mimic denervation, suggesting that the neurotransmitters released by nerve endings in the tumor microenvironment activate cancer cell proliferation and invasion. Furthermore, investigations in mouse models have shown that prostate stromal and cancer cells express both β-adrenergic and muscarinic receptors, and that these receptors participate in tumor cell growth and invasion (Magnon et al., 2013). In gastric cancer, the suppression of tumorigenesis induced by vagal denervation in mouse models involved the inhibition of cholinergic signaling and muscarinic receptors (Hayakawa et al., 2017; Zhao et al., 2014). This is similar to the involvement of acetylcholine muscarinic receptors in cardiomyocyte progenitor proliferation during heart regeneration (Mahmoud et al., 2015). Also, the involvement of stromal cells as targets of nerves is comparable with the situation in regeneration, where the mesenchymal blastema cells differentiate into various stromal cells including fibroblast and endothelial cells under the influence of nerves (Satoh et al., 2010, 2016). Therefore nerves not only impact cancer cells directly, but also stromal cells, and induce a remodeling of the tumor microenvironment.

There is extensive evidence that cancer cells express neurotransmitter receptors and can be stimulated toward growth by exogenous neurotransmitters, as described with β-adrenergic receptors and the stimulatory impact of noradrenaline and the sympathetic nervous system on cancer progression (Cole et al., 2015). In ovarian cancer, the activation of the tyrosine

kinase SRC by β-adrenergic receptors is a switch for tumor metastasis (Armaiz-Pena et al., 2013), and adrenergic signaling leads to increased metastasis via prostaglandin E2 synthesis (Nagaraja et al., 2016). In addition, the effect of β-adrenergic receptors may extend to angiogenesis, as they are expressed in endothelial cells and improve endothelial progenitor cell-mediated neo-angiogenesis (Galasso et al., 2013). Also, the role of sympathetic nerves in cancer progression could be related to the reported effect of the intake of β blockers on the survival of cancer patients. Beta blockers are traditionally used for the treatment of cardiovascular disorders and anxiety, but in prostate (Grytli et al., 2014), breast (Barron et al., 2011; Melhem-Bertrandt et al., 2011; Raimondi et al., 2016) and ovarian (Watkins et al., 2015) cancers, β blockers have been associated with improved patient survival. Catecholamines are secreted not only by nerves, but also by the adrenal gland in response to stress. The effect of β blockers may therefore also be related to the inhibition of stress. Stress can have an impact on tumor progression, through the stimulation of the sympathetic nervous system and β-adrenergic receptors (Sloan et al., 2010). Also, dopamine, a stress inhibitory catecholamine, can decrease cancer growth through an anti-angiogenic effect (Moreno-Smith et al., 2011, 2013). While the issue of the impact of β blockers in cancer is still debated (Nagaraja et al., 2013; Weberpals et al., 2016), further studies are needed to elucidate the mechanism of action. Although the effect of β blockers on cardiovascular health and stress will be difficult to isolate from the effect on nerves in cancer, it may be hypothesized that β blockers could also inhibit the impact of catecholamines released by nerve endings in the tumor microenvironment.

Nerve-Stem Cell Connection

Nerves seem to be part of the normal stem cell niche. In bone marrow, sympathetic nerves regulate hematopoietic stem cells (Yamazaki et al., 2011), in particular to egress bone marrow (Katayama et al., 2006). Chemotherapy-induced nerve injury in the bone marrow impairs hematopoietic regeneration (Lucas et al., 2013) and sympathetic neuropathy promotes malignancy in the hematopoietic stem cell niche (Hanoun et al., 2014). In the intestinal epithelium, enteric nerves innervating the crypts stimulate the proliferation of stem/progenitor cells, thus contributing to the maintenance of the intestinal epithelial barrier (Lundgren et al., 2011). This study proposed that the development of stem/progenitor cells is under the control of cholinergic nerves, which are influenced by mucosal afferent neurons releasing acetylcholine, substance P, and calcitonin gene-related peptide.

In gastric cancer (Zhao et al., 2014), vagal denervation induces the inhibition of tumorigenesis and is associated with a decrease in Wnt signaling and the suppression of stem cell expansion through an M3 receptor-mediated cholinergic signaling. Wnt signaling is crucial to morphogenesis in both development and cancer, and is a potential therapeutic target in oncology (Kahn, 2014). In planarian worm regeneration, the transcription of Wnt family genes in stem cells along the body's pre-existing nervous system is regulated by hedgehog (HH) signaling and is responsible for the establishment of the anterior-posterior polarity (Yazawa et al., 2009). Canonical Wnt signaling is necessary in the epithelium during digit tip regeneration (Takeo et al., 2013) and is associated to a stem cell population positive for Lgr6 (leucin-rich repeat-containing G protein-coupled receptor 6) that is required for proper regeneration (Lehoczky and Tabin, 2015). Therefore, Wnt regulation by nerves in gastric cancer in relation to stem cells (Zhao et al., 2014) pointed to common cellular and molecular mechanisms of nerve dependence between regeneration and cancer.

A relationship between nerve dependence and cancer stem cells has been further confirmed in basal cell carcinomas (Peterson et al., 2015), in which tumors arise from stem cells within the hair follicle and mechanosensory niches. Sensory cutaneous nerves are required for tumor formation from touch domes and this nerve dependence is mediated by HH signaling. This is in line with previous findings showing that nerve-derived HH signaling defines a niche for hair follicle stem cells capable of becoming epidermal stem cells (Brownell et al., 2011). Here again, there are similarities with regeneration, where HH signaling in mesenchymal cells of the blastema is involved in the establishment of the anterior-posterior polarity observed in the presence of nerves (Nacu et al., 2016). Furthermore, digit tip regeneration also involves nerves that impact the behavior of the stem/progenitor cell compartment of the epidermis by increasing their multiplication (Rinkevich et al., 2014).

Interestingly, a recent transcriptomic analysis of prostate cancer has revealed a neurogenic gene expression profile associated to stem cells in aggressive prostate tumors (Zhang et al., 2016a), suggesting that cancer stem cells can develop a profile of gene expression oriented toward the stimulation of nerve infiltration. Therefore, there is increasing evidence in various models that nerves directly activate the stem cell compartment, presumably via the release of neurotransmitters, and this may constitute a mechanism that generally applies to cancer progression.

Neuro-Immune Regulations

The regulation of inflammation by innervation may also constitute a mechanism involved in nerve dependence. As reviewed recently (Hanoun et al., 2015), there is a neural regulation of inflammation that plays a role in cancer. For instance, in breast cancer, macrophage infiltration in the tumor is induced by sympathetic activation mediated by β-adrenergic receptors, and contributes to metastasis (Sloan et al., 2010). This echoes the recently described involvement of macrophages in the regenerative blastema (Godwin et al., 2013) (Petrie et al., 2014), further emphasizing the parallels between cancer and regeneration. The interaction between innervation and inflammation in cancer progression can be complex, as shown with splenic vagal denervation that results in the expansion of myeloid-derived suppressor cells and the subsequent suppression of cytotoxic T cells, ultimately promoting carcinogenesis (Dubeykovskaya et al., 2016). Future investigations will need to clarify the complex signaling pathways involving neurotransmitters and cytokines in the interplay between immune and cancer cells.

The Emerging Role of Schwann Cells

There is recent evidence pointing to Schwann cells as active players of nerve dependence in cancer. In pancreatic and colon cancer, Schwann cells colonize neoplastic sites before the onset of cancer invasion (Demir et al., 2014). This study demonstrated that dedifferentiated Schwann cells from nerves around the primary tumor can migrate toward cancer cells. NGF secreted by

cancer cells was demonstrated to be a mediator of Schwann cell chemoattraction through a $p75^{NTR}$-mediated signaling. In addition, nerve-derived Schwann cells can promote pancreatic cancer progression through the induction of cancer cell dispersion and invasion (Deborde et al., 2016; Demir et al., 2015). A direct contact between dedifferentiated Schwann cells and cancer cells, mediated by NCAM1, was found necessary not only to perineural invasion, but also to the stimulation of cancer cell invasion (Deborde et al., 2016). These data are reminiscent of the role of Schwann cells in limb (Kumar et al., 2007) and digit tip regeneration (Johnston et al., 2016), suggesting a broader implication of Schwann cells in nerve dependence.

Overall, the impact of nerve infiltration in tumor progression encompasses a direct effect on cancer growth and invasion, not only through the stimulation of cancer and stromal cells, but also via the activation of Schwann cells, angiogenesis, and the modulation of inflammation. Future studies will need to clarify the network of cellular and molecular interactions involved.

Nerve Dependence in Cancer Initiation?

The data obtained so far about nerve dependence in cancer have been mainly related to cancer progression. Surgical and chemical denervation of tumors in cancer animal models was the experimental cornerstone of most investigations and, as a consequence, the role of nerves has been interpreted more in the context of tumor progression than preneoplasia. Interestingly, cancer initiation has been compared with chronic wound repair, because both involve hyperplasia and tissue remodeling, and nerves are also thought to play a role in wound repair. Denervation impairs cutaneous wound healing (Fukai et al., 2005; Smith and Liu, 2002). Various clinical situations also indicate the role of nerves in wound healing. In diabetes, loss of innervation and axon plasticity accompany impaired diabetic wound healing (Cheng et al., 2013), and a defective wound healing is classically observed in patients with paraplegia and quadriplegia (Basson and Burney, 1982). Of note, NGF is a potent accelerator of wound healing (Li et al., 1980), further pointing to the role of nerve infiltration in hyperplasia and tissue remodeling. So far, the data indicating that nerves are likely to be important for cancer initiation and preneoplasia come from gastric cancer (Zhao et al., 2014) and basal cell carcinomas (Peterson et al., 2015). In gastric cancer, vagus denervation attenuates (but does not completely block) tumorigenesis at the preneoplastic stage in mouse models of gastric cancer, as demonstrated with tumor incidence 6 months after surgery: 76% versus 14% in control and denervated animals, respectively (Zhao et al., 2014). In basal cell carcinomas, denervation attenuates the early formation of tumors (Peterson et al., 2015). In this study, nerve-derived factors released by cutaneous nerves were able to promote tumor initiation from the mechanosensory niche of the touch domes within hair follicles. In addition, in pancreatic cancer Schwann cells seem to precede cancer invasion (Deborde et al., 2016). However, there are also investigations suggesting a stimulating effect of denervation on tumor initiation. In the skin, denervation has previously been reported to induce the formation of tumors (Pawlowski and Weddell, 1967), and partial gastrectomy with denervation promotes the development of cancer-related lesions in the gastric remnant (Kaminishi et al., 1997). Therefore, further investigations are needed to clarify the impact of nerves in preneoplasia and cancer initiation, to determine how the nerve-cancer interaction starts and how neural-dependent signaling might modulate epithelial or mesenchymal progenitor cells during early tumorigenesis.

Cancer Cell Stimulation of Tumor Axonogenesis

An essential aspect of nerve dependence in cancer is the ability of the tumor to stimulate and maintain nerve infiltration (axonogenesis). The expression of neurotrophic growth factors and corresponding receptors by cancer cells has been extensively described, as illustrated with NGF and other neurotrophins in breast cancer (Hondermarck, 2012), and was usually interpreted in the context of autocrine and paracrine loops of stimulation of cancer cell growth. Cancer cells express various neurotrophic growth factors/receptors, and the corresponding signaling pathways lead to the activation of cancer cell survival, proliferation, and invasion (Adriaenssens et al., 2008; Lagadec et al., 2009; Vaishnavi et al., 2013; Vanhecke et al., 2011). However, aside from the stimulation of cancer cells, there is increasing evidence that neurotrophic growth factors released by cancer cells also stimulate the outgrowth of nerves in the tumor microenvironment.

In prostate cancer, the release of the precursor for NGF (proNGF) by cancer cells is able to induce neuronal outgrowth (Pundavela et al., 2014) and could therefore contribute to nerve infiltration in prostate tumors. Whether or not proNGF is processed into NGF or exhibits a neurotrophic activity in its own right remains to be elucidated, but the production of proNGF by prostate cancer cells can stimulate tumor axonogenesis and correlates with tumor grade (Pundavela et al., 2014). Granulocyte-colony stimulating factor is also a potential driver of sympathetic nerve infiltration in prostate cancer (Dobrenis et al., 2015). Similarly, in breast cancer, nerve infiltration is associated with tumor aggressiveness and correlates with NGF release by cancer cells (Pundavela et al., 2015), and NGF receptor signaling promotes the expansion of the stem cell compartment (Tomellini et al., 2015). In gastric cancer, the expression of NGF family members (Du et al., 2003) and brain-derived neurotrophic factor (Okugawa et al., 2013) is associated with tumor aggressiveness. Interestingly, NGF has recently been shown to promote gastric tumorigenesis through aberrant cholinergic signaling (Hayakawa et al., 2017). The mechanism involves the liberation of acetylcholine from nerves, which induces NGF in gastric cancer cells and stimulates tumor axonogenesis (Hayakawa et al., 2017). In pancreatic cancer, NGF is also involved in attracting Schwann cells that in return attract cancer cells (Demir et al., 2014), favoring perineural invasion. A crucial role for NGF has also been shown in stimulating the innervation required for heart regeneration (Mahmoud et al., 2015), and therefore NGF and proNGF may be crucial drivers of axonogenesis in both cancer and regeneration. Other neurotrophic factors are likely to be involved in tumor axonogenesis, as illustrated in pancreatic cancer where the expression of the neurotrophic factor neurturin, a member of the GDNF family, is associated with neuronal plasticity (Wang et al., 2014). Together, epithelial and mesenchymal proliferating cells in the tumor release neurotrophic growth factors that stimulate axonogenesis. This is similar to the situation in the blastema and neurotrophic factors are involved in the innervation of the tumor and the blastema (Table 1), here again pointing to

common mechanisms of nerve dependence in regeneration and cancer.

Axon guidance molecules, which play a role in directing nerve outgrowth during development, are expressed in solid tumors, where their signaling can be altered (Biankin et al., 2012). Semaphorin 4F expression is associated with prostate cancer aggressiveness (Ding et al., 2013) and, in breast cancer, semaphorin 3B fosters a prometastatic environment through elevated interleukin-8 expression leading to dissemination to the lung (Rolny et al., 2008). The Robo-Slit pathway, which is a nerve repulsive pathway, is recurrently mutated (Bailey et al., 2016) and interacts with smoking in modifying the risk of pancreatic cancer (Tang et al., 2014). Interestingly, Robo1 and Slit2 also act as enhancers of host tolerance to chemotherapy in colorectal cancer and facilitate intestinal regeneration after treatment (Zhou et al., 2013). However, it should be noted that the presence of axon guidance molecules does not necessarily implicate nerve dependence, as these trophic factors can be expressed ectopically for a growth-activating purpose independent of nerves, and further investigations are necessary to clarify the involvement of axon guidance molecules in tumor axonogenesis.

The significance of neurotrophic growth factors and axonal guidance molecules in cancer has been generally interpreted in terms of a direct effect on cancer cells (attachment and mobility), but the recent developments on nerve infiltration in the tumor microenvironment suggest that they may also be involved in directing tumor axonogenesis. Together, it is clear that the role of neurotrophic factors and axon guidance molecules in cancer should be revisited in the context of the nerve-cancer cell crosstalk.

In translational terms, alternatively to surgical or chemical denervation, targeting neurotrophic signaling in cancer should be further explored as an innovative therapeutic approach to prevent tumor innervation. In development, injection of anti-NGF antibodies has been shown to prevent sympathetic and sensory innervation of organs (Aloe et al., 1981), and injection of anti-NGF antibodies can also prevent tumor growth and metastasis (Adriaenssens et al., 2008). Therefore, preventing or inhibiting tumor innervation via the targeting of neurotrophic factors may prove to be an efficient therapy in oncology.

Concluding Remarks

The emerging importance of nerves in cancer progression echoes the long-reported nerve dependence in tissue regeneration. The molecular mechanisms of nerve dependence remain to be fully elucidated, but in both regeneration and cancer the release of trophic factors by nerves significantly impacts the tissue microenvironment to stimulate cell growth and migration. In the regenerative blastema and the tumor, there is a bidirectional communication between growing nerves and proliferating cells, and the nerve-stem cell interaction is an area that warrants further investigation. The neural compartment appears to be an essential part of the tumor microenvironment and, similar to angiogenesis, there is accumulating evidence that axonogenesis is stimulated by malignant cells and contributes to cancer growth and metastasis.

Clinical ramifications of the nerve-cancer cell crosstalk are promising: neuronal biomarkers and anti-neurogenic therapies are increasingly regarded as innovative tools for cancer diagnosis and treatment (Cole et al., 2015; Jobling et al., 2015; Vaishnavi et al., 2015). However, nerve dependence in cancer being in the early phase of investigation, it is difficult at this point in time to anticipate the clinical relevance. To date, there are no examples that might indicate how targeting nerves may affect cancer growth in human patients and surgical denervation or targeted inhibition of neurotrophic growth factors are to be further explored as therapeutic approaches to denervate tumors or prevent the innervation of precancerous lesions. At this stage, the neural compartment of the tumor microenvironment is an untapped source for developing new diagnostic and therapeutic tools, and the neurobiology of cancer is an emerging field that opens new perspectives for innovation in basic and translational oncology.

Finally, on a more philosophical note, it is important to broaden the perspective of cancer research by breaking the artificial walls with other disciplines, toward a more comprehensive and holistic approach incorporating ideas from development, regeneration, stem cells, and neuroscience. The two parallel literatures on the role of nerves in regeneration and cancer point to the common neural mechanisms involved. Not only does this provide clues for cancer research, but also cancer research findings may sow new concepts and tools for regenerative medicine. Furthermore, the notion that cancer and normal stem cells are innervated, and thus communicate with the nervous system, raises a larger question, which is the possibility of a higher-order control of cancer growth and regeneration, and possibly integration with sensory input. This is again a reason that more expertise from the neuroscience field is needed in cancer biology.

ACKNOWLEDGMENTS

This work was supported by the University of Newcastle, the Hunter Medical Research Institute (HMRI 15-70), the Hunter Cancer Research Alliance (pilot project prostate cancer), and the Hunter New England Local Health District (G1601109). We thank Professor Robert Rush (Flinders University, Australia) for critical reading of the manuscript and helpful comments.

REFERENCES

Adriaenssens, E., Vanhecke, E., Saule, P., Mougel, A., Page, A., Romon, R., Nurcombe, V., Le Bourhis, X., and Hondermarck, H. (2008). Nerve growth factor is a potential therapeutic target in breast cancer. Cancer Res. *68*, 346–351.

Aloe, L., Cozzari, C., Calissano, P., and Levi-Montalcini, R. (1981). Somatic and behavioral postnatal effects of fetal injections of nerve growth factor antibodies in the rat. Nature *291*, 413–415.

Amit, M., Na'ara, S., and Gil, Z. (2016). Mechanisms of cancer dissemination along nerves. Nat. Rev. Cancer *16*, 399–408.

Armaiz-Pena, G.N., Allen, J.K., Cruz, A., Stone, R.L., Nick, A.M., Lin, Y.G., Han, L.Y., Mangala, L.S., Villares, G.J., Vivas-Mejia, P., et al. (2013). Src activation by beta-adrenoreceptors is a key switch for tumour metastasis. Nat. Commun. *4*, 1403.

Athippozhy, A., Lehrberg, J., Monaghan, J.R., Gardiner, D.M., and Voss, S.R. (2014). Characterization of in vitro transcriptional responses of dorsal root ganglia cultured in the presence and absence of blastema cells from regenerating salamander limbs. Regeneration (Oxf) *1*, 1–10.

Ayala, G.E., Dai, H., Powell, M., Li, R., Ding, Y., Wheeler, T.M., Shine, D., Kadmon, D., Thompson, T., Miles, B.J., et al. (2008). Cancer-related axonogenesis and neurogenesis in prostate cancer. Clin. Cancer Res. *14*, 7593–7603.

Bailey, P., Chang, D.K., Nones, K., Johns, A.L., Patch, A.M., Gingras, M.C., Miller, D.K., Christ, A.N., Bruxner, T.J., Quinn, M.C., et al. (2016). Genomic analyses identify molecular subtypes of pancreatic cancer. Nature *531*, 47–52.

Barnbrook, D.H. (1953). Pheochromocytoma; an alternative surgical approach. Can Med. Assoc. J. *68*, 245–247.

Barron, T.I., Connolly, R.M., Sharp, L., Bennett, K., and Visvanathan, K. (2011). Beta blockers and breast cancer mortality: a population- based study. J. Clin. Oncol. *29*, 2635–2644.

Basson, M.D., and Burney, R.E. (1982). Defective wound healing in patients with paraplegia and quadriplegia. Surg. Gynecol. Obstet. *155*, 9–12.

Batkin, S., Piette, L.H., and Wildman, E. (1970). Effect of muscle denervation on growth of transplanted tumor in mice. Proc. Natl. Acad. Sci. USA *67*, 1521–1527.

Bauduin, B., Lassalle, B., and Boilly, B. (2000). Stimulation of axon growth from the spinal cord by a regenerating limb blastema in newts. Brain Res. Dev. Brain Res. *119*, 47–54.

Biankin, A.V., Waddell, N., Kassahn, K.S., Gingras, M.C., Muthuswamy, L.B., Johns, A.L., Miller, D.K., Wilson, P.J., Patch, A.M., Wu, J., et al. (2012). Pancreatic cancer genomes reveal aberrations in axon guidance pathway genes. Nature *491*, 399–405.

Boilly, B., and Bauduin, B. (1988). Production in vitro by spinal cord of growth factor(s) acting on newt limb regeneration: influence of regeneration of the nerve fibers. Brain Res. *466*, 155–160.

Boilly, B., Cavanaugh, K.P., Thomas, D., Hondermarck, H., Bryant, S.V., and Bradshaw, R.A. (1991). Acidic fibroblast growth factor is present in regenerating limb blastemas of axolotls and binds specifically to blastema tissues. Dev. Biol. *145*, 302–310.

Borovikova, L.V., Ivanova, S., Zhang, M., Yang, H., Botchkina, G.I., Watkins, L.R., Wang, H., Abumrad, N., Eaton, J.W., and Tracey, K.J. (2000). Vagus nerve stimulation attenuates the systemic inflammatory response to endotoxin. Nature *405*, 458–462.

Bower, D.V., Lee, H.K., Lansford, R., Zinn, K., Warburton, D., Fraser, S.E., and Jesudason, E.C. (2014). Airway branching has conserved needs for local parasympathetic innervation but not neurotransmission. BMC Biol. *12*, 92.

Brownell, I., Guevara, E., Bai, C.B., Loomis, C.A., and Joyner, A.L. (2011). Nerve-derived Sonic hedgehog defines a niche for hair follicle stem cells capable of becoming epidermal stem cells. Cell Stem Cell *8*, 552–565.

Cannata, S.M., Bagni, C., Bernardini, S., Christen, B., and Filoni, S. (2001). Nerve-independence of limb regeneration in larval *Xenopus laevis* is correlated to the level of fgf-2 mRNA expression in limb tissues. Dev. Biol. *231*, 436–446.

Carter, R.L., Foster, C.S., Dinsdale, E.A., and Pittam, M.R. (1983). Perineural spread by squamous carcinomas of the head and neck: a morphological study using antiaxonal and antimyelin monoclonal antibodies. J. Clin. Pathol. *36*, 269–275.

Cheng, C., Singh, V., Krishnan, A., Kan, M., Martinez, J.A., and Zochodne, D.W. (2013). Loss of innervation and axon plasticity accompanies impaired diabetic wound healing. PLoS One *8*, e75877.

Chou, H.J., Lai, D.M., Huang, C.W., McLennan, I.S., Wang, H.D., and Wang, P.Y. (2013). BMP4 is a peripherally-derived factor for motor neurons and attenuates glutamate-induced excitotoxicity in vitro. PLoS One *8*, e58441.

Cole, S.W., Nagaraja, A.S., Lutgendorf, S.K., Green, P.A., and Sood, A.K. (2015). Sympathetic nervous system regulation of the tumour microenvironment. Nat. Rev. Cancer *15*, 563–572.

De Sousa Pereira, A. (1946). A basis for sympathectomy for cancer of the cervix uteri. Arch. Surg. *52*, 260–285.

Deborde, S., Omelchenko, T., Lyubchik, A., Zhou, Y., He, S., McNamara, W.F., Chernichenko, N., Lee, S.Y., Barajas, F., Chen, C.H., et al. (2016). Schwann cells induce cancer cell dispersion and invasion. J. Clin. Invest. *126*, 1538–1554.

Demir, I.E., Boldis, A., Pfitzinger, P.L., Teller, S., Brunner, E., Klose, N., Kehl, T., Maak, M., Lesina, M., Laschinger, M., et al. (2014). Investigation of Schwann cells at neoplastic cell sites before the onset of cancer invasion. J. Natl. Cancer Inst. *106*, pii: dju184.

Demir, I.E., Friess, H., and Ceyhan, G.O. (2015). Neural plasticity in pancreatitis and pancreatic cancer. Nat. Rev. Gastroenterol. Hepatol. *12*, 649–659.

Ding, Y., He, D., Florentin, D., Frolov, A., Hilsenbeck, S., Ittmann, M., Kadmon, D., Miles, B., Rowley, D., and Ayala, G. (2013). Semaphorin 4F as a critical regulator of neuroepithelial interactions and a biomarker of aggressive prostate cancer. Clin. Cancer Res. *19*, 6101–6111.

Dobrenis, K., Gauthier, L.R., Barroca, V., and Magnon, C. (2015). Granulocyte colony-stimulating factor off-target effect on nerve outgrowth promotes prostate cancer development. Int. J. Cancer *136*, 982–988.

Drachman, D.B., and Singer, M. (1971). Regeneration in botulinum-poisoned forelimbs of the newt. Triturus. Exp. Neurol. *32*, 1–11.

Du, J.J., Dou, K.F., Peng, S.Y., Qian, B.Z., Xiao, H.S., Liu, F., Wang, W.Z., Guan, W.X., Gao, Z.Q., Liu, Y.B., and Han, Z.G. (2003). Expression of NGF family and their receptors in gastric carcinoma: a cDNA microarray study. World J. Gastroenterol. *9*, 1431–1434.

Dubeykovskaya, Z., Si, Y., Chen, X., Worthley, D.L., Renz, B.W., Urbanska, A.M., Hayakawa, Y., Xu, T., Westphalen, C.B., Dubeykovskiy, A., et al. (2016). Neural innervation stimulates splenic TFF2 to arrest myeloid cell expansion and cancer. Nat. Commun. *7*, 10517.

Endo, T., Bryant, S.V., and Gardiner, D.M. (2004). A stepwise model system for limb regeneration. Dev. Biol. *270*, 135–145.

Fukai, T., Takeda, A., and Uchinuma, E. (2005). Wound healing in denervated rat skin. Wound Repair Regen. *13*, 175–180.

Galasso, G., De Rosa, R., Ciccarelli, M., Sorriento, D., Del Giudice, C., Strisciuglio, T., De Biase, C., Luciano, R., Piccolo, R., Pierri, A., et al. (2013). beta2-Adrenergic receptor stimulation improves endothelial progenitor cell-mediated ischemic neoangiogenesis. Circ. Res. *112*, 1026–1034.

Garaci, E., Caroleo, M.C., Aloe, L., Aquaro, S., Piacentini, M., Costa, N., Amendola, A., Micera, A., Calio, R., Perno, C.F., and Levi-Montalcini, R. (1999). Nerve growth factor is an autocrine factor essential for the survival of macrophages infected with HIV. Proc. Natl. Acad. Sci. USA *96*, 14013–14018.

Geraudie, J., and Singer, M. (1977). Relation between nerve fiber number and pectoral fin regeneration in the teleost. J. Exp. Zool. *199*, 1–8.

Gil, Z., Cavel, O., Kelly, K., Brader, P., Rein, A., Gao, S.P., Carlson, D.L., Shah, J.P., Fong, Y., and Wong, R.J. (2010). Paracrine regulation of pancreatic cancer cell invasion by peripheral nerves. J. Natl. Cancer Inst. *102*, 107–118.

Godwin, J.W., Pinto, A.R., and Rosenthal, N.A. (2013). Macrophages are required for adult salamander limb regeneration. Proc. Natl. Acad. Sci. USA *110*, 9415–9420.

Goss, R.J. (1969). Principles of Regeneration (Academic Press).

Grassme, K.S., Garza-Garcia, A., Delgado, J.P., Godwin, J.W., Kumar, A., Gates, P.B., Driscoll, P.C., and Brockes, J.P. (2016). Mechanism of action of secreted newt anterior gradient protein. PLoS One *11*, e0154176.

Grothe, C., Meisinger, C., and Claus, P. (2001). In vivo expression and localization of the fibroblast growth factor system in the intact and lesioned rat peripheral nerve and spinal ganglia. J. Comp. Neurol. *434*, 342–357.

Grytli, H.H., Fagerland, M.W., Fossa, S.D., and Tasken, K.A. (2014). Association between use of beta-blockers and prostate cancer-specific survival: a cohort study of 3561 prostate cancer patients with high-risk or metastatic disease. Eur. Urol. *65*, 635–641.

Hanoun, M., Zhang, D., Mizoguchi, T., Pinho, S., Pierce, H., Kunisaki, Y., Lacombe, J., Armstrong, S.A., Duhrsen, U., and Frenette, P.S. (2014). Acute myelogenous leukemia-induced sympathetic neuropathy promotes malignancy in an altered hematopoietic stem cell niche. Cell Stem Cell *15*, 365–375.

Hanoun, M., Maryanovich, M., Arnal-Estape, A., and Frenette, P.S. (2015). Neural regulation of hematopoiesis, inflammation, and cancer. Neuron *86*, 360–373.

Hardcastle, Z., Mo, R., Hui, C.C., and Sharpe, P.T. (1998). The Shh signalling pathway in tooth development: defects in Gli2 and Gli3 mutants. Development *125*, 2803–2811.

Hayakawa, Y., Sakitani, K., Konishi, M., Asfaha, S., Niikura, R., Tomita, H., Renz, B.W., Tailor, Y., Macchini, M., Middelhoff, M., et al. (2017). Nerve growth factor promotes gastric tumorigenesis through aberrant cholinergic signaling. Cancer Cell *31*, 21–34.

Hondermarck, H. (2012). Neurotrophins and their receptors in breast cancer. Cytokine Growth Factor Rev. *23*, 357–365.

Huet, M. (1975). [Role of the nervous system during the regeneration of an arm in a starfish: *Asterina gibbosa* Penn. (Echinodermata, Asteriidae)]. J. Embryol. Exp. Morphol. *33*, 535–552.

Jobling, P., Pundavela, J., Oliveira, S.M., Roselli, S., Walker, M.M., and Hondermarck, H. (2015). Nerve-cancer cell cross-talk: a novel promoter of tumor progression. Cancer Res. *75*, 1777–1781.

Johnston, A.P., Yuzwa, S.A., Carr, M.J., Mahmud, N., Storer, M.A., Krause, M.P., Jones, K., Paul, S., Kaplan, D.R., and Miller, F.D. (2016). Dedifferentiated Schwann cell precursors secreting paracrine factors are required for regeneration of the mammalian digit tip. Cell Stem Cell *19*, 433–448.

Kahn, M. (2014). Can we safely target the WNT pathway? Nat. Rev. Drug Discov. *13*, 513–532.

Kaminishi, M., Shimizu, N., Shimoyama, S., Yamaguchi, H., Tsuji, E., Aoki, F., Nomura, S., Yoshikawa, A., Kuramoto, S., Oohara, T., et al. (1997). Denervation promotes the development of cancer-related lesions in the gastric remnant. J. Clin. Gastroenterol. *25*, S129–S134.

Katayama, Y., Battista, M., Kao, W.M., Hidalgo, A., Peired, A.J., Thomas, S.A., and Frenette, P.S. (2006). Signals from the sympathetic nervous system regulate hematopoietic stem cell egress from bone marrow. Cell *124*, 407–421.

Kaucka, M., and Adameyko, I. (2014). Non-canonical functions of the peripheral nerve. Exp. Cell Res. *321*, 17–24.

Kersigo, J., and Fritzsch, B. (2015). Inner ear hair cells deteriorate in mice engineered to have no or diminished innervation. Front Aging Neurosci. *7*, 33.

Khattak, S., Schuez, M., Richter, T., Knapp, D., Haigo, S.L., Sandoval-Guzman, T., Hradlikova, K., Duemmler, A., Kerney, R., and Tanaka, E.M. (2013). Germline transgenic methods for tracking cells and testing gene function during regeneration in the axolotl. Stem Cell Rep. *1*, 90–103.

King, R.S., and Newmark, P.A. (2012). The cell biology of regeneration. J. Cell Biol. *196*, 553–562.

Knox, S.M., Lombaert, I.M., Haddox, C.L., Abrams, S.R., Cotrim, A., Wilson, A.J., and Hoffman, M.P. (2013). Parasympathetic stimulation improves epithelial organ regeneration. Nat. Commun. *4*, 1494.

Kragl, M., Knapp, D., Nacu, E., Khattak, S., Maden, M., Epperlein, H.H., and Tanaka, E.M. (2009). Cells keep a memory of their tissue origin during axolotl limb regeneration. Nature *460*, 60–65.

Kumar, A., and Brockes, J.P. (2012). Nerve dependence in tissue, organ, and appendage regeneration. Trends Neurosci. *35*, 691–699.

Kumar, A., Godwin, J.W., Gates, P.B., Garza-Garcia, A.A., and Brockes, J.P. (2007). Molecular basis for the nerve dependence of limb regeneration in an adult vertebrate. Science *318*, 772–777.

Kumar, A., Gates, P.B., Czarkwiani, A., and Brockes, J.P. (2015). An orphan gene is necessary for preaxial digit formation during salamander limb development. Nat. Commun. *6*, 8684.

Lagadec, C., Meignan, S., Adriaenssens, E., Foveau, B., Vanhecke, E., Romon, R., Toillon, R.A., Oxombre, B., Hondermarck, H., and Le Bourhis, X. (2009). TrkA overexpression enhances growth and metastasis of breast cancer cells. Oncogene *28*, 1960–1970.

Lehoczky, J.A., and Tabin, C.J. (2015). Lgr6 marks nail stem cells and is required for digit tip regeneration. Proc. Natl. Acad. Sci. USA *112*, 13249–13254.

Lehoczky, J.A., Robert, B., and Tabin, C.J. (2011). Mouse digit tip regeneration is mediated by fate-restricted progenitor cells. Proc. Natl. Acad. Sci. USA *108*, 20609–20614.

Lehrberg, J., and Gardiner, D.M. (2015). Regulation of axolotl (*Ambystoma mexicanum*) limb blastema cell proliferation by nerves and BMP2 in organotypic slice culture. PLoS One *10*, e0123186.

Li, A.K., Koroly, M.J., Schattenkerk, M.E., Malt, R.A., and Young, M. (1980). Nerve growth factor: acceleration of the rate of wound healing in mice. Proc. Natl. Acad. Sci. USA *77*, 4379–4381.

Liebl, F., Demir, I.E., Rosenberg, R., Boldis, A., Yildiz, E., Kujundzic, K., Kehl, T., Dischl, D., Schuster, T., Maak, M., et al. (2013). The severity of neural invasion is associated with shortened survival in colon cancer. Clin. Cancer Res. *19*, 50–61.

Lucas, D., Scheiermann, C., Chow, A., Kunisaki, Y., Bruns, I., Barrick, C., Tessarollo, L., and Frenette, P.S. (2013). Chemotherapy-induced bone marrow nerve injury impairs hematopoietic regeneration. Nat. Med. *19*, 695–703.

Lundgren, O., Jodal, M., Jansson, M., Ryberg, A.T., and Svensson, L. (2011). Intestinal epithelial stem/progenitor cells are controlled by mucosal afferent nerves. PLoS One *6*, e16295.

Magnon, C., Hall, S.J., Lin, J., Xue, X., Gerber, L., Freedland, S.J., and Frenette, P.S. (2013). Autonomic nerve development contributes to prostate cancer progression. Science *341*, 1236361.

Mahmoud, A.I., O'Meara, C.C., Gemberling, M., Zhao, L., Bryant, D.M., Zheng, R., Gannon, J.B., Cai, L., Choi, W.Y., Egnaczyk, G.F., et al. (2015). Nerves regulate cardiomyocyte proliferation and heart regeneration. Developmental Cell *34*, 387–399.

Makanae, A., Mitogawa, K., and Satoh, A. (2014). Co-operative Bmp- and Fgf-signaling inputs convert skin wound healing to limb formation in urodele amphibians. Dev. Biol. *396*, 57–66.

Makanae, A., Mitogawa, K., and Satoh, A. (2016). Cooperative inputs of Bmp and Fgf signaling induce tail regeneration in urodele amphibians. Dev. Biol. *410*, 45–55.

Martinez, J.A., Kobayashi, M., Krishnan, A., Webber, C., Christie, K., Guo, G., Singh, V., and Zochodne, D.W. (2015). Intrinsic facilitation of adult peripheral nerve regeneration by the Sonic hedgehog morphogen. Exp. Neurol. *271*, 493–505.

Melhem-Bertrandt, A., Chavez-Macgregor, M., Lei, X., Brown, E.N., Lee, R.T., Meric-Bernstam, F., Sood, A.K., Conzen, S.D., Hortobagyi, G.N., and Gonzalez-Angulo, A.M. (2011). Beta-blocker use is associated with improved relapse-free survival in patients with triple-negative breast cancer. J. Clin. Oncol. *29*, 2645–2652.

Mescher, A.L., Connell, E., Hsu, C., Patel, C., and Overton, B. (1997). Transferrin is necessary and sufficient for the neural effect on growth in amphibian limb regeneration blastemas. Dev. Growth Differ. *39*, 677–684.

Mescher, A.L., Neff, A.W., and King, M.W. (2016). Inflammation and immunity in organ regeneration. Dev. Comp. Immunol. *66*, 98–110.

Monaghan, J.R., Epp, L.G., Putta, S., Page, R.B., Walker, J.A., Beachy, C.K., Zhu, W., Pao, G.M., Verma, I.M., Hunter, T., et al. (2009). Microarray and cDNA sequence analysis of transcription during nerve-dependent limb regeneration. BMC Biol. *7*, 1.

Moreno-Smith, M., Lu, C., Shahzad, M.M., Pena, G.N., Allen, J.K., Stone, R.L., Mangala, L.S., Han, H.D., Kim, H.S., Farley, D., et al. (2011). Dopamine blocks stress-mediated ovarian carcinoma growth. Clin. Cancer Res. *17*, 3649–3659.

Moreno-Smith, M., Lee, S.J., Lu, C., Nagaraja, A.S., He, G., Rupaimoole, R., Han, H.D., Jennings, N.B., Roh, J.W., Nishimura, M., et al. (2013). Biologic effects of dopamine on tumor vasculature in ovarian carcinoma. Neoplasia *15*, 502–510.

Morgan, T.H. (1901). Regeneration and liability to injury. Science *14*, 235–248.

Mullen, L.M., Bryant, S.V., Torok, M.A., Blumberg, B., and Gardiner, D.M. (1996). Nerve dependency of regeneration: the role of Distal-less and FGF signaling in amphibian limb regeneration. Development *122*, 3487–3497.

Nacu, E., Gromberg, E., Oliveira, C.R., Drechsel, D., and Tanaka, E.M. (2016). FGF8 and SHH substitute for anterior-posterior tissue interactions to induce limb regeneration. Nature *533*, 407–410.

Nagaraja, A.S., Sadaoui, N.C., Lutgendorf, S.K., Ramondetta, L.M., and Sood, A.K. (2013). Beta-blockers: a new role in cancer chemotherapy? Expert Opin. Investig. Drugs *22*, 1359–1363.

Nagaraja, A.S., Dorniak, P.L., Sadaoui, N.C., Kang, Y., Lin, T., Armaiz-Pena, G., Wu, S.Y., Rupaimoole, R., Allen, J.K., Gharpure, K.M., et al. (2016). Sustained adrenergic signaling leads to increased metastasis in ovarian cancer via increased PGE2 synthesis. Oncogene *35*, 2390–2397.

Nedvetsky, P.I., Emmerson, E., Finley, J.K., Ettinger, A., Cruz-Pacheco, N., Prochazka, J., Haddox, C.L., Northrup, E., Hodges, C., Mostov, K.E., et al.

(2014). Parasympathetic innervation regulates tubulogenesis in the developing salivary gland. Developmental Cell *30*, 449–462.

Noy, R., and Pollard, J.W. (2014). Tumor-associated macrophages: from mechanisms to therapy. Immunity *41*, 49–61.

Okugawa, Y., Tanaka, K., Inoue, Y., Kawamura, M., Kawamoto, A., Hiro, J., Saigusa, S., Toiyama, Y., Ohi, M., Uchida, K., et al. (2013). Brain-derived neurotrophic factor/tropomyosin-related kinase B pathway in gastric cancer. Br. J. Cancer *108*, 121–130.

Olar, A., He, D., Florentin, D., Ding, Y., and Ayala, G. (2014). Biologic correlates and significance of axonogenesis in prostate cancer. Hum. Pathol. *45*, 1358–1364.

Pawlowski, A., and Weddell, G. (1967). Induction of tumours in denervated skin. Nature, 1234–1236.

Peterson, S.C., Eberl, M., Vagnozzi, A.N., Belkadi, A., Veniaminova, N.A., Verhaegen, M.E., Bichakjian, C.K., Ward, N.L., Dlugosz, A.A., and Wong, S.Y. (2015). Basal cell carcinoma preferentially arises from stem cells within hair follicle and mechanosensory niches. Cell Stem Cell *16*, 400–412.

Petrie, T.A., Strand, N.S., Yang, C.T., Rabinowitz, J.S., and Moon, R.T. (2014). Macrophages modulate adult zebrafish tail fin regeneration. Development *141*, 2581–2591.

Pundavela, J., Demont, Y., Jobling, P., Lincz, L.F., Roselli, S., Thorne, R.F., Bond, D., Bradshaw, R.A., Walker, M.M., and Hondermarck, H. (2014). ProNGF correlates with Gleason score and is a potential driver of nerve infiltration in prostate cancer. Am. J. Pathol. *184*, 3156–3162.

Pundavela, J., Roselli, S., Faulkner, S., Attia, J., Scott, R.J., Thorne, R.F., Forbes, J.F., Bradshaw, R.A., Walker, M.M., Jobling, P., and Hondermarck, H. (2015). Nerve fibers infiltrate the tumor microenvironment and are associated with nerve growth factor production and lymph node invasion in breast cancer. Mol. Oncol. *9*, 1626–1635.

Rageh, M.A., Mendenhall, L., Moussad, E.E., Abbey, S.E., Mescher, A.L., and Tassava, R.A. (2002). Vasculature in pre-blastema and nerve-dependent blastema stages of regenerating forelimbs of the adult newt, *Notophthalmus viridescens*. J. Exp. Zool. *292*, 255–266.

Raimondi, S., Botteri, E., Munzone, E., Cipolla, C., Rotmensz, N., DeCensi, A., and Gandini, S. (2016). Use of beta-blockers, angiotensin-converting enzyme inhibitors and angiotensin receptor blockers and breast cancer survival: systematic review and meta-analysis. Int. J. Cancer *139*, 212–219.

Raju, B., Haug, S.R., Ibrahim, S.O., and Heyeraas, K.J. (2007). Sympathectomy decreases size and invasiveness of tongue cancer in rats. Neuroscience *149*, 715–725.

Rathbone, M.P., Petri, J., Choo, A.F., Logan, D.M., Carlone, R.L., and Foret, J.E. (1980). Noradrenaline and cyclic AMP-independent growth stimulation in newt limb blastemata. Nature *283*, 387–388.

Rinkevich, Y., Lindau, P., Ueno, H., Longaker, M.T., and Weissman, I.L. (2011). Germ-layer and lineage-restricted stem/progenitors regenerate the mouse digit tip. Nature *476*, 409–413.

Rinkevich, Y., Montoro, D.T., Muhonen, E., Walmsley, G.G., Lo, D., Hasegawa, M., Januszyk, M., Connolly, A.J., Weissman, I.L., and Longaker, M.T. (2014). Clonal analysis reveals nerve-dependent and independent roles on mammalian hind limb tissue maintenance and regeneration. Proc. Natl. Acad. Sci. USA *111*, 9846–9851.

Rolny, C., Capparuccia, L., Casazza, A., Mazzone, M., Vallario, A., Cignetti, A., Medico, E., Carmeliet, P., Comoglio, P.M., and Tamagnone, L. (2008). The tumor suppressor semaphorin 3B triggers a prometastatic program mediated by interleukin 8 and the tumor microenvironment. J. Exp. Med. *205*, 1155–1171.

Rosenberg, A.F., Wolman, M.A., Franzini-Armstrong, C., and Granato, M. (2012). In vivo nerve-macrophage interactions following peripheral nerve injury. J. Neurosci. *32*, 3898–3909.

Saha, S., Aranda, E., Hayakawa, Y., Bhanja, P., Atay, S., Brodin, N.P., Li, J., Asfaha, S., Liu, L., Tailor, Y., et al. (2016). Macrophage-derived extracellular vesicle-packaged WNTs rescue intestinal stem cells and enhance survival after radiation injury. Nat. Commun. *7*, 13096.

Saloman, J.L., Albers, K.M., Li, D., Hartman, D.J., Crawford, H.C., Muha, E.A., Rhim, A.D., and Davis, B.M. (2016). Ablation of sensory neurons in a genetic model of pancreatic ductal adenocarcinoma slows initiation and progression of cancer. Proc. Natl. Acad. Sci. USA *113*, 3078–3083.

Sandoval-Guzman, T., Wang, H., Khattak, S., Schuez, M., Roensch, K., Nacu, E., Tazaki, A., Joven, A., Tanaka, E.M., and Simon, A. (2014). Fundamental differences in dedifferentiation and stem cell recruitment during skeletal muscle regeneration in two salamander species. Cell Stem Cell *14*, 174–187.

Satoh, A., Cummings, G.M., Bryant, S.V., and Gardiner, D.M. (2010). Neurotrophic regulation of fibroblast dedifferentiation during limb skeletal regeneration in the axolotl (*Ambystoma mexicanum*). Dev. Biol. *337*, 444–457.

Satoh, A., Bryant, S.V., and Gardiner, D.M. (2012). Nerve signaling regulates basal keratinocyte proliferation in the blastema apical epithelial cap in the axolotl (*Ambystoma mexicanum*). Dev. Biol. *366*, 374–381.

Satoh, A., Makanae, A., Nishimoto, Y., and Mitogawa, K. (2016). FGF and BMP derived from dorsal root ganglia regulate blastema induction in limb regeneration in *Ambystoma mexicanum*. Dev. Biol. *417*, 114–125.

Singer, M. (1947). The nervous system and regeneration of the forelimb of adult Triturus; the relation between number of nerve fibers and surface area of amputation. J. Exp. Zool. *104*, 251–265.

Sloan, E.K., Priceman, S.J., Cox, B.F., Yu, S., Pimentel, M.A., Tangkanangnukul, V., Arevalo, J.M., Morizono, K., Karanikolas, B.D., Wu, L., et al. (2010). The sympathetic nervous system induces a metastatic switch in primary breast cancer. Cancer Res. *70*, 7042–7052.

Smith, P.G., and Liu, M. (2002). Impaired cutaneous wound healing after sensory denervation in developing rats: effects on cell proliferation and apoptosis. Cell Tissue Res. *307*, 281–291.

Smith, M.J., Globus, M., and Vethamany-Globus, S. (1995). Nerve extracts and substance P activate the phosphatidylinositol signaling pathway and mitogenesis in newt forelimb regenerates. Dev. Biol. *167*, 239–251.

Soo, K.C., Carter, R.L., O'Brien, C.J., Barr, L., Bliss, J.M., and Shaw, H.J. (1986). Prognostic implications of perineural spread in squamous carcinomas of the head and neck. Laryngoscope *96*, 1145–1148.

Stopczynski, R.E., Normolle, D.P., Hartman, D.J., Ying, H., DeBerry, J.J., Bielefeldt, K., Rhim, A.D., DePinho, R.A., Albers, K.M., and Davis, B.M. (2014). Neuroplastic changes occur early in the development of pancreatic ductal adenocarcinoma. Cancer Res. *74*, 1718–1727.

Takeo, M., Chou, W.C., Sun, Q., Lee, W., Rabbani, P., Loomis, C., Taketo, M.M., and Ito, M. (2013). Wnt activation in nail epithelium couples nail growth to digit regeneration. Nature *499*, 228–232.

Tang, H., Wei, P., Duell, E.J., Risch, H.A., Olson, S.H., Bueno-de-Mesquita, H.B., Gallinger, S., Holly, E.A., Petersen, G., Bracci, P.M., et al. (2014). Axonal guidance signaling pathway interacting with smoking in modifying the risk of pancreatic cancer: a gene- and pathway-based interaction analysis of GWAS data. Carcinogenesis *35*, 1039–1045.

Thorimbert, V., Konig, D., Marro, J., Ruggiero, F., and Jazwinska, A. (2015). Bone morphogenetic protein signaling promotes morphogenesis of blood vessels, wound epidermis, and actinotrichia during fin regeneration in zebrafish. FASEB J. *29*, 4299–4312.

Todd, T.J. (1823). On the process of reproduction of the members of the aquatic salamander. Q. J. Sci. Lit. Arts *16*, 84–96.

Tomellini, E., Touil, Y., Lagadec, C., Julien, S., Ostyn, P., Ziental-Gelus, N., Meignan, S., Lengrand, J., Adriaenssens, E., Polakowska, R., and Le Bourhis, X. (2015). Nerve growth factor and proNGF simultaneously promote symmetric self-renewal, quiescence, and epithelial to mesenchymal transition to enlarge the breast cancer stem cell compartment. Stem Cells *33*, 342–353.

Tomlinson, B.L., Globus, M., and Vethamany-Globus, S. (1981). Promotion of mitosis in cultured newt limb regenerates by a diffusible nerve factor. In Vitro *17*, 167–172.

Tsuji, T., Satoyoshi, R., Aiba, N., Kubo, T., Yanagihara, K., Maeda, D., Goto, A., Ishikawa, K., Yashiro, M., and Tanaka, M. (2015). Agr2 mediates paracrine effects on stromal fibroblasts that promote invasion by gastric signet-ring carcinoma cells. Cancer Res. *75*, 356–366.

Tu, S., and Johnson, S.L. (2011). Fate restriction in the growing and regenerating zebrafish fin. Dev. Cell *20*, 725–732.

Vaishnavi, A., Capelletti, M., Le, A.T., Kako, S., Butaney, M., Ercan, D., Mahale, S., Davies, K.D., Aisner, D.L., Pilling, A.B., et al. (2013). Oncogenic and drug-sensitive NTRK1 rearrangements in lung cancer. Nat. Med. *19*, 1469–1472.

Vaishnavi, A., Le, A.T., and Doebele, R.C. (2015). TRKing down an old oncogene in a new era of targeted therapy. Cancer Discov. *5*, 25–34.

Vanhecke, E., Adriaenssens, E., Verbeke, S., Meignan, S., Germain, E., Berteaux, N., Nurcombe, V., Le Bourhis, X., and Hondermarck, H. (2011). Brain-derived neurotrophic factor and neurotrophin-4/5 are expressed in breast cancer and can be targeted to inhibit tumor cell survival. Clin. Cancer Res. *17*, 1741–1752.

Wang, L., Marchionni, M.A., and Tassava, R.A. (2000). Cloning and neuronal expression of a type III newt neuregulin and rescue of denervated, nerve-dependent newt limb blastemas by rhGGF2. J. Neurobiol. *43*, 150–158.

Wang, K., Demir, I.E., D'Haese, J.G., Tieftrunk, E., Kujundzic, K., Schorn, S., Xing, B., Kehl, T., Friess, H., and Ceyhan, G.O. (2014). The neurotrophic factor neurturin contributes toward an aggressive cancer cell phenotype, neuropathic pain and neuronal plasticity in pancreatic cancer. Carcinogenesis *35*, 103–113.

Watkins, J.L., Thaker, P.H., Nick, A.M., Ramondetta, L.M., Kumar, S., Urbauer, D.L., Matsuo, K., Squires, K.C., Coleman, R.L., Lutgendorf, S.K., et al. (2015). Clinical impact of selective and nonselective beta-blockers on survival in patients with ovarian cancer. Cancer *121*, 3444–3451.

Weberpals, J., Jansen, L., Carr, P.R., Hoffmeister, M., and Brenner, H. (2016). Beta blockers and cancer prognosis - the role of immortal time bias: a systematic review and meta-analysis. Cancer Treat. Rev. *47*, 1–11.

Xiao, Y., Thoresen, D.T., Williams, J.S., Wang, C., Perna, J., Petrova, R., and Brownell, I. (2015). Neural Hedgehog signaling maintains stem cell renewal in the sensory touch dome epithelium. Proc. Natl. Acad. Sci. USA *112*, 7195–7200.

Yamazaki, S., Ema, H., Karlsson, G., Yamaguchi, T., Miyoshi, H., Shioda, S., Taketo, M.M., Karlsson, S., Iwama, A., and Nakauchi, H. (2011). Nonmyelinating Schwann cells maintain hematopoietic stem cell hibernation in the bone marrow niche. Cell *147*, 1146–1158.

Yazawa, S., Umesono, Y., Hayashi, T., Tarui, H., and Agata, K. (2009). Planarian Hedgehog/Patched establishes anterior-posterior polarity by regulating Wnt signaling. Proc. Natl. Acad. Sci. USA *106*, 22329–22334.

Yin, V.P., and Poss, K.D. (2008). New regulators of vertebrate appendage regeneration. Curr. Opin. Genet. Dev. *18*, 381–386.

Yin, Y., Cui, Q., Li, Y., Irwin, N., Fischer, D., Harvey, A.R., and Benowitz, L.I. (2003). Macrophage-derived factors stimulate optic nerve regeneration. J. Neurosci. *23*, 2284–2293.

Zenjari, C., Boilly, B., Hondermarck, H., and Boilly-Marer, Y. (1997). Nerve-blastema interactions induce fibroblast growth factor-1 release during limb regeneration in *Pleurodeles waltl*. Dev. Growth Differ. *39*, 15–22.

Zhang, D., Park, D., Zhong, Y., Lu, Y., Rycaj, K., Gong, S., Chen, X., Liu, X., Chao, H.P., Whitney, P., et al. (2016a). Stem cell and neurogenic gene-expression profiles link prostate basal cells to aggressive prostate cancer. Nat. Commun. *7*, 10798.

Zhang, J., Jin, Y., Xu, S., Zheng, J., Zhang, Q.I., Wang, Y., Chen, J., Huang, Y., He, X., and Zhao, Z. (2016b). AGR2 is associated with gastric cancer progression and poor survival. Oncol. Lett. *11*, 2075–2083.

Zhao, C.M., Hayakawa, Y., Kodama, Y., Muthupalani, S., Westphalen, C.B., Andersen, G.T., Flatberg, A., Johannessen, H., Friedman, R.A., Renz, B.W., et al. (2014). Denervation suppresses gastric tumorigenesis. Sci. Transl. Med. *6*, 250ra115.

Zhou, W.J., Geng, Z.H., Spence, J.R., and Geng, J.G. (2013). Induction of intestinal stem cells by R-spondin 1 and Slit2 augments chemoradioprotection. Nature *501*, 107–111.

2.2 Neurotrophin family of growth factors and receptors

Neurotrophins (NTs) are a cluster of largely conserved polypeptide growth factors that are important regulators of neuronal growth, survival and differentiation [1, 2]. In humans, this group of proteins consists of four neurotrophic factors: nerve growth factor (NGF), brain-derived neurotrophic factor (BDNF), neurotrophin-3 (NT-3) and neurotrophin-4/5 (NT-4/5) [3]. Each of the NTs and their corresponding precursors (proNGF, proBDNF, proNT-3 and proNT-4/5) arise from the same gene and mRNA sequence, resulting in an array of shared characteristics between pro and mature form [4]. All proNTs have a molecular weight (MW) of approximately 26 kilodaltons (kDa) and are comprised of the mature NT (approximately 13 kDa) joined to the N-terminus of the pro-peptide sequence [5]. NTs are manufactured through the proteolytic maturation of their precursors, a process which begins in the endoplasmic reticulum (ER) and involves the segregation of pre-proNTs from their signal peptide into the proNTs. The sequestered proNTs are then subjected to a range of cleaving mechanisms at dibasic amino acid sites, either intracellularly (via furin) or extracellularly (via metalloproteases or plasmin), resulting in the formation of mature NTs [6-8].

Mature NTs, which exist as non-covalently associated homodimers, induce neuronal responses by interacting with two distinct classes of cell membrane receptors: $p75^{NTR}$ (**n**euro**t**rophin **r**eceptor), of the tumour necrosis factor receptor superfamily, and the Trk (tropomyosin-related kinase, also named NTRK1) family of receptor tyrosine kinases **(Figure 1)** [9]. Up until recently, proNTs were thought of as purely a source used for the production of mature NTs, however what has now been revealed is that they do indeed have a distinct functional role [10]. Lee et al. determined that proNTs promote neuronal apoptosis, in comparison to their mature counterparts, which induce survival and differentiation [6]. Following this discovery, Nykjaer et al. identified a receptor capable of binding to all proNTs, namely sortilin **(Figure 1)** [11, 12]. Activation of a complex between $p75^{NTR}$/sortilin regulates a pro-apoptotic effect on neurons, usually taking place during neuronal development and aging, and involves the inhibition of the RAC

(Rho GTPase) pathway [13]. Conversely, an interaction between sortilin and the Trk receptors enhances axonal transport and neurotrophin signalling via the activation of the MAPK pathway, as well as phosphatidylinositol 3-kinase and phospholipase C-γ1 signalling [14].

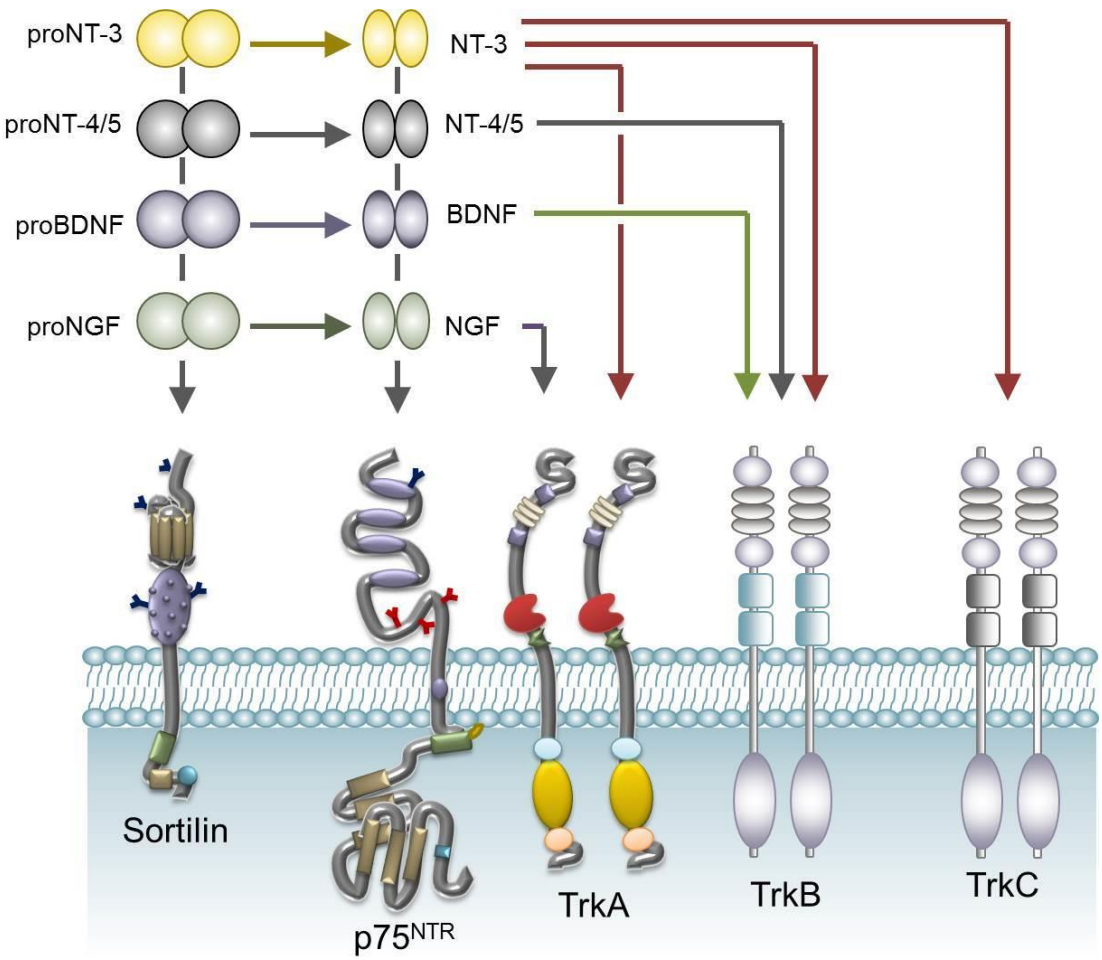

Figure 1 | Binding of neurotrophins and pro-neurotrophins to their receptors. NGF, BDNF, NT-3, NT-4/5 in addition to their respective precursor proteins (proNGF, proBDNF, proNT, proNT-4/5) all bind to p75NTR with approximate equal affinity whereas Trk receptors (TrkA, TrkB, TrkC) bind neurotrophins with different specificities. Sortilin only binds to the pro-neurotrophins. Adapted from Bradshaw et al. 2014 [15].

Importantly, It has been shown that NTs and their precursors are also capable of inducing a variety of non-neuronal responses in healthy and diseased tissue [1]. This is due not only to the existence of proNTs, NTs and their receptors in areas outside of the nervous system, but also as a result of the intracellular signalling

controlled by their specific receptors being very important to downstream pathways controlling the survival, proliferations and differentiation of cells [5].

2.2.1 Nerve growth factor (NGF)

NGF is a 13.5 kDa monomer crucial to the development of the sympathetic and sensory neurons [16]. NGF carries out its neurotrophic activity via the establishment of a trimeric complex with TrkA and $p75^{NTR}$, which induces downstream signalling pathways critical for the survival and differentiation of central and peripheral neurons [17]. NGF facilitates connections between the nervous system and peripheral organ sites during embryogenesis and post-natal development. More specifically, NGF is manufactured and secreted by organs which need to be innervated, in order to attract nerve fibres into them. Once these connections have been well-established during development, then the foremost peripheral effect of NGF in the adult is indeed the promotion of pain [18], where inhibition of NGF and its receptor TrkA, which happens to be a nociceptor, have substantial analgesic effects [19]. In particular, anti-NGF blocking antibodies have entered clinical trials for the treatment of chronic rheumatoid and back pain [20, 21]. More recently, neurotrophic factors such as NGF have been implicated in tumour neoneurogenesis [22], which will be discussed in more detail throughout the forthcoming pages of this thesis.

2.2.2 Structure and function of proNGF

ProNGF is a 25 kDa protein comprised of the mature NGF polypeptide (13.5 kDa) in combination with an inactive pro-segment (11.5 kDa) in N-term **(Figure 2)** [6]. In addition to being a reservoir for the production of NGF, proNGF has recently been rendered capable of eliciting its own biological effects, independent to pathways of survival and differentiation mediated by NGF, as it can bypass the cleaving processes that follow its synthesis and release **(Figure 2)** [9, 23]. The role of proNGF in the nervous system is multifunctional, having both neurotrophic and pro-apoptotic activities reported **(Figure 3)** [24]. For inducing its pro-apoptotic effect on neurons, the proNGF protein binds to and forms a trimeric complex with the $p75^{NTR}$ and sortilin receptors, resulting in the inhibition of the RAC (Rho GTPase) pathway **(Figure 3)** [3, 11]. Sortilin is a 95-kDa plasma trans-membrane receptor that has the ability to bind the pro-segment of proNGF [25, 26]. However, opposing studies have also described proNGF in terms of having

neurotrophic activities, by stimulating the survival and differentiation of neurons via interactions with a complex of TrkA and p75^{NTR}, resulting in the downstream activation of the mitogen-activated protein kinase (MAPK) pathway **(Figure 3)** [27]. In the CNS, proNGF has been reported as being more abundant than mature NGF, where it is capable of exhibiting similar neurotrophic activity [28]. It has been suggested that proNGF induces neurotrophic or apoptotic activities based on the relative levels of its receptors, p75^{NTR} and TrkA, as well tissue type [29]. More specifically, proNGF promotes apoptotic activity in cases of injury where p75^{NTR} is dominant [30-32], whereas proNGF overexpression is neurotrophic in undamaged tissue containing a higher proportion of TrkA [33]. Even though the bulk of ligand-receptor binding for proNGF is carried out through both p75^{NTR} and sortilin, TrkA phosphorylation, as a result of receptor stimulation by proNGF, has also been identified and the downstream signalling reported, primarily through activation of the MAPK pathway [34]. As a result, proNGF is not only categorized as a reservoir for the mature NGF protein, but also as an active agent produced from the *NGF* gene that can exert a range of distinct biological effects.

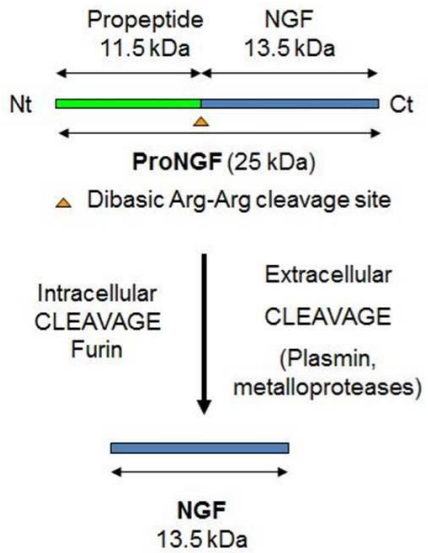

Figure 2 | Structure of proNGF and NGF. NGF is synthesized as a 25-kDa precursor protein, termed proNGF, that yields the mature NGF polypeptide of 13.5-kDa and an inactive pro segment of 11.5-kDa. Cleavage of the pro-peptide from the N-terminus occurs intracellularly by furin, or extracellularly by pro-convertases.

2.2.3 Structural and functional characteristics of receptors for proNGF

ProNGF is capable of binding to and activating a complex between sortilin with that of either p75^{NTR} and TrkA, resulting in a variety of downstream signalling cascades. [34]. The stimulation of p75^{NTR} results in the activation of c-Jun N-terminal Kinase (JNK) and nuclear factor-κB (NFkB), whereas TrkA primarily

activates Ras, Rac, ERKs, phosphatidylinositol 3-kinase, phospholipase C-γ1 signalling, as well as their downstream effectors [1]. Although the receptors for proNGF have a tight association with one another, their structures, activations and biological impacts are quite distinct and are presented below.

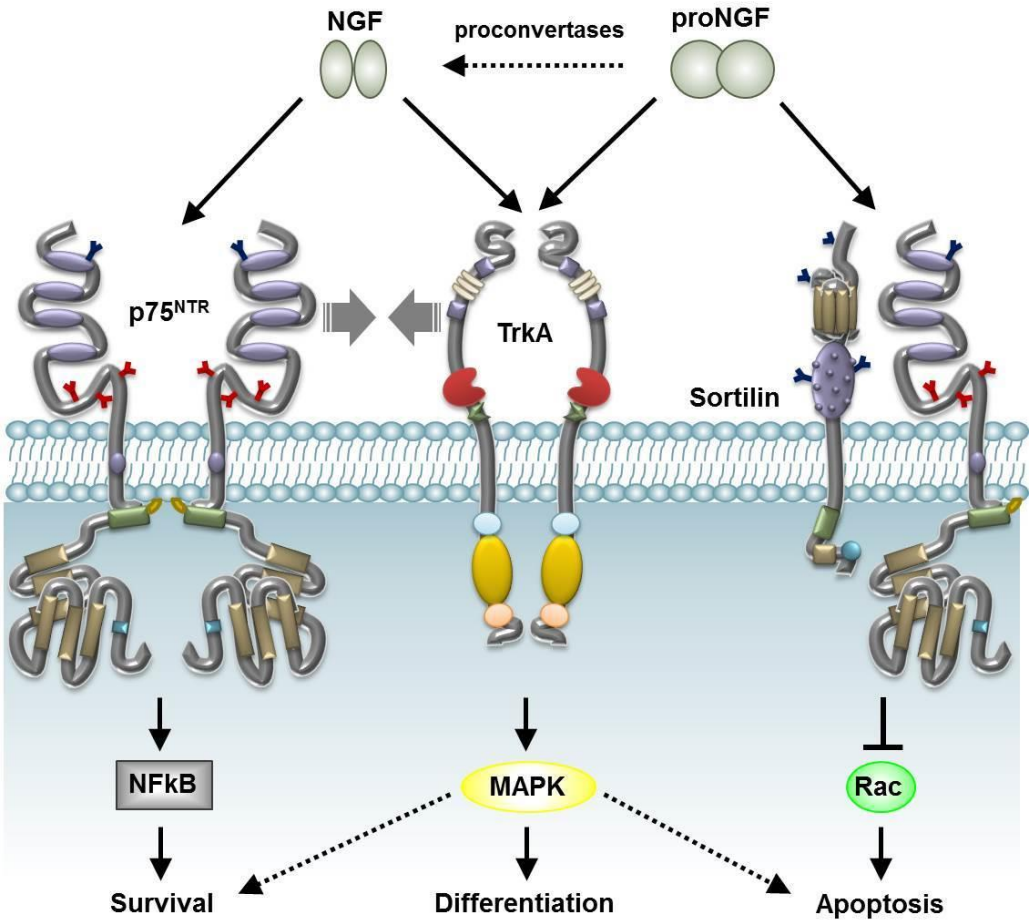

Figure 3 | Biological function of proNGF and NGF in neurons. ProNGF induces neuron apoptosis via the activation of a complex between $p75^{NTR}$ and sortilin. NGF promotes neuron survival and differentiation through the TrkA and $p75^{NTR}$ receptors. In some models, proNGF has been reported to induce differentiation of neurons via interactions with a complex of TrkA and $p75^{NTR}$ [29]. This illustrates the diversity of these proteins with respect to their biological effects. Adapted from Bradshaw et al. 2014 [15]

2.2.4 P75^{NTR} (p75 neurotrophin receptor)

P75^{NTR} is the common receptor to all neurotrophins and pro-neurotrophins. It was first identified as the receptor for NGF and was logically called NGFR [35], however, subsequent studies revealed that all pro/neurotrophins were ligands for this particular receptor, thus it was renamed p75^{NTR} [36-38]. P75^{NTR} is a 75 kDa, type I receptor **(Figure 4)** member of the superfamily of TNF (tumour necrosis factor) receptors [17, 39]. The extracellular domain is involved in membrane targeting, conformation and ligand binding [40] and contains four cysteine-rich domains (CRDs) **(Figure 4)** [41-43]. An essential characteristic of the intracellular part of p75^{NTR} is the presence of 5 death domains (DD) **(Figure 4)** [41] and it is classified it as a type II DD receptor associated with activating the caspase pathway and regulating apoptosis [44]. This notably involves the activation of the NF-kB transcription factor [1]. Initial 3D analysis of p75^{NTR} structure and binding to NGF/proNGF indicated a ligand-receptor interaction with an asymmetrical ratio of 2:1, in which homodimeric proNGF binds to a single p75^{NTR} [45]. In contrast, a recent model including the extracellular domain of an N-glycosylated p75^{NTR} showed a 2:2 complex ratio, with proNGF homodimer binding to a dimeric p75^{NTR} [46]. In this latest hypothesis, a S-S bridge is formed between two p75^{NTR} molecules in the transmembrane region [40].

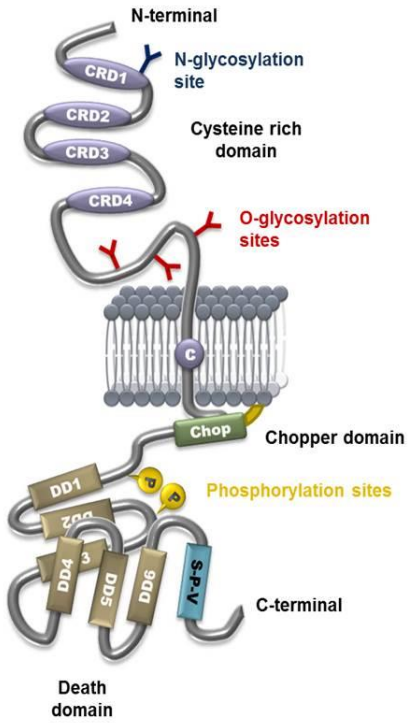

Figure 4 | The neurotrophin receptor p75^{NTR}. P75^{NTR} is made of an extracellular 'cysteine rich' domain (CRD), containing four repeated cysteine residues. The transmembrane domain includes one cysteine that is involved in signal transduction. The intracellular domain, made up of a Chopper domain and 5 death domains (DD), plays a role in the regulation of post-translational modifications (PTMs), and in particular O-glycosylation, cleavage, protein interactions and activation of downstream signaling [44]. Adapted from Hondermarck et al. 2015 [47].

2.2.5 Sortilin receptor

Sortilin is a 95 kDa member of the family of Vps (Vacuolar protein sorting) 10p-domain receptor found predominantly in the brain, spinal cord and muscles [48, 49]. It was originally discovered as the neurotensin receptor [50] but it was later found as being a co-receptor for proNGF and other pro-neurotrophins [11, 51]. ProNGF does not bind and elicit a response in $p75^{NTR}$ without the presence of sortilin. Sortilin is co-receptor for proNGF and mediator of interaction with $p75^{NTR}$ [11]. Once its signal peptide of 33 aa is released, sortilin is a protein of 798 aa with an N-glycosylation [52, 53] **(Figure 5)** [54]. Sortilin interacts with all pro-neurotrophins, and its interaction with proNGF has been more particularly described. Nykjaer et al. have shown that proNGF binds to sortilin with high affinity (kd of 5 nM), while NGF has only a low affinity for this receptor (kd of 87 nM) [13]. Sortilin signal transduction is solely dependent on the specific interaction it has with a variety of its co-receptors. Sortilin/$p75^{NTR}$ promotes the c-Jun N-terminal kinase (JNK) 3 and caspases 3, 6 and 9 pathways, leading to neuronal apoptosis [13]. Conversely, sortilin may associate with TrkA, leading to an anterograde axonal transport and expression of TrkA on the plasma membrane. This increased receptor expression results in enhanced NT signalling, and thus cell survival, via activation of the the PLCγ, Akt and Ras pathways [13].

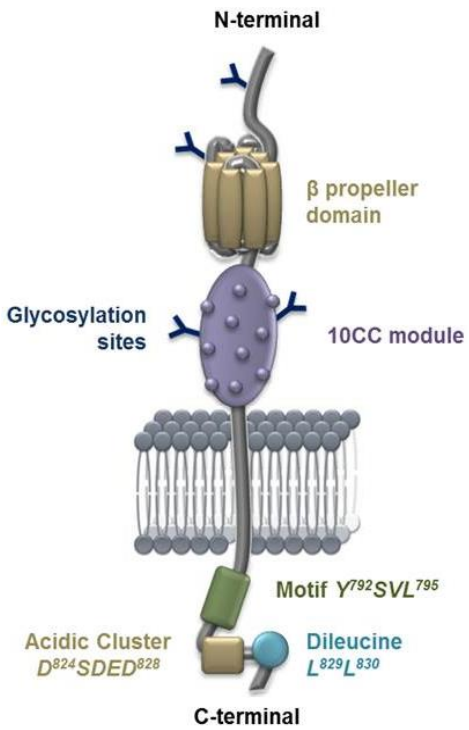

Figure 5 | Structure of the sortilin receptor. Sortilin is made up of one transmembrane domain, a cytosolic tail and a long extracellular domain. Its VPS10P domain (~700 aa) composes its N-terminus, and is essential to ligand binding. It is made of 10 conserved cysteine residues establishing five disulfide bounds, as well as a β propeller domain. The intracellular domain is composed of sequences implicated in its internalization and intracellular traffic: the $Y^{792}SVL^{795}$ motif, the $D^{824}SDED^{828}$ acidic cluster and the di-leucine $L^{829}L^{830}$ domain. Adapted from Hondermarck et al. 2015 [47].

2.2.6 TrkA receptor

Tropomyosin related kinase A (TrkA) is a tyrosine kinase receptor with a molecular weight of around 140 kDa **(Figure 6)**. The extracellular domain, which is glycosylated, controls the dimerization, whereas the intracellular domain presents several tyrosines, which can eventually be phosphorylated **(Figure 6)**. TrkA was originally described as a tyrosine kinase protein associated with tropomyosin A, for which NGF was identified as its ligand [55]. Binding between proNGF and the TrkA receptor is disputed. ProNGF induces the death of sympathetic neurons by binding to sortilin and $p75^{NTR}$ without the activation TrkA [6]. However, other groups have shown that proNGF is co-immunoprecipitated with TrkA in sympathetic neurons and PC12 cells and that it enables neuritogenesis (and not apoptosis), though with lower efficacy than NGF [28]. Structural analyses have shown that TrkA binds to proNGF with less affinity than NGF [11]. The masking of tryptophan by the pro-peptide of proNGF seems to reduce its association with TrkA as compared to NGF [56-58]. Furthermore, Al-Shawi et al. [24] demonstrated that neurons from young rodents respond to proNGF by increasing survival and neuritogenesis, and neurons from elderly rodents die by apoptosis upon stimulation by proNGF. Also, work by Masoudi et al has shown that proNGF can activate phosphorylation of TrkA and underlying MAPKs, leading to neuronal survival and differentiation, although to a lesser extent than NGF [29]. Ultimately, it seems that proNGF is a weak ligand for TrkA and that the stoichiometry of the various receptors, including $p75^{NTR}$ and sortilin, controls the interaction of proNGF with TrkA and the observed antagonistic biological effects (apoptosis vs. neuronal outgrowth). These observations explain why proNGF is reported to be neurotoxic or neurotrophic, depending on the study.

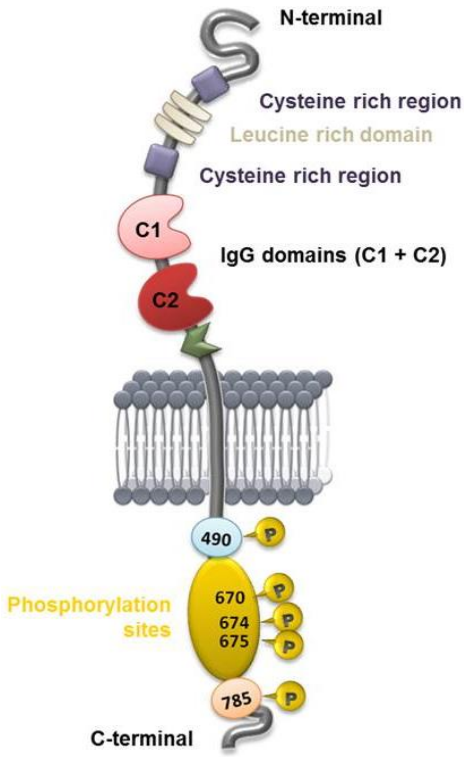

Figure 6 | Diagrammatic representation of tropomyosin related kinase A (TrkA). TrkA is composed of a transmembrane, glycosylated, type I protein of approximately 800 aa. The extracellular domain comprise a leucine rich domain with two cysteine rich regions, two immunoglobulin domains (C1-C2) and an insert (green) that increases the specificity of TrkA for its ligands. The intracellular domain presents a tyrosine kinase domain that transautophosphorylates upon stimulation of TrkA [58, 59]. Adapted from Hondermarck et al. 2015 [47].

2.3 NGF, proNGF and their receptors in cancer

It has been suggested that proNTs, NTs and their receptors play a role in cancer, however to date the majority of studies into this family of growth factors and receptors have been in relation to the nervous system [3]. Mature NGF, prior to its discovery and sequencing, was first identified as a factor secreted by proliferating tissue, in particular by murine sarcomas, which is capable of enhancing the growth and attraction of nerve fibres [60]. There is also preclinical evidence in animal models showing that NGF inhibition leads to a decrease in pain, particularly in breast and prostate cancers [61, 62]. Studies that have demonstrated that NGF and proNGF are involved in cancers are detailed below.

2.3.1 Breast cancer

In breast cancer, there has been many reports showing that targeting NTs and their receptors in a preclinical setting results in the inhibition of breast cancer cell growth and features of aggressiveness, such as migration and invasion [5]. Descamps et al. were the first group to describe an active role for NGF in stimulating the proliferation of a series of breast tumour-derived cancer cell lines, as compared with normal human breast epithelial cells [63]. This was mediated

by NGF binding to its receptor TrkA, leading to the downstream activation of MAPKs **(Figure 7)**. Subsequent studies further elucidated the role of $p75^{NTR}$, for which NGF binding results in the downstream TRADD mediated activation of NF-kB, leading to enhanced cell survival **(Figure 7)** [64, 65]. The synthesis and secretion of NGF by breast cancer cells also underpins the presence of a positive autocrine feedback loop, involving the dual activation of both TrkA and $p75^{NTR}$ [66]. Furthermore, inhibiting components of this pathway in a preclinical animal model resulted in a reduction in tumour growth, further sparking interest in the potential utility of NGF and its receptors as targets for therapeutic intervention [67]. A separate study by Lagadec et al. reinforced the emerging importance of the NGF/TrkA axis in breast cancer progression [68]. TrkA, as well as its active counterpart phospho-TrkA, were both overexpressed in a series of breast carcinomas as compared with normal breast tissue. Following on, stable overexpression and constitutive activation of TrkA in a breast cancer cell line resulted in enhanced cell growth, migration and invasion, mediated by the downstream activation of PI3K-Akt and ERK-p38 MAPK. These *in vitro* discoveries were emulated *in vivo* using a murine xenograft model, in which TrkA overexpression promoted growth, angiogenesis, as well as metastasis, primarily to the lung, of the tumours [68]. These findings were further explored by the group in a subsequent article, which revealed that the protein Ku86, which is involved in repairing DNA double stranded breaks [69], was not only found to be increased in TrkA overexpressing breast cancer cells, but was vital for the observed TrkA mediated stimulation of invasion [70].

Similarly, to that of mature NGF, ProNGF is secreted by breast tumour cells and can act in an autocrine manner to significantly impact tumour cell growth and metastasis through various signalling pathways [16]. More specifically, proNGF stimulates the migration/invasion of breast cancer cells through an autocrine loop which is mediated by the receptors TrkA and sortilin **(Figure 7)**. This signalling pathway requires the phosphorylation of TrkA as well as the activation of Src and Akt, but not the MAP-kinases. Moreover, in contrast to what has previously been described regarding the biologically active receptors and subsequent downstream pathway activation for proNGF, $p75^{NTR}$ is not involved, which was the first indication or evidence of an active TrkA-sortilin relationship. In addition,

a comparison between proNGF levels and patient clinicopathological parameters, in a series of breast cancer TMAs, revealed a positive correlation with lymph node invasion, suggesting a link to metastasis [16]. A study by Roselli et al. analysed the expression and biological function of sortilin in a large cohort of breast tumours as well as *in vitro* using established breast cancer cell lines [71]. Sortilin was detected in epithelial cells, with increased levels in tumours, as compared to normal breast tissue. Further analysis of the clinicopathological parameters revealed an association between sortilin expression and enhanced lymph node invasion, suggesting a relationship with metastatic potential. Analysis of sortilin expression *in vitro* illustrated that sortilin levels were higher in cancer cell lines as compared to non-tumorigenic breast epithelial cells and that functional assays utilizing siRNA knockdown of sortilin resulted in the inhibition of cancer cell adhesion, migration and invasion [71].

The NGF-proNGF-p75^{NTR} axis has also been linked to breast cancer stem cell (CSC) differentiation, plasticity and self-renewal [72]. More specifically, NGF or proNGF enrich for CSCs in several breast cancer cell lines and p75^{NTR} mediated breast CSC self-renewal, via the regulation of key transcription factors [72]. In addition, the secretion of NGF by breast cancer cells has also been shown to induce nerve infiltration in breast tumours, as described in this thesis, resulting in neuronal outgrowth (axonogenesis or neo-neurogenesis) **(Figure 7)**. Whilst studies of this particular nature are still relatively in their infancy, the hypothesis that NGF, or even its precursor proNGF, may play a role in the crosstalk between the peripheral nervous system and breast tumours warrants further exploration [73]. Angiogenesis is another important factor in the progression of solid tumours. Romon et al. demonstrated that NGF could be an important stimulator for breast cancer angiogenesis whereas proNGF has thus far not been implicated [74]. Consequently, NGF, proNGF and their receptors, TrkA, p75^{NTR} and sortilin, may serve as diagnostic or metastatic biomarkers and as potential therapeutic targets in breast cancer, thus exploration into a variety of different tumour types is warranted.

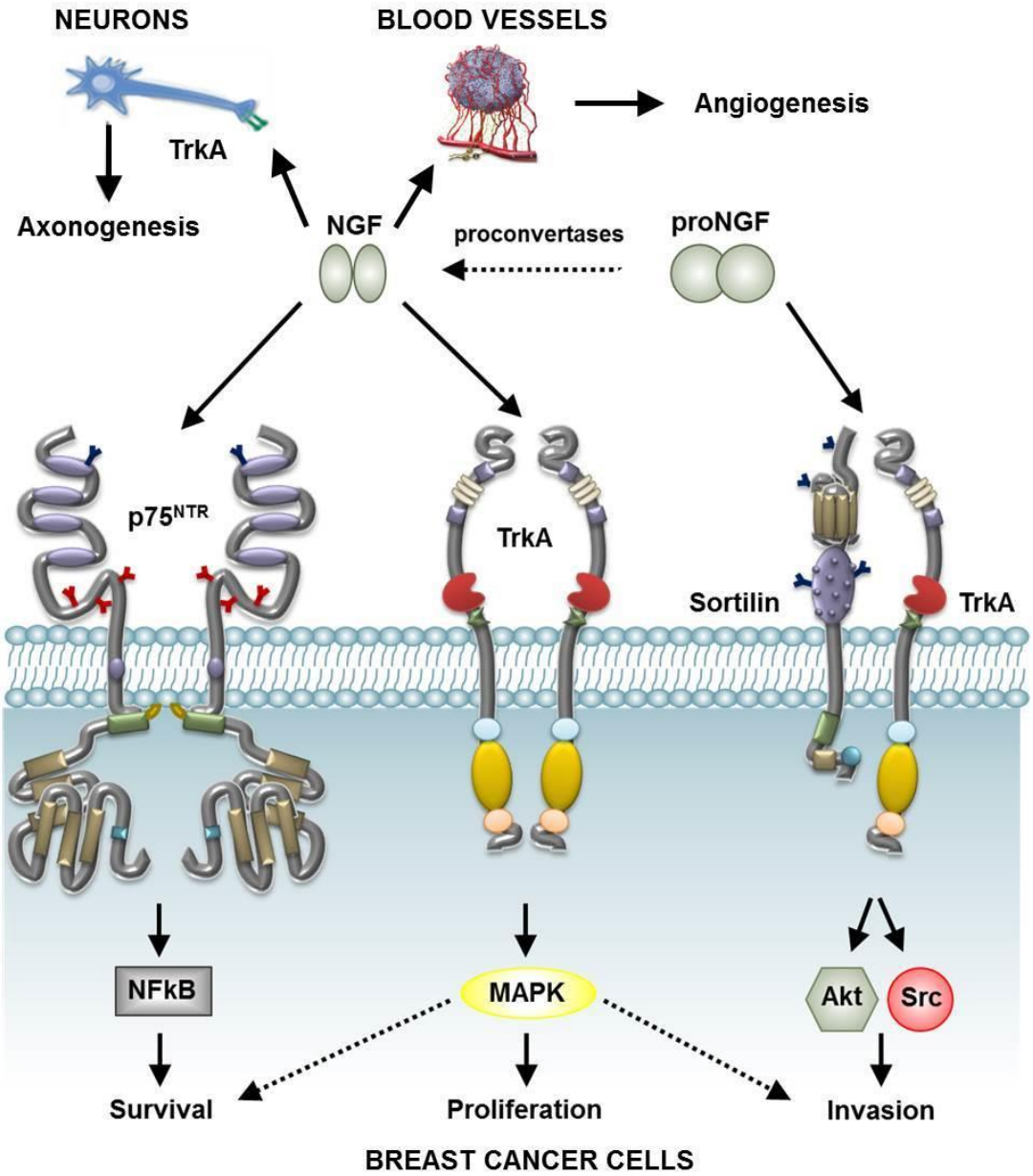

Figure 7 | ProNGF/NGF signaling in breast cancer cells. In breast cancer cells, NGF stimulates TrkA and $p75^{NTR}$ leading to the activation of cell proliferation and survival, respectively. ProNGF binds to a complex TrkA/sortilin to stimulate cancer cell migration and invasion via the activation of Src and Akt. NGF liberation by breast cancer cells may also act on and induce neuron outgrowth of surrounding nerves (axonogenesis or neo-neurogenesis – this Thesis) [73] and/or angiogenesis [74]. Adapted from Bradshaw et al. 2014 [15].

2.3.2 Pancreatic cancer

The expression of NGF in normal pancreatic tissue has been described, where it is thought to contribute to innervation [75]. NGF is expressed in pancreatic vasculature whereas TrkA is found localised within β-cells contained within regions of endocrine tissue known as the islets of Langerhans, where they play

a role in glucose-induced insulin secretion [75]. More specifically, high glucose levels rapidly increase NGF secretion and subsequent TrkA phosphorylation. Conversely, a reduction in NGF or disruption to TrkA signalling results in impaired glucose tolerance and insulin secretion [75]. Thus far however, research into the expression, modulation and role of NGF in pancreatic tumours has been limited. Research carried out in 1999 by Zhu et al. reported high immuno-reactivity of NGF in pancreatic cancer as compared to normal pancreatic tissue in humans [76]. Comparisons between this NGF overexpression with the clinocopathlogical parameters of the patients revealed a positive correlation between NGF immuno-reactivity with that of perineural invasion (PNI), a mechanism by which cancer cells surround and invade nerves, as well as pain sensation [76]. Murine studies also carried out by the same team reported that TrkA stimulation and downstream activation of its signalling pathways significantly enhanced the growth and tumorigenic capacity of pancreatic tumours [77]. Pancreatic neuroplasticity during the development and progression of pancreatic cancer, involving not only increased neural hypertrophy and density, but also alterations to neural subpopulations [78]. More specifically, a crosstalk between the changing neuronal environment with that of pancreatic cancer cells is mediated by the presence or recruitment of a variety of neuronal cells, such as Schwann cells [79], as well as the secretion of neuronal mediators or neuropeptides, which in turn may modulate inflammation and tumour growth [78]. NGF, proNGF and their receptors are one such family of proteins for which their increased expression has been correlated to poor prognosis [80]. Blocking of NGF signalling with neutralising antibodies or direct targeting of NGF, TrkA and $p75^{NTR}$ using siRNA has been shown to inhibit the proliferation of pancreatic cancer cells as well as their ability to migrate towards dorsal root ganglia (DRG), *in vitro [80]*. Furthermore, a recent study has shown that gold nano-cluster delivery of siRNA against NGF effectively downregulated NGF protein expression in animal models, resulting in decreased aggressiveness and tumour progression [81].

The existence of proNGF in pancreatic cancer cells has only been illustrated in one study [82], therefore, its importance as a possible biomarker or candidate for therapeutic intervention has not yet been established. Sortilin has also been shown to play a role in stimulating pancreatic secretions for lipid digestion as well

as a protective agent against for pancreatic beta cells against cytotoxic molecules [83]. However, compelling research carried out by Mijatovic and colleagues has also linked sortilin to the migration of pancreatic cancer cells [84], which could in turn and by association implicate its ligand proNGF.

2.3.3 Melanoma

Melanocytes share a common neuroectodermal origin with that of the nervous system, thus, it is not surprising that they express all NTs [85, 86]. With respect to melanoma, NGF and its receptors were first shown to be expressed in human melanoma cells in the 1970s [87, 88]. For the common NT receptor $p75^{NTR}$, immunostaining was previously described as negative in normal melanocytes and detectable in benign nevi [89], whereas it has since been found to be overexpressed in both desmoplastic and spindle cell melanomas [90-92]. TrkA was also found to be expressed in cases of both primary and metastatic melanoma as well as being associated with poor prognosis [93, 94]. Truzzi et al. demonstrated that NGF is synthesised and secreted by primary and metastatic melanoma cell lines and that its receptors TrkA and $p75^{NTR}$ are also expressed [95]. Targeting TrkA and $p75^{NTR}$, with the inhibitor K252a or transfection with $p75^{NTR}$ siRNA, respectively, inhibited both the proliferation and migration of these melanoma cells, *in vitro [95]*. A previous study demonstrated that proNGF could exert powerful stimulatory effects on the migration of melanoma cells, for which the required concentration is 20 times less than that of its derivative protein, NGF [96]. Truzzi et al. confirmed these findings, from which it was made apparent that proNGF strongly induces motility of melanoma cells [95]. In addition, the same authors observed that normal melanocytes express sortilin, a key receptor for proNGF, at comparably lower levels than in that of cancer cells. Treatment of these normal melanocytes with a known tumour promoter, namely tetradecanoyl phorbol acetate (TPA), leads to the overexpression of sortilin in these cells, suggesting that expression of this receptor may be increased during tumoural transformation. Furthermore, utilising melanoma cells expressing varying levels of sortilin, this study also demonstrated that sortilin expression positively correlates with migratory capacity [95]. More recently, a study by Pasini et al. found an overexpression of the TrkA gene in up to 50% of their cohort of metastatic melanoma cases, which were also correlated with poor clinical

outcome [97]. Surprisingly, induction of the NGF-TrkA signalling cascade in melanoma cell lines, triggering downstream MAPK activity, resulted in oncogene-induced cessation of growth [97]. This may point to a differential role for NGF as compared with proNGF in melanoma.

2.3.4 Prostate and gastric cancer

The mechanisms or agents responsible for stimulating the growth of peripheral neurons into the prostate and gastric tumour microenvironment are yet to be fully elucidated, however, it has been suggested that this neurogenesis, as well as cancer progression, could be mediated by the synthesis and liberation of neurotrophic growth factors [98]. With respect to prostate cancer, Pundavela et al. demonstrated that proNGF is overexpressed, primarily in that of the cytoplasm of cancer cells, in a cohort of 120 human prostate tumour samples [27]. Furthermore, the quantification of proNGF intensity or immunoreactivity within these samples was positively correlated with that of Gleason score [27]. These findings support the very initial observations by Delsite and Djakiew in 1999, which identified the expression of proNGF in human prostatic stromal cells, however, mature NGF was not detected by either group, suggesting a more dominant role for proNGF [27, 99]. Pundavela et al. also determined that prostate cancer cells can induce axonogenesis in two neuronal cell lines (PC-12 and 50B11) via the secretion of proNGF, *in vitro*. Conversely, blocking antibodies directed against proNGF inhibited this observed effect [27]. Until very recently, work carried out looking at the expression and biological function of NGF in gastric cancer has been sparse. Du et al. were one of the first lab groups to demonstrate the expression of NGF and its Trk receptor, using cDNA microarrays, in both normal gastric mucosa and gastric carcinomas [100]. Ahluwalia et al. have also described the expression of NGF and its receptor TrkA in gastric mucosal endothelial cells isolated from rats, where they play a critical role in promoting angiogenesis [101]. Very recently, in a major study, NGF overexpression in gastric epithelial cells, induced by cholinergic stimulation with acetylcholine (ACh), has been linked with expanding enteric nerves, ultimately resulting in enhanced carcinogenesis [102]. More specifically, tuft cells (chemosensory cells) positive for the Doublecortin-like kinase gene (*DCLK1*) and nerves of the stomach are both a rich source of ACh. Cholinergic signalling within

the gastric epithelium, facilitated by the agonist carbachol, was found to promote the overexpression of NGF, in turn altering enteric nerve morphology and enhancing epithelial proliferation and tumorigenesis [102]. Abolition of cholinergic signalling via surgical vagotomy successfully reversed NGF overexpression in gastric tumours. Furthermore, the inhibition of Trk receptor activation, using the small molecule inhibitor PLX-7486, was also capable of supressing the growth of stromal nerves in NGF-overexpressing mice [102]. Overall, this landmark study suggests a role for Trk inhibitors and potentially anti-NGF blocking antibodies for disrupting the role of the ACh-NGF axis in enhancing neuronal growth and tumorigenesis in gastric cancer [102]. These studies further highlight the interplay between proNTs, NTs and their receptors with that of the nervous system, in a range of human cancers, in turn highlighting a compelling target for therapeutic intervention.

CHAPTER 3 | Nerve fibers infiltrate the tumor microenvironment and are associated with nerve growth factor production and lymph node invasion in breast cancer

3.1 Preface

Chapter 3 contains an original research article entitled **"Nerve fibers infiltrate the tumor microenvironment and are associated with nerve growth factor production and lymph node invasion in breast cancer"** which has been published in the journal *Molecular Oncology*. The infiltration and manifestation of nerves within the tumour microenvironment has been previously described for several human cancers, such as the prostate and pancreas, and has been directly correlated with aggressiveness. Breast cancer neurogenesis has also been described, however the data remains fragmentary and the molecular mediators driving this infiltration have not been elucidated. This chapter contains the first demonstration of a NGF-driven nerve infiltration in the microenvironment of breast tumours. More specifically, patients with a higher degree of nerve infiltration had more aggressive cases of disease as well as increased NGF protein expression. Furthermore, *in vitro* analyses of breast cancer cells co-cultured with neuronal-like cell lines elucidated a function role for NGF in this neurotrophic response.

3.2 Publication

MOLECULAR ONCOLOGY 9 (2015) 1626–1635

available at www.sciencedirect.com

ScienceDirect

www.elsevier.com/locate/molonc

Nerve fibers infiltrate the tumor microenvironment and are associated with nerve growth factor production and lymph node invasion in breast cancer

Jay Pundavela[a,b,1], *Severine Roselli*[a,b,1], *Sam Faulkner*[a,b], *John Attia*[b,c], *Rodney J. Scott*[a,b], *Rick F. Thorne*[b], *John F. Forbes*[b,c], *Ralph A. Bradshaw*[d], *Marjorie M. Walker*[b,c], *Phillip Jobling*[a,b,1], *Hubert Hondermarck*[a,b,*,1]

[a]*School of Biomedical Sciences and Pharmacy, Faculty of Health and Medicine, University of Newcastle, Callaghan, NSW 2308, Australia*
[b]*Hunter Medical Research Institute, New Lambton Heights, NSW 2305, Australia*
[c]*School of Medicine and Public Health, Faculty of Health and Medicine, University of Newcastle, Callaghan, NSW 2308, Australia*
[d]*Department of Pharmaceutical Chemistry, University of California, San Francisco, CA 94158, USA*

ARTICLE INFO

Article history:
Received 18 March 2015
Received in revised form
1 May 2015
Accepted 4 May 2015
Available online 14 May 2015

Keywords:
Nerve fibers (axons)
Tumor microenvironment
Nerve growth factor
Breast cancer

ABSTRACT

Infiltration of the tumor microenvironment by nerve fibers is an understudied aspect of breast carcinogenesis. In this study, the presence of nerve fibers was investigated in a cohort of 369 primary breast cancers (ductal carcinomas in situ, invasive ductal and lobular carcinomas) by immunohistochemistry for the neuronal marker PGP9.5. Isolated nerve fibers (axons) were detected in 28% of invasive ductal carcinomas as compared to only 12% of invasive lobular carcinomas and 8% of ductal carcinomas in situ ($p = 0.0003$). In invasive breast cancers, the presence of nerve fibers was observed in 15% of lymph node negative tumors and 28% of lymph node positive tumors ($p = 0.0031$), indicating a relationship with the metastatic potential. In addition, there was an association between the presence of nerve fibers and the expression of nerve growth factor (NGF) in cancer cells ($p = 0.0001$). *In vitro*, breast cancer cells were able to induce neurite outgrowth in PC12 cells, and this neurotrophic activity was partially inhibited by anti-NGF blocking antibodies. In conclusion, infiltration by nerve fibers is a feature of the tumor microenvironment that is associated with aggressiveness and involves NGF production by cancer cells. The potential participation of nerve fibers in breast cancer progression needs to be further considered.

Abbreviations: DCIS, ductal carcinoma in situ; IDC, invasive ductal carcinoma; ILC, invasive lobular carcinoma; EGF, epidermal growth factor; IHC, immunohistochemistry; NGF, nerve growth factor; PGP9.5, protein gene product 9.5; TMA, tumor microarrays.

* *Corresponding author.* School of Biomedical Sciences and Pharmacy, Life Sciences Building (LS3-35), University of Newcastle, Callaghan, NSW 2308, Australia. Tel.: +61 2492 18830; fax: +61 2492 16903.
E-mail address: hubert.hondermarck@newcastle.edu.au (H. Hondermarck).

[1] Contributed equally to this work.

http://dx.doi.org/10.1016/j.molonc.2015.05.001

1. Introduction

The role of the nervous system in cancer etiology, and in particular the influence of nerve fibers in the tumor microenvironment, is an understudied aspect of cancer biology (Ondicova and Mravec, 2010). It is well established that cancer cells can grow around existing nerves and eventually invade them in a process called perineural invasion (Marchesi et al., 2010). This is generally associated with a poor prognosis and can cause pain as demonstrated in pancreatic cancer (Bapat et al., 2011). Conversely, the infiltration of tumors by growing nerves, or tumor axonogenesis, has only recently been suggested to actively participate in cancer progression. Indeed, a recent report (Magnon et al., 2013) has revealed that tumor infiltration by nerve fibers is essential for prostate cancer progression from early initiation to metastasis. The mechanism remains unclear but includes liberation of catecholamines and acetylcholine in the vicinity of cancer cells, resulting in the stimulation of tumor growth and invasion. In addition, another recent study has shown that denervation suppresses gastric tumorigenesis (Zhao et al., 2014a), further pointing to the role of the nervous system in carcinogenesis. These pioneering studies in prostate and gastric cancer suggest a potential value of anti-neurogenic therapies (Jobling et al., 2015) and raise the possibility that tumor infiltration by nerve fibers may also be important in other types of cancer.

In breast cancer, little is known about nerve fibers in the tumor microenvironment. A study in mice has shown that nerve infiltration in bone metastases participates in the stimulation of metastatic growth (Campbell et al., 2012) and recent investigations have evidenced the presence of nerves in human primary breast tumors (Zhao et al., 2014b; Huang et al., 2014). Anatomical and histological studies have shown that the normal breast is innervated by both sympathetic and sensory fibers from the 4–6th thoracic nerves (Sarhadi et al., 1996). Sensory fibers supply the nipple and skin, whereas sympathetic fibers innervate blood vessels and ducts. Therefore, it is conceivable that nerve fibers could be attracted into breast tumors, especially in light of the evidence that breast cancer cells can produce neurotrophic growth factors such as the neurotrophins (Hondermarck, 2012). In particular, nerve growth factor (NGF), which can stimulate the growth of sympathetic and sensory nerves, is produced and secreted by breast cancer cells (Adriaenssens et al., 2008). During embryonic development, NGF plays a major role in directing nerves to their correct targets (Skaper, 2012) and similarly it can be hypothesized that the production of NGF by breast cancer cells may result in the attraction of nerve fibers into primary breast tumors.

In the present study, the hypothesis that nerve fibers are a significant component of the breast tumor microenvironment has been explored by analyzing a cohort of breast cancers. Nerve fibers were detected in a significant proportion of invasive breast cancers and their presence was associated with lymph node invasion, suggesting a relationship with metastatic potential. An association was found between the presence of nerve fibers and the expression of NGF by cancer cells, and in co-culture with neuronal cells, breast cancer cells were able to induce neuronal outgrowth via the release of NGF.

2. Materials and methods

2.1. *Breast cancer tissue samples and cell lines*

High-density tumor microarrays (TMAs) of invasive ductal carcinomas (IDC), invasive lobular carcinomas (ILC) and ductal carcinomas in situ (DCIS) of the breast were obtained from Biomax (Maryland, USA, catalog number BR1921, BR1921a and BR8011). They included 159 IDC, 160 ILC and 50 DCIS. Histopathological subtypes were reviewed by a pathologist (MMW). Clinical annotation included age at diagnosis, tumor size, lymph node status, estrogen receptor, progesterone receptor, human epidermal growth factor (EGF) receptor 2 (HER2). MDA-MB-231, MCF-7, BT-474, and SKBR-3 breast cancer cell lines were from the American Type Culture Collection. JIMT-1 cells were from DSMZ (Germany). Brain metastatic 231-BR cells and HME human mammary epithelial cells (transformed but non-tumorigenic) were a generous gift from Barbara Steeg (Bethesda, USA) and Robert Weinberg (Boston, USA), respectively. Individual cell line authentication was performed after DNA extraction (Promega genomic purification kit, catalog number A1120) and using the GenePrint 10 PCR amplification kit (Promega catalog number B9510). All breast epithelial cell lines were maintained in RPMI-1640 with 10% foetal calf serum (JRH Biosciences) and 2 mM L-glutamine. The neuron-like PC12 cell line was from Ralph A. Bradshaw (University of California San Francisco). They were maintained in Dulbecco's modified eagle medium (DMEM) from Life Technologies (Australia) with 5% foetal calf serum, 10% horse serum (Sigma), and 2 mM L-glutamine. All cell lines were grown in 75 cm^2 tissue culture flasks in a humidified incubator at 37 °C with 5% CO_2. The study was approved by the Human Research Ethic Committee of the University of Newcastle, Australia.

2.2. *Immunohistochemistry*

After deparaffinization and rehydration of the TMAs following standard procedures, heat induced epitope retrieval was carried out in a citrate based low pH buffer (Vector Laboratories) using a decloaking chamber (Biocare) at 95 °C for 20 min. Immunohistochemistry (IHC) was then performed using an ImmPRESS detection kit (Vector Laboratories) as per the manufacturer's recommendations. Briefly, after inactivation of endogenous peroxidases with H_2O_2, and blocking with 2.5% horse serum, rabbit PGP9.5 antibody (Abcam, catalog number ab15503), or rabbit NGF antibody (Abcam, catalog number ab52918), or non-immune rabbit IgG control (Alpha Diagnostic, catalog number 20009-1-200) were applied at a 1:200 dilution. ImmPRESS HRP anti-rabbit IgG (peroxidase) was then applied to the sections and revealed with DAB peroxidase substrate solution (Vector laboratories). Finally, TMA slides were counterstained with hematoxylin (Gill's formulation, Vector laboratories), dehydrated and cleared in Xylene before mounting in Ultramount #4 mounting media (Thermo Scientific). Imaging was performed using an Axioplan-2 microscope fitted with an AxioCam Mrc5 digital camera (Carl Zeiss AG). The presence or absence of nerve fibers was recorded for

each tumor sample of the TMAs by two independent observers including a pathologist (MMW).

2.3. Digital quantification of immunohistochemistry

For quantification of NGF staining, TMA slides were digitized at 200× absolute resolution using an Aperio AT2 scanner (Leica Biosystems). Quantitative IHC analyses were performed using the Halo™ image analysis platform (Indica Labs) under the supervision of a pathologist. Five random areas containing cancer cells were selected and the pixel intensities of DAB staining calculated using the Area Quantification algorithm. Pixel intensity values were then used to determine h-scores for each core (index ranging from 0 to 300 calculated as the sum of 3 × % of pixels with strong staining + 2 × % of pixels with intermediate staining + 1 × % pixels with weak staining). To compare NGF levels across the cohort, the h-scores were used to divide cases into 4 classifications (0 = h-score <50; 1 = h-score 50–100, 2 = h-score 101–150, 3 = h-score h > 150).

2.4. Association between nerve fibers and clinicopathological parameters

The presence of nerve fibers was compared with clinicopathological parameters (patient age at diagnosis, tumor size, histological subtype, lymph node invasion, estrogen receptor (ER), progesterone receptor (PR), human epidermal growth factor receptor 2 (HER2), molecular subtype) and NGF staining intensity. For statistical analysis, simple unadjusted associations between nerve fibers and other pathological variables were performed using a chi-squared test. We used log-linear models to adjust the various bivariate associations for other potential confounders. The log linear models provided a Chi-squared test adjusted for all other variables in the model; these included cancer type (lobular vs ductal), lymph node involvement (yes/no), estrogen receptor positivity (yes/no), progesterone receptor positivity (yes/no), HER2+ (yes/no) and nerve fibers (negative/positive). The model was specified as a Poisson generalized linear model with a log-link function. Using hierarchical nesting of models, all 3-way then 2-way interactions involving nerve fibers were examined. Goodness of fit was tested using G2 Chi-squared statistics, as well as AIC and BIC. These models were fitted using SAS (SAS Institute, North Carolina, USA).

2.5. Preparation of conditioned medium and dot-blot analysis

Subconfluent breast cancer cells were seeded at 5×10^6 cells per 100 mm culture dish and grown in 10 mL serum free media for 24 h. The collected medium was centrifuged (800× *g* for 5 min at 4 °C) and the supernatant was concentrated and desalted using 10-kDa cut-off Amicon Ultra-15 filter unit (Millipore) for 30 min (4000× *g*, 4 °C). The recovered 250 μL concentrate was stored at −80 °C. Dot-blot analysis was performed by spotting 20 μL of concentrated medium onto nitrocellulose membrane using the Bio-Dot microfiltration system (Bio-Rad). Then the membrane was saturated with blocking buffer (LI-COR Biosciences) for 1 h at room temperature before incubation with rabbit anti-NGF polyclonal IgG (Santa Cruz Biotechnology, catalog number sc548) overnight at 4 °C. After washing with PBS containing 0.1% Tween-20, membranes were probed with goat anti-rabbit IR-Dye 680 secondary antisera (LI-COR Biosciences, catalog number 926-68073), then washed twice. Densitometric analysis was performed using the Odyssey infrared imaging system (LI-COR Biosciences).

2.6. Neurite outgrowth assay

The neurotrophic ability of breast cancer cells was tested in co-culture experiments with the neuronal-like PC12 cells and neurite outgrowth was measured. PC12 cells are extensively used for studying neurite elongation (Suter and Miller, 2011). For co-culture experiments, PC12 cells (5×10^4 in 1 ml) were seeded on bottom wells of 12-well Transwell plates (Corning) coated with rat-tail collagen I (Invitrogen). After 24 h, they were serum starved in DMEM containing 1% horse serum. Breast cancer cells were grown in Transwell inserts (12.0 mm in diameter with 0.4 μm pores, Corning). Differentiation of PC12 cells was allowed for 3 days, with or without anti-NGF mouse monoclonal blocking antibody (Alomone, catalog number alm-006) and neurite elongation was measured. PC12 cells exhibiting neurites of at least twice the size of the cell body were considered as differentiated. Pictures were taken using a Zeiss Axiovert 200 inverted microscope fitted with an AxioCam HRm digital camera (Zeiss AG). One-way ANOVA statistical test (GraphPad Prism 5.01) was used.

3. Results

3.1. Breast tumors are infiltrated by nerve fibers

To test the hypothesis that nerve fibers could infiltrate breast tumors, we have explored TMAs containing 319 invasive breast cancers (IDC + ILC) and 50 DCIS by immunohistochemistry against the neuronal marker PGP9.5. Typical morphological features corresponding to both nerves and isolated nerve fibers (axons) were observed (Figure 1). The presence of nerve trunks (composed of many fibers or axons) with perineural invasion (Figure 1A) was occasionally observed in 6 out of the 319 cases of invasive cancers, but this does not constitute a reliable quantification due to the bias introduced by sampling in relation to the location of nerve trunks. Importantly, isolated nerve fibers (axons) were also observed (Figure 1B–H). The reactivity to the neuronal marker PGP9.5 and typical morphology were characteristic of axons. Nerve fibers were localized around cancer cells and adipocytes (Figure 1B), in the tumor stroma next to cancer cells (Figure 1C–F), around arterioles (Figure 1G) and blood vessels (Figure 1H). In Table 1, breast cancers were classified as nerve fiber positive *versus* nerve fiber negative tumors, and comparison was made with clinicopathological parameters. TMAs do not contain enough tissue for analyzing and dissecting precisely nerve fiber densities in tumors and therefore we have chosen to present the data in terms of presence *versus* absence of nerve fibers (this may lead to an underestimation of the innervation). The presence of nerve fibers was detected in 8% of DCIS, 12% of ILC and 28% of IDC ($p = 0.0003$), indicating that

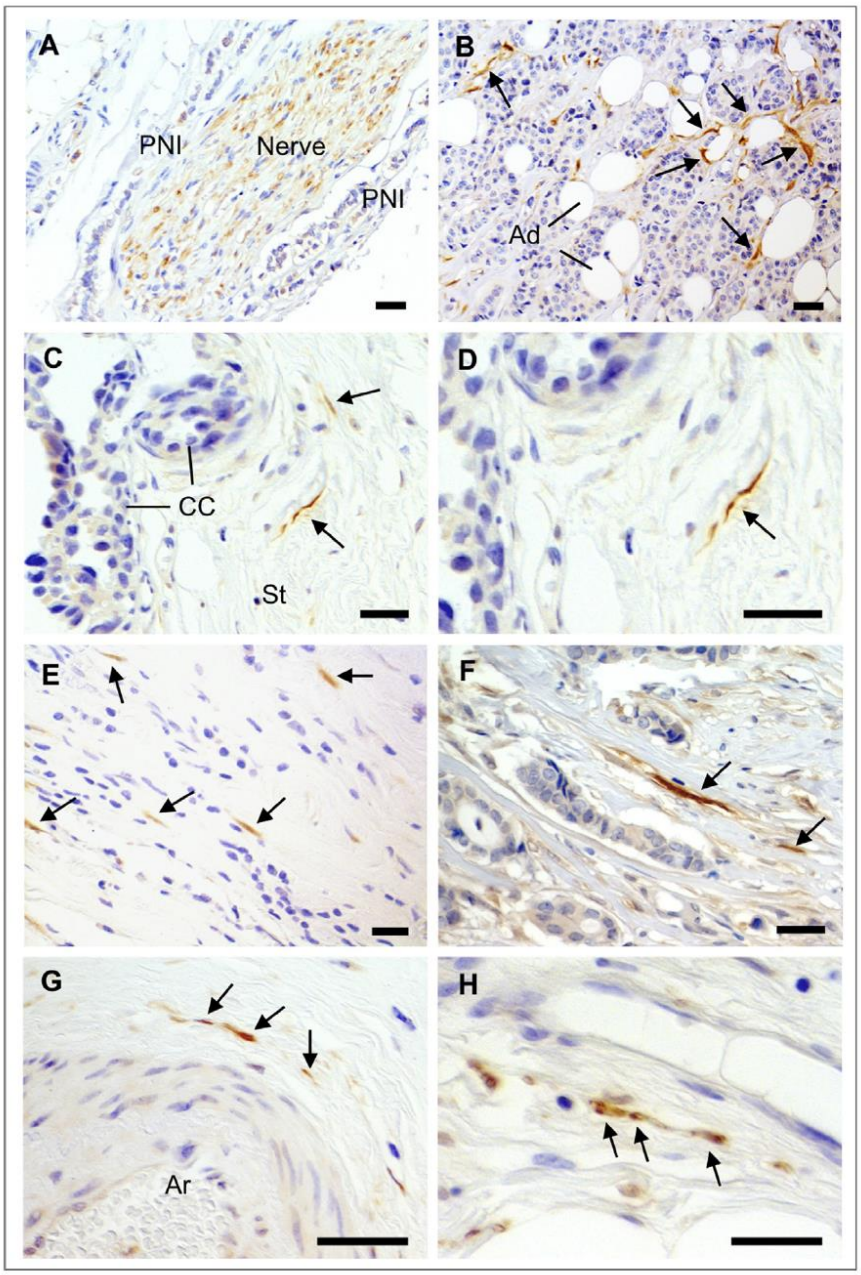

Figure 1 – Detection of nerve fibers in breast cancers. IHC for the neuronal marker PGP9.5 was performed on a series of 319 breast cancer samples. A) Nerve trunks (composed of many nerve fibers), occasionally present in breast tumors, were positive for PGP9.5. Perineural invasion (PNI) could be observed, as shown here. B–H) In some breast cancers, isolated nerve fibers (axons) positive for PGP9.5 were observed and are indicated by arrows. B) Nerve fibers around cancer cells and adipocytes (Ad). C) Nerve fibers in the tumor stroma (St) adjacent to cancer cells (CC). D) Enlargement of C. E, F) Nerve fibers among scattered breast cancer cells and in tumor stroma. G) Nerve fibers around an arteriole (Ar). H) Nerve fibers close to a thin walled blood vessel in the tumor stroma. Scale bar = 50 μm.

nerve fibers are predominantly associated with invasive ductal carcinomas. This association was confirmed in Log-Linear modeling, two-way analysis ($p < 0.001$). In invasive breast tumors, there was no association between the presence of nerve fibers and age at diagnosis, HER2, estrogen receptor, progesterone receptor, tumor size and molecular subtype (defined as TNBC: ER−/PR−/HER2−, luminal A: ER+ and/or PR+/HER2−, luminal B: ER+ and/or PR+/HER2+, HER2+: ER−/PR−/HER2+). The tumors that presented innervation were not enriched in any particular molecular subtypes. A more detailed analysis of innervation in function of ER/PR/HER2 status is shown in Supplementary Table 1 and indicates the absence of statistically significant differences between the subgroups.

Table 1 – Association between the presence of nerve fibers and clinicopathological parameters in breast carcinomas.

Parameter	Nerve fibers negative	Nerve fibers positive	*p*-value
All cases (n = 369)	301 (82%)	68 (18%)	
Pathological subtype			**0.0003**[a]
DCIS (n = 50)	46 (92%)	4 (8%)	
ILC (n = 160)	140 (88%)	20 (12%)	
IDC (n = 159)	115 (72%)	44 (28%)	
Clinical parameters in invasive carcinomas			
Patient age			
50≤ (n = 183)	142 (77%)	41 (22%)	0.1201
>50 (n = 136)	115 (84%)	21 (15%)	
Lymph node status (N)			**0.0031**[a]
Negative (n = 164)	140 (85%)	24 (15%)	
Positive (n = 135)	97 (72%)	38 (28%)	
Undetermined (n = 20)	16 (80%)	4 (20%)	
HER2			0.2162
HER2 negative (n = 252)	205 (81%)	47 (19%)	
HER2 positive (n = 67)	50 (75%)	17 (15%)	
Estrogen receptor			0.3093
ER negative (n = 182)	149 (82%)	33 (18%)	
ER positive (n = 137)	106 (77%)	31 (13%)	
Progesterone receptor			0.8143
PR negative (n = 208)	167 (80%)	41 (20%)	
PR positive (n = 111)	88 (79%)	23 (21%)	
Molecular subtype			0.5801
TNBC (n = 123)	98 (80%)	25 (20%)	
Luminal A (n = 129)	107 (83%)	22 (17%)	
Luminal B (n = 34)	25 (74%)	9 (26%)	
HER2+ (n = 33)	25 (76%)	8 (24%)	
Tumor size (T)			0.5284
1 (n = 25)	19 (76%)	6 (14%)	
2 (n = 228)	183 (80%)	45 (20%)	
3 (n = 32)	28 (88%)	4 (12%)	
4 (n = 30)	22 (73%)	8 (27%)	
Nerve growth factor			**0.0001**[a]
NGF negative (n = 167)	149 (89%)	18 (11%)	
NGF positive (n = 152)	107 (70%)	45 (30%)	

DCIS = ductal carcinomas in situ; ER = estrogen receptor; HER2 = Human EGF receptor 2; IDC = invasive ductal carcinomas; ILC = invasive lobular carcinomas; NGF = nerve growth factor; TNBC = triple negative breast cancer.
a Statistically significant *p*-values ($p < 0.05$ using chi-square test).
Molecular subtypes were defined as TNBC: ER−/PR−/HER2−, luminal A: ER+ and/or PR+/HER2−, luminal B: ER+ and/or PR+/HER2+, HER2+: ER−/PR−/HER2+.

3.2. *The presence of nerve fibers in invasive breast tumors is associated with lymph node invasion and NGF production*

The presence of nerve fibers was associated with lymph node invasion and NGF production in cancer cells (Table 1). Individual nerve fibers were observed in only 15% of invasive tumors with no lymph node invasion whereas 28% of lymph node positive tumors contained nerve fibers ($p = 0.0031$), indicating a relationship between the presence of nerve fibers and metastatic potential/poorer prognosis. The association between nerve fibers and lymph node invasion was confirmed in Log-linear modeling ($p = 0.0064$ in two-way analysis). Together this association with lymph node invasion and the fact that only 8% of DCIS presented with nerve fibers indicate that the presence of nerve fibers in breast tumors is related to aggressiveness/invasiveness.

In addition, as we have previously shown that the neurotrophic growth factor NGF is expressed in breast tumors (Adriaenssens et al., 2008), we tested the hypothesis that the presence of nerve fibers in breast cancers could be related to NGF expression. Interestingly, there was an association between the presence of nerve fibers and the expression of NGF in cancer cells (Table 1). Nerve fibers were observed in only 11% of NGF negative tumors (h-score<50), as compared to 30% of NGF positive tumors (h-score≥50) ($p = 0.0001$). The digital quantification of NGF intensity staining is presented (Figure 2). NGF intensity staining (h-score) was significantly higher in IDC than in DCIS and ILC ($p < 0.0001$) (Figure 2A), thus corroborating the higher proportion of IDC presenting with nerve fibers. The frequency distribution of NGF staining intensity in DCIS, ILC and IDC is presented as categories (Figure 2B), with 0 = h-score <50, 1 = h-score 50–100, 2 = h-score 101–150, 3 = h-score>150. The percentage of cases with NGF labeling was 2% in DCIS, 15% in ILC and 79% in IDC ($p < 0.0001$). In invasive tumors (Figure 2C), the proportion of cases with high NGF labeling (intensity labeling 2 and 3) was 12% in nerve fibers negative tumors and 31% in nerve fibers positive tumors ($p < 0.0001$), confirming the association between NGF and the presence of nerve fibers. Overall, the Spearman correlation factor between nerve fibers and NGF level was 0.28 ($p < 0.0001$). Furthermore, in serial sections with NGF and PGP9.5 staining, nerve fibers were observed around cancer cells producing NGF (Figure 3). Together, these results suggested that NGF produced by breast cancer cells could participate in tumor infiltration by nerves and have prompted an examination of a NGF-mediated neurotrophic effect (ability to induce neuronal outgrowth) of breast cancer cells.

3.3. *Breast cancer cells can induce neuronal outgrowth through NGF secretion*

Given the association between the presence of nerve fibers and the production of NGF in breast tumors, the neurotrophic ability of breast cancer cells was investigated. Co-cultures between breast cancer cell lines and the neuronal-like PC12 cells (Figure 4A) were performed and neurite outgrowth of PC12 cells was measured as a percentage of cells with elongated neurites (Figure 4B). MCF-7, MDA-MB-231 and 231-BR induced a strong neurite outgrowth, whereas only a slight induction was observed with SKBR-3 and JIMT-1. In contrast, no neurite outgrowth was detected with BT-474. Interestingly, the non-tumorigenic HME cells were not able to induce neurite outgrowth. Representative pictures of PC12 cells co-cultured in presence of breast cancer cells are shown (Figure 4C). NGF was quantified in dot blot analyses of conditioned media from breast cancer cell lines (Figure 4D). The dot blot was prepared from an equivalent number of cells and the densitometric quantification indicated different levels of NGF between cell lines. Interestingly, the levels of NGF in the conditioned media of breast cancer cells partly corroborated their ability to induce neurite outgrowth (as shown in Figure 4B), suggesting that NGF participates in the

neurotrophic effect induced by breast cancer cells. MCF-7 exhibited the highest level of NGF secretion and the highest neurotrophic effect (as reported in panel B). The non-tumorigenic HME had a low level of NGF and exhibited a limited neurotrophic effect. However, MDA-MB-231 cells exhibited a significant neurotrophic effect whereas the level of NGF was low, and BT-474 had an intermediate NGF level and only a low impact on neuritogenesis. This suggested that NGF is probably not the only neurotrophic factor produced by breast cancer cells and able to stimulate neuron outgrowth. The involvement of NGF in breast cancer-induced neurite outgrowth was confirmed by use of blocking antibodies against NGF (Figure 4E). As shown with MCF-7 cells, blocking antibodies against NGF could partly inhibit breast cancer cell-induced neurite outgrowth whereas a control IgG antibody had no effect. Representative pictures showing the effect of anti-NGF antibody on neurite outgrowth induced by MCF-7 cells are shown (Figure 4F). The inhibitory activity of anti-NGF blocking antibody for breast cancer-induced neurite outgrowth has been confirmed using the 50B11 cell line (Supplementary Figure 1), which is derived from dorsal root ganglia and morphologically responsive to NGF (Bhattacherjee et al., 2014). Together these data indicate that breast cancer cells have the ability to stimulate axonogenesis through the production and release of NGF, and that other neurotrophic factors may also be involved.

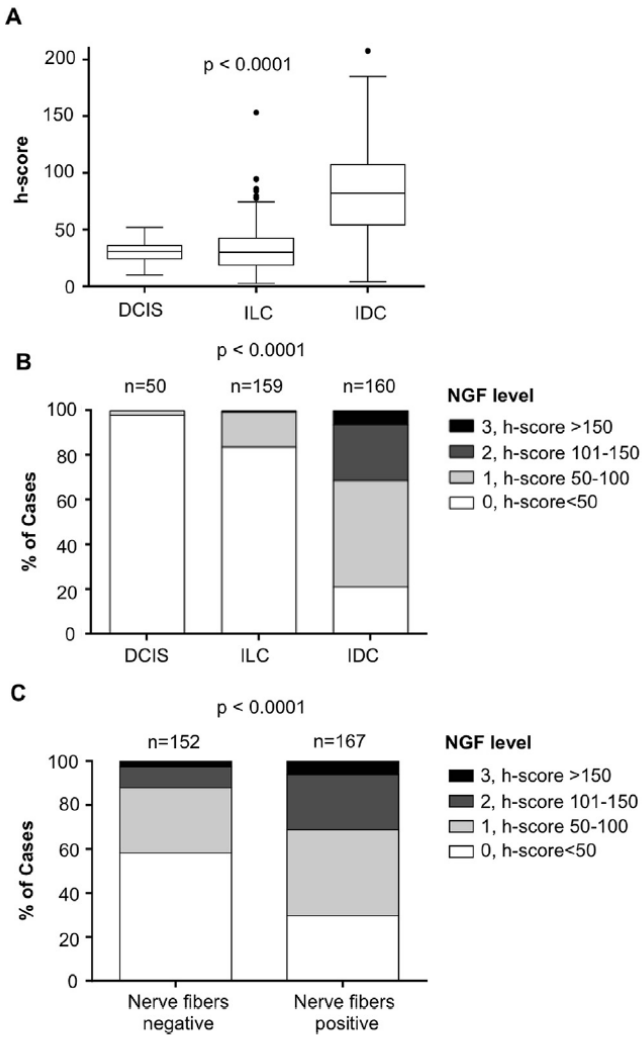

Figure 2 – Frequency distribution of NGF level in breast cancers according to the presence of nerve fibers. NGF levels were obtained after digital quantification. A) Distribution of NGF intensity staining (h-score) in ductal carcinomas in situ (DCIS), invasive lobular carcinomas (ILC) and invasive ductal carcinomas (IDC). Box and Whisker plots comparing median NGF levels using h-scores as a measure of IHC staining (n = 50, 160 and 160, respectively). The box limits indicate the 25th and 75th percentiles with the whiskers extending 1.5 times the interquartile range from the 25th and 75th percentiles (outliers are represented by dots; prepared using BoxPlotR). B) Distribution of NGF staining intensity in DCIS, ILC and IDC. Categorization is presented as 0 = h-score < 50, 1 = h-score 50–100, 2 = h-score 101–150, 2 = h-score > 150. C) Distribution of NGF staining intensity in invasive tumors (nerve fibers positive *versus* nerve fibers negative tumors). Categories of NGF staining (0, 1, 2, 3) were the same as in B. Tumors presenting with nerve fibers were more likely to have higher NGF expression than tumors without nerve fibers. Number of cases (n) is indicated. ***One-way ANOVA was used for A and Chi square for B and D.

4. Discussion

The tumor microenvironment is crucial to breast cancer progression and the interaction of breast cancer cells with the components of the stroma, endothelial and immune cells, fibroblasts and extracellular matrix, is well established (Hanahan and Weinberg, 2011). In contrast, the presence of nerve fibers in the breast tumor microenvironment and a possible interaction with cancer cells has not been studied in detail. The present study demonstrates the presence of thin and isolated nerve fibers (axons) in the breast tumor microenvironment and their association with NGF production in cancer cells. In prostate cancer, nerve infiltration correlates with tumor aggressiveness (Magnon et al., 2013), and is driven by the production of proNGF (Pundavela et al., 2014) and granulocyte colony-stimulating factor (G-CSF) (Dobrenis et al., 2015). The results presented here suggest that a similar situation occurs in breast cancer as infiltration by nerve fibers was found associated to lymph node invasion. Lymph node status is the single most important prognostic variable for the management of patients with primary breast cancer. However, the occurrence of false negatives, along with heterogeneity of clinical outcomes among lymph node positive patients, highlights the need to improve the classification and management of invasive breast cancer. This study points to the potential value of using the presence of nerve fibers as a new predictive biomarker in breast cancer.

The production and release of neurotrophic factors by breast cancer cells has been described (Hondermarck, 2012). NGF expression is increased in breast cancer cells as compared to normal breast epithelial cells (Adriaenssens et al., 2008), resulting in an autocrine stimulation of breast cancer cells through the tyrosine kinase receptor TrkA and the TNF-receptor family member $p75^{NTR}$ (Lagadec et al., 2009; Verbeke et al., 2010). However, until now, the possibility that NGF produced by breast cancer cells could stimulate tumor nerve infiltration had not been investigated. The present

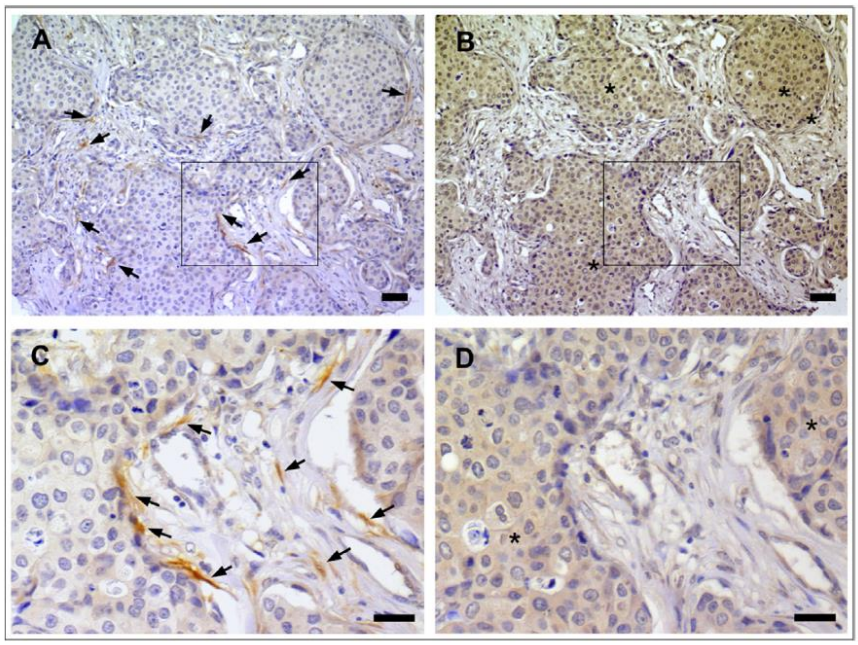

Figure 3 – Co-localization between nerve fibers and NGF in breast cancer. A) IHC for PGP9.5 indicating the presence of many nerve fibers in the stroma and along cancer cells of an invasive ductal carcinoma. Arrows point to few nerve fibers. B) IHC against NGF in a section serial to that presented in panel A. NGF immunoreactivity (indicated by stars) was observed in cancer cells adjacent to nerve fibers. C) Enlargement of the area boxed in panel A. D) Enlargement of the area boxed in panel B. Scale bar = 50 μm.

study reveals that breast cancer cells can activate neuronal outgrowth through a NGF-mediated mechanism. In bone metastases of breast cancer, one study has already shown that NGF production by tumor cells can attract nerves (Bloom et al., 2011) and our study demonstrates that nerve infiltration is also a characteristic of primary breast tumors that is partially driven by NGF production. However, the correlation between NGF and nerve outgrowth, both in tumor samples and in cell cultures, was only partial, suggesting that NGF is not the only factor involved. There are many growth factors (neurotrophins and others) that can exhibit a neurotrophic activity, and several are produced in breast cancers. Brain-derived neurotrophic factor (BDNF) and neurotrophin-4/5 (Hernandez-Bedolla et al., 2015; Vanhecke et al., 2011), Artemin (Kang et al., 2009) or fibroblast growth factors (Penault-Llorca et al., 1995), as well as axon guidance molecules such as netrins (Harburg and Hinck, 2011) are expressed by breast cancer cells and could also contribute to the attraction of nerve fibers. The development of the nervous system involves a variety of neurotrophic molecules that act on different neuronal subtypes, and it is possible that a similar diversity of mechanisms also participates in tumor innervation. Further investigations are warranted to clarify the possible involvement of neurotrophic factors and axon guidance molecules in the infiltration of breast tumors by nerve fibers.

The presence of nerve fibers could be particularly relevant in terms of tumor growth and metastasis, via the secretion of active neuropeptides and neurotransmitters. Breast cancer cells have been reported to express receptors for a number of neuropeptides and neurotransmitters, like norepinephrine and epinephrine (Luthy et al., 2009) or substance P (Garcia-Recio et al., 2013). As a consequence tumor cells are able to transduce neurotransmitter-induced intracellular signaling pathways, which have been described to eventually lead to the activation of their growth and metastasis (Entschladen et al., 2004). The presence of nerve fibers in the breast tumor microenvironment suggests that they could liberate neurotransmitters directly in the vicinity of breast cancer cells. We have observed tyrosine hydroxylase positivity in some nerve trunks as well as axons (Supplementary Figure 2), indicating that some of the nerve fibers present in breast cancer are of sympathetic origin and could therefore liberate catecholamines. It has been shown that the expression of the beta-adrenergic receptor for catecholamines is associated with a poor clinical outcome in breast cancer patients (Powe et al., 2011) and that stress-induced activation of the sympathetic nervous system can induce a metastatic switch (Sloan et al., 2010). The mechanism involved the stimulation of beta-adrenergic receptors at the surface of breast cancer cells by circulating catecholamines, but our study suggests that a local production by nerves may also be involved. In addition, epidemiological studies have suggested that blockers of the beta-adrenergic receptors, traditionally used for the treatment of cardiovascular disorders and anxiety, can increase breast cancer patient survival (Barron et al., 2011; Melhem-Bertrandt et al., 2011); the mechanism is unclear, but beta-blockers could potentially inhibit the stimulatory effect of catecholamines liberated by nerves. Although further experiments are necessary to test these hypotheses and determine if infiltrating nerve fibers have an impact on cancer and

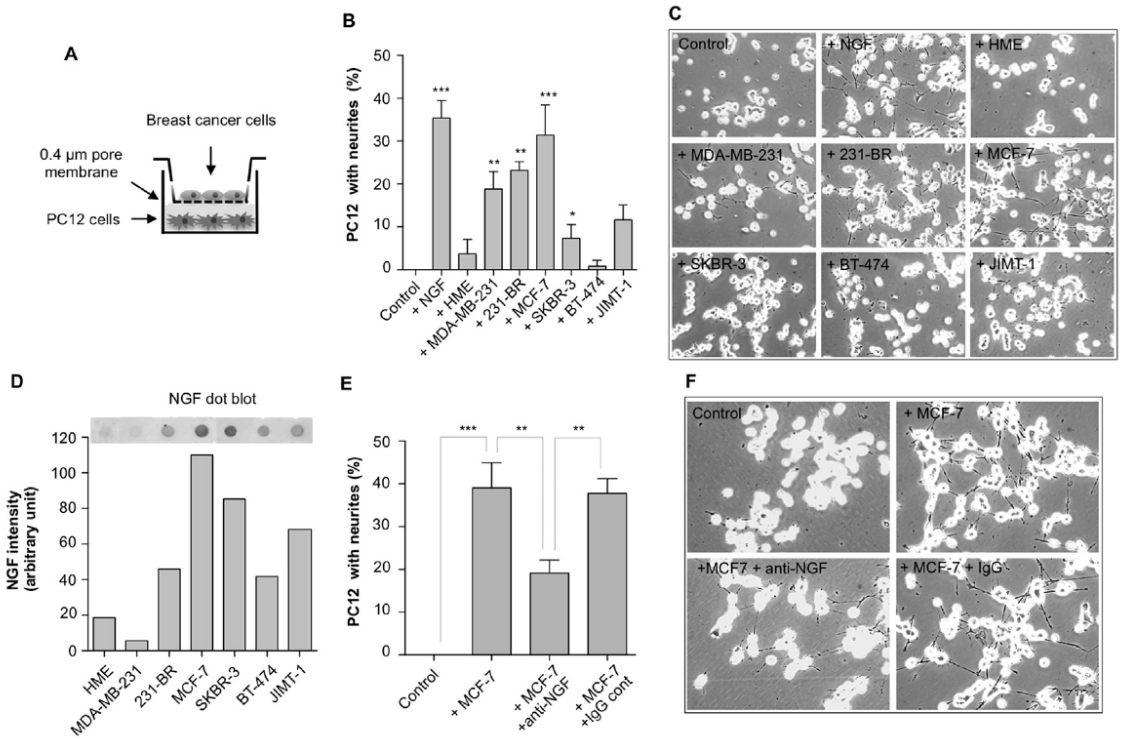

Figure 4 – NGF-mediated neurotrophic effect of breast cancer cells. A) Co-culture experiments were performed in Transwell Boyden chambers with breast epithelial cells in the upper part and PC12 cells in the lower part. B) Some breast cancer cell lines were able to induce a neurotrophic effect on PC12 cells. Neurite outgrowth was induced in presence of MDA-MB-231, 231-BR, MCF-7, SKBR-3, JIMT-1, but not in presence of BT-474 and the non-tumorigenic HME. A negative control (with no breast cancer cells) and a positive control (addition of 50 ng/ml NGF) have been added. The results represent the mean of 3 independent experiments ± SD. $^{*}p < 0.05$, $^{**}p < 0.01$, $^{***}p < 0.001$ for comparison with control. C) Representative pictures showing the effect of breast cancer cell lines and HME on PC12 cells. Quantifications are presented in panel B. D) Dot-blot analysis for the detection of NGF in breast cancer cell conditioned media and quantification of NGF signal intensity in different breast epithelial cells. E) Impact of blocking anti-NGF antibodies on breast cancer cell-induced neurite outgrowth. MCF-7 cells were co-cultured for 72 h with PC12 cells in presence or absence of anti-NGF blocking antibodies (1 µg/ml). Control was without MCF-7 cells, and isotype antibodies were also tested. The results represent the mean of 3 independent experiments ± SD. $^{***}p < 0.001$. F) Representative pictures corresponding to the experiment described in panel E.

stromal cells, our results open the theoretical possibility that, similarly to prostate cancer (Magnon et al., 2013), nerve fibers could be involved in breast cancer progression.

In conclusion, the nerve-breast cancer connection described here bridges a gap in knowledge about the neuronal component of the breast tumor microenvironment and points to NGF as a driver of nerve infiltration. This opens a new perspective of crosstalk between nerves and breast cancer cells, and warrants more studies to investigate the impact of nerve fibers in breast cancer progression.

Contributions

SR performed the immunohistochemistry. Tissue slide analyses were performed by MMW (histopathologist), and confirmed by PJ (neuroanatomist) and HH. Digital quantification of IHC was performed by RT. JP performed all *in vitro* experiments and participated in IHC; he also prepared all Figures and Tables. JA supervised the statistical analyses. SF contributed to cell culture. HH and PJ conceived the study. HH, MMW, RJS, RAB and JFF supervised the study. HH drafted the manuscript. All authors have read and approved the final manuscript.

Conflict of interest

The authors disclosed no competing interests.

Acknowledgments

This work was supported by the University of Newcastle, Australia and the Hunter Cancer Research Alliance. We thank Dr. Christopher Oldmeadow from the Clinical Research Design, IT, and Statistical Support (CReDITSS) Unit of the University of Newcastle.

Appendix A.
Supplementary data

Supplementary data related to this article can be found at http://dx.doi.org/10.1016/j.molonc.2015.05.001.

REFERENCES

Adriaenssens, E., Vanhecke, E., Saule, P., Mougel, A., Page, A., Romon, R., Nurcombe, V., Le Bourhis, X., Hondermarck, H., 2008. Nerve growth factor is a potential therapeutic target in breast cancer. Cancer Res. 68, 346–351.

Bapat, A.A., Hostetter, G., Von Hoff, D.D., Han, H., 2011. Perineural invasion and associated pain in pancreatic cancer. Nat. Rev. Cancer 11, 695–707.

Barron, T.I., Connolly, R.M., Sharp, L., Bennett, K., Visvanathan, K., 2011. Beta blockers and breast cancer mortality: a population- based study. J. Clin. Oncol. 29, 2635–2644.

Bhattacherjee, A., Liao, Z., Smith, P.G., 2014. Trophic factor and hormonal regulation of neurite outgrowth in sensory neuron-like 50B11 cells. Neurosci. Lett. 558, 120–125.

Bloom, A.P., Jimenez-Andrade, J.M., Taylor, R.N., Castaneda-Corral, G., Kaczmarska, M.J., Freeman, K.T., Coughlin, K.A., Ghilardi, J.R., Kuskowski, M.A., Mantyh, P.W., 2011. Breast cancer-induced bone remodeling, skeletal pain, and sprouting of sensory nerve fibers. J. Pain 12, 698–711.

Campbell, J.P., Karolak, M.R., Ma, Y., Perrien, D.S., Masood-Campbell, S.K., Penner, N.L., Munoz, S.A., Zijlstra, A., Yang, X., Sterling, J.A., Elefteriou, F., 2012. Stimulation of host bone marrow stromal cells by sympathetic nerves promotes breast cancer bone metastasis in mice. PLoS Biol. 10, e1001363.

Dobrenis, K., Gauthier, L.R., Barroca, V., Magnon, C., 2015. Granulocyte colony-stimulating factor off-target effect on nerve outgrowth promotes prostate cancer development. Int. J. Cancer 136, 982–988.

Entschladen, F., Drell, T.L.t, Lang, K., Joseph, J., Zaenker, K.S., 2004. Tumour-cell migration, invasion, and metastasis: navigation by neurotransmitters. Lancet Oncol. 5, 254–258.

Garcia-Recio, S., Fuster, G., Fernandez-Nogueira, P., Pastor-Arroyo, E.M., Park, S.Y., Mayordomo, C., Ametller, E., Mancino, M., Gonzalez-Farre, X., Russnes, H.G., Engel, P., Costamagna, D., Fernandez, P.L., Gascon, P., Almendro, V., 2013. Substance P autocrine signaling contributes to persistent HER2 activation that drives malignant progression and drug resistance in breast cancer. Cancer Res. 73, 6424–6434.

Hanahan, D., Weinberg, R.A., 2011. Hallmarks of cancer: the next generation. Cell 144, 646–674.

Harburg, G.C., Hinck, L., 2011. Navigating breast cancer: axon guidance molecules as breast cancer tumor suppressors and oncogenes. J. Mammary Gland Biol. Neoplasia 16, 257–270.

Hernandez-Bedolla, M.A., Carretero-Ortega, J., Valadez-Sanchez, M., Vazquez-Prado, J., Reyes-Cruz, G., 2015. Chemotactic and proangiogenic role of calcium sensing receptor is linked to secretion of multiple cytokines and growth factors in breast cancer MDA-MB-231 cells. Biochim. Biophys. Acta 1853, 166–182.

Hondermarck, H., 2012. Neurotrophins and their receptors in breast cancer. Cytokine Growth Factor Rev. 23, 357–365.

Huang, D., Su, S., Cui, X., Shen, X., Zeng, Y., Wu, W., Chen, J., Chen, F., He, C., Liu, J., Huang, W., Liu, Q., Su, F., Song, E., Ouyang, N., 2014. Nerve fibers in breast cancer tissues indicate aggressive tumour progression. Medicine (Baltimore) 93, e172.

Jobling, P., Pundavela, J., Oliverira, S.M.R., Roselli, S., Walker, M.M., Hondermarck, H., 2015. Nerve-cancer cell crosstalk: a novel promoter of tumour progression. Cancer Res. 75, 1–5.

Kang, J., Perry, J.K., Pandey, V., Fielder, G.C., Mei, B., Qian, P.X., Wu, Z.S., Zhu, T., Liu, D.X., Lobie, P.E., 2009. Artemin is oncogenic for human mammary carcinoma cells. Oncogene 28, 2034–2045.

Lagadec, C., Meignan, S., Adriaenssens, E., Foveau, B., Vanhecke, E., Romon, R., Toillon, R.A., Oxombre, B., Hondermarck, H., Le Bourhis, X., 2009. TrkA overexpression enhances growth and metastasis of breast cancer cells. Oncogene 28, 1960–1970.

Luthy, I.A., Bruzzone, A., Pinero, C.P., Castillo, L.F., Chiesa, I.J., Vazquez, S.M., Sarappa, M.G., 2009. Adrenoceptors: non conventional target for breast cancer? Curr. Med. Chem. 16, 1850–1862.

Magnon, C., Hall, S.J., Lin, J., Xue, X., Gerber, L., Freedland, S.J., Frenette, P.S., 2013. Autonomic nerve development contributes to prostate cancer progression. Science 341, 1236361.

Marchesi, F., Piemonti, L., Mantovani, A., Allavena, P., 2010. Molecular mechanisms of perineural invasion, a forgotten pathway of dissemination and metastasis. Cytokine Growth Factor Rev. 21, 77–82.

Melhem-Bertrandt, A., Chavez-Macgregor, M., Lei, X., Brown, E.N., Lee, R.T., Meric-Bernstam, F., Sood, A.K., Conzen, S.D., Hortobagyi, G.N., Gonzalez-Angulo, A.M., 2011. Beta-blocker use is associated with improved relapse-free survival in patients with triple-negative breast cancer. J. Clin. Oncol. 29, 2645–2652.

Ondicova, K., Mravec, B., 2010. Role of nervous system in cancer aetiopathogenesis. Lancet Oncol. 11, 596–601.

Penault-Llorca, F., Bertucci, F., Adelaide, J., Parc, P., Coulier, F., Jacquemier, J., Birnbaum, D., deLapeyriere, O., 1995. Expression of FGF and FGF receptor genes in human breast cancer. Int. J. Cancer 61, 170–176.

Powe, D.G., Voss, M.J., Habashy, H.O., Zanker, K.S., Green, A.R., Ellis, I.O., Entschladen, F., 2011. Alpha- and beta-adrenergic receptor (AR) protein expression is associated with poor clinical outcome in breast cancer: an immunohistochemical study. Breast Cancer Res. Treat. 130, 457–463.

Pundavela, J., Demont, Y., Jobling, P., Lincz, L.F., Roselli, S., Thorne, R., Bond, D., Bradshaw, R.A., Walker, M.M., Hondermarck, H., 2014. ProNGF correlates with Gleason score and is a potential driver of nerve infiltration in prostate cancer. Am. J. Pathol. 184, 3156–3162.

Sarhadi, N.S., Shaw Dunn, J., Lee, F.D., Soutar, D.S., 1996. An anatomical study of the nerve supply of the breast, including the nipple and areola. Br. J. Plast. Surg. 49, 156–164.

Skaper, S.D., 2012. The neurotrophin family of neurotrophic factors: an overview. Methods Mol. Biol. 846, 1–12.

Sloan, E.K., Priceman, S.J., Cox, B.F., Yu, S., Pimentel, M.A., Tangkanangnukul, V., Arevalo, J.M., Morizono, K., Karanikolas, B.D., Wu, L., Sood, A.K., Cole, S.W., 2010. The sympathetic nervous system induces a metastatic switch in primary breast cancer. Cancer Res. 70, 7042–7052.

Suter, D.M., Miller, K.E., 2011. The emerging role of forces in axonal elongation. Prog. Neurobiol. 94, 91–101.

Vanhecke, E., Adriaenssens, E., Verbeke, S., Meignan, S., Germain, E., Berteaux, N., Nurcombe, V., Le Bourhis, X., Hondermarck, H., 2011. Brain-derived neurotrophic factor and neurotrophin-4/5 are expressed in breast cancer and can be targeted to inhibit tumor cell survival. Clin. Cancer Res. 17, 1741–1752.

Verbeke, S., Meignan, S., Lagadec, C., Germain, E., Hondermarck, H., Adriaenssens, E., Le Bourhis, X., 2010. Overexpression of p75(NTR) increases survival of breast cancer cells through p21(waf1). Cell Signal. 22, 1864–1873.

Zhao, C.M., Hayakawa, Y., Kodama, Y., Muthupalani, S., Westphalen, C.B., Andersen, G.T., Flatberg, A., Johannessen, H., Friedman, R.A., Renz, B.W., Sandvik, A.K., Beisvag, V., Tomita, H., Hara, A., Quante, M., Li, Z., Gershon, M.D., Kaneko, K., Fox, J.G., Wang, T.C., Chen, D., 2014a. Denervation suppresses gastric tumorigenesis. Sci. Transl Med. 6, 250ra115.

Zhao, Q., Yang, Y., Liang, X., Du, G., Liu, L., Lu, L., Dong, J., Han, H., Zhang, G., 2014b. The clinicopathological significance of neurogenesis in breast cancer. BMC Cancer 14, 484.

3.3 Supplemental Files

Supplementary Table 1. Association between the presence of nerve fibers and ER/PR/HER2 status of invasive breast carcinomas. Chi-square test was used for p-value calculation.

	Nerve Fibers Negative	Nerve Fibers Positive	*p*-value
ER/PR/HER2 status			0.0620
ER-/PR-/HER2- (n=123)	98 (80%)	25 (20%)	
ER+/PR+/HER2+ (n=14)	8 (57%)	6 (43%)	
ER+/PR-/HER2+ (n=13)	10 (77%)	3 (23%)	
ER-/PR+/HER2+ (n=7)	7 (100%)	0 (0%)	
ER+/PR-/HER2- (n=39)	34 (87%)	5 (13%)	
ER-/PR+/HER2- (n=19)	19 (100%)	0 (0%)	
ER+/PR+/HER2- (n=71)	54 (76%)	17 (24%)	
ER-/PR-/HER2+ (n=33)	25 (76%)	8 (24%)	

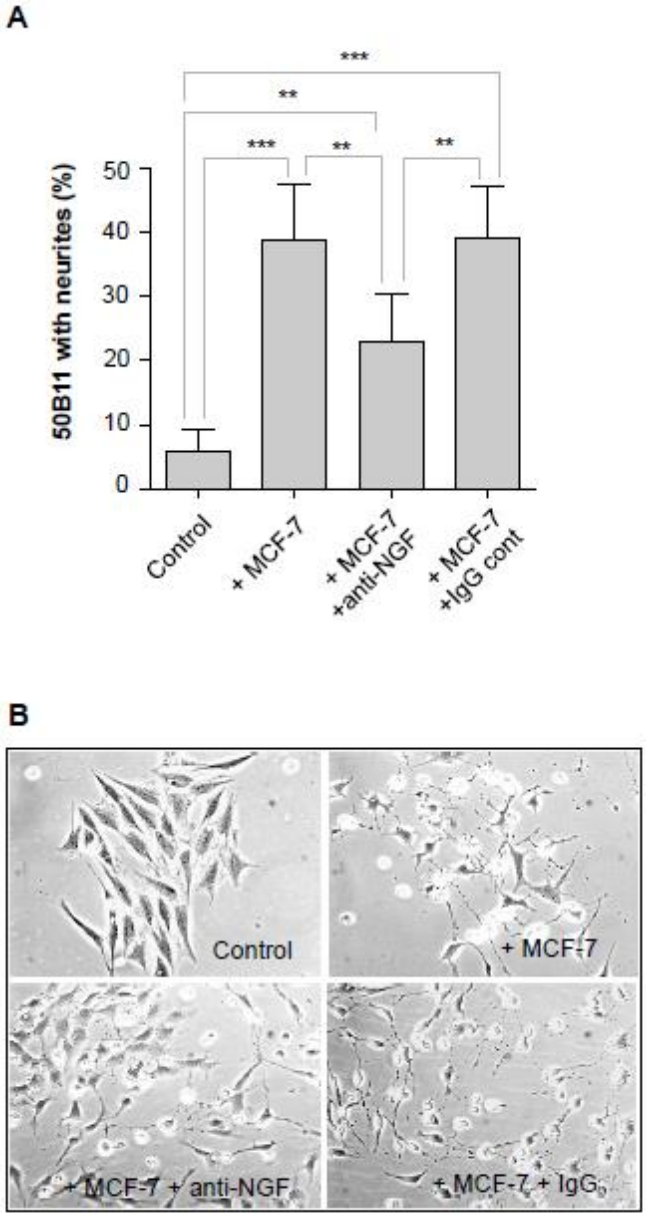

Supplemental Figure S1. NGF-mediated neurotrophic effect of breast cancer cells for 50B11 cells from dorsal root ganglia. Immortalized dorsal root ganglia (DRG) neurons 50B11 were obtained from Dr A. Höke (John Hopkins University, Baltimore USA). The coculture with breast cancer cells was performed as described for PC12 cells in the Material and Methods section. For co-culture with the breast cancer cells, the same protocol as for PC12 cells was used (see Material and Methods section), but the culture media included 5µM forskolin (necessary to obtain neurite outgrowth with these cells). **A)** MCF-7 cells were able to induce neurite outgrowth in 50B11 cells. This neurotrophic effect was partially inhibited by addition of anti-NGF antibody but not by IgG control. **B)** Representative pictures of each experimental condition are shown. The results represent the mean of 3 independent experiments +/- SD. *** $p<0.001$; ** $p<0.05$.

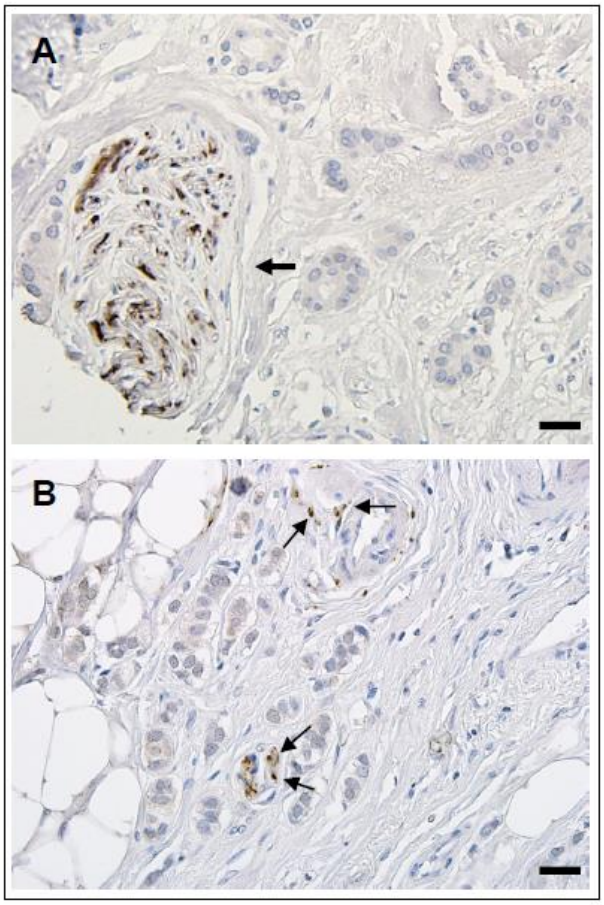

Supplemental Figure S2. Detection of tyrosine hydroxylase positive nerve fibers in breast cancer. Tyrosine hydroxylase was detected by IHC using the same protocol as described in Material and Methods, with anti-tyrosine hydroxylase (Millipore, catalogue number AB152). **A)** Nerve trunk composed of many fibers positive for tyrosine hydroxylase is shown by an arrow. **B)** Individual nerve fibers (axons) positive for tyrosine hydroxylase are indicated by arrows. Scale bar=50 µm.

CHAPTER 4 | ProNGF is a potential diagnostic biomarker for thyroid cancer

4.1 Preface

Chapter 4 contains an original research article entitled **"ProNGF is a potential diagnostic biomarker for thyroid cancer"** which has been published in the journal *Oncotarget*. Subsequent to revealing the extent of neural invasion within primary breast tumours, as well as identifying NGF as a potential inducer, we looked to extend these findings to determine if a similar mechanism is at play in human thyroid cancer. We observed neural infiltration in only 5% of thyroid tumours which is significantly less than what we reported for breast cancer (~28%). Additionally, we found proNGF to be overexpressed in thyroid tumours as compared with both benign adenomas and normal thyroid tissue, highlighting its potential as a novel diagnostic biomarker. However, this overexpression was not associated with the presence of nerve fibres.

4.2 Publication

www.impactjournals.com/oncotarget/ Oncotarget, Advance Publications 2016

ProNGF is a potential diagnostic biomarker for thyroid cancer

Sam Faulkner[1,2,*], Severine Roselli[1,2,*], Yohann Demont[3,7], Jay Pundavela[1,2], Genevieve Choquet[4], Philippe Leissner[4], Christopher Oldmeadow[5], John Attia[2,6], Marjorie M. Walker[2,6], Hubert Hondermarck[1,2]

[1]School of Biomedical Sciences & Pharmacy, Faculty of Health and Medicine, University of Newcastle, Callaghan NSW 2308, Australia

[2]Hunter Medical Research Institute, University of Newcastle, New Lambton NSW 2305, Australia

[3]Inserm U908, Growth Factor Signaling and Functional Proteomics of Breast Cancer, University of Lille, 59655 Villeneuve d'Ascq, France

[4]Medical Diagnostic Discovery Department, bioMérieux, 69280 Marcy l'Etoile, France

[5]School of Mathematical and Physical Sciences, Faculty of Science and Information Technology, University of Newcastle, Callaghan NSW 2308, Australia

[6]School of Public Health & Medicine, Faculty of Health and Medicine, University of Newcastle, Callaghan NSW 2308, Australia

[7]Present address: INSERM U1138 team 11, Centre de Recherche des Cordeliers, 15 rue de l'Ecole de Medecine, 75006 Paris, France

[*]These authors have contributed equally to this work

Correspondence to: *Hubert Hondermarck,* ***e-mail:*** *hubert.hondermarck@newcastle.edu.au*

Keywords: *growth factors, proNGF, thyroid cancer, diagnostic biomarker*

Received: *January 11, 2016* ***Accepted:*** *March 28, 2016* ***Published:*** *April 08, 2016*

ABSTRACT

The precursor for nerve growth factor (proNGF) is expressed in some cancers but its clinicopathological significance is unclear. The present study aimed to define the clinicopathological significance of proNGF in thyroid cancer. ProNGF expression was analysed by immunohistochemistry in two cohorts of cancer *versus* benign tumors (adenoma) and normal thyroid tissues. In the first cohort (40 thyroid cancers, 40 thyroid adenomas and 80 normal thyroid tissues), proNGF was found overexpressed in cancers compared to adenomas and normal samples (p<0.0001). The area under the receiver-operating characteristic (ROC) curve was 0.84 (95% CI 0.75-0.93, p<0.0001) for cancers *versus* adenomas, and 0.99 (95% CI 0.98-1.00, p<0.0001) for cancers *versus* normal tissues. ProNGF overexpression was confirmed in a second cohort (127 cancers of various histological types and 55 normal thyroid tissues) and using a different antibody (p<0.0001). ProNGF staining intensity was highest in papillary carcinomas compared to other histological types (p<0.0001) and there was no significant association with age, gender, tumor size, stage and lymph node status. In conclusion, proNGF is increased in thyroid cancer and should be considered as a new potential diagnostic biomarker.

INTRODUCTION

Thyroid cancer is a common malignancy with a rapidly increasing global incidence [1]. Although mortality from thyroid cancer is relatively low, the rate of disease recurrence or persistence is high, leading to increased patient morbidity and mortality [1]. Histological types of thyroid cancer include the relatively differentiated papillary, follicular and medullary cancers, as well as the undifferentiated anaplastic cancers. Aside from thyroid cancers, benign thyroid tumors (adenomas) represent the majority of clinically detected thyroid nodules. In clinical practice, microscopic examination of fine needle aspiration biopsy (FNAB) is the critical diagnostic test for evaluation of the cancerous nature of thyroid nodules. Unfortunately, in 10-15% of cases a definitive diagnosis cannot be made after FNAB, and the tumor is classified by the pathologist as "indeterminate" or "suspicious" [1]. No individual thyroid cancer biomarker has been found with sufficient sensitivity and specificity [2]. To resolve

this diagnosis dilemma, new biomarkers of thyroid cancer are needed.

The precursor for nerve growth factor (proNGF) consists of the mature NGF polypeptide plus a propeptide of equivalent molecular mass at the N-terminus [3]. ProNGF can also generate NGF after processing by various proteolytic enzymes, such as furin or matrix metalloproteases [3]. However, proNGF also exhibits its own biological activities on neurons through the stimulation of specific receptors [3, 4]. ProNGF binds to the membrane protein sortilin [3, 4], a member of the Vacuolar Protein Sorting 10 protein (VPS10P) [5], to activate the neurotrophin receptor $p75^{NTR}$ and the tyrosine kinase receptor TrkA (NTRK1) [3]. Original findings have described proNGF as an inducer of neuron apoptosis [6], but other studies have reported that its neurotrophic activities result in neuron survival and differentiation [7, 8]. These seemingly contradictory data can be explained by differential levels of sortilin, $p75^{NTR}$ and TrkA at the neuronal cell surface, resulting in differential activations of downstream signaling pathways, such as those involving ERK, SRC or PI3K [9].

ProNGF is also expressed in some malignancies. In breast cancer, proNGF stimulates cancer cell invasion *via* the stimulation of TrkA and sortilin [10], and this tumor promoting effect is particularly relevant for the stem cell compartment of breast tumors [11]. In prostate cancer, proNGF expression correlates with aggressiveness and the growth of nerves into the tumor [12]. ProNGF also stimulates the invasion of melanoma cells through an interaction with $p75^{NTR}$ and sortilin [13]. In thyroid cancer, oncogenic rearrangements of TrkA have been described, particularly in the histological type papillary carcinoma [14, 15]. TrkA as well as its TRK-T1 fusion protein induce neoplastic transformation of the thyroid epithelium [16, 17]. The expression of $p75^{NTR}$ has also been reported in papillary thyroid carcinoma [18, 19]. Although NGF has been described in thyroid cancer, it has not been associated with any clinicopathological features [19]. In contrast, proNGF expression, to our knowledge, has not been reported.

In the present study, we aimed to determine the expression and clinicopathological significance of proNGF in thyroid cancer. The expression of proNGF was analyzed by immunohistochemistry in two cohorts of cancers *versus* normal thyroid tissues. The data show that proNGF is overexpressed in thyroid cancer and therefore could constitute a novel biomarker for diagnosis.

RESULTS

ProNGF expression in cohort 1: comparison of thyroid cancers *versus* adenomas and normal tissues

ProNGF expression was investigated by immunohistochemistry, using a polyclonal antibody, in a series of 40 cases of thyroid cancer, 40 adenomas and 80 normal thyroid tissues. ProNGF was detected in epithelial cells with a marked increase in cancers compared to normal tissue (Figure 1A–1D). No labeling was observed in the stroma (including endothelial cells, fibroblasts and the extracellular matrix). Digital quantification of staining intensities (Figure 1E) revealed a median h-score of 19.7 in normal thyroid tissues, 35.5 in adenomas and 69.3 in cancer ($p<0.0001$). The corresponding ROC curves are presented (Figure 1F–1H). The area under the ROC curve (AUROC) of cancer *versus* normal tissue (Figure 1F) was 0.99 (95% CI 0.98-1.00, $p<0.0001$). Similarly, the AUROC of cancers *versus* adenomas (Figure 1G) was 0.84 (95% CI 0.75-0.93, $p<0.0001$). When considering cancers *versus* adenomas + normal tissue (Figure 1H), the AUROC was 0.95 (95% CI 0.92-0.98, $p<0.0001$). For analysing the correlations between proNGF expression and clinicopathological parameters, proNGF staining intensities were categorized as 0 (h-score <25), 1 (h-score 25-50), 2 (h-score 50-75), and 3 (h-score >75). The frequency distribution is presented in Table 1 and indicated that 100% of thyroid cancer (including papillary, follicular and medullary histological types) were positive for proNGF as compared to 87% adenoma and 22% of normal tissues ($p<0.0001$). Importantly, the proportion of samples with intermediate and high levels of proNGF (staining intensities 2 and 3) shifted from 0% in normal tissues to 27% in adenomas and 82% in cancer. The analysis of association with clinicopathological parameters indicated that 96% of papillary carcinomas presented high levels (staining intensities 2 and 3) of proNGF compared to 88% of follicular carcinomas and 17% of medullary carcinomas ($p=0.0006$). Overall and for each histological type, there was no association between proNGF expression and other clinicopathological parameters (age, gender, tumor size, stage and lymph node status).

ProNGF expression in cohort 2: comparison of thyroid cancer of different histological types and normal tissues

ProNGF expression was analysed by immunohistochemistry, using a monoclonal antibody, in a series of 127 thyroid cancers of various histological types, 6 adenomas and 55 normal thyroid tissues. ProNGF was preferentially detected in thyroid cancer cells and rarely in normal thyroid tissues (Figure 2A–2F). ProNGF staining appeared in all tumor types including papillary, follicular, medullary and anaplastic carcinomas. Digital quantification of staining intensities (Figure 2G) confirmed the overexpression of proNGF in cancers as observed in cohort 1. The median h-score for proNGF staining was 7.2 in normal thyroid tissues, 21.7 in adenomas and and 54.6 in cancers ($p<0.0001$). The difference in h-score was not different between normal and adenomas, but was significantly different between cancer and adenomas ($p<0.0001$). The ROC curve of cancer versus normal (Figure 2H) indicated an AUROC of 0.98 (95% CI 0.97-0.99, $p<0.0001$). There were not

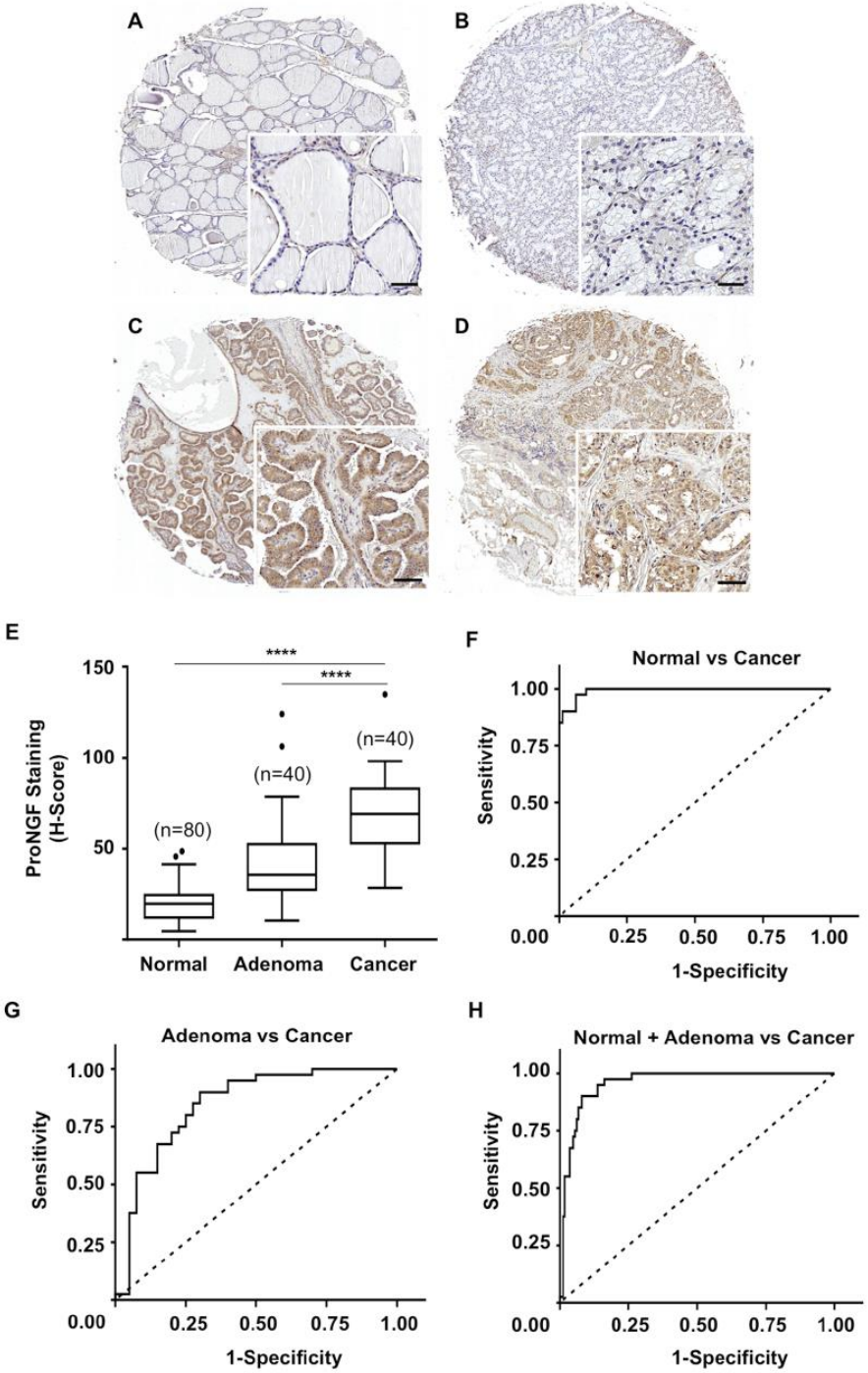

Figure 1: ProNGF expression in cohort 1 of thyroid cancers *versus* adenomas and normal tissues. A–D. Immunohistochemical detection of proNGF was performed with a polyclonal antibody on a series of thyroid cancers (n=40), adenoma (n=40) and normal thyroid tissues (n=80). ProNGF was found in epithelial cells with a marked increased in cancer tissues. Representative pictures are shown for normal thyroid tissue (A), adenoma (B), papillary carcinoma (C), follicular carcinoma (D). Scale = 50µm. **E.** Quantification of proNGF staining intensities was performed using the Halo™ image analysis platform, h-scores were calculated and used to establish the ROC curves. ProNGF staining intensities were significantly higher for cancers (median h-score = 69.3) than adenomas (median h-score = 35.5) and normal tissues (median h-score = 19.7) ($p<0.0001$). The box limits indicate the 25th and 75th percentiles with the whiskers extending 1.5 times the interquartile range from the 25th and 75th percentiles (outliers are represented by dots) (****$p<0.0001$). **F–H.** ROC curves for proNGF staining intensity levels in thyroid cancers versus adenomas and normal thyroid tissues were established and analyzed using GraphPad™. The area under the curve was 0.99 (95% CI 0.98-1.00, $p<0.0001$) for cancers *versus* normal samples (F), 0.84 (95% CI 0.75-0.93, $p<0.0001$) for cancers *versus* adenomas (G), and 0.95 (95% CI 0.85-0.96, $p<0.0001$) for cancers *versus* adenomas and normal samples (H).

Table 1: ProNGF expression in thyroid cancers versus adenomas and normal tissues (cohort 1) and associations with clinicopathological parameters

Parameters	ProNGF Intensity				*p*-value
	0	1	2	3	
Normal vs. Cancer					**< 0.0001**
Normal (n=80)	62 (78%)	18 (22%)	0 (0%)	0 (0%)	
Adenoma (n=40)	5 (13%)	24 (60%)	8 (20%)	3 (7%)	
Cancer (n=40)	0 (0%)	7 (18%)	17 (42%)	16 (40%)	
Clinical Parameters in Cancers					
Histological Type					**0.0006**
Follicular (n=8)	0 (0%)	1 (12%)	5 (63%)	2 (25%)	
Papillary (n=26)	0 (0%)	1 (4%)	11 (42%)	14 (54%)	
Medullary (n=6)	0 (0%)	5 (83%)	1 (17%)	0 (0%)	
Gender					0.9952
Female (n=30)	0 (0%)	5 (17%)	13 (43%)	12 (40%)	
Male (n=10)	0 (0%)	2 (20%)	4 (40%)	4 (40%)	
Age (Years)					0.4385
<50 (n=24)	0 (0%)	4 (17%)	8 (33%)	12 (50%)	
≥50 (n=16)	0 (0%)	3 (19%)	9 (56%)	4 (25%)	
Tumour Size (T)					0.9254
T1 + T2 (n=14)	0 (0%)	3 (21%)	5 (36%)	6 (43%)	
T3 + T4 (n=26)	0 (0%)	4 (15%)	12 (46%)	10 (39%)	
Lymph Node Status					0.9055
Negative (n=37)	0 (0%)	6 (16%)	16 (43%)	15 (41%)	
Positive (n=3)	0 (0%)	1 (33%)	1 (33%)	1 (33%)	
Stage					0.6106
I + II (n=25)	0 (0%)	4 (16%)	9 (36%)	12 (48%)	
III + IV (n=15)	0 (0%)	3 (20%)	8 (54%)	4 (26%)	

Pro NGF immunohistochemical staining in each sample was quantified and categorized as 0 = no staining (h-score <25), 1 = low staining (h-score 25-50), 2 = intermediate staining (h-score 50-75), 3 = strong staining (h-score >75). Representative pictures and corresponding ROC curves are presented in Figure 1. For each category, the number of cases is indicated, and the corresponding percentage is under brackets. Statistically significant p-values ($p<0.05$ using chi-square test) are shown in bold and were confirmed in Log linear analysis.

enough adenoma cases (n=6) in this cohort to draw a relevant ROC curve for proNGF intensities between adenomas and cancer. The categorization of proNGF staining intensities is presented in Table 2. High levels of proNGF (staining intensities 2 and 3) were found in 60% of thyroid cancer, particularly in the papillary and follicular types, as compared to 0% of normal tissue and adenoma samples (p<0.0001). Considering the distribution of proNGF in the different histological types of thyroid cancers, papillary carcinomas presented with 74% of high proNGF staining intensities (staining intensities 2 and 3) compared to 34% of follicular carcinomas and 25% of anaplastic carcinomas (p<0.0001). This association of proNGF expression with papillary histological types was confirmed in Log linear analysis (p=0.0098), controlling for stage and gender. In addition, the odds of papillary relative to follicular cancer were increased by a factor of 2.07 for increased proNGF level (p=0.039). There was evidence of crude associations of proNGF expression with

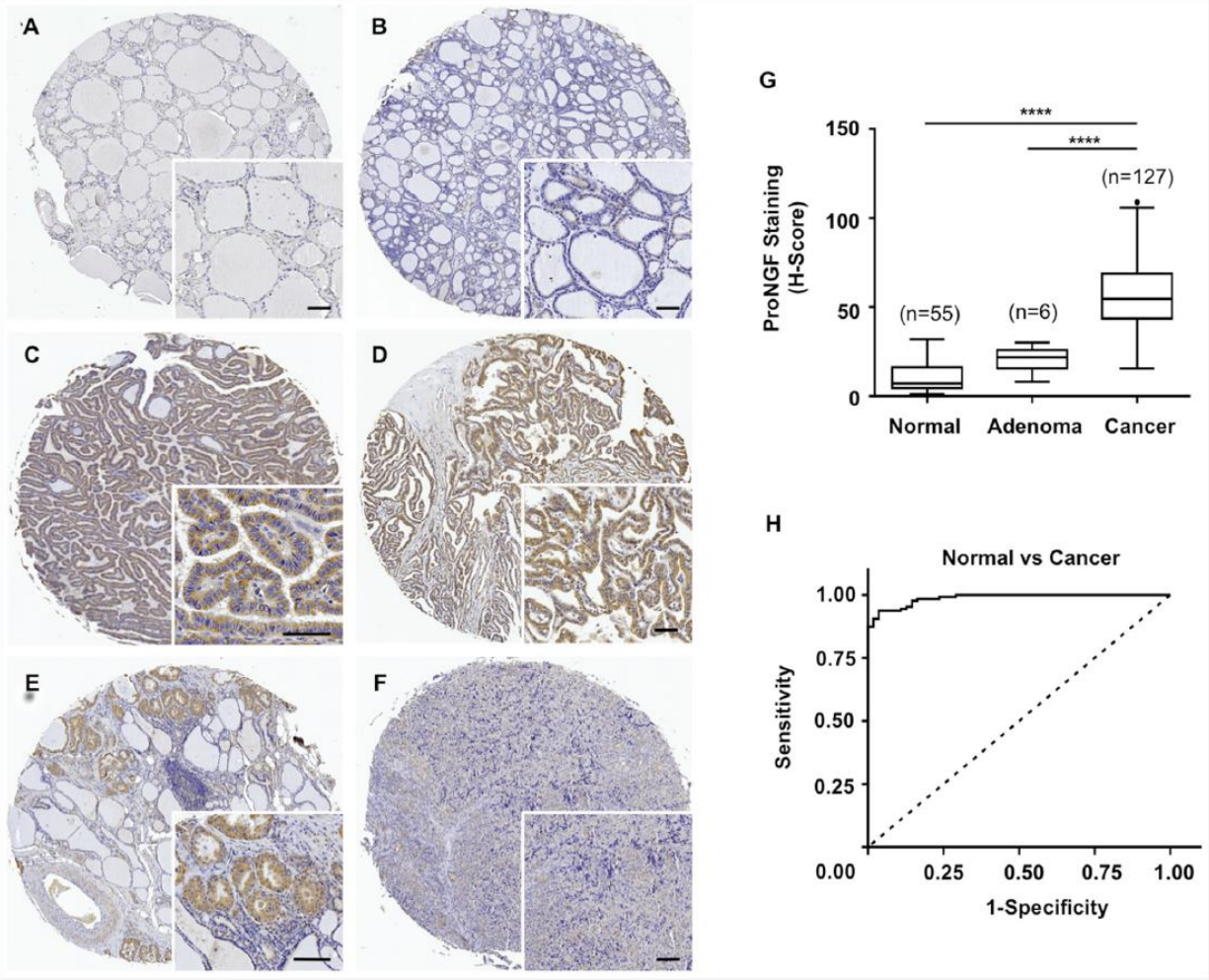

Figure 2: ProNGF expression in cohort 2 of thyroid carcinomas of different histological types *versus* normal tissues. A-F. Immunohistochemical detection of proNGF in thyroid cancers of various histological types (n=127 cases), adenomas (n=6) and normal thyroid tissues (n=55) was performed witha monoclonal antibody. ProNGF was found in epithelial cells with a marked increased in cancer tissues. Representative pictures are shown for normal thyroid tissue (A), adenoma (B), papillary carcinoma (C), follicular carcinoma (D), medullary carcinoma (E), and anaplastic carcinoma (F). Scale = 50µm. **G.** Quantification of proNGF staining intensities was performed using the Halo™ image analysis platform, h-scores were calculated and used to establish the ROC curves. ProNGF staining intensities were significantly higher for cancers (median h-score = 54.6) than adenomas (median h-score = 21.7) and normal tissues (median h-score = 7.2). The box limits indicate the 25th and 75th percentiles with the whiskers extending 1.5 times the interquartile range from the 25th and 75th percentiles (outliers are represented by dots) (****$p<0.0001$). **H.** The ROC curve for proNGF staining intensity levels in thyroid cancers *versus* normal thyroid tissues was established and analyzed using GraphPad™. The area under the ROC curve was 0.98 (95% CI 0.97-0.99, $p<0.0001$).

gender ($p=0.004$), but this was not confirmed in Log linear analysis. No significant associations ($p<0.05$) were found between proNGF expression and other clinicopathological parameters (age, tumor size, stage and lymph node status).

DISCUSSION

This study reports for the first time the expression of proNGF in thyroid cancer, and has shown a potential value of this growth factor as a biomarker to differentiate thyroid cancer from adenoma and normal thyroid. The molecular pathogenesis of thyroid cancer remains to be clarified, but abnormalities in key signaling pathways have been described [20]. Genetic and epigenetic alterations in thyroid tumors include mutations ($BRAF^{V600E}$, Ras, PI3K, PTEN, p53, b-catenin, anaplastic lymphoma kinase), translocation (RET-PTC) and paired box 8 (PAX8)-peroxisome proliferator-activated receptor-g (PPARG) as well as aberrant gene methylation (retinoic acid receptor beta, and tissue inhibitor of metalloprotease 3) [20]. Gene amplifications and copy-number gains have also

Table 2: ProNGF expression in thyroid cancers of different histological types (cohort 2) and associations with clinicopathological parameters

Parameter	ProNGF Intensity				*p*-value
	0	1	2	3	
Normal vs. Cancer					**< 0.0001**
Normal (n=55)	53 (96%)	2 (4%)	0 (0%)	0 (0%)	
Adenoma (n=6)	5 (83%)	1 (17%)	0 (0%)	0 (0%)	
Cancer (n=127)	8 (6%)	43 (34%)	53 (42%)	23 (18%)	
Clinical Parameters in Cancers					
Histological Type					**< 0.0001**
Follicular (n=26)	1 (4%)	16 (62%)	7 (26%)	2 (8%)	
Papillary (n=79)	1 (1%)	20 (25%)	38 (49%)	20 (25%)	
Anaplastic (n=12)	5 (42%)	4 (33%)	3 (25%)	0 (0%)	
Others (n=10)	1 (10%)	3 (30%)	5 (50%)	1 (10%)	
Gender					**0.0004**[#]
Female (n=100)	2 (2%)	35 (35%)	41 (41%)	22 (22%)	
Male (n=27)	6 (22%)	8 (30%)	12 (44%)	1 (4%)	
Age (Years)					0.8519
<50 (n=74)	4 (5%)	24 (33%)	31 (42%)	15 (20%)	
≥50 (n=53)	4 (8%)	19 (35%)	22 (42%)	8 (16%)	
Tumour Size (T)					0.0929
T1 + T2 (n=29)	2 (7%)	6 (21%)	15 (51%)	6 (21%)	
T3 + T4 (n=59)	4 (7%)	28 (47%)	21 (36%)	6 (10%)	
Missing (n=39)	2 (5%)	9 (23%)	17 (44%)	11 (28%)	
Lymph Node Status					0.3055
Negative (n=68)	6 (9%)	24 (35%)	27 (40%)	11 (16%)	
Positive (n=17)	0 (0%)	9 (53%)	7 (41%)	1 (6%)	
Missing (n=42)	2 (5%)	10 (24%)	19 (45%)	11 (26%)	
Stage					0.1041
I + II (n=54)	1 (2%)	22 (41%)	22 (41%)	9 (16%)	
III + IV (n=34)	5 (15%)	12 (35%)	14 (41%)	3 (9%)	
Missing (n=39)	2 (5%)	9 (23%)	17 (44%)	11 (28%)	

Pro NGF immunohistochemical staining in each sample was quantified and categorized as 0= no staining (h-score <25), 1 = low staining (h-score 25-50), 2 = intermediate staining (h-score 50-75), 3 = strong staining (h-score >75). Representative pictures and corresponding ROC curves are presented in Figure 2. For each category, the number of cases is indicated and the corresponding percentage is under brackets. Statistically significant p-values ($p<0.05$ using chi-square test) are shown in bold and were confirmed in Log linear analysis for normal vs cancer and histological types.
[#]The association with gender was not confirmed in Log linear analysis.

been described, particularly for genes encoding receptor tyrosine kinases such as EGFR, VEGFR, KIT, MET and PDGF [20]. Interestingly, gene rearrangements of the neurotrophin receptor TrkA have also been reported to play a role in thyroid tumor progression [21, 14, 15, 16]. Although the molecular alterations described so far in thyroid cancer provided opportunities for clinical development as biomarkers and therapeutic targets, their clinicopathological significance has not been demonstrated. Molecular markers such as RAS,

BRAF, PAX8/PPARc, RET/PTC, may be considered for indeterminate cytology according to American Thyroid Association guidelines [22]. However, the American Association of Clinical Endocrinologists and the European Thyroid Association do not currently recommend these markers in routine practice but reserved them for selected cases due to theirs inconsistent results and relatively high costs [23]. In this context, our study demonstrating the overexpression of proNGF in thyroid cancer points to the potential clinical utility of a novel and reliable growth factor as a new diagnostic biomarker. A microquantification of proNGF could eventually be applied to fine needle aspirates, and help to categorize the indeterminate/suspicious samples, but this warrants further technical investigations. The accurate preoperative diagnosis of thyroid cancer continues to be a significant challenge. No individual thyroid cancer biomarker has been found with sufficient sensitivity and specificity [2]. However, a panel comprised of GAL3, CK19 and HBME1 is by far the most studied to date and offers some improvement over individual marker performance alone [2]. In the future, it would be important to evaluate the diagnostic performance of proNGF in comparison and combination with the currently used biomarkers.

In terms of gene expression, NGF mRNA abundance has not been reported to be linked to a particular clinicopathological parameter in thyroid cancer. Before investigating proNGF protein levels by immunohistochemistry, we have performed a data mining of NGF gene expression, using cBioportal [24], of thyroid datasets in The Cancer Genome Atlas (TCGA) database [25]. NGF mRNA upregulation was found in only 23 out of 507 patient cases, representing only 5% of the total number of cases. Also, a point mutation (K153R) was found in one single patient. No cases of NGF mRNA downregulation were detected. Initial studies in yeast have suggested a correlation of about 50% between mRNA and protein levels [26], and in humans, global transcriptomic and proteomic analyses have shown that only an estimated 30% of changes in protein levels can be explained by corresponding variations in mRNA [27]. Interestingly, a recent proteogenomic investigation in colorectal cancer has also revealed that mRNA abundance does not reliably predict differences in tumoral protein levels [28]. This emphasizes the importance of analysing proteins directly in cancer tissue, to define new biomarkers and therapeutic targets in oncology.

ProNGF expression has been reported in melanoma [13], breast [10] and prostate [10] cancers. In melanoma and breast cancer, proNGF stimulates invasion of cancer cells [10, 12], whereas in prostate cancer, proNGF participates in nerve infiltration into the tumor [12]. Interestingly, in breast and prostate cancers, higher levels of proNGF were reported in malignant tumors compared to benign tissues [10, 12]. Therefore, proNGF overexpression appears to be a feature of several cancers, including thyroid cancer as demonstrated in the present study. The use of two different antibodies (polyclonal and monoclonal) further strengthens the demonstration that proNGF is overexpressed in thyroid cancer. Unspecific cross-reactivity of antibodies is a potential pitfall of IHC. Not only we have performed the necessary negative controls, but also the same overexpression of proNGF was observed using the two antibodies, and this is reassuring that it is indeed specific to proNGF. In addition, we have not detected any association between proNGF expression and the presence of nerve fibers in thyroid tumors. Nerve fibers were seen in less than 5% of thyroid cancers and this was independent of proNGF expression (data not shown). Therefore, in contrast to prostate cancer [12], the expression of proNGF in thyroid cancer is not related to nerve infiltration. In the nervous system, proNGF binds to a complex between sortilin and $p75^{NTR}$ or TrkA, depending on the relative receptor concentrations at the cell surface [2, 29]. In thyroid cancer, TrkA expression and gene rearrangements have been reported [21, 14, 15, 30] and given the tyrosine kinase activity of TrkA, it participates in the deregulation of thyroid cancer cell growth [16, 17]. It has also been shown that $p75^{NTR}$ is widely expressed in papillary thyroid carcinoma [18] and sortilin is expressed in thyroid epithelial cells, where it contributes to the recycling of the thyroid hormone precursor thyroglobulin [31]. However, the determination of a biological activity for proNGF has not been investigated here. Also additional questions arise, such as the effects of proNGF expression on therapeutic and external accidental ionizing radiation of the thyroid. Together, further *in vitro* and *in vivo* experiments are warranted to define a possible function for this growth factor in thyroid cancer progression.

In conclusion, this study demonstrates an increased level of proNGF in thyroid cancers and suggests that this growth factor has potential as a new diagnostic biomarker. In addition, as proNGF is a secreted protein, its potential value as a blood biomarker should also be considered. Together, further investigations to assess the impact and clinical utility of proNGF in thyroid cancer are warranted.

MATERIALS AND METHODS

Thyroid tissue samples

High-density tumor microarrays (TMA, TH801, TH802, TH804, TH641, TH8010) were obtained from Biomax (Maryland, USA). Cohort 1 included 40 thyroid cancers (26 papillary, 8 follicular, 6 medullary) (TH802), 40 adenomas (TH802) and 80 normal thyroid glands (TH804). Cohort 2 included 127 thyroid cancers (79 papillary, 26 follicular, 12 anaplastic, 10 from other histological subtypes) (TH801, TH641, TH8010), 6 adenomas (TH641) and 55 normal thyroid tissues (TH801, TH8010). Cohort 2 also included the following clinicopathological information: patient age and sex,

histological type, tumor size, lymph node status and stage. No information on treatment and patient survival was available. The small core size (1.5 mm diameter) and the bias introduced by sampling is a general limitation of using TMAs. Biomax (USA) quality controls are described as follows. Each single tissue spot on every array slide is individually examined by pathologists certified according to WHO published standardizations of diagnosis, classification and pathological grade. Pathological re-confirmation report is generated and digital image captured. Standard immunohistochemistry tests are also performed to ensure the accuracy and specificity of tissue array products. Each specimen collected from any clinic was consented to by both hospital and individual. Discrete legal consent form was obtained and the rights to hold research uses for any purpose or further commercialized uses were waived. The study was approved by the Human Research Ethic Committee of the University of Newcastle, Australia.

Immunohistochemistry

After deparaffinization and rehydration of TMA slides following standard procedures, heat induced epitope retrieval was carried out in a low pH, citrate based antigen unmasking solution (Vector Laboratories, California, USA, catalogue number H-3300) using a decloaking chamber (Biocare, West Midlands, United Kingdom) at 95°C for 20min. After inactivation of endogenous peroxidases with 0.3% H_2O_2, and blocking with 2.5% horse serum, anti-proNGF antibodies were applied to the sections and revealed with DAB Peroxidase (HRP) Substrate Kit (Vector Laboratories, California, USA, catalogue number SK-4100). Two different anti-proNGF antibodies were used. A polyclonal anti-proNGF antibody (Merck Millipore, Darmstadt, Germany, catalogue number AB9040) was used at 1/200 for cohort 1, and a monoclonal anti-proNGF antibody made against the proNGF propeptide sequence (in house from Biomerieux, Marcy l'Etoile, France) was used at 2.5 µg/ml for cohort 2. Specific controls of the used antibodies are shown in Supplementary Figure S1. In Western-blotting both the polyclonal and monoclonal antibodies recognized proNGF but not NGF (Supplementary Figure S1A). In addition, negative controls with no primary antibodies or control isotype antibodies (Mouse (G3A1) mAb IgG1 Isotype Control, Cell Signaling Technology, Massachusetts, USA, catalogue number #5415) were also performed (Supplementary Figure S1B, C). TMA slides were also counterstained with hematoxylin (Gill's formulation, Vector Laboratories, California, USA), dehydrated and cleared in xylene before mounting in Ultramount #4 mounting media (Thermo Fisher Scientific, Victoria, Australia). Imaging was performed on an Axioplan-2 microscope (Carl Zeiss AG, Oberkochen, Germany).

Digital quantification of immunohistochemistry

For quantification of proNGF staining, TMA slides were digitized at 200x absolute resolution using an Aperio AT2 scanner (Leica Biosystems, Victoria, Australia). Quantitative IHC analyses were performed using the Halo™ image analysis platform (Indica Labs, New Mexico, USA) under the supervision of a pathologist (MMW). The pixel intensities of DAB staining were calculated using the Area Quantification algorithm. Pixel intensity values were then used to determine the h-scores for each core (index calculated as the sum of 3 x % of pixels with strong staining + 2 x % of pixels with intermediate staining + 1 x % pixels with weak staining). To compare proNGF levels across the cohort, the h-scores were used to divide cases into 4 categories (0 = h-score <25, 1 = h-score 25-50, 2 = h-score 50-75, 3 = h-score >75).

Statistical analyses and determination of associations with clinicopathological parameters

The staining intensity for proNGF was compared with clinicopathological parameters: normal *versus* malignant, patient age and gender, histological type, tumor size, stage, lymph node status. For statistical analysis, simple unadjusted associations with pathological variables were performed using a chi-squared test. We used log-linear models to adjust the various bivariate associations for other potential confounders. The log linear models provided a Chi-squared test adjusted for all other variables in the model. The model for the cross-classified counts was specified as a Poisson generalised linear model with a log-link function. Using hierarchical nesting of models we looked at all 3-way then 2-way interactions involving proNGF intensity (modelled as an ordinal variable). Goodness of fit was tested using G^2 Chi-squared statistics (comparing the log likelihood to that obtained from the saturated model). Nested models were compared by calculating differences in G^2 statistics and were used to assess removal (a non-significant reduction in fit) of terms to the model. The prognostic value of the biomarker was expressed using the area under the receiver-operating characteristic (AUROC) curve; values close to 0.5 indicate performance close to chance, while values close to 1 indicate near perfect discrimination. These models were fitted using SAS (SAS Institute, North Carolina, USA).

Abbreviations

AUROC, area under the receiver-operating characteristic curve; **CI,** confidence interval; **FNAB**, fine needle aspiration biopsy; **NTRK1,** neurotrophin receptor tyrosine kinase 1; **p75^{NTR}**, p75 neurotrophin receptor; **NGF**, nerve growth factor; **proNGF,** NGF precursor; **TMA,** tumor microarray.

ACKNOWLEDGMENTS

This work was supported by the University of Newcastle (Australia), the Hunter Cancer Research Alliance (Australia) and the INSERM (France). We thank Mrs Helen Carpenter for excellent technical assistance, and the Clinical Research Design, IT, and Statistical Support (CReDITSS) Unit of the University of Newcastle.

CONFLICTS OF INTEREST

HH, YD and GC are inventors on patent US 20130171173 A1 "Method for proNGF assay for *in vitro* diagnosis of cancer in particular breast, thyroid or lung cancer and therapeutic use of proNGF".

Author contributions

SF, SR and YD performed the immunohistochemistry. Tissue slide analyses and quantification were performed by MMW (histopathologist), and confirmed by HH. SF prepared all Figures and Tables. GC, PL and JP contributed to the elaboration of the monoclonal antibody against proNGF. JA and CO supervised the statistical analyses. HH conceived and supervised the study and also drafted the manuscript. All authors have read and approved the final manuscript.

REFERENCES

1. Tuttle RM, Ball DW, Byrd D, Dilawari RA, Doherty GM, Duh QY, Ehya H, Farrar WB, Haddad RI, Kandeel F, Kloos RT, Kopp P, Lamonica DM, Loree TR, Lydiatt WM, McCaffrey JC, Olson JA, Jr., Parks L, Ridge JA, Shah JP, Sherman SI, Sturgeon C, Waguespack SG, Wang TN, Wirth LJ, National Comprehensive Cancer Network. Thyroid carcinoma. J Natl Compr Canc Netw. 2010; 8:1228-74.
2. Griffith OL, Chiu CG, Gown AM, Jones SJ, Wiseman SM. Biomarker panel diagnosis of thyroid cancer: a critical review. Expert Rev Anticancer Ther. 2008; 8:1399-413.
3. Bradshaw RA, Pundavela J, Biarc J, Chalkley RJ, Burlingame AL, Hondermarck H. NGF and ProNGF: Regulation of neuronal and neoplastic responses through receptor signaling. Adv Biol Regul. 2015; 58:16-27.
4. Lee R, Kermani P, Teng KK, Hempstead BL. Regulation of cell survival by secreted proneurotrophins. Science 2001; 294:1945-8.
5. Nykjaer A, Willnow TE. Sortilin: a receptor to regulate neuronal viability and function. Trends Neurosci. 2012; 35:261-70.
6. Nykjaer A, Lee R, Teng KK, Jansen P, Madsen P, Nielsen MS, Jacobsen C, Kliemannel M, Schwarz E, Willnow TE, Hempstead BL, Petersen CM. Sortilin is essential for proNGF-induced neuronal cell death. Nature 2004; 427:843-8.
7. Fahnestock M, Yu G, Michalski B, Mathew S, Colquhoun A, Ross GM, Coughlin MD. The nerve growth factor precursor proNGF exhibits neurotrophic activity but is less active than mature nerve growth factor. J Neurochem. 2004; 89:581-92.
8. Howard L, Wyatt S, Nagappan G, Davies AM. ProNGF promotes neurite growth from a subset of NGF-dependent neurons by a p75NTR-dependent mechanism. Development 2013; 140:2108-17.
9. Masoudi R, Ioannou MS, Coughlin MD, Pagadala P, Neet KE, Clewes O, Allen SJ, Dawbarn D, Fahnestock M. Biological activity of nerve growth factor precursor is dependent upon relative levels of its receptors. J Biol Chem. 2009; 284:18424-33.
10. Demont Y, Corbet C, Page A, Ataman-Onal Y, Choquet-Kastylevsky G, Fliniaux I, Le Bourhis X, Toillon RA, Bradshaw RA, Hondermarck H. Pro-nerve growth factor induces autocrine stimulation of breast cancer cell invasion through tropomyosin-related kinase A (TrkA) and sortilin protein. J Biol Chem. 2012; 287:1923-31.
11. Tomellini E, Touil Y, Lagadec C, Julien S, Ostyn P, Ziental-Gelus N, Meignan S, Lengrand J, Adriaenssens E, Polakowska R, Le Bourhis X. Nerve growth factor and proNGF simultaneously promote symmetric self-renewal, quiescence, and epithelial to mesenchymal transition to enlarge the breast cancer stem cell compartment. Stem Cells 2015; 33:342-53.
12. Pundavela J, Demont Y, Jobling P, Lincz LF, Roselli S, Thorne R, Bond D, Bradshaw RA, Walker MM, Hondermarck H. ProNGF correlates with gleason score and is a potential Driver of Nerve Infiltration in Prostate Cancer. Am J Pathol. 2014; 184:3156-62.
13. Truzzi F, Marconi A, Lotti R, Dallaglio K, French LE, Hempstead BL, Pincelli C. Neurotrophins and their receptors stimulate melanoma cell proliferation and migration. J Invest Dermatol 2008; 128:2031-40.
14. Frattini M, Ferrario C, Bressan P, Balestra D, De Cecco L, Mondellini P, Bongarzone I, Collini P, Gariboldi M, Pilotti S, Pierotti MA, Greco A. Alternative mutations of BRAF, RET and NTRK1 are associated with similar but distinct gene expression patterns in papillary thyroid cancer. Oncogene 2004; 23:7436-40.
15. Greco A, Miranda C, Pierotti MA. Rearrangements of NTRK1 gene in papillary thyroid carcinoma. Mol Cell endocrinol. 2010; 321:44-9.
16. McGregor LM, McCune BK, Graff JR, McDowell PR, Romans KE, Yancopoulos GD, Ball DW, Baylin SB, Nelkin BD. Roles of trk family neurotrophin receptors in medullary thyroid carcinoma development and progression. Proc Natl Acad Sci USA 1999; 96:4540-5.
17. Russell JP, Powell DJ, Cunnane M, Greco A, Portella G, Santoro M, Fusco A, Rothstein JL. The TRK-T1 fusion protein induces neoplastic transformation of thyroid epithelium. Oncogene 2000; 19:5729-35.

18. Rocha AS, Risberg B, Magalhaes J, Trovisco V, de Castro IV, Lazarovici P, Soares P, Davidson B, Sobrinho-Simoes M. The p75 neurotrophin receptor is widely expressed in conventional papillary thyroid carcinoma. Hum Pathol. 2006; 37: 562-8.
19. van der Laan BF, Freeman JL, Asa SL. Expression of growth factors and growth factor receptors in normal and tumorous human thyroid tissues. Thyroid 1995; 5:67-73.
20. Xing M. Molecular pathogenesis and mechanisms of thyroid cancer. Nat Rev Cancer 2013; 13:184-99.
21. Bongarzone I, Vigneri P, Mariani L, Collini P, Pilotti S, Pierotti MA. RET/NTRK1 rearrangements in thyroid gland tumors of the papillary carcinoma family: correlation with clinicopathological features. Clin Cancer Res. 1998; 4:223-8.
22. American Thyroid Association (ATA) Guidelines Taskforce on Thyroid Nodules and Differentiated Thyroid Cancer, Cooper DS, Doherty GM, Haugen BR, Kloos RT, Lee SL, Mandel SJ, Mazzaferri EL, McIver B, Pacini F, Schlumberger M, Sherman SI, Steward DL, Tuttle RM. Revised American Thyroid Association management guidelines for patients with thyroid nodules and differentiated thyroid cancer. Thyroid 2009; 19:1167-214.
23. Gharib H, Papini E, Paschke R, Duick DS, Valcavi R, Hegedus L, Vitti P, Nodules AAETFoT. American Association of Clinical Endocrinologists, Associazione Medici Endocrinologi, and European Thyroid Association medical guidelines for clinical practice for the diagnosis and management of thyroid nodules: executive summary of recommendations. J Endocrinol Invest 2010; 33:51-6.
24. Cerami E, Gao J, Dogrusoz U, Gross BE, Sumer SO, Aksoy BA, Jacobsen A, Byrne CJ, Heuer ML, Larsson E, Antipin Y, Reva B, Goldberg AP, Sander C, Schultz N. The cBio cancer genomics portal: an open platform for exploring multidimensional cancer genomics data. Cancer Discov. 2012; 2:401-4.
25. Cancer Genome Atlas N. Comprehensive molecular portraits of human breast tumours. Nature 2012; 490:61-70.
26. Gygi SP, Rochon Y, Franza BR, Aebersold R. (1999) Correlation between protein and mRNA abundance in yeast. Mol Cell Biol. 1999; 19:1720-30.
27. Vogel C, Marcotte EM. Insights into the regulation of protein abundance from proteomic and transcriptomic analyses. Nat Rev Genet 2012; 13:227-32.
28. Zhang B, Wang J, Wang X, Zhu J, Liu Q, Shi Z, Chambers MC, Zimmerman LJ, Shaddox KF, Kim S, Davies SR, Wang S, Wang P, Kinsinger CR, Rivers RC, Rodriguez H, Townsend RR, Ellis MJ, Carr SA, Tabb DL, Coffey RJ, Slebos RJ, Liebler DC, Nci C. Proteogenomic characterization of human colon and rectal cancer. Nature 2014; 513:382-7.
29. Clewes O, Fahey MS, Tyler SJ, Watson JJ, Seok H, Catania C, Cho K, Dawbarn D, Allen SJ. Human ProNGF: biological effects and binding profiles at TrkA, P75NTR and sortilin. J Neurochem 2008; 107:1124-35.
30. Rabes HM, Demidchik EP, Sidorow JD, Lengfelder E, Beimfohr C, Hoelzel D, Klugbauer S. Pattern of radiation-induced RET and NTRK1 rearrangements in 191 post-chernobyl papillary thyroid carcinomas: biological, phenotypic, and clinical implications. Clin Cancer Res. 2000; 6:1093-103.
31. Botta R, Lisi S, Pinchera A, Giorgi F, Marcocci C, Taddei AR, Fausto AM, Bernardini N, Ippolito C, Mattii L, Persani L, de Filippis T, Calebiro D, Madsen P, Petersen CM, Marino M. Sortilin is a putative postendocytic receptor of thyroglobulin. Endocrinology 2009; 150: 509-18.

4.3 Supplementary Files

www.impactjournals.com/oncotarget/ Oncotarget, Supplementary Materials 2016

SUPPLEMENTARY FIGURE

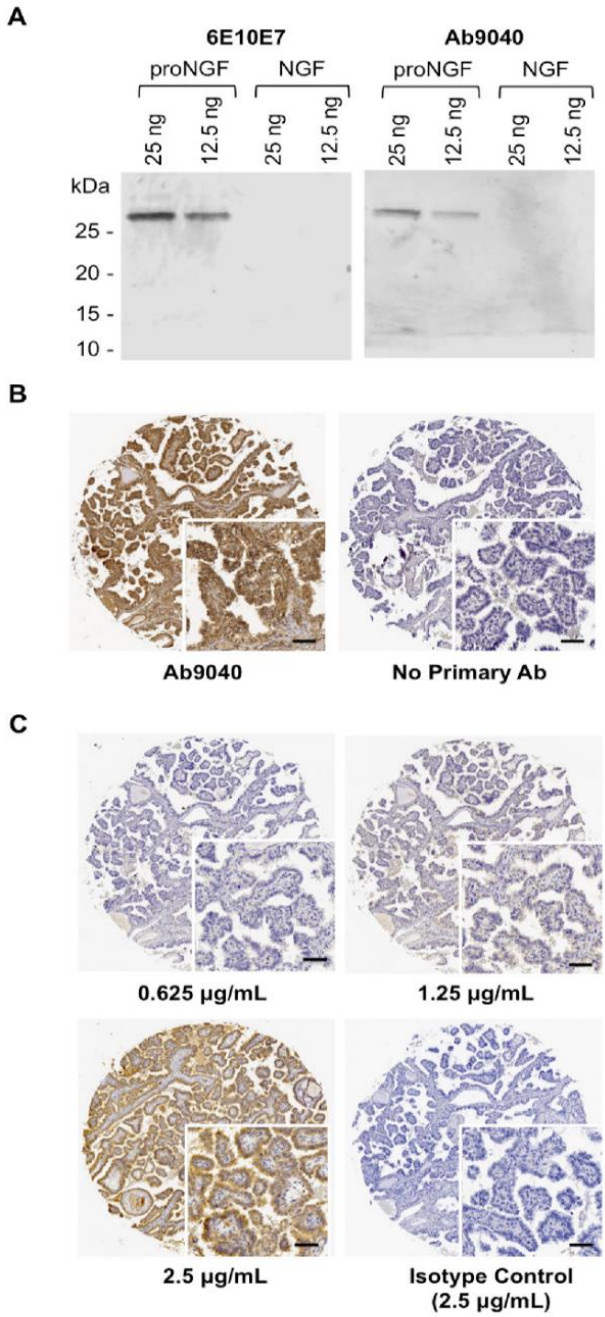

Supplementary Figure S1: Specific controls for proNGF antibodies. A polyclonal anti-proNGF (Ab9040) and a monoclonal anti-proNGF (6E10E7) were tested in Western-blotting and immunohistochemistry. **A.** Western-blotting was performed against proNGF and NGF. Two different quantities per lane (25 ng and 12.5 ng) were used for proNGF and NGF. The two antibodies recognized proNGF but not NGF. **B.** Negative control with no primary antibody in immunohistochemistry (with a papillary thyroid cancer) for the Ab9040 antibody. **C.** Dilution of the 6E10E7 antibody in immunohistochemistry (0.625, 1.25 and 2.5 µg/mL with a papillary carcinoma) and negative control using an isotype control antibody at the concentration of 2.5 µg/mL.

CHAPTER 5 | Neurotrophin Receptors TrkA, p75^{NTR} and Sortilin are Increased and Targetable in Thyroid Cancer

5.1 Preface

Chapter 5 contains an original research article entitled "**Neurotrophin Receptors TrkA, p75^{NTR} and Sortilin are Increased and Targetable in Thyroid Cancer"** which has been accepted for publication in *The American Journal of Pathology*. It serves to build on our findings from Chapter 4 through examining the expression and function of the receptors for proNGF, namely TrkA, p75^{NTR} and sortilin, in thyroid cancer. We show that the expression of TrkA, p75^{NTR} and sortilin is increased in a cohort of thyroid tumours, as compared with adenomas and normal thyroid tissue. Furthermore, TrkA was expressed in nerves found within the tumour microenvironment, whereas p75^{NTR} and sortilin were absent. Additionally, we implicate their activation and downstream signalling as potential principal constituents of tumour aggressiveness in two anaplastic thyroid cancer cell lines.

5.2 Publication

The American Journal of Pathology, Vol. 188, No. 1, January 2018

ELSEVIER

The American Journal of PATHOLOGY

ajp.amjpathol.org

TUMORIGENESIS AND NEOPLASTIC PROGRESSION

Neurotrophin Receptors TrkA, p75^{NTR}, and Sortilin Are Increased and Targetable in Thyroid Cancer

Sam Faulkner,[*†] Philip Jobling,[*†] Christopher W. Rowe,[†‡§] S.M. Rodrigues Oliveira,[*†] Severine Roselli,[*†] Rick F. Thorne,[†] Christopher Oldmeadow,[†¶] John Attia,[†‡] Chen Chen Jiang,[†‡] Xu Dong Zhang,[*†] Marjorie M. Walker,[†‡‖] and Hubert Hondermarck[*†]

From the School of Biomedical Sciences & Pharmacy, Faculty of Health and Medicine, the Hunter Medical Research Institute,[†] the School of Mathematical and Physical Sciences,[¶] Faculty of Science and Information Technology, and the School of Medicine & Public Health,[‡] Faculty of Health and Medicine, University of Newcastle, Callaghan, New South Wales; and the Departments of Endocrinology[§] and Anatomical Pathology,[‖] John Hunter Hospital, Callaghan, New South Wales, Australia*

Accepted for publication September 21, 2017.

Address correspondence to Hubert Hondermarck, Ph.D., School of Biomedical Sciences & Pharmacy, University of Newcastle, Life Sciences Building, Callaghan, NSW 2308, Australia. E-mail: hubert.hondermarck@newcastle.edu.au.

Neurotrophin receptors are emerging targets in oncology, but their clinicopathologic significance in thyroid cancer is unclear. In this study, the neurotrophin tyrosine receptor kinase TrkA (also called NTRK1), the common neurotrophin receptor p75^{NTR}, and the proneurotrophin receptor sortilin were analyzed with immunohistochemistry in a cohort of thyroid cancers ($n = 128$) and compared with adenomas and normal thyroid tissues ($n = 62$). TrkA was detected in 20% of thyroid cancers, compared with none of the benign samples ($P = 0.0007$). TrkA expression was independent of histologic subtypes but associated with lymph node metastasis ($P = 0.0148$), suggesting the involvement of TrkA in tumor invasiveness. Nerves in the tumor microenvironment were positive for TrkA. p75^{NTR} was overexpressed in anaplastic thyroid cancers compared with papillary and follicular subtypes ($P < 0.0001$). Sortilin was overexpressed in thyroid cancers compared with benign thyroid tissues ($P < 0.0001$). Neurotrophin receptor expression was confirmed in a panel of thyroid cancer cell lines at the mRNA and protein levels. Functional investigations using the anaplastic thyroid cancer cell line CAL-62 found that siRNA against TrkA, p75^{NTR}, and sortilin decreased cell survival and cell migration through decreased SRC and ERK activation. Together, these data reveal TrkA, p75^{NTR}, and sortilin as potential therapeutic targets in thyroid cancer. *(Am J Pathol 2018, 188: 229–241; https://doi.org/10.1016/j.ajpath.2017.09.008)*

Thyroid cancer is the most common endocrine malignant tumor. Most tumors are derived from thyroid follicular epithelial cells, including papillary thyroid carcinoma (PTC), follicular thyroid carcinoma (FTC), and undifferentiated anaplastic thyroid carcinoma (ATC), whereas medullary thyroid carcinoma (MTC) is derived from neuroendocrine parafollicular cells. Worldwide, the incidence of thyroid cancer is increasing.[1] In part, this is explained by increased detection of indolent disease,[2] and there is a need for improved diagnostic strategies for clinically significant carcinomas.[3] However, recent data have indicated an increase in mortality during the past 3 decades for patients diagnosed with advanced thyroid cancer, suggesting not only a true increase in incidence but also the need for novel treatment strategies for this subgroup.[4] In particular, ATC, the most lethal histologic subtype, carries a high mortality rate, with median survival of <1 year after diagnosis.[5] Thus, the identification of new targets for the diagnosis and treatment of clinically significant thyroid cancer is essential.

Neurotrophin receptors are known to be overexpressed in some human cancers, where they participate in the stimulation of tumor growth and dissemination.[6,7] In particular, recent data have indicated the crucial stimulatory impact of nerve growth factor (NGF) in gastric[8] and pancreatic cancer,[9] where targeting NGF resulted in a strong reduction of tumor growth and metastasis. In thyroid cancer, the overexpression of the precursor for NGF (proNGF) has been

Supported by the University of Newcastle (Australia) and the Hunter Cancer Research Alliance.

Disclosures: None declared.

https://doi.org/10.1016/j.ajpath.2017.09.008

found, suggesting a role in pathogenesis.[10] However, the status of NGF/proNGF receptors in thyroid tissue is not clear. ProNGF binds to a complex between the membrane protein sortilin and the neurotrophin receptor $p75^{NTR}$, initiating various signaling pathways, including NF-κB, RhoA, and JNK.[11] In addition, proNGF has also been found to activate the neurotrophin tyrosine receptor kinase 1 (NTRK1 or TrkA).[11] In thyroid cancer, the expression of sortilin has never been reported, and although $p75^{NTR}$[12] and TrkA[13] are expressed, their clinicopathologic significance is not defined.

In this study, we found the increased expression of TrkA, $p75^{NTR}$, and sortilin in a cohort of thyroid cancers compared with benign thyroid tissues (adenomas and normal thyroid tissues). Furthermore, *in vitro* experiments revealed that targeting these neurotrophin receptors resulted in a decreased growth and invasion of ATC cells, suggesting a potential utility as therapeutic targets.

Materials and Methods

Thyroid Tissue Samples

High-density tumor microarrays (TH801, TH641, TH8010) were obtained from US Biomax Inc. (Rockville, MD) and included 128 thyroid cancers (79 PTCs, 27 FTCs, 12 ATCs, 10 other subtypes), 6 adenomas, and 56 normal thyroid tissues. The other subtypes were follicular papillary carcinomas ($n = 6$), sarcomatoid carcinomas ($n = 1$), and MTCs ($n = 3$). Within the 27 cases of FTC, 3 cases were characterized as poorly differentiated, and 5 were characterized as moderately differentiated. The following information was available: patient age and sex, histologic subtype, tumor size, lymph node status, and stage. US Biomax Inc. quality controls are described as follows. Each single tissue spot on every array slide is individually examined by pathologists certified according to World Health Organization published standardizations of diagnosis, classification, and pathologic grade. Each specimen collected was consented to by both hospital and individual. Discrete legal consent was obtained, and the rights to hold research uses for any purpose or further commercialized uses were waived. The study was approved by the Human Research Ethics Committee of the University of Newcastle, Australia.

Immunohistochemistry and Digital Quantification

Immunohistochemistry and digital quantification of staining intensities were performed as previously described.[10] Antibodies against TrkA (1/200 dilution, catalog number 2508; Cell Signaling Technology, Danvers, MA), $p75^{NTR}$ (1/400 dilution, catalog number 4201; Cell Signaling Technology), sortilin (0.8 μg/mL, catalog number ANT-009; Alomone Labs, Jerusalem, Israel), or PGP9.5 (1/200 dilution, catalog number ab15503; Abcam, Cambridge, United Kingdom) were applied. Negative controls with a rabbit monoclonal antibody IgG Isotype Control (DA1E, catalog number 3900; Cell Signaling Technology) were also performed (Supplemental Figure S1A). The specificity of the antibodies used for immunohistochemistry was assessed using Western blot analysis in a panel of thyroid tumor tissue samples (Supplemental Figure S1B). Thyroid tumor samples included one FTC and three PTCs. Specificity was also confirmed in the PC-12 cell line, which is known to express neurotrophin receptors (Supplemental Figure S1C). TrkA, $p75^{NTR}$, and sortilin were all found to be expressed at their expected molecular weights (140 kDa for TrkA, 75 kDa for $p75^{NTR}$, and 100 kDa for sortilin) in both the thyroid tumor tissue samples (Supplemental Figure S1B) and PC-12 cells (Supplemental Figure S1C). For quantification of $p75^{NTR}$ and sortilin staining intensity, pixel intensity values were used to determine the h-scores for each core (index calculated as the sum of 3 × percentage of pixels with strong staining + 2 × percentage of pixels with intermediate staining + 1 × percentage of pixels with weak staining). Staining intensities were categorized as negative (h-score < 25), low (h-score of 25 to 100), or high (h-score >100). For TrkA, because of the limited proportion of cells that tested positive for TrkA, it was not possible to calculate a representative h-score; therefore, positivity versus negativity for TrkA staining was recorded. For statistical analyses, staining intensities for $p75^{NTR}$, sortilin, and positivity or negativity for TrkA, were compared with clinicopathologic parameters: normal versus malignant, patient age and sex, histologic type, tumor size, lymph node status, stage, and grade. Simple unadjusted associations with pathologic variables were performed using a χ^2 test with SAS statistical software version 9.4 (SAS Institute, Cary, NC).

Cell Culture

Thyroid cancer cell lines CAL-62 (ATC), BCPAP (PTC), and ML-1 (MTC) were purchased from DSMZ (Braunschweig, Germany), which uses STR verification of cell line authenticity. The TPC-1 (PTC) cell line was obtained from Dr. Mareel's laboratory (University of Gent, Gent, Belgium). The 8505c (ATC) cell line was a generous gift from Prof. Alfred Lam (Griffith University, Queensland, Australia). TPC-1 cell authenticity was validated using the GenePrint 10 System (catalog number B9510, Promega, Madison WI). PC-12 cells were obtained from Prof. Ralph A. Bradshaw (University of California, San Francisco, CA). All cell lines were maintained in RPMI-1640 with 10% (v/v) fetal calf serum (FCS) (JRH Biosciences, Lenexa, KS) and 2 mmol/L L-glutamine in a humidified incubator at 37°C with 5% (v/v) CO_2. Routine *Mycoplasma* testing was performed using the MycoAlert *Mycoplasma* Detection Kit (catalog number LT07-118; Lonza, Basel, Switzerland). Cells were not maintained in culture for longer than 3 months to ensure passage number remained fit for purpose.

Preparation of Conditioned Media

Conditioned media was prepared as previously described.[14] Briefly, 5×10^6 cells were seeded per T-75 cm^2 culture flask and grown in 10 mL of serum free media for 24 hours. The collected medium was centrifuged ($800 \times g$ for 5 minutes at 4°C) and the supernatant was concentrated and desalted using 10-kDa cut-off Amicon Ultra-15 filtration unit (catalog number UFC900324; Merck Millipore, Darmstadt, Germany) for 30 minutes ($4000 \times g$, 4°C). The recovered concentrate was stored at −80°C.

Protein Extraction and Western Blotting

Protein extraction from cell lines and Western blotting experiments were performed as previously described.[15] For protein extraction from thyroid tumors, thyroid tumor tissue samples (obtained from the biobank of the Department of Endocrinology, John Hunter Hospital, Newcastle, Australia) were snap frozen with liquid nitrogen, crushed using a mortar and pestle, and transferred to individual 1.5 mL Precellys CK28 Lysing Tubes (catalog number KT03961-1-007.2; Bertin Technologies, Montigny-le-Bretonneux, France). Samples were lysed on ice using 1 mL of SDS extraction buffer (2% SDS, 1% IGEPAL, 0.5% sodium deoxycholate, 50 mmol/L Tris pH 7.5, 5 mmol/L EDTA). Complete mini-protease inhibitor cocktail tablets (catalog number 4693124001; Roche, Basel, Switzerland) and PhosSTOP phosphatase inhibitor tablets (catalog number 4906837001; Roche) were also used. Samples were homogenized in a Precellys 24 Homogenizer (Bertin Technologies) at $1500 \times g$ (6×30 seconds intervals). Finally, samples were centrifuged at $16{,}000 \times g$ for 15 minutes at 4°C, and the supernatant was extracted and stored at −80°C. Anti-TrkA (catalog number ANT018; Alomone Labs), anti-p75^{NTR} (catalog number sc-6188; Santa Cruz Biotechnology, Dallas, TX), and anti-sortilin (catalog number ANT009; Alomone Labs) antibodies were used at a dilution of 1:500. Anti-proNGF (catalog number ab9040; Merck Millipore) and anti-NGF (catalog number sc-548; Santa Cruz Biotechnology) antibodies were used at a dilution of 1:200. β-Actin detection (1/5000 dilution, catalog number A2066; Sigma-Aldrich, St. Louis, MO) was used as the equal loading control. Antibodies from Cell Signaling Technology were used to assess cellular signaling pathways: anti−phospho-TrkA (anti−p-TrkA) (Tyr490, catalog number 9141), anti-Src (catalog number 2100), anti−phospho-Src (anti−p-Src) (Tyr416, catalog number 2101), anti-Erk1/2 (catalog number 9107), and anti−phospho-Erk1/2 (anti−p-Erk1/2) (Thr202/Tyr204, catalog number 4370).

Real-Time RT-PCR

Total RNA was isolated from thyroid cancer cell lines using the illustra RNAspin Mini RNA Isolation Kit (catalog number 25-0500-70; GE Healthcare Life Sciences, Little Chalfont, UK). Reverse transcription was performed with 1 μg of total RNA using the iScript cDNA Synthesis Kit (catalog number 1708890; Bio-Rad Laboratories Inc., Hercules, CA). Real-time PCR was performed using 2 μL of 1/10 cDNA using iTaq Universal SYBR Green Supermix (catalog number 172-5120; Bio-Rad Laboratories Inc.). The primers used were as follows: sortilin primers were Quantitect Primer Assay QT00073318 (Qiagen, Venlo, Netherlands); p75^{NTR} primers were 5′-ACGG CTACTACCAGGATGAG-3′ (forward) and 5′-TGGCCTCG TCGGAATACGTG-3′ (reverse) (Sigma-Aldrich); TrkA primers were Quantitect Primer Assay QT00054110 (Qiagen); primers used for the reference gene *GAPDH* were 5′-CAC-CAGGGCTGCTTTTAACTCCTGTA-3′ (forward) and 5′-CCTTGACGGTGCCATGGAATTTG-3′ (reverse) (Sigma-Aldrich). PCR was performed in a ABI7500 Real-Time PCR System (Applied Biosystems, Thermo Fisher Scientific, Waltham, MA) using the following conditions: 95°C for 10 minutes, 40 cycles of 95°C for 15 seconds, and 60°C for 60 seconds followed by a continuous Melt curve from 65°C to 95°C. Data were analyzed using the ABI7500 Real-Time software version 2.3 (Applied Biosystems, Thermo Fisher Scientific). Relative expression was obtained using the $2^{-\Delta\Delta Ct}$ method.

Transfection with siRNA

ATC cell lines CAL-62 and 8505c were transfected for 72 hours with 15 nmol/L of siRNA using lipofectamine RNAiMAX (catalog number 13778150; Life Technologies, Carlsbad, CA), according to the manufacturer's recommendations. Cells were seeded in 6-well plates and transfected 24 hours later with siRNA against TrkA (siTrkA, CGAGAACCCA-CAAUACUUCAGUGAT, catalog number SR303249; OriGene Technologies Inc., Rockville, MD), p75^{NTR} (siP75^{NTR}, GGAAUUGACUUCGACUGUGACCUGT, catalog number SR303174; OriGene Technologies Inc.), and sortilin (siSort, CUCUGCUGUUAACACCACC[dT][dT]; Sigma-Aldrich) as well as a commercially available siRNA control sequence: MISSION siRNA Universal negative control 1 (catalog number SIC001; Sigma-Aldrich). The efficiency of TrkA, p75^{NTR}, and sortilin knockdown was assessed using Western blot analysis at 24, 48, and 72 hours after transfection, using anti-TrkA (catalog number ANT018; Alomone Labs), anti-p75^{NTR} (catalog number sc-6188; Santa Cruz Biotechnology), and anti-sortilin (catalog number ANT009; Alomone Labs) antibodies, respectively. β-Actin (catalog number A2066; Sigma-Aldrich) was used as an equal loading control.

Cell Growth and Apoptosis Assay

A total of 7×10^5 ATC cells (CAL-62 and 8505c) were seeded in 2 mL of culture medium (RPMI containing 10% FCS and 2 mmol/L L-glutamine) on 6-well plates and were allowed to adhere overnight in a humidified incubator at 37°C and 5% CO_2. Cells were transfected the following day with siTrkA, siP75^{NTR}, siSort, a combination of the three

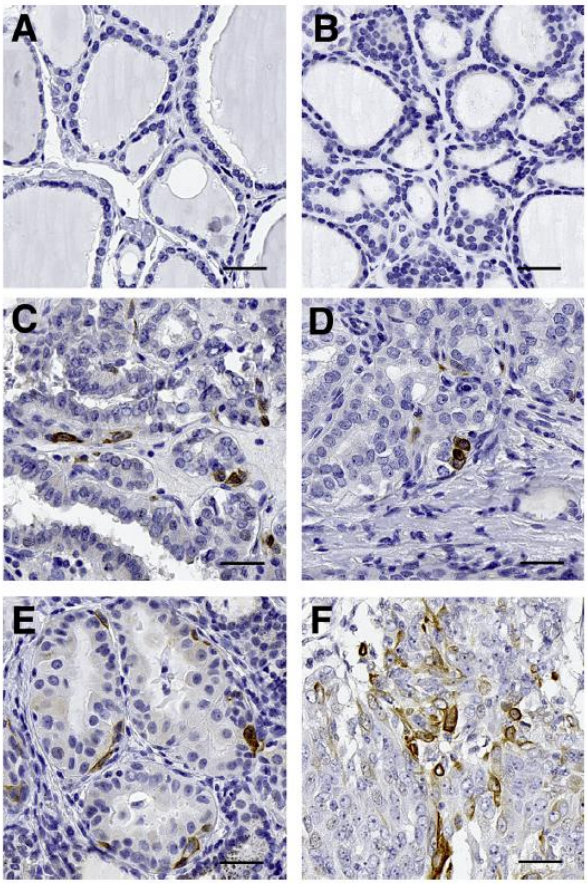

Figure 1 TrkA expression in thyroid cancers. **A–F:** TrkA immunostaining was performed on a cohort of thyroid cancers, adenomas, and normal thyroid tissues. TrkA is not observed in normal thyroid tissues (**A**) or adenomas (**B**). In contrast, TrkA staining is found in papillary thyroid carcinom a (**C** and **D**), follicular thyroid carcinoma (**E**), and anaplastic thyroid carcinoma (**F**) histologic subtypes. Only a small proportion of cancer cells are positive for TrkA. Recording of TrkA positivity is reported in Table 1. n = 128 thyroid cancers, 6 adenomas, and 56 normal thyroid tissues. Scale bars: 50 μm. Original magnification, ×400.

siRNAs (siCombo), or control siRNA (siCont). Images were obtained after 72 hours, and viable cell number was counted using Trypan Blue with a hemocytometer. For assessing apoptosis, 1×10^6 cells were incubated with 100 μL of Muse Annexin V and Dead Cell Reagent (catalog number MCH100105; Merck Millipore, Darmstadt, Germany) for 20 minutes at room temperature as per the manufacturer's instructions. The Muse Cell Analyzer (Merck Millipore) was used to determine apoptosis, and the statistics obtained revealed the percentages of the cells represented by alive, apoptotic, and dead populations.

Cell Migration and Wound-Healing Assay

A total of 5×10^5 ATC cells (CAL-62 and 8505c) were seeded on 6-well plates in complete growth medium (RPMI containing 10% FCS and 2 mmol/L L-glutamine) and were allowed to adhere overnight in a humidified incubator at 37°C and 5% CO_2. Cells were transfected the following day with siTrkA, siP75^{NTR}, siSort, a combination of the three siRNAs (siCombo), or control siRNA (siCont). After 72 hours, during which the cells were allowed to grow to confluence, the cell monolayer was scratched with a 200-μL pipette tip, rinsed three times with phosphate-buffered saline to remove floating cellular debris, and replaced with media that contained 0.1% (v/v) FCS. The wound area that resulted from the scratch was monitored using the JuLI Stage automated cell imaging system (NanoEnTek Inc., Seoul, Korea). Images were taken automatically every 5 hours during a 20-hour postscratch period. Results are shown as the percentage reduction of the wound area, measured using ImageJ version 1.60_20 (NIH, Bethesda, MD; *http://imagej.nih.gov/ij*).

Cell Invasion Assay

Cell invasion assays were performed on CAL-62 and 8505c ATC cells using the QCM ECMatrix Cell Invasion Assay (catalog number ECM554; Merck Millipore), which is made up of 24-well plates and contains upper invasion chamber inserts with 8-μm pore size membranes. The extracellular matrix layer was rehydrated with 300 μL of prewarmed serum free media for 30 minutes at room temperature. Cells were loaded into the invasion chamber insert using 2×10^5 siRNA transfected cells (72 hours after transfection with siTrkA, siP75^{NTR}, siSort, siCombo, and siCont.) in 250 μL of media that contained 0.1% (v/v) FCS. Five hundred microliters of media, in the presence of a chemoattractant (10% FCS), was added to the lower chamber. After a 20-hour incubation period, the upper invasion chamber inserts were rinsed with phosphate-buffered saline, and cells at the upper surface of the membranes were gently scraped and removed. Invading cells were dislodged by placing the invasion chambers in 225 μL of pre-warmed cell detachment buffer before being stained by CyQuant GR Dye (1:75 with 4× lysis buffer) for 15 minutes. Two hundred microliters of the mixture from each sample was transferred to a black 96-well plate (catalog number CLS3792-100; Sigma-Aldrich), and the fluorescence was recorded at 480/520 nm using a FLUOstar OPTIMA fluorescence plate reader (BMG Labtech, Durham, NC). Samples without cells but containing cell detachment buffer, lysis buffer, and CyQuant Dye were used as blanks, and background fluorescence was subtracted from all samples. The number of invading cells was determined by running a fluorescent cell dose standard curve.

Statistical Analysis for *in Vitro* Assays

For cell proliferation, apoptosis, and migration and invasion assays, each condition was performed at least in triplicate, and experiments were repeated on three separate occasions. Statistical analysis was conducted using the GraphPad Prism software version 6 (GraphPad Software Inc., La Jolla, CA). Cell proliferation, apoptosis, migration, and invasion assays

were analyzed using ordinary one-way analysis of variance. For assessing multiple comparisons, Dunnett's multiple comparisons test was used.

Results

The expression of TrkA, p75^{NTR}, and sortilin was analyzed by immunohistochemistry in a series of 128 thyroid cancers of various histologic types, six adenomas, and 55 normal thyroid tissues. In addition, these neurotrophin receptors were detected in thyroid cancer cells in culture, and the functional impact of their targeting using siRNA was investigated.

Gene Versus Protein Expression

We initially started with data mining of gene expression, using cBioportal,[16] of thyroid data sets in The Cancer Genome Atlas database.[17] The results indicated that mRNA for TrkA, p75^{NTR}, and sortilin are overexpressed in 4%, 6%, and 1% of thyroid cancers, respectively. However, mRNA abundance in tumors does not reliably predict differences in protein levels.[18] Therefore, we proceeded with analyzing protein expression.

TrkA Expression in Thyroid Cancers

TrkA staining was not observed in normal thyroid tissue or adenoma samples (Figure 1, A and B). In contrast, TrkA staining was observed in a proportion of PTC (Figure 1C), FTC (Figure 1D), MTC (Figure 1E), and ATC (Figure 1F) histologic subtypes. TrkA staining was observed in only a small proportion (5% to 10%) of cancer cells; hence, digital quantification with h-score calculation did not provide a meaningful comparison of staining intensities among samples. Therefore, TrkA staining was analyzed in terms of TrkA-positive versus TrkA-negative samples (Table 1).

Table 1 TrkA, p75^{NTR}, and Sortilin Expression in Thyroid Cancers and Associations with Clinicopathologic Parameters

	TrkA intensity			p75^{NTR} intensity				Sortilin intensity			
Parameter	Negative, Total (%)	Positive, Total (%)	*P* value	Negative, Total (%)	Low, Total (%)	High, Total (%)	*P* value	Negative, Total (%)	Low, Total (%)	High, Total (%)	*P* value
Normal versus cancer			**0.0007**				**<0.0001**				**<0.0001**
Normal (n = 56)	56 (100)	0 (0)		6 (11)	49 (87)	1 (2)		56 (100)	0 (0)	0 (0)	
Adenoma (n = 6)	6 (100)	0 (0)		0 (0)	6 (100)	0 (0)		4 (67)	2 (33)	0 (0)	
Cancer (n = 128)	102 (80)	26 (20)		3 (2)	57 (45)	68 (53)		48 (38)	79 (61)	1 (1)	
Cancer histologic subtype			0.1020				**<0.0001**				**0.0415**
Papillary (n = 79)	58 (73)	21 (27)		1 (1)	28 (36)	50 (63)		26 (33)	52 (66)	1 (1)	
Follicular (n = 27)	25 (93)	2 (7)		2 (7)	20 (74)	5 (19)		7 (26)	20 (74)	0 (0)	
Anaplastic (n = 12)	9 (75)	3 (25)		0 (0)	1 (8)	11 (92)		9 (75)	3 (25)	0 (0)	
Others (n = 10)	10 (100)	0 (0)		0 (0)	8 (80)	2 (20)		6 (60)	4 (40)	0 (0)	
Sex			1.0000				0.5750				0.8201
Female (n = 101)	80 (80)	21 (20)		3 (3)	46 (45)	52 (52)		37 (37)	63 (62)	1 (1)	
Male (n = 27)	22 (81)	5 (19)		0 (0)	11 (41)	16 (59)		11 (41)	16 (59)	0 (0)	
Age, years			0.3826				0.6287				0.4647
<50 (n = 74)	61 (82)	13 (18)		1 (1)	34 (46)	39 (53)		30 (41)	43 (58)	1 (1)	
≥50 (n = 54)	41 (76)	13 (24)		2 (3)	23 (42)	29 (55)		18 (33)	36 (67)	0 (0)	
Tumor size (T)			0.3686				0.4064				0.3686
T1 + T2 (n = 29)	24 (83)	5 (17)		2 (7)	13 (45)	14 (48)		5 (17)	24 (83)	0 (0)	
T3 + T4 (n = 59)	47 (80)	12 (20)		1 (2)	31 (53)	27 (45)		17 (29)	41 (69)	1 (2)	
Missing (n = 40)	31 (78)	9 (22)		0 (0)	13 (31)	27 (69)		26 (65)	14 (35)	0 (0)	
Lymph node (N)			**0.0148**				0.6772				0.8318
Negative (n = 68)	59 (87)	9 (13)		3 (5)	34 (50)	31 (45)		17 (25)	50 (73)	1 (2)	
Positive (n = 17)	10 (59)	7 (41)		0 (0)	9 (53)	8 (47)		5 (29)	12 (71)	0 (0)	
Missing (n = 43)	33 (77)	10 (23)		0 (0)	14 (31)	29 (69)		26 (60)	17 (40)	0 (0)	
Stage			0.5827				0.6381				0.4719
I + II (n = 54)	45 (83)	9 (17)		2 (4)	29 (53)	23 (43)		12 (22)	41 (76)	1 (2)	
III + IV (n = 35)	27 (77)	8 (23)		1 (3)	16 (44)	18 (53)		11 (31)	24 (69)	0 (0)	
Missing (n = 39)	30 (77)	9 (23)		0 (0)	12 (31)	27 (69)		25 (64)	14 (36)	0 (0)	

Immunohistochemical staining for each neurotrophin receptor was quantified. For TrkA, because only a small proportion of cancer cells were positive for TrkA, immunohistochemical staining in each sample was categorized only as negative versus positive. Representative images for TrkA staining are presented in Figure 1. For p75^{NTR} and sortilin, immunohistochemical staining in each sample was digitally quantified and categorized as negative (h-score <25), low staining (h-score of 25 to 100), or high staining (h-score >100). Representative images for p75^{NTR} and sortilin staining are presented in Figures 3 and 4, respectively. Statistically significant *P* values ($P < 0.05$, using the χ^2 test) are shown in bold.

TrkA positivity was found in 20% of thyroid cancers compared with none of the benign samples ($P = 0.0007$). An association was found between TrkA expression and lymph node metastases, with TrkA positivity observed in 41% of lymph node–positive cancers compared with only 13% of lymph node–negative cancers ($P = 0.0148$). There was no association between TrkA expression and other clinicopathologic parameters (sex, age, tumor size, and stage).

Some staining for TrkA also appears to be in endothelial and other stromal cells. In other models, endothelial cells[19] and fibroblasts[20] have been reported to express TrkA; therefore, it is not unexpected to find some TrkA expression in stromal cells. Interestingly, TrkA expression was also detecte in nerves present in thyroid cancers (Figure 2). The presence of nerves in the tumor microenvironment was validated using the neuronal marker PGP9.5 (Figure 2, A and E). TrkA staining was observed in nerves (Figure 2, B and F), whereas $p75^{NTR}$ (Figure 2C) and sortilin (Figure 2D) were not detected in serial tumor microarray cores.

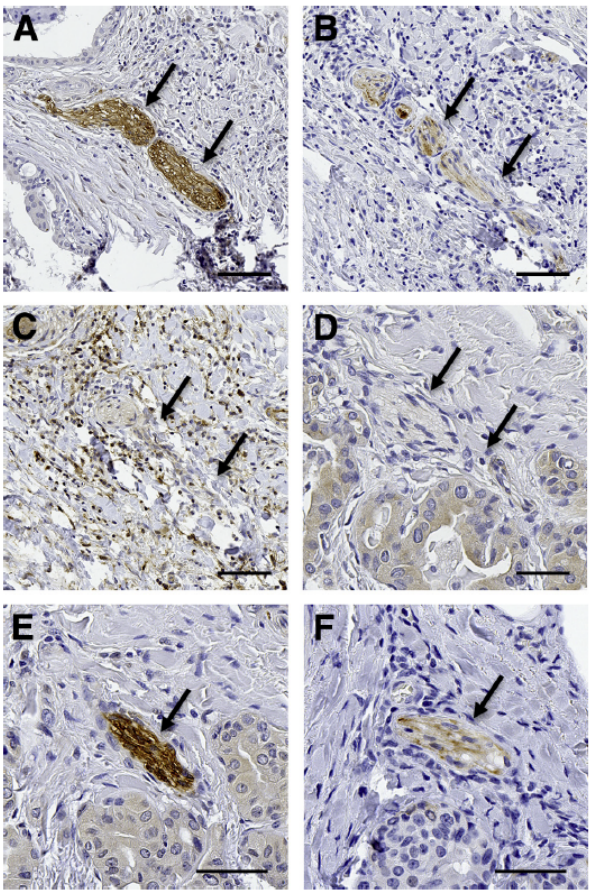

Figure 2 TrkA expression in nerves present in thyroid cancers. Immunohistochemical detection of the neuronal marker PGP9.5 was used to detect nerves in thyroid cancers, and the detection of TrkA, $p75^{NTR}$, and sortilin was performed in serial sections. **A:** Nerves stained for the neuronal marker PGP9.5. **B–D:** Serial sections for the detection of TrkA (**B**), $p75^{NTR}$ (**C**), and sortilin (**D**) in the nerve shown in **A**. **E:** Another nerve stained for PGP9.5. **F:** TrkA staining observed in a serial section of the nerve shown in **E**. **Arrows** indicate the location of nerves. Scale bars: 50 μm. Original magnification, ×400.

$p75^{NTR}$ Expression in Thyroid Cancers

Expression of $p75^{NTR}$ was detected in most benign thyroid tissues and cancers (Figure 3, A–F). Digital quantification of $p75^{NTR}$ staining intensities (Figure 3G) indicated a median combined h-score of 57.86 for benign thyroid tissue compared with 102.5 for thyroid malignant tumors. Within cancer histologic subtypes, $p75^{NTR}$ was expressed at higher levels in ATC, with a median h-score of 130.60 ($P < 0.0001$) compared with 109.30 ($P < 0.0001$) and 76.82 ($P = 0.0054$) in PTC and FTC, respectively (Figure 3G). For analysis of the associations between $p75^{NTR}$ expression and clinicopathologic parameters, $p75^{NTR}$ staining intensities were categorized as negative (h-score <25), low (h-score of 25 to 100), or high (h-score >100). The frequency distribution of staining intensities (Table 1) indicated that most normal tissues, adenomas, and cancers were positive for $p75^{NTR}$, whereas only 0% to 2% of normal tissues and adenomas presented intense $p75^{NTR}$ staining compared with 53% of cancers ($P < 0.0001$). By histologic subtypes, $p75^{NTR}$ was expressed at higher levels in ATC, with high $p75^{NTR}$ staining observed in 92% of ATC compared with 19% of FTC and 63% of PTC ($P < 0.0001$). There was no association between $p75^{NTR}$ expression and sex, age, tumor size, lymph node invasion, and stage (Table 1).

Sortilin Expression in Thyroid Cancers

Sortilin was not detected in normal thyroid tissues (Figure 4A). In adenomas (Figure 4B), weak sortilin labeling was observed in epithelial cells of some tissue samples. Thyroid cancers were positive for sortilin, and the labeling was specifically observed in cancer cells (Figure 4, C–F). Digital quantification of staining intensities (Figure 4G) indicated that sortilin was higher in thyroid cancers compared with normal tissues and adenomas. Normal and adenoma thyroid tissues had a combined median h-score of 15.04 compared with 29.69 ($P < 0.0001$) and 40.80 ($P < 0.0001$) in the FTC and PTC cancer subtypes, respectively (Figure 4G). Sortilin expression in ATC yielded a median h-score of 24.11, which was not significantly different than benign thyroid tissues (normal and adenoma) (Figure 4G). For analysis of the association between sortilin expression and clinicopathologic parameters, sortilin staining intensities were categorized as negative (h-score <25), low (h-score of 25 to 100), or high (h-score >100). The frequency distribution of staining intensities (Table 1) indicated that 62% of thyroid cancers were positive for sortilin compared with 33% of adenomas and 0% of normal tissues ($P < 0.0001$). In terms of histologic subtypes, stronger sortilin staining was observed in FTC and PTC compared with ATC ($P = 0.0415$). There was no association between sortilin expression and other clinicopathologic parameters (sex, age, tumor size, lymph node invasion, and stage).

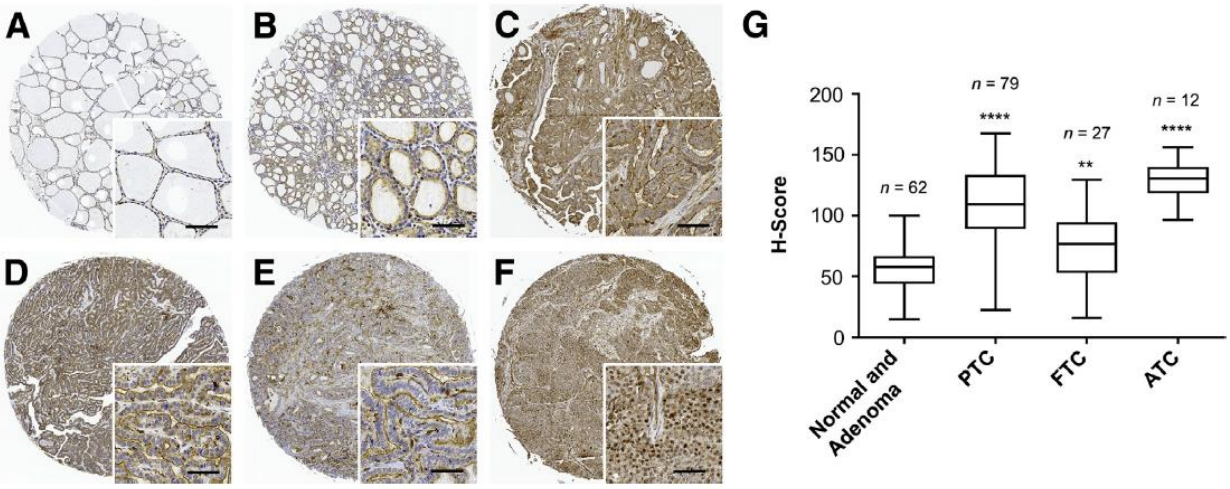

Figure 3 p75^{NTR} expression in thyroid cancers. **A–F:** Immunohistochemical detection of p75^{NTR} in thyroid cancers of various histologic types, adenomas, and normal thyroid tissues was performed. p75^{NTR} was found in epithelial cells of normal tissue (**A**), adenomas (**B**), and thyroid cancers of various histologic subtypes: papillary thyroid carcinoma (PTC) (**C** and **D**), follicular thyroid carcinoma (FTC) (**E**), and anaplastic thyroid carcinoma (ATC) (**F**). **Insets** show higher magnification. **G:** p75^{NTR} staining was quantified using the Halo image analysis platform; h-scores were calculated. p75^{NTR} staining intensities are significantly higher for ATC (median h-score = 130.60), PTC (median h-score = 109.30), and FTC (median h-score = 76.82) compared with normal and adenoma thyroid tissues combined (median h-score = 57.86). Data are expressed as means (horizontal line in center of box), 25th and 75th percentiles (box limits), and interquartile ranges (whiskers) (**G**). n = 128 thyroid cancers, 6 adenomas, and 56 normal thyroid tissues. $^{**}P < 0.01$, $^{****}P < 0.0001$ versus normal/adenoma tissue controls. Scale bars: 50 μm (**A–F**). Original magnification: ×50 (**A–F, main images**); ×400 (**insets**).

TrkA, p75^{NTR}, and Sortilin Expression in Thyroid Cancer Cell Lines

Real-time RT-PCR and Western blot analysis were used to detect TrkA, p75^{NTR}, and sortilin at the mRNA and protein levels in a series of thyroid cancer cell lines. The data (Figure 5) indicate that the three receptors are expressed in the four tested cancer cell lines (CAL-62, ML-1, BCPAP, and TPC-1). All three receptors were detected at their expected theoretical molecular mass: 140 kDa for TrkA, 75 kDa for p75^{NTR}, and 100 kDa for sortilin. TrkA mRNA was present at higher levels in BCPAP, but again this difference

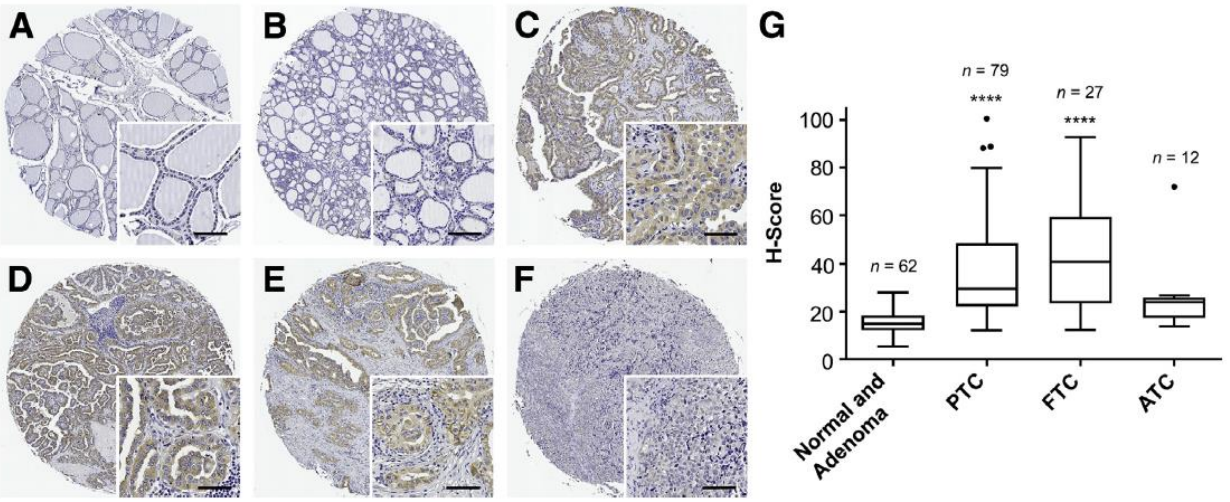

Figure 4 Sortilin expression in thyroid cancer versus normal thyroid tissue. **A–F:** Immunohistochemical detection of sortilin was performed on a cohort of thyroid cancers, adenomas, and normal thyroid tissues. Sortilin is not found in normal thyroid tissues (**A**) and in most adenomas (**B**). In contrast, sortilin staining is observed in cancer cells of papillary thyroid carcinoma (PTC) (**C** and **D**), follicular thyroid carcinoma (FTC) (**E**), and anaplastic thyroid carcinoma (ATC) (**F**). **Insets** show higher magnification. **G:** Sortilin staining was quantified using the Halo image analysis platform; h-scores were calculated. Sortilin staining intensities are significantly higher for PTC (median h-score = 29.69) and FTC (median h-score = 40.80) compared with normal and adenomas combined (median h-score = 15.04). Data are expressed as means (horizontal line in center of box), 25th and 75th percentiles (box limits), interquartile ranges (whiskers), and outliers (dots). n = 128 thyroid cancers, 6 adenomas, and 56 normal thyroid tissues. $^{****}P < 0.0001$ versus normal/adenoma tissue controls. Scale bars: 50 μm (**A–F**). Original magnification: ×50 (**A–F, main images**); ×400 (**insets**).

was not found at the protein level, and all cell lines had comparable levels of TrkA. For p75^{NTR}, BCPAP cells expressed a higher level of mRNA than the other cell lines, but this difference was not found at the protein level, where p75^{NTR} appears similar among cell lines. For sortilin, the mRNA and protein levels were similar among cell lines. The protein expression of NGF and its precursor proNGF was also examined in two ATC cell lines, CAL-62 and 8505c (Supplemental Figure S2). NGF and proNGF were detected in protein extracts from both cell lines. Furthermore, the conditioned culture media obtained from CAL-62 and 8505c cells revealed that proNGF was secreted by CAL-62 and 8505c cells, whereas NGF was secreted only by 8505c cells. The concomitant expression of TrkA, p75^{NTR}, and sortilin with NGF and proNGF suggest the existence of an autocrine loop of stimulation in thyroid cancer cells.

Functional Impact of Targeting TrkA, p75^{NTR}, and Sortilin

In vitro assays were performed on the highly aggressive CAL-62 (Figure 6). Cells were transfected with siRNA directed against TrkA, p75^{NTR}, sortilin, and the impact on cell growth, apoptosis, migration, and invasion was assessed. The efficacy of the targeted siRNAs was determined using Western blot analysis at 24, 48, and 72 hours after transfection (Figure 6A). Sortilin protein expression was reduced after 24 hours and completely inhibited after 48 hours. However, maximal inhibition of TrkA and p75^{NTR} expression was achieved 72 hours after transfection, indicating that it was necessary to evaluate the effects of the siRNAs after 72 hours. The combination of the three siRNA (siCombo) against TrkA, p75^{NTR}, and sortilin similarly decreased the level of the three receptors 72 hours after transfection (Figure 6A).

Signaling Pathways

The effects of inhibiting TrkA, p75^{NTR}, and sortilin on various tumorigenic and metastatic-related signaling pathways were explored using Western blot analysis (Figure 6A). p-TrkA was markedly decreased in response to siTrkA, siP75^{NTR}, and siSort, suggesting that the activation of TrkA requires the presence of both p75^{NTR} and sortilin. Total ERK1/2 and p-ERK1/2 were comparable for siCont, siP75^{NTR}, and siSort; however, siTrkA resulted in a decreased level of p-ERK. Inhibition of TrkA, p75^{NTR}, and sortilin all reduced the level of p-SRC. Targeting all three receptors simultaneously mirrored data obtained when targeting each receptor alone; however, the observed effect was not potentiated (Figure 6A).

Cell Growth and Apoptosis

CAL-62 cell growth was analyzed at 72 hours after transfection, and the effects of siTrkA, siP75^{NTR}, siSort, and siCombo were compared with siCont-treated cells (Figure 6B). Treatment of cells with siTrkA, siP75^{NTR},

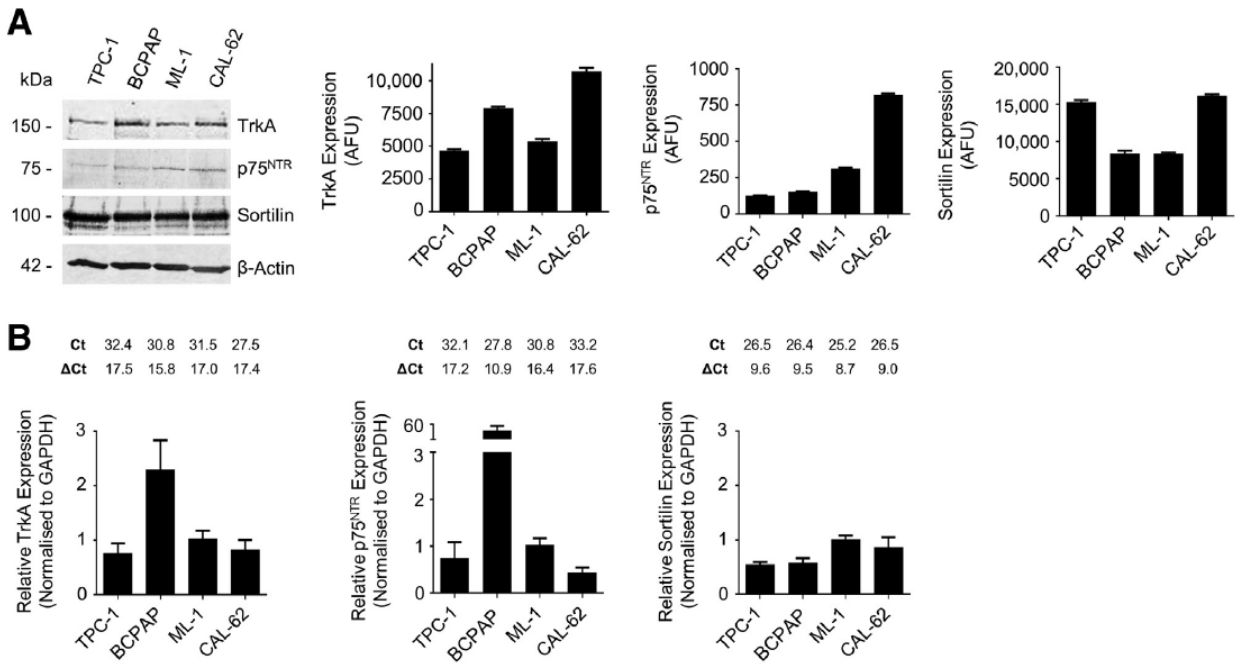

Figure 5 TrkA, p75^{NTR}, and sortilin expression in thyroid cancer cell lines. The levels of mRNA and protein for TrkA, p75^{NTR}, and sortilin were measured by real-time RT-PCR and Western blot analysis. **A:** Western blot analysis. TrkA, p75^{NTR}, and sortilin are detected at the expected molecular weight of 140, 75, and 100 kDa, respectively. Densitometric quantification indicates no significant differences among cell lines. β-Actin was used for normalization. **B:** Real-time RT-PCR. Relative quantification identifies mRNA for TrkA, p75^{NTR}, and sortilin at various levels among thyroid cancer cell lines. The value 1 represents the level obtained in ML-1 cells. mRNA levels were normalized with glyceraldehyde-3-phosphate dehydrogenase (GAPDH) as internal control. Cycle threshold (Ct) and △Ct values are indicated. Data are representative of at least three independent experiments. AFU, arbitrary fluorescence unit.

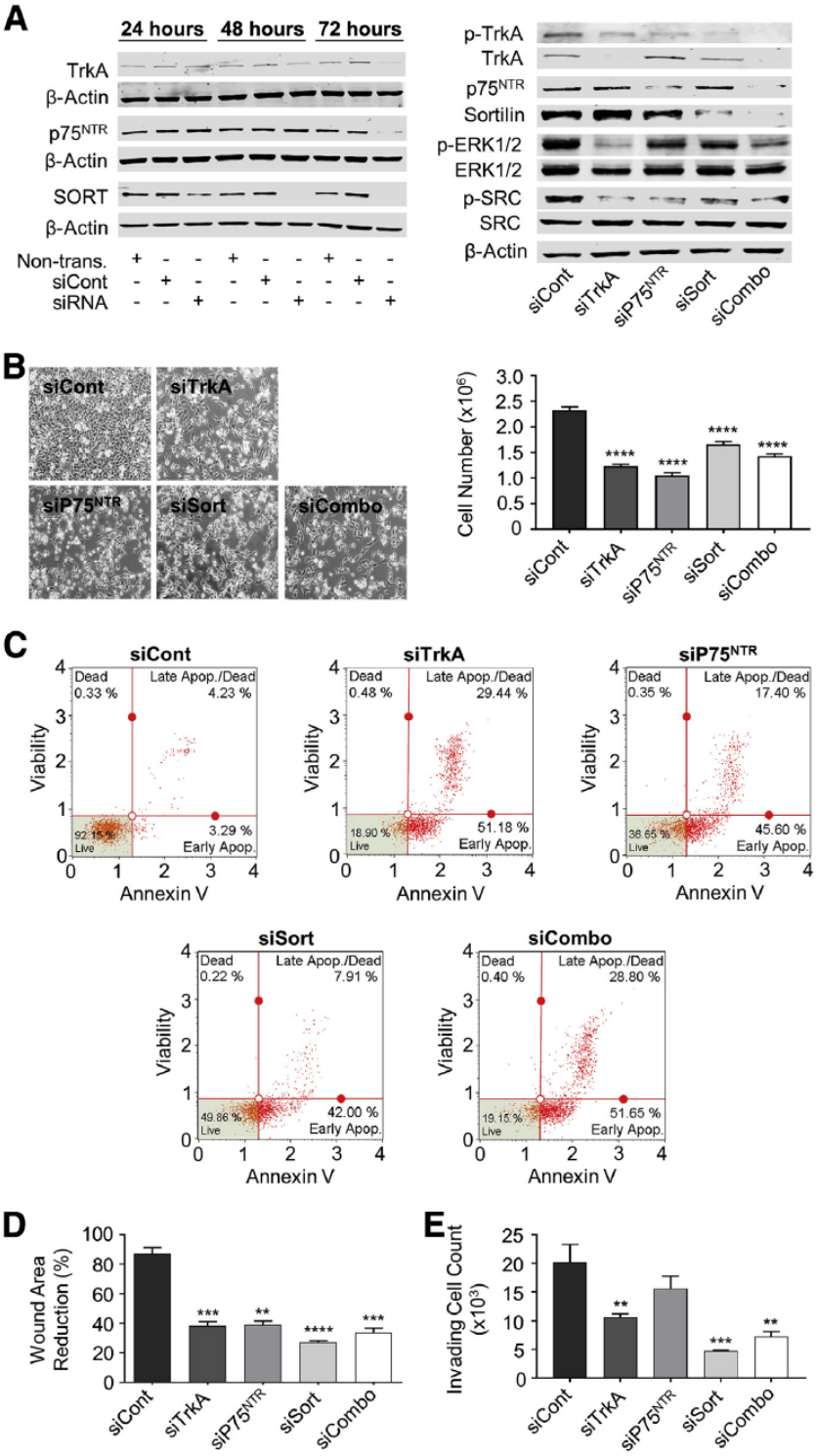

Figure 6 Impact of targeting TrkA, p75^{NTR}, and sortilin in the CAL-62 anaplastic thyroid cancer cell line. CAL-62 cells were transfected with siRNA against TrkA (siTrkA), p75^{NTR} (siP75^{NTR}), and sortilin (siSort), alone and in combination (siCombo), as well as with a universal negative control siRNA (siCont). **A:** Effect of siRNA on protein levels and cell signaling. The impact of siRNA transfection in inhibiting the protein level of TrkA, p75^{NTR}, and sortilin was measured by Western blot analysis 24, 48, and 72 hours after transfection. Non-transfected cells (nontrans.) were also analyzed. β-Actin protein expression was used as an equal loading control. TrkA protein level significantly decreases after 48 hours and further at 72 hours. p75^{NTR} protein level is inhibited after 72 hours. Sortilin is completely decreased after 48 and 72 hours. For cell signaling, siTrkA and siCombo decreased the level of phosphor-TrkA (p-TrkA), phosphor-ERK1/2 (p-ERK1/2), and phospho-SRC (p-SRC). siP75^{NTR} and siSort decrease p-ERK1/2 and p-SRC. **B:** Cell growth. The number of cells was measured by cell counting at 72 hours after transfection, and siRNA-treated cells were compared with siCont cells. SiRNA against TrkA, p75^{NTR}, and sortilin, alone or combined (siCombo), all significantly inhibit cell growth. **C:** Apoptosis (Apop.). The proportion of apoptotic cells was measured in flow cytometry using Annexin V, and siRNA-treated cells were compared with siCont cells. siRNA against TrkA, p75^{NTR}, and sortilin, alone or in combination, all increase the percentage of apoptotic cells compared with siCont. The numbers indicate the percentages of the cells represented by alive, apoptotic, and dead populations. **D:** Cell migration. Scratching of the cell monolayer was performed 72 hours after transfection with siRNA, and reduction in gap area was measured 20 hours later. Targeting of all three receptors, alone and in combination (siCombo), resulted in the inhibition of wound scratch healing. **E:** Cell invasion. Transwell assays were set up 72 hours after siRNA transfection, and cells were allowed to invade for 20 hours. Only siSort and siTrkA, and siCombo significantly inhibited cancer cell invasion. Data are expressed as means ± SD (**B**, **D**, and **E**). Data are representative of at least three technical replicates, each consisting of at least three biological replicates. $^{**}P < 0.01$, $^{***}P < 0.001$, and $^{****}P < 0.0001$ versus controls.

siSort, and siCombo all resulted in a reduction in CAL-62 cell number compared with siCont treated cells ($P < 0.0001$). To further elucidate the effects of targeting TrkA, p75^{NTR}, and sortilin, we determined the impact on apoptosis using Annexin V expression flow cytometry profiling (Figure 6C). In comparison with siCont cells (7.5% apoptotic cells), the percentage of CAL-62 apoptotic cells increased after knockdown of TrkA (80.62%), p75^{NTR} (63%), and sortilin (49.9%). Simultaneous knockdown of all three receptors resulted in 80.4% of cells entering apoptosis (Figure 6C).

Cell Migration and Invasion

Cellular migration was assessed using a scratch wound healing assay, in which a scratch was made to a cell monolayer to create a wound area. The rate of closure was monitored and quantitated (Figure 6D). Transfection with siTrkA ($P = 0.0002$), siP75^{NTR} ($P = 0.0019$), siSort ($P < 0.0001$), and siCombo ($P = 0.0002$) all inhibited the migration of CAL-62 cells compared with siCont. The invasiveness of CAL-62 cells, in response to transfection with siRNA against TrkA, p75^{NTR}, and sortilin or the combination (siCombo), was assessed using a Transwell assay (Figure 6E). Invasion of CAL-62 cells was significantly inhibited by siTrkA ($P = 0.0085$), siSort ($P = 0.001$), and siCombo ($P = 0.0021$) compared with siCont cells. In contrast, knocking down p75^{NTR} expression did not significantly alter the invasion of CAL-62 cells ($P = 0.1268$).

The 8505c ATC cell line was also analyzed (Supplemental Figure S3). The impact of siRNA against the three receptors, alone or in combination, was studied following the same experimental procedures as for CAL-62. Similar results were obtained with 8505c cells compared with the CAL-62 cells, with respect to the decreased cell, growth (Supplemental Figure S3B), apoptosis (Supplemental Figure S3C), migration (Supplemental Figure S3D), and invasion (Supplemental Figure S3E). In terms of cell signaling, similar decreased level of p-TrkA, ERK1/2, and SRC were obtained using siCombo, but the individual siRNAs had a less clear impact on signaling pathways (Supplemental Figure S3A), probably indicating a synergic effect of inhibiting the three receptors simultaneously. Interestingly, 8505c cells did not express the membrane receptor p75^{NTR} (Supplemental Figure S3A); thus, targeting this receptor with siRNA yielded similar results to that obtained with siCont cells. This finding highlights the specificity of the siRNA targeting in our experiment and points to a potential diversity of anaplastic cells in regard to neurotrophin receptor expression.

Discussion

New therapeutic strategies are required for treatment of thyroid cancers that do not respond to current treatment, in particular, ATC and metastatic differentiated thyroid cancer. We report that neurotrophin signaling may be an important component of tumor aggressiveness in ATC and differentiated thyroid carcinomas, which invites further examination as a potential drug target.

TrkA Expression and Targeting

This study found that TrkA protein expression is present in approximately 20% of thyroid cancers and is a marker of tumor aggressiveness, being associated with lymph node metastasis. Furthermore, targeting TrkA expression resulted in a decreased activation of SRC and ERK, ultimately resulting in decreased thyroid cancer cell growth and invasion. TrkA participates in the stimulation of cancer cell invasion in several cancers,[6] including those of the breast,[21,22] prostate,[23,24] and pancreas,[23,25] and is increasingly being considered as a therapeutic target in oncology. In breast cancer, TrkA activation participates in cancer cell invasion,[21] and in lung cancer, Trk inhibitors are in clinical trials.[26] The present data confirm the role of TrkA as an oncogenic protein and suggest a potential utility of targeting this pathway in thyroid cancer therapy.

In addition, TrkA expression was detected in the nerves present in the microenvironment of thyroid cancer. Although innervation of thyroid cancers has not been previously reported, using the neuronal marker PGP9.5, we found nerves in <5% of thyroid cancers (S.F., P.J., C.W.R., S.M.R.O., S.R., R.F.T., C.O., J.A., C.C.J., X.D.Z., M.M.W., H.H., unpublished data). This proportion of innervated tumors may be an underestimate because of the small sampling radius and depth of the tumor microarray cores. In developing neurons, TrkA activation results in the stimulation of various tyrosine kinase—induced signaling pathways, leading to neurite extension.[11] The thyroid gland is principally innervated by the autonomic nervous system, with parasympathetic nerves from the vagus and sympathetic nerves distributed from the sympathetic trunk, entering the gland along blood vessels.[27] Interestingly, the nerves observed in thyroid cancers were positive for TrkA but not for sortilin and p75^{NTR}. Given that NGF[28] and proNGF[10] are expressed and released by thyroid cancer cells,[10] it can be hypothesized that the activation of TrkA in nerves may lead to a stimulation of neurogenesis in the tumor microenvironment. NGF and TrkA are involved in perineural invasion in other cancers, as in pancreatic cancer,[29] and TrkA may play a similar role in thyroid cancer. In any case, the nerve-cancer cell crosstalk is increasingly regarded as a promoter of cancer progression,[30,31] and the expression of TrkA in nerves suggests a potential association with neural infiltration in thyroid cancer.

p75^{NTR} Expression and Targeting

Although previous studies have found that p75^{NTR} is expressed in PTC and is associated with the presence of *BRAF* (V600E) mutations,[12] this study provides the first data that p75^{NTR} is expressed in normal thyroid tissue, although at a significantly lower level than in thyroid cancers. In addition, we found for the first time the expression of p75^{NTR} in FTC and ATC. p75^{NTR} is the common receptor for all neurotrophins and proneurotrophins.[11] It belongs to the tumor necrosis factor receptor gene family, and the proteins recruited by p75^{NTR} signaling are the tumor necrosis factor receptor—associated factor proteins followed by the activation of the NF-κB transcription factor. In addition, p75^{NTR} interacts with sortilin and TrkA and can modulate the tyrosine kinase activity of the latter on stimulation by neurotrophins.[11] Presumably because of its wide

range of interaction with various receptors and signaling, p75^{NTR} exhibits various biological activities in neurons, including the stimulation of survival or apoptosis, differentiation, and neurite outgrowth. In cancer, the same variety of effects are observed.[32] p75^{NTR} acts as a tumor suppressor in gastric, bladder, and prostate cancers by blocking cell cycle progression and inducing apoptosis.[33,34] In most other tumors, including melanoma,[35] glioma,[36] and breast cancer,[37] p75^{NTR} favors tumor development, in particular through the stimulation of the stem cell compartment.[7] Interestingly, our data indicate that p75^{NTR} is overexpressed in most ATC. ATC has a poor survival rate (approximately 5% after 5 years), and at this stage there is no targeted treatment.[5] Therefore, our data warrant future functional exploration to determine the interest of p75^{NTR} as a therapeutic target in thyroid cancer.

Sortilin Expression and Targeting

This study is the first report of sortilin expression in thyroid cancer. Sortilin is expressed in thyroid epithelial cells, where it contributes to the recycling of the thyroid hormone precursor thyroglobulin,[38] but its protein expression in thyroid cancer was previously unknown. Sortilin is a neuronal type 1 membrane protein, encoded by the *SORT1* gene.[39] It belongs to the vacuolar protein sorting 10 protein (VPS10P) family of receptors and is most abundantly expressed in the central and peripheral nervous systems. Initially described as neurotensin receptor 3, sortilin is more generally involved in sorting and trafficking of target proteins to distinct destinations.[39] It is a common binding partner of tyrosine kinase receptors, G-protein—coupled receptors, and ion channels, for which it facilitates ligand-induced signaling.[39] Sortilin has been identified as a co-receptor for proneurotrophins, including proNGF, in which it acts in a complex with the neurotrophin receptor p75^{NTR} to induce neuron apoptosis.[40] A few cancer cell lines express sortilin. In HT29 colon cancer cells, sortilin participates in the control of the growth-promoting activity induced by brain-derived growth factor through interacting with its tyrosine kinase receptor TrkB (NTRK2).[41] In addition, sortilin mediates the release and transfer of exosomes in the A549 lung cancer cell line[42] and regulates progranulin stimulatory activity of prostate cancer cells.[43] In melanoma cell lines, sortilin is a co-receptor for proNGF and acts in cooperation with the neurotrophin receptor p75^{NTR} to promote cancer cell invasion.[35] In breast cancer, sortilin expression is increased in invasive carcinomas compared with healthy tissues,[15] and sortilin expression in the primary tumor is also associated with lymph node invasion.[15] *In vitro*, sortilin participates in the proinvasive effect of proNGF in breast cancer cells.[15] In the present study, similar to breast cancer, sortilin expression was increased in thyroid cancer compared with normal tissues and adenomas. This increased level of sortilin protein in thyroid cancers, compared with benign thyroid tissues, suggested a potential role in the initiation and progression of the disease. Intriguingly, sortilin was expressed at higher levels in PTC and FTC compared with ATC. Sortilin is a ubiquitous receptor; its functions go beyond the sole control of cell growth and migration,[39] and this probably accounts for the fact that its expression is not strictly related to tumor aggressiveness in thyroid cancer. However, siRNA-targeting sortilin resulted in an inhibition of anaplastic thyroid cancer cell growth, migration, and invasion. Although the molecular mechanism of sortilin activity and its direct interacting signaling partners remain to be fully elucidated in thyroid cancer, our data suggest that targeting sortilin is a potential therapeutic strategy in thyroid cancer.

Conclusion

The present study found an increased level of TrkA, p75^{NTR}, and sortilin in thyroid cancers, which signals the potential value of these neurotrophin receptors as novel therapeutic targets. Further preclinical investigations *in vivo* are warranted to explore the therapeutic interest of targeting neurotrophin receptors in the different forms of thyroid cancers and particularly in ATCs, which are resistant to current treatment options. In addition, pain is a reported event in thyroid cancer, particularly in MTC and ATC.[44] Neurotrophins and their receptors have been well characterized as important mediators of pain initiation and maintenance,[45] and pharmacotherapies targeting the NGF/TrkA pathway are undergoing trials in the treatment of a variety of pain conditions,[46] including cancer.[47] Therefore, targeting neurotrophin receptors in ATC may potentially address the issue of pain, which also merits further attention.

Acknowledgments

We thank Sheridan Keene for excellent technical assistance and the Clinical Research Design, IT, and Statistical Support (CReDITSS) Unit of the University of Newcastle (Callaghan, New South Wales, Australia). The 8505c (ATC) cell line was a generous gift from Prof. Alfred Lam (Griffith University, Queensland, Australia).

H.H. conceived and supervised the study and drafted the manuscript; S.F., S.R., and C.C.J. performed immunohistochemistry and quantified staining; tissue slide analyses and quantification were supervised by M.M.W. (histopathologist) and confirmed by R.F.T.; S.M.R.O. and P.J. performed nerve analysis; S.F. performed all cell culture experiments and prepared all figures and tables; C.W.R. and X.Z. provided clinical insights; J.A. and C.O. supervised statistical analyses; and all authors read and approved the final manuscript.

Supplemental Data

Supplemental material for this article can be found at *https://doi.org/10.1016/j.ajpath.2017.09.008*.

References

1. Kitahara CM, Sosa JA: The changing incidence of thyroid cancer. Nat Rev Endocrinol 2016, 12:646–653
2. Ahn HS, Kim HJ, Welch HG: Korea's thyroid-cancer "epidemic"—screening and overdiagnosis. N Engl J Med 2014, 371:1765–1767
3. Cabanillas ME, McFadden DG, Durante C: Thyroid cancer. Lancet 2016, 388:2783–2795
4. Lim H, Devesa SS, Sosa JA, Check D, Kitahara CM: Trends in thyroid cancer incidence and mortality in the United States, 1974-2013. JAMA 2017, 317:1338–1348
5. Ranganath R, Shah MA, Shah AR: Anaplastic thyroid cancer. Curr Opin Endocrinol Diabetes Obes 2015, 22:387–391
6. Demir IE, Tieftrunk E, Schorn S, Friess H, Ceyhan GO: Nerve growth factor & TrkA as novel therapeutic targets in cancer. Biochim Biophys Acta 2016, 1866:37–50
7. Chopin V, Lagadec C, Toillon RA, Le Bourhis X: Neurotrophin signaling in cancer stem cells. Cell Mol Life Sci 2016, 73:1859–1870
8. Hayakawa Y, Sakitani K, Konishi M, Asfaha S, Niikura R, Tomita H, Renz BW, Tailor Y, Macchini M, Middelhoff M, Jiang Z, Tanaka T, Dubeykovskaya ZA, Kim W, Chen X, Urbanska AM, Nagar K, Westphalen CB, Quante M, Lin CS, Gershon MD, Hara A, Zhao CM, Chen D, Worthley DL, Koike K, Wang TC: Nerve growth factor promotes gastric tumorigenesis through aberrant cholinergic signaling. Cancer Cell 2017, 31:21–34
9. Lei Y, Tang L, Xie Y, Xianyu Y, Zhang L, Wang P, Hamada Y, Jiang K, Zheng W, Jiang X: Gold nanoclusters-assisted delivery of NGF siRNA for effective treatment of pancreatic cancer. Nat Commun 2017, 8:15130
10. Faulkner S, Roselli S, Demont Y, Pundavela J, Choquet G, Leissner P, Oldmeadow C, Attia J, Walker MM, Hondermarck H: ProNGF is a potential diagnostic biomarker for thyroid cancer. Oncotarget 2016, 7:28488–28497
11. Bradshaw RA, Pundavela J, Biarc J, Chalkley RJ, Burlingame AL, Hondermarck H: NGF and ProNGF: regulation of neuronal and neoplastic responses through receptor signaling. Adv Biol Regul 2015, 58:16–27
12. Rocha AS, Risberg B, Magalhaes J, Trovisco V, de Castro IV, Lazarovici P, Soares P, Davidson B, Sobrinho-Simoes M: The p75 neurotrophin receptor is widely expressed in conventional papillary thyroid carcinoma. Hum Pathol 2006, 37:562–568
13. Bevan S, Pal T, Greenberg CR, Green H, Wixey J, Bignell G, Narod SA, Foulkes WD, Stratton MR, Houlston RS: A comprehensive analysis of MNG1, TCO1, fPTC, PTEN, TSHR, and TRKA in familial nonmedullary thyroid cancer: confirmation of linkage to TCO1. J Clin Endocrinol Metab 2001, 86:3701–3704
14. Pundavela J, Roselli S, Faulkner S, Attia J, Scott RJ, Thorne RF, Forbes JF, Bradshaw RA, Walker MM, Jobling P, Hondermarck H: Nerve fibers infiltrate the tumor microenvironment and are associated with nerve growth factor production and lymph node invasion in breast cancer. Mol Oncol 2015, 9:1626–1635
15. Roselli S, Pundavela J, Demont Y, Faulkner S, Keene S, Attia J, Jiang CC, Zhang XD, Walker MM, Hondermarck H: Sortilin is associated with breast cancer aggressiveness and contributes to tumor cell adhesion and invasion. Oncotarget 2015, 6:10473–10486
16. Cerami E, Gao J, Dogrusoz U, Gross BE, Sumer SO, Aksoy BA, Jacobsen A, Byrne CJ, Heuer ML, Larsson E, Antipin Y, Reva B, Goldberg AP, Sander C, Schultz N: The cBio cancer genomics portal: an open platform for exploring multidimensional cancer genomics data. Cancer Discov 2012, 2:401–404
17. Cancer Genome Atlas Research Network, Weinstein JN, Collisson EA, Mills GB, Shaw KR, Ozenberger BA, Ellrott K, Shmulevich I, Sander C, Stuart JM: The Cancer Genome Atlas Pan-Cancer Analysis Project. Nat Genet 2013, 45:1113–1120
18. Zhang B, Wang J, Wang X, Zhu J, Liu Q, Shi Z, Chambers MC, Zimmerman LJ, Shaddox KF, Kim S, Davies SR, Wang S, Wang P, Kinsinger CR, Rivers RC, Rodriguez H, Townsend RR, Ellis MJ, Carr SA, Tabb DL, Coffey RJ, Slebos RJ, Liebler DC, Nci C: Proteogenomic characterization of human colon and rectal cancer. Nature 2014, 513:382–387
19. Romon R, Adriaenssens E, Lagadec C, Germain E, Hondermarck H, Le Bourhis X: Nerve growth factor promotes breast cancer angiogenesis by activating multiple pathways. Mol Cancer 2010, 9:157
20. Palazzo E, Marconi A, Truzzi F, Dallaglio K, Petrachi T, Humbert P, Schnebert S, Perrier E, Dumas M, Pincelli C: Role of neurotrophins on dermal fibroblast survival and differentiation. J Cell Physiol 2012, 227:1017–1025
21. Lagadec C, Meignan S, Adriaenssens E, Foveau B, Vanhecke E, Romon R, Toillon RA, Oxombre B, Hondermarck H, Le Bourhis X: TrkA overexpression enhances growth and metastasis of breast cancer cells. Oncogene 2009, 28:1960–1970
22. Demont Y, Corbet C, Page A, Ataman-Onal Y, Choquet-Kastylevsky G, Fliniaux I, Le Bourhis X, Toillon RA, Bradshaw RA, Hondermarck H: Pro-nerve growth factor induces autocrine stimulation of breast cancer cell invasion through tropomyosin-related kinase A (TrkA) and sortilin protein. J Biol Chem 2012, 287:1923–1931
23. Miknyoczki SJ, Wan W, Chang H, Dobrzanski P, Ruggeri BA, Dionne CA, Buchkovich K: The neurotrophin-trk receptor axes are critical for the growth and progression of human prostatic carcinoma and pancreatic ductal adenocarcinoma xenografts in nude mice. Clin Cancer Res 2002, 8:1924–1931
24. Festuccia C, Muzi P, Gravina GL, Millimaggi D, Speca S, Dolo V, Ricevuto E, Vicentini C, Bologna M: Tyrosine kinase inhibitor CEP-701 blocks the NTRK1/NGF receptor and limits the invasive capability of prostate cancer cells in vitro. Int J Oncol 2007, 30:193–200
25. Zhang Y, Dang C, Ma Q, Shimahara Y: Expression of nerve growth factor receptors and their prognostic value in human pancreatic cancer. Oncol Rep 2005, 14:161–171
26. Vaishnavi A, Le AT, Doebele RC: TRKing down an old oncogene in a new era of targeted therapy. Cancer Discov 2015, 5:25–34
27. Dumont J, Opitz R, Christophe D, Vassart G, Roger PP, Maenhaut C: Ontogeny, anatomy, metabolism and physiology of the thyroid. In Endotext. Edited by De Groot LJ, Beck-Peccoz P, Chrousos G, Dungan K, Grossman A, Hershman JM, Koch C, McLachlan R, New M, Rebar R, Singer F, Vinik A, Weickert MO. South Dartmouth, MA: MDText.com, 2000
28. van der Laan BF, Freeman JL, Asa SL: Expression of growth factors and growth factor receptors in normal and tumorous human thyroid tissues. Thyroid 1995, 5:67–73
29. Bapat AA, Hostetter G, Von Hoff DD, Han H: Perineural invasion and associated pain in pancreatic cancer. Nat Rev Cancer 2011, 11:695–707
30. Jobling P, Pundavela J, Oliveira SM, Roselli S, Walker MM, Hondermarck H: Nerve-cancer cell cross-talk: a novel promoter of tumor progression. Cancer Res 2015, 75:1777–1781
31. Boilly B, Faulkner S, Jobling P, Hondermarck H: Nerve dependence: from regeneration to cancer. Cancer Cell 2017, 31:342–354
32. Tomellini E, Touil Y, Lagadec C, Julien S, Ostyn P, Ziental-Gelus N, Meignan S, Lengrand J, Adriaenssens E, Polakowska R, Le Bourhis X: Nerve growth factor and proNGF simultaneously promote symmetric self-renewal, quiescence, and epithelial to mesenchymal transition to enlarge the breast cancer stem cell compartment. Stem Cells 2015, 33:342–353
33. Jin H, Pan Y, Zhao L, Zhai H, Li X, Sun L, He L, Chen Y, Hong L, Du Y, Fan D: p75 neurotrophin receptor suppresses the proliferation of human gastric cancer cells. Neoplasia 2007, 9:471–478
34. Khwaja F, Tabassum A, Allen J, Djakiew D: The p75(NTR) tumor suppressor induces cell cycle arrest facilitating caspase mediated apoptosis in prostate tumor cells. Biochem Biophys Res Commun 2006, 341:1184–1192
35. Truzzi F, Marconi A, Lotti R, Dallaglio K, French LE, Hempstead BL, Pincelli C: Neurotrophins and their receptors stimulate melanoma cell proliferation and migration. J Invest Dermatol 2008, 128:2031–2040

36. Johnston AL, Lun X, Rahn JJ, Liacini A, Wang L, Hamilton MG, Parney IF, Hempstead BL, Robbins SM, Forsyth PA, Senger DL: The p75 neurotrophin receptor is a central regulator of glioma invasion. PLoS Biol 2007, 5:e212
37. Vanhecke E, Adriaenssens E, Verbeke S, Meignan S, Germain E, Berteaux N, Nurcombe V, Le Bourhis X, Hondermarck H: Brain-derived neurotrophic factor and neurotrophin-4/5 are expressed in breast cancer and can be targeted to inhibit tumor cell survival. Clin Cancer Res 2011, 17:1741−1752
38. Botta R, Lisi S, Pinchera A, Giorgi F, Marcocci C, Taddei AR, Fausto AM, Bernardini N, Ippolito C, Mattii L, Persani L, de Filippis T, Calebiro D, Madsen P, Petersen CM, Marino M: Sortilin is a putative postendocytic receptor of thyroglobulin. Endocrinology 2009, 150:509−518
39. Nykjaer A, Willnow TE: Sortilin: a receptor to regulate neuronal viability and function. Trends Neurosci 2012, 35:261−270
40. Nykjaer A, Lee R, Teng KK, Jansen P, Madsen P, Nielsen MS, Jacobsen C, Kliemannel M, Schwarz E, Willnow TE, Hempstead BL, Petersen CM: Sortilin is essential for proNGF-induced neuronal cell death. Nature 2004, 427:843−848
41. Akil H, Perraud A, Melin C, Jauberteau MO, Mathonnet M: Fine-tuning roles of endogenous brain-derived neurotrophic factor, TrkB and sortilin in colorectal cancer cell survival. PLoS One 2011, 6: e25097
42. Wilson CM, Naves T, Vincent F, Melloni B, Bonnaud F, Lalloue F, Jauberteau MO: Sortilin mediates the release and transfer of exosomes in concert with two tyrosine kinase receptors. J Cell Sci 2014, 127: 3983−3997
43. Tanimoto R, Morcavallo A, Terracciano M, Xu SQ, Stefanello M, Buraschi S, Lu KG, Bagley DH, Gomella LG, Scotlandi K, Belfiore A, Iozzo RV, Morrione A: Sortilin regulates progranulin action in castration-resistant prostate cancer cells. Endocrinology 2015, 156: 58−70
44. Chiacchio S, Lorenzoni A, Boni G, Rubello D, Elisei R, Mariani G: Anaplastic thyroid cancer: prevalence, diagnosis and treatment. Minerva Endocrinol 2008, 33:341−357
45. Pezet S, McMahon SB: Neurotrophins: mediators and modulators of pain. Annu Rev Neurosci 2006, 29:507−538
46. Chang DS, Hsu E, Hottinger DG, Cohen SP: Anti-nerve growth factor in pain management: current evidence. J Pain Res 2016, 9: 373−383
47. Lam DK: Emerging factors in the progression of cancer-related pain. Pain Manag 2016, 6:487−496

5.3 Supplemental Files

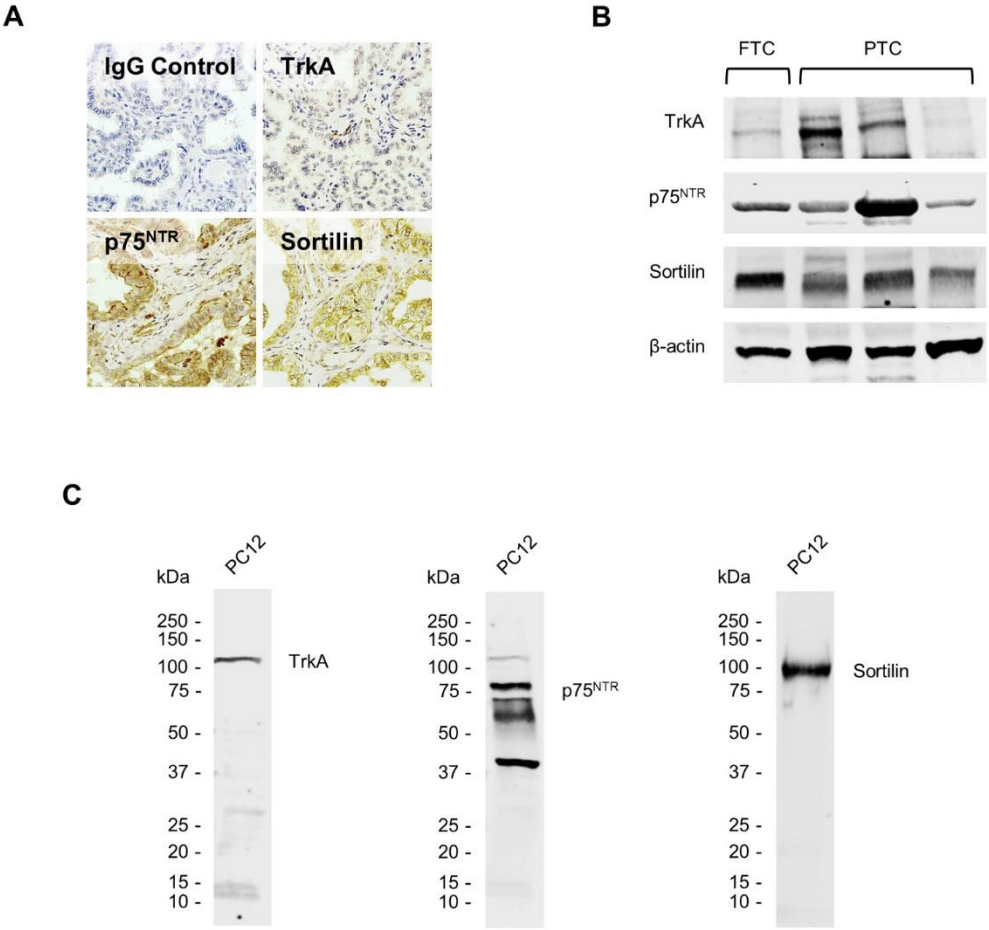

Supplemental Figure S1. Validation of antibodies used for immunohistochemistry. The specificity of antibodies used for immunohistochemistry was validated with IgG isotype controls in a matched case of papillary thyroid carcinoma (PTC). In addition, using the same antibodies, Western blot analysis for TrkA, p75^{NTR}, and sortilin was performed in thyroid tumor samples and PC-12 cells, which are known to express neurotrophins. A: Immunohistochemical detection of TrkA, p75^{NTR}, and sortilin, along with matched isotype IgG negative control, in a case of PTC. B: Western blotting detection of TrkA, p75^{NTR}, and sortilin in a panel of thyroid tumor samples, including follicular thyroid carcinoma (FTC) (n = 1) and PTC (n = 3). β-Actin was used as an equal loading control. C: Western blotting for TrkA, p75^{NTR}, and sortilin using PC-12 cells. In B and C, TrkA, p75^{NTR} and sortilin were detected at the expected molecular weight of 140, 75, and 100 kDa, respectively.

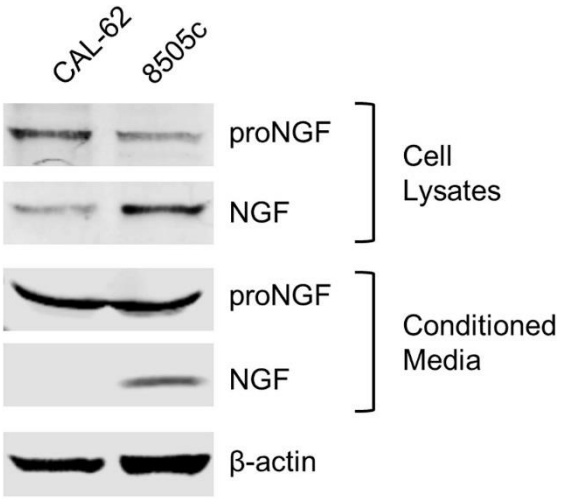

Supplemental Figure S2. Nerve growth factor (NGF) and precursor for NGF (proNGF) protein expression and secretion in anaplastic thyroid carcinoma cell lines. The protein level of NGF and proNGF was measured using Western blot analysis in the anaplastic carcinoma cell lines, CAL-62 and 8505c, as well as in their conditioned culture medium. ProNGF was detected in the protein extract and conditioned medium of both cell lines. NGF was detected in the cell extract from both cell lines; however, only 8505c cells secreted NGF. β-actin was used as an equal loading control.

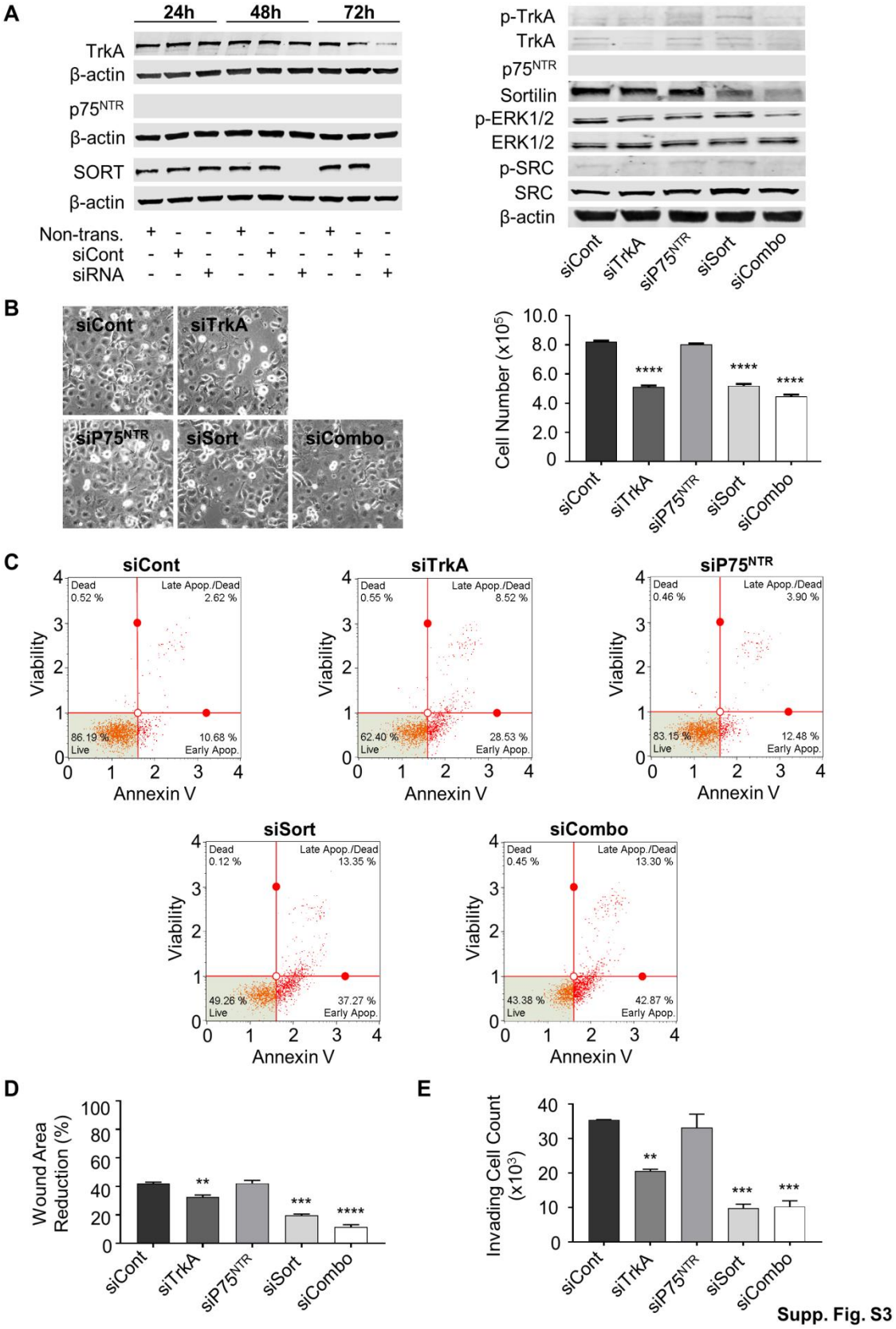
A
24h
48h
72h
TrkA
β-actin
p75NTR
β-actin
SORT
β-actin
Non-trans.
siCont
siRNA
p-TrkA
TrkA
p75NTR
Sortilin
p-ERK1/2
ERK1/2
p-SRC
SRC
β-actin
siCont
siTrkA
siP75NTR
siSort
siCombo
B
siCont
siTrkA
siP75NTR
siSort
siCombo
Cell Number (x10^5)
C
siCont
siTrkA
siP75NTR
siSort
siCombo
Viability
Annexin V
Dead
Late Apop./Dead
Live
Early Apop.
D
Wound Area Reduction (%)
E
Invading Cell Count (x10^3)

Supp. Fig. S3

Supplemental Figure S3. Impact of targeting TrkA, $p75^{NTR}$, and sortilin in the anaplastic thyroid cancer cell line 8505c. 8505c cells were transfected with siRNA against TrkA (siTrkA), $p75^{NTR}$ ($siP75^{NTR}$), and sortilin (siSort) alone and in combination (siCombo), as well as with a universal negative control siRNA (siCont). A: Effect of siRNA on protein levels. The impact of siRNA transfection in inhibiting the protein level of TrkA, $p75^{NTR}$, and sortilin was measured by Western blot analysis 24, 48, and 72 hours after transfection. Nontransfected cells (nontrans.) were also analyzed. β-Actin protein expression was used as an equal loading control. TrkA protein level is inhibited after 72 hours. $p75^{NTR}$ expression is absent in 8505c cells. Sortilin level completely decreases after transfection for 48 and 72 hours. For cell signaling, the impact of siRNA against the three receptors is less strong than for CAL-62 cells (Figure 6). siCombo decreases the level of phosphor-TrkA (p-TrkA), phosphor-ERK1/2 (p-ERK1/2), and phospho-SRC (p-SRC), but the impact of individual siRNA is less clear, suggesting a synergistic effect of the combined inhibition. B: Cell growth. The number of cells was measured by cell counting at 72 hours after transfection, and siRNA-treated cells were compared with siCont cells. SiRNA against TrkA and sortilin, alone and in combination (siCombo), significantly inhibited cell growth compared with siCont. Consistent with the absence of $p75^{NTR}$ in these cells (A), $siP75^{NTR}$ has no effect. C: Apoptosis. The proportion of apoptotic cells was measured in flow cytometry using Annexin V, and siRNA-treated cells were compared with siCont cells. siRNA against TrkA and sortilin, alone or in combination, increases the percentage of apoptotic cells compared with siCont. Consistent with the absence of $p75^{NTR}$ in these cells (A), $siP75^{NTR}$ has no effect. The numbers indicate the percentages of the cells represented by alive, apoptotic, and dead populations. D: Cell migration. Cell layers were scratched 72 hours after transfection with siRNA, and reduction in gap area was measured 20 hours later. Targeting TrkA and sortilin, alone and in combination (siCombo), results in the inhibition of wound scratch healing. Consistent with the absence of $p75^{NTR}$ in these cells (A), $siP75^{NTR}$ has no effect. E: Cell invasion. Transwell assays were set up 72 hours after siRNA transfection, and cells were allowed to invade for 20 hours. Only siTrkA and siSort significantly inhibit cancer cell invasion. Similar results were observed when using the siRNAs in combination (siCombo). Consistent with the absence of $p75^{NTR}$ in these cells (A), $siP75^{NTR}$ has no effect. Data are expressed as means ± SD (B, D, and E). Data are representative of at least three technical replicates, each consisting of at least three biological replicates. $^{**}P < 0.01$, $^{***}P < 0.001$, and $^{****}P < 0.0001$ versus controls.

CHAPTER 6 | General Discussion

The primary focus of this thesis was to further clarify the current understanding of the involvement of both nerves and neurotrophins in mediating the development and progression of human cancers. More specifically, this was addressed by examining the presence of nerve fibre infiltration within the tumour microenvironment, using the neuronal marker PGP9.5, as well as the expression of NGF, proNGF and their receptors (TrkA, $p75^{NTR}$ and sortilin) in cohorts of both breast and thyroid primary tumours. Following immunohistochemical detection, functional experiments were carried out, *in vitro*, using representative neuronal and cancer cell lines, to further elucidate the potential mediators underpinning the nerve-cancer cell crosstalk as well as the related molecular mechanisms influencing tumour growth and metastasis.

The study presented in Chapter 3 of this thesis reveals the presence of individual nerve fibres, commonly referred to as axons, within a significant proportion of primary breast cancers. With respect to histological subtype, invasive ductal carcinomas were more susceptible to neural manifestations as compared with both invasive lobular carcinomas and in situ lesions. Furthermore, these manifestations were associated with certain characteristics of metastatic cancers, namely lymph node invasion. Prior to our investigation, a limited number of studies had reported the presence of nerves within primary breast tumours [103, 104], in which neural infiltration was also found to be associated with features of tumour aggressiveness. Despite these findings, no follow up studies were carried out for the purpose of identifying the molecular drivers of this breast cancer related neurogenesis. A previous study by Adriaenssens et al. revealed that nerve growth factor (NGF) is produced and secreted by breast cancer cells [67], where it was later determined to act in an autocrine manner, stimulating its receptors TrkA and $p75^{NTR}$ [68, 105]. Given the major role of NGF in directing nerves to specific sites for the innervation and development of organs during embryonic growth [1], we hypothesised that the production of NGF by breast cancer cells may play a similar role in directing nerves into the microenvironment of primary breast tumours. Interestingly, an association was found between the

presence of nerve fibres in the microenvironment and the expression of NGF by cancer cells, which was particularly apparent in the more clinically aggressive cases of disease, highlighting their individual or possible joint utility as predictive biomarkers. This finding prompted us to explore the potential mechanism by which NGF may mediate the neurogenesis of the breast tumour microenvironment. *In vitro*, a series of breast cancer cell lines were found to secrete NGF as well as being capable of inducing neurite outgrowth in the neuronal cell line, PC12, during co-culture. The specificity of this finding was confirmed using anti-NGF blocking antibodies, which diminished the observed effect. Therefore, work carried out within this chapter of my thesis provided novel information regarding the presence and impact of the neuronal component in the breast tumour microenvironment. In addition, we elucidated a potential mechanistic role for NGF in initiating and regulating this infiltration. In terms of potential clinical applications, future preclinical studies in animal models will have to confirm the relevance of anti-NGF strategies to inhibit nerve infiltration *in vivo*.

The nature or origin of the nerves infiltrating the breast tumour microenvironment remains to be clarified. Given that PGP9.5 is a broad neuronal marker, future studies will need to be conducted in order to clarify the distribution of sympathetic, parasympathetic or sensory nerves and to identify the mechanism(s) by which each of these neuronal subpopulations influence the nature of cancer cells. Furthermore, the extent and nature of tumour innervation may have been underestimated. Paraffin embedded TMAs generally do not contain a sufficient amount of tissue, with respect to both area and depth of the core, for the purpose of precisely measuring and dissecting neural infiltration and densities in tumours. Subsequent studies looking to extend on this research should utilise thicker sections as well as whole tumour tissue samples to precisely characterise the density and source of tumour innervation. Additionally, immunofluorescent microscopy of fresh or frozen sections should be applied for simultaneously assessing the immunoreactivity of sympathetic, parasympathetic or sensory nerves.

Subsequent to revealing the extent of neural invasion within primary breast tumours, as well as identifying NGF as a potential inducer and mediator of this phenomena, Chapters 4 and 5 of this thesis focus on further clarifying the

expression and role of both nerves and neurotrophic growth factors in another human cancer, specifically that of the thyroid. Recent data has shown an increase in mortality over the past three decades for patients diagnosed with late stage thyroid cancer, signifying not only rise in incidence, but also the need for novel treatment strategies for this particular subgroup of patients [106]. In particular, anaplastic thyroid carcinoma, the most lethal histological subtype, carries a high mortality rate, with median survival less than one year after diagnosis [107]. Thus, the identification of new targets for the diagnosis and treatment of clinically significant thyroid cancer is essential.

Chapter 4 of this thesis highlights the prevalence of neural infiltration as well as the protein expression of proNGF in a cohort of clinically annotated thyroid tumours, as compared with both adenomas and normal thyroid tissue. Although innervation of thyroid cancers has not been previously reported, we observed nerve fibres in only 5% of cases (data not shown). This proportion is significantly less than what we reported for breast cancer, in which up to 28% of invasive ductal carcinomas contained neural manifestations. Due to this difference between breast and thyroid cancer, it was not at all surprising to find no association of nerve fibres presence in the tumour with any clinically relevant features of thyroid tumours (data not shown). Previous studies have revealed that NGF expression has no association with any clinicopathological features of thyroid cancer [108]. NGF protein expression has previously been described as diffuse throughout the cytoplasm of the majority of cells found within both normal and cancerous thyroid tissue [108]. However, its precursor protein, namely proNGF, was previously unexplored within the context of thyroid cancer but has been implicated in several other tumour models, including melanoma and breast cancer [16, 95]. For the first time, we found proNGF to be overexpressed in thyroid tumours as compared with both benign adenomas and normal thyroid tissue. A recent study by Pundavela et al. demonstrated that proNGF is also overexpressed in prostate cancer, where it is involved in stimulating axonogenesis (nerve infiltration) [109]. This prompted us to investigate any association between proNGF expression and that of neural invasion in our thyroid tumours. We hypothesised that perhaps proNGF was a driver of nerve infiltration in the thyroid tumour microenvironment, as in the prostate and similar to the role

we found for NGF in breast cancer. However, in contrast with prostate and breast tumours, the expression of proNGF was not associated with the presence of nerve fibres or with any of the other clinicopathological parameters of the patients. Despite these findings, the overexpression of proNGF in thyroid tumours as compared with that of adenomas and normal thyroid tissue nonetheless highlighted its potential utility as a novel diagnostic biomarker. Given that proNGF has previously been shown to be secreted by breast and prostate cancer cells [16, 109], and more recently by anaplastic thyroid cancer cells (Chapter 5 of this thesis), its value as a blood biomarker should also not be overlooked and should be investigated in the future. In collaboration with our industrial partner BioSensis Lty Ptd (Prof Robert Rush, Adelaide), we have developed ProNGF ELISA kits that are currently on the market and have been specifically designed for assaying human serum samples. Prospective studies should follow up on the potential use of proNGF as a novel blood biomarker, with respect to both diagnostic and prognostic utility.

The overexpression of proNGF observed in our cohort of thyroid tumours (Chapter 4) suggests a potential role in pathogenesis, however, the status of its receptors remained unclear. ProNGF acts as a ligand and is capable of binding to a receptor complex between the membrane protein sortilin and $p75^{NTR}$, initiating various signalling pathways (NFKB, RhoA and JNK) [15]. In addition, proNGF has also been shown to activate TrkA, which in turn has been shown to regulate the MAPK pathway [15]. In thyroid cancer, the expression of sortilin had never been reported and although $p75^{NTR}$ [110] and TrkA [111] are expressed, their clinicopathological significance remains unclear. Therefore, the study contained within Chapter 5 of this thesis looked to define the expression of TrkA, $p75^{NTR}$ and sortilin in thyroid cancer, as well as to determine if targeting these receptors reduced features of aggressiveness. We demonstrated the expression of TrkA, $p75^{NTR}$ and sortilin was increased in a cohort of thyroid tumours, as compared with adenomas and normal thyroid tissue. TrkA was also expressed within the neural population of the tumour microenvironment, whereas both $p75^{NTR}$ and sortilin were absent. In developing neurons, TrkA activation results in the stimulation of various tyrosine kinase-induced signalling pathways leading to neurite extension [15]. Therefore, based on our observation that proNGF is

expressed and secreted by thyroid cancer cells, we can hypothesise that it may bind to and activate TrkA receptors on nerves, which could in turn represent a previously unreported mechanism of neurogenesis in thyroid cancer. Interestingly, our data also shows that $p75^{NTR}$ is overexpressed in most cases of anaplastic thyroid cancer. This undifferentiated subtype has a poor survival rate (only around 5% after 5 years) and at this stage there is no targeted treatment, Given that TrkA was also expressed and knowing that sortilin is an essential co-receptor for proNGF, we followed up these findings, *in vitro*, using two representative anaplastic thyroid cancer cell lines. Our data revealed that targeting these neurotrophin receptors with specific siRNA resulted in a decreased growth and invasion, suggesting their potential utility as novel therapeutic targets. New therapeutic strategies are required for treatment of thyroid cancers that do not respond to current treatment, in particular, anaplastic thyroid carcinoma and metastatic differentiated thyroid cancer. Here we show for the first time that the expression of proNGF and its receptors, TrkA, $p75^{NTR}$ and sortilin are all increased in thyroid tumours, as compared with benign lesions and normal thyroid tissue. Additionally, we implicate their activation and downstream signaling as a potential principal constituent of tumour aggressiveness in anaplastic thyroid carcinomas, which warrants further assessment of their utility as novel targets for therapeutic intervention. A number of orthotopic and more recently genetically engineered immunocompetent mouse models of anaplastic thyroid carcinoma have been developed to enhance the understanding of this insidious disease [112, 113]. Interestingly, one such orthotopic model uses the same cell line in which we have carried out our *in* vitro functional assays [112], namely 8505c, thus a direct comparison using this particular model would prove critical for confirming our findings. Future studies should look at targeting the TrkA, $p75^{NTR}$ and sortilin signaling axis using these models to fully assess any potential for clinical utility.

In translational terms, recent studies in prostate [114], gastric [115], pancreatic [116] and basal cell [117] carcinomas have demonstrated that targeting tumour innervation can result in the inhibition of both tumour growth and metastasis. However, the major issue with repurposing neurotoxic drugs, such as botulinum toxin (or BOTOX), is their ability to pass through the blood brain barrier, resulting

in potentially devastating neurotoxicity and non-specific targeting of non-neuronal cells [118, 119]. Therefore, NGF, proNGF and their receptors, TrkA, $p75^{NTR}$ and sortilin, may provide alternate means for therapeutic intervention, for the purpose of targeting both tumour neurogenesis and cancer-related pathways promoting tumour growth and metastasis. At the present time, blocking antibodies developed against NGF (Tanezumab) [18], as well as small molecule inhibitors designed to disrupt TrkA and $p75^{NTR}$ signalling have been developed to combat pain [120], however, these may also be re-purposed to potentially target both tumour progression and cancer-related pain.

Overall, this thesis has contributed to provide novel evidence supporting the importance of nerve infiltration in both breast and thyroid tumours, clarified NGF as a potential regulator of this manifestation in the breast, as well as highlighted the potential role of NGF, proNGF and their receptors, TrkA, $p75^{NTR}$ and sortilin, as therapeutic targets in breast and thyroid cancer progression. The study of nerve-dependence in cancer is still in its infancy and the coming years should see more translational investigations into this new area of cancer research.

Appendices

A.1 Additional publications supplemental to this thesis

Faulkner S, Dun MD, Hondermarck H, 'Proteogenomics: Emergence and promise', Cellular and Molecular Life Sciences, 72 953-957 (2015)

http://dx.doi.org/10.1007/s00018-015-1837-y

Removed for Copyright Reasons

Sortilin is associated with breast cancer aggressiveness and contributes to tumor cell adhesion and invasion

Séverine Roselli[1,2], Jay Pundavela[1,2], Yohann Demont[3,5], Sam Faulkner[1,2], Sheridan Keene[1,2], John Attia[2,4], Chen Chen Jiang[1,2], Xu Dong Zhang[1,2], Marjorie M. Walker[2,4], Hubert Hondermarck[1,2]

[1]School of Biomedical Sciences & Pharmacy, Faculty of Health and Medicine, University of Newcastle, Callaghan NSW 2308, Australia

[2]Hunter Medical Research Institute, University of Newcastle, New Lambton NSW 2305, Australia

[3]INSERM U908, IFR-147, Universite Lille 1, Villeneuve d'Ascq 59655, France

[4]School of Public Health & Medicine, Faculty of Health and Medicine, University of Newcastle, Callaghan NSW 2308, Australia

[5]INSERM U1138, Equipe 11, Centre de Recherche des Cordeliers, Paris 75006, France

Correspondence to:
Hubert Hondermarck, **e-mail:** hubert.hondermarck@newcastle.edu.au

Keywords: breast cancer, sortilin, protein expression, cell adhesion, cell invasion

Received: January 21, 2015 ***Accepted:*** February 16, 2015 ***Published:*** March 18, 2015

ABSTRACT

The neuronal membrane protein sortilin has been reported in a few cancer cell lines, but its expression and impact in human tumors is unclear. In this study, sortilin was analyzed by immunohistochemistry in a series of 318 clinically annotated breast cancers and 53 normal breast tissues. Sortilin was detected in epithelial cells, with increased levels in cancers, as compared to normal tissues (p = 0.0088). It was found in 79% of invasive ductal carcinomas and 54% of invasive lobular carcinomas (p < 0.0001). There was an association between sortilin expression and lymph node involvement (p = 0.0093), suggesting a relationship with metastatic potential. In cell culture, sortilin levels were higher in cancer cell lines compared to non-tumorigenic breast epithelial cells and siRNA knockdown of sortilin inhibited cancer cell adhesion, while proliferation and apoptosis were not affected. Breast cancer cell migration and invasion were also inhibited by sortilin knockdown, with a decrease in focal adhesion kinase and SRC phosphorylation. In conclusion, sortilin participates in breast tumor aggressiveness and may constitute a new therapeutic target against tumor cell invasion.

INTRODUCTION

The expression of nervous system related proteins in cancer is an intriguing feature of several carcinomas that probably stems from the shared developmental origin of neurons and epithelial cells, which both derive from the neuroepithelial layer of the embryo. Neurotrophic growth factors [1], neuronal guidance molecules [2] or receptors for neurotransmitters [3] are expressed in tumors and, similarly to their role in the nervous system, may contribute to the plasticity of cancer cells.

Sortilin is a neuronal type-1 membrane protein, encoded by the *SORT1* gene, that belongs to the Vacuolar Protein Sorting 10 protein (VPS10P) family of receptors and is most abundantly expressed in both the central and peripheral nervous systems [4]. Sortilin is composed of a transmembrane segment and a short cytoplasmic tail, including motifs for interaction with cytosolic adaptor molecules. Initially described as the neurotensin receptor-3, sortilin is more generally involved in protein sorting and trafficking via a complex pattern whereby it shuttles between the cell surface and various intracellular compartments, directing target proteins to distinct destinations [5]. It is a common binding partner of tyrosine kinase receptors, G-protein coupled receptors and ion-channels, for which it facilitates ligand-induced signalling [6]. Sortilin has been identified as a co-receptor for neurotensin and pro-nerve growth factor (proNGF), and in the latter case acts in a

complex with the neurotrophin receptor p75^{NTR} to induce neuron apoptosis [6, 7]. Further to its neuronal death-promoting activity, sortilin has also recently been identified as a receptor for apolipoprotein E and is a key factor in the catabolism of amyloid-β peptide in the brain [8]. Overall, sortilin is an essential regulator of neuronal viability and a potential therapeutic target in neurodegenerative diseases, but its role outside the nervous system, and particularly in cancer remains to be determined.

In non-neuronal tissues, sortilin expression has been reported in skeletal and heart muscles, adrenal gland, thyroid, lymphocyte B cells as well as keratinocytes and adipocytes [9–12]. A few cancer cell lines have been shown to express sortilin and are impacted by its disruption. In the HT29 colon cancer cells, sortilin participates in the control of growth promoting activity by brain-derived growth factor, through interacting with its tyrosine kinase receptor TrkB [13]. Additionally, sortilin mediates the release and transfer of exosomes in the A549 lung cancer cell line [14]. In prostate cancer cells, sortilin has been shown to regulate progranulin stimulatory activity of cancer cell growth [15]. In melanoma cell lines, sortilin is a co-receptor for pro-nerve growth factor (proNGF), and acts in cooperation with the neurotrophin receptor p75^{NTR} to promote cancer cell invasion [16]. Similarly, in breast cancer cell lines sortilin has been shown to participate in proNGF induced-cell invasion through cooperation with the tyrosine kinase receptor TrkA [17]. Together, data about the impact of sortilin in cancer are fragmentary, and as the expression of sortilin has never been reported in a cohort of human cancers, its clinicopathological significance in oncology is unclear.

In the present study, sortilin protein levels were analyzed by immunohistochemistry in a cohort of clinically annotated breast cancers and normal breast tissues. The expression of sortilin was found increased in breast cancer, particularly in ductal invasive carcinomas, and there was an association with lymph node invasion. In addition, decreasing sortilin protein level resulted in a diminished adhesion and invasion of breast cancer cells.

RESULTS

Sortilin protein expression in breast cancers

Sortilin was analyzed by immunohistochemistry in a series of 318 clinically annotated breast cancers and 53 adjacent normal tissues. Sortilin expression was found only in epithelial cells of both normal and cancerous samples (Fig. 1). No labeling was observed in the stroma: fibroblasts, endothelial cells, adipocytes and extracellular matrix were all negative. The frequency distribution of sortilin levels (Fig. 2) showed that the majority of normal tissues had low levels of sortilin (staining intensity 0 and 1), while the proportion of cases with intermediate (staining intensity 2) and high (staining intensity 3) levels of sortilin increased in cancers and in particular in invasive ductal carcinomas (IDC) and lymph node positive tumors. There was a clear difference between sortilin positive and sortilin negative cases (Fig. 1) and among sortilin positive cases, the staining intensities were fairly homogeneous (mostly staining intensities 1 and 2). Therefore, the data were expressed in terms of sortilin positive *versus* sortilin negative cancer cases (Table 1). Analysis of relationships between sortilin expression and clinicopathological parameters revealed sortilin expression in 66% of breast cancers compared to 47% of adjacent normal tissues ($p = 0.0088$). A difference in expression between invasive ductal carcinomas (IDC) and invasive lobular carcinomas (ILC) was observed: 79% of IDC were positive for sortilin as compared to 54% of ILC ($p < 0.0001$). No significant association of sortilin expression was observed with tumor size, grade, patient age, ER and PR, and molecular subtypes of breast cancer (luminal A and B, HER2+, triple negative). Sortilin was expressed in 59% of triple negative breast cancers. In addition, there was a trend toward more tumors expressing sortilin among HER2-positive tumors (77%) than among HER2-negative tumors (63%) but the p-value was limited ($p = 0.0349$). A significant association was found between sortilin expression and lymph node invasion. Sortilin was expressed in 60% of lymph node negative cancers *versus* 75% of lymph node positive cancers ($p = 0.0093$), suggesting a positive relationship between sortilin expression and the metastatic potential. In Log-Linear modeling, two-way analyses confirmed the association, adjusted for all other variables, of sortilin with histological type (ductal vs. lobular invasive carcinomas, $p = 0.002$) and lymph node invasion (OR = 1.55 for lymph node positivity, $p = 0.096$).

Sortilin expression in breast cancer cell lines

A series of normal, immortalized and cancerous breast epithelial cells was analyzed for sortilin expression by RT-PCR and Western-blotting (Fig. 3). qRT-PCR analysis showed varying levels of sortilin mRNA in normal and cancer cell lines (Fig. 3A). All breast cancer cell lines expressed more mRNA for sortilin than the normal breast epithelial cells (HMEC). In Western-blotting, a band at about 100 kDa, which corresponds to the expected migration of sortilin, was observed in all tested cells (Fig. 3B). In MCF-7, SKBR-3 and BT-474 cells, an additional minor band at 50 kDa was also detected. This additional band may represent a degraded form of sortilin, which requires further characterization. Overall, there was more sortilin in cancer cell lines than in the normal HMEC. In the HMEC-derivatives model of breast carcinogenesis [18], there was an increase of sortilin in the tumorigenic HMLE and HMLER as compared to the normal HMEC and the transformed but non-tumorigenic HME (Fig. 3C) (the entire blot is shown in Supplemental Data).

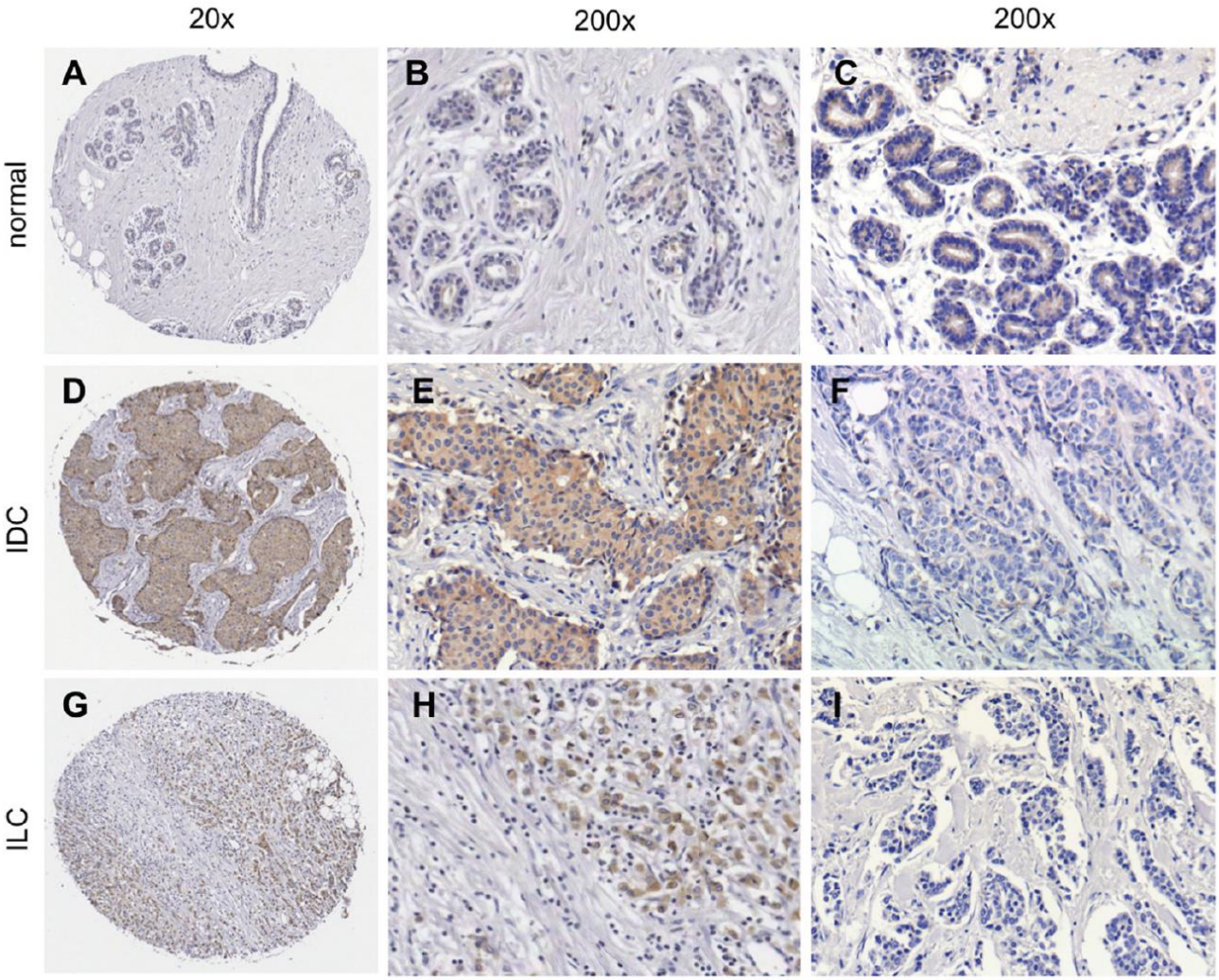

Figure 1: Immunohistological detection of sortilin in breast cancers. The expression of sortilin was assessed by immunohistochemistry in a series of invasive breast cancers and normal adjacent tissues. Representative photos of sortilin immunolabeling are shown. **(A)** Entire core and **(B, C)** higher magnifications obtained for normal breast adjacent tissue; **(D)** Entire core and **(E)**) higher magnification obtained for an invasive ductal carcinoma (IDC) positive for sortilin; **(F)** Sortilin negative IDC. **(G)** Entire core and **(H)** higher magnification obtained for an invasive lobular carcinoma (ILC) positive for sortilin; **(I)** Sortilin negative ILC. Magnification (20x, 200x) is indicated.

Impact of sortilin inhibition on breast cancer cell phenotype

The functional analysis was performed on the highly invasive and triple negative MDA-MB-231 breast cancer cell line, the HER2 overexpressing SKBR-3, and the luminal A type MCF-7 cells. Breast cancer cell lines were transfected with siRNA against sortilin *versus* control siRNA and the impact on cell growth, survival, adhesion, migration and invasion was measured. The efficacy of siRNA was assessed by Western-blotting at 24, 48 and 72 h after transfection (Fig. 4A). In MDA-MB-231 cells, a strong decrease in sortilin protein was observed from 24 h and was maintained after 72 h. In SKBR-3 and MCF-7 cells, the inhibition was complete only at 48 h, but was also maintained at 72 h. Microscopic observation 72 h after transfection (Fig. 4B) suggested that there were fewer cells in siRNA sortilin than in control siRNA, with a lower attachment (higher proportion of round cells). The decrease in cell number was confirmed by cell counting (Fig. 4C). This has prompted us to analyze cell cycle and apoptosis. Flow cytometry after propidium iodide incorporation (Fig. 4D) indicated no change in the proportion of cells in each phase of the cell cycle (G1/G0, S, G2M) between the siRNA sortilin and the siRNA control conditions. This demonstrated that the sortilin siRNA had no impact on cell proliferation. In addition there was also no change

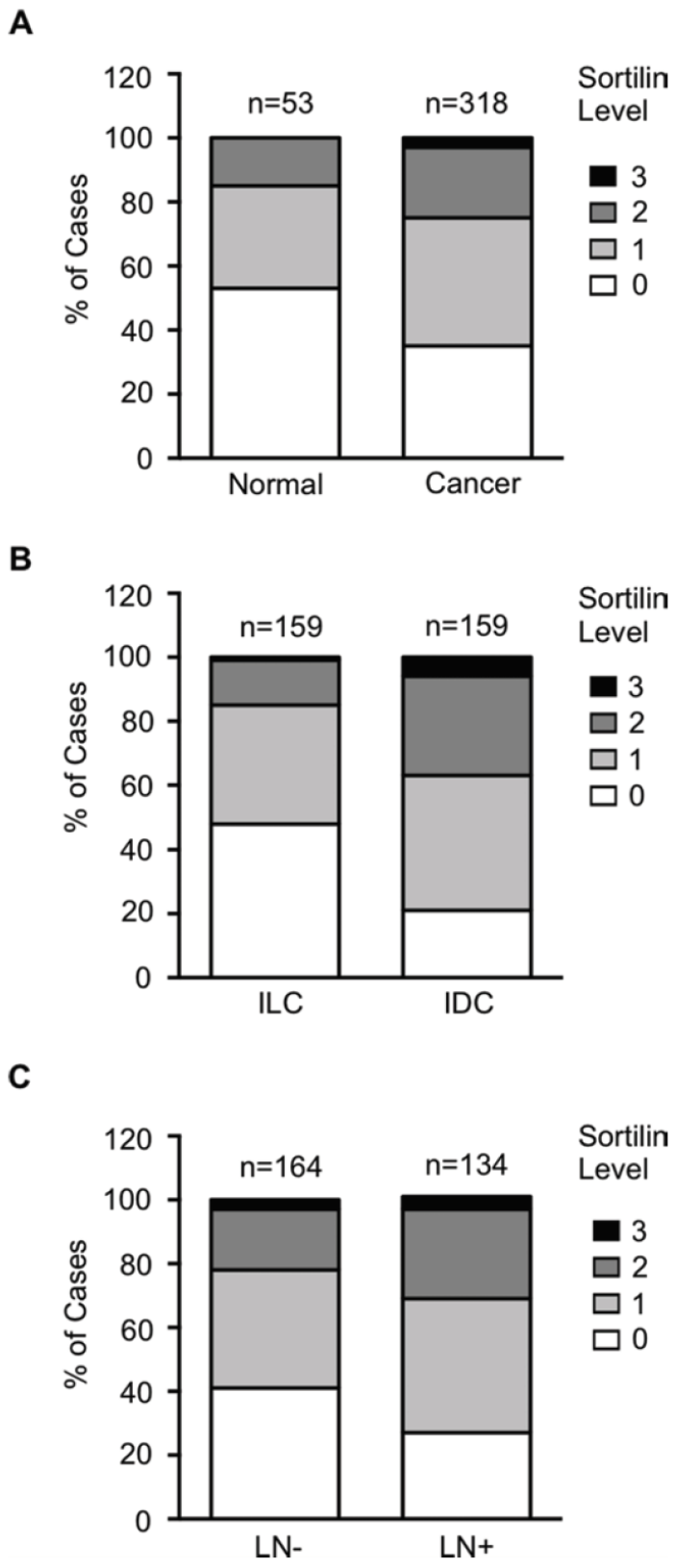

Figure 2: Frequency distribution of sortilin levels. Sortilin levels (0 = no staining, 1 = low intensity staining, 2 = intermediate intensity staining, 3 = high intensity staining) were measured in breast cancers and normal breast tissues. **(A)** Distribution in normal tissues versus breast tumors. **(B)** Distribution in invasive lobular carcinomas (ILC) versus invasive ductal carcinomas (IDC). **(C)** Distribution in lymph node negative (LN-) versus lymph node positive (LN+) cancers. Number of cases (n) is indicated. Statistical significance of the difference between groups are reported in Table 1.

Table 1: Association between sortilin expression and clinicopathological parameters in breast cancer

	Sortilin negative	Sortilin positive	*p*-value
Normal vs cancer			
Normal (n = 53)	28 (53%)	25 (47%)	0.0088
Cancer (n = 318)	107 (34%)	211 (66%)	
Pathological type			
IDC (n = 159)	34 (21%)	125 (79%)	< 0.0001[a]
ILC (n = 159)	73 (46%)	86 (54%)	
Age (years)			
< 50 (n = 171)	54 (32%)	117 (68%)	0.4075
≥ 50 (n = 147)	53 (36%)	94 (64%)	
Tumor size			
T1 (n = 25)	11 (44%)	14 (56%)	0.0951
T2 (n = 228)	75 (33%)	153 (67%)	
T3 (n = 31)	15 (48%)	16 (52%)	
T4 (n = 29)	6 (26%)	23 (74%)	
Lymph node status			
LN- (n = 164)	65 (40%)	99 (60%)	0.0093[a]
LN+ (n = 134)	34 (25%)	100 (75%)	
HER2			
HER2- (n = 252)	92 (37%)	160 (63%)	0.0349
HER2+ (n = 66)	15 (23%)	51 (77%)	
Estrogen receptor			
ER- (n = 182)	67 (37%)	115 (63%)	0.1670
ER+ (n = 136)	40 (29%)	96 (71%)	
Progesterone receptor			
PR- (n = 208)	75 (36%)	133 (64%)	0.2111
PR+ (n = 110)	32 (29%)	78 (71%)	
Breast cancer subtypes			
luminal A (n = 129)	44 (34%)	85 (66%)	0.1329
luminal B (n = 33)	9 (27%)	24 (73%)	
HER2 (n = 33)	7 (21%)	26 (79%)	
TNBC (n = 122)	50 (41%)	72 (59%)	

Abbreviations: IDC = Invasive ductal carcinoma; ILC = Invasive lobular carcinomas; HER2 = Human epidermal growth factor receptor 2; ER = estrogen receptor; PR = progesterone receptor; TNBC = Triple negative breast cancer.
Chi-square test was used to test statistical association. Statistically significant *P*-values ($p < 0.05$) are shown in bold.
[a]The association with histological type and lymph node invasion was confirmed by two-way Log-Linear analysis, but not the association with HER2+

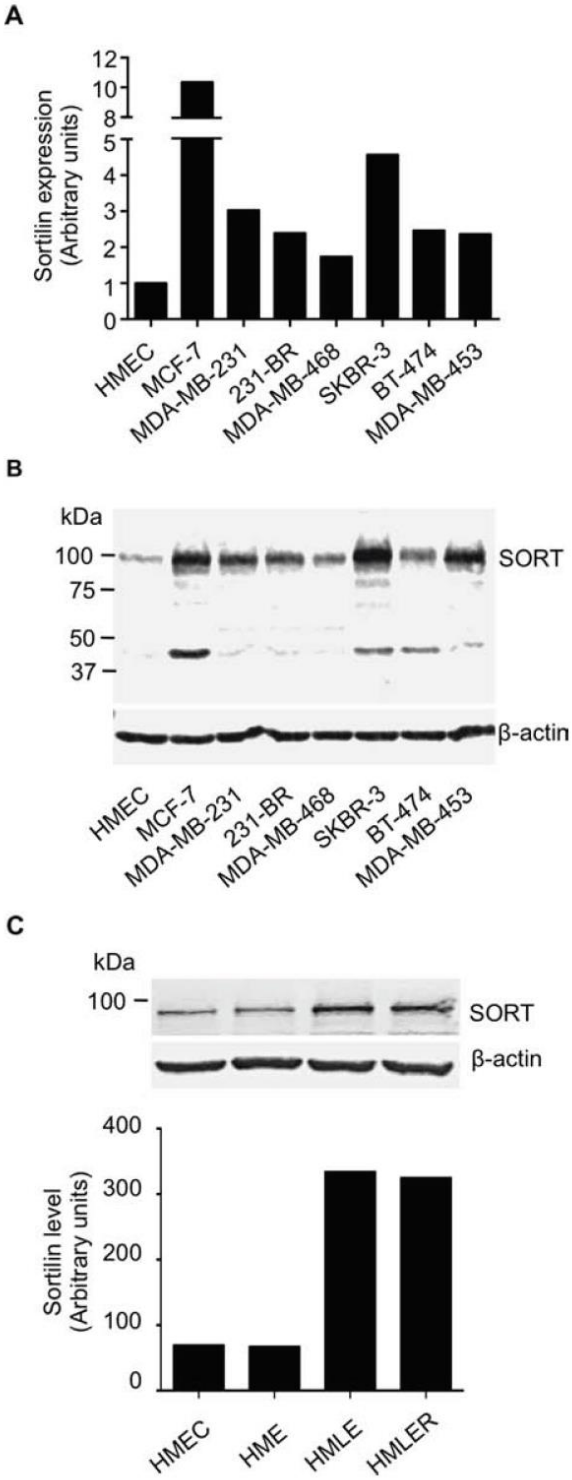

Figure 3: Expression of sortilin in breast cancer cell lines. (A) Quantitative RT-PCR analysis of sortilin gene expression in a range of breast cancer cell lines. Human mammary epithelial cells (HMEC) and the breast cancer cell lines MCF-7, MDA-MB-231 and their brain metastatic derivatives 231-BR, SKBR-3, MDA-MB-468, BT-474 and MDA-MB-453 were analyzed. Normalization was performed using β actin and the value obtained for HMEC was considered as 1. **(B)** Western-blotting detection of sortilin in the same breast cancer cell lines. A band at about 100 kDa, the expected molecular weight of sortilin, was observed in all cell lines. In MCF-7, SKBR-3 and BT474 cells, an additional band at 50 kDa was also detected. **(C)** Sortilin was detected in the HMEC derivatives model of breast tumorigenic progression. The intensity of the sortilin band was higher in the tumorigenic HMLE and HMLER cells compared to the precancerous HME and the normal non-transformed HMEC.

in subG0/G1, suggesting that siRNA against sortilin did not induce cell death. This was confirmed by Hoechst staining (Fig. 4D), as no particular nuclei fragmentation or condensation could be observed in the anti-sortilin siRNA condition. About 5% of apoptosis could be observed for all cell lines with or without anti-sortilin siRNA. Therefore, the decrease in cell number observed after sortilin siRNA transfection was not due to a decrease in cell proliferation or an increase in cell death. This has prompted us to test the impact of the sortilin siRNA on cell adhesion. Interestingly, breast cancer cell adhesion was affected by sortilin siRNA knockdown (Fig. 4E). SiRNA against sortilin resulted in 30% inhibition of MCF-7 cell adhesion, as measured 20 h after cell seeding. In SKBR-3, the inhibition of cell adhesion was ~50% and it reached ~80% in MDA-MB-231 cells. These results indicated that sortilin is involved in breast cancer cell adhesion. We then investigated the impact of sortilin knockdown on breast cancer cell migration and invasion (Fig. 5). In wound healing assay, anti-sortilin siRNA inhibited the migration of MDA-MB-231 cells (Fig. 5A). In contrast the migration of MCF-7 and SKBR-3 cells was not affected (Fig. 5A). We then looked for the invasive property of MDA-MB-231 in Transwell assays. The invasion of MDA-MB-231 cells was significantly inhibited by anti-sortilin siRNA (Fig. 5B). To take under account the potential impact of the inhibition of cell adhesion on the invasion of MDA-MB-231 cells, we counted the number of cells attached in both the upper part and the down-side of the Transwell filters (Fig.5B left panel). We then expressed the percentage (%) of invading cells, as compared to attached cells (Fig. 5B right panel). The results show that the invasion of cancer cells that had attached was inhibited and therefore, siRNA against sortilin had a direct inhibitory effect on MDA-MB-231 cell invasion. We have then explored the level of activation of various cell invasion-related signaling pathways (Fig. 5C) (the entire blots are shown in Supplemental Data). Western-blotting experiments revealed that the level of vimentin was not affected by siRNA against sortilin, indicating that the EMT (epithelial-mesenchymal transition) phenotype of MDA-MB-231 was not altered. Akt and Erk1/2 phosphorylation was also not modified, but in contrast, the activation of SRC and focal adhesion kinase (FAK) was inhibited by anti-sortilin siRNA. Therefore, the sortilin knockdown-induced inhibition of MDA-MB-231 breast cancer cell invasion involves a decrease in SRC/FAK signaling pathways.

DISCUSSION

This study is the first to report sortilin expression in a series of human tumors. The results highlight an increase in sortilin protein level in breast cancer cells, particularly in invasive ductal carcinomas, as well as an association between sortilin and lymph node invasion. Furthermore, the *in vitro* data point to a participation of sortilin in adhesion and invasion of breast cancer cells.

In terms of gene expression, sortilin mRNA abundance has not been reported to be linked to a particular molecular subtype of breast cancer or clinicopathological parameter. Data mining, using cBioportal [19] of The Cancer Genome Atlas (TCGA) database [20], which contains 1062 samples of invasive breast carcinomas, indicated that sortilin is altered in 7.2% of breast tumors with 5 cases of amplification, 2 homozygous deletions, 4 mutations, 59 mRNA up regulations, and 8 mRNA down regulations (data not shown). The 59/1062 cases of mRNA amplifications represented 5.5% of all breast cancer cases. In addition, using the Gene Expression-Based Outcome for Breast cancer Online (GOBO) [21] with datasets GSE1456, 3494, 7390, representing a total of 737 breast cancers, no relationship was found between sortilin mRNA abundance and clinicopathological parameters (molecular subtypes, lymph node invasion, ER, PR, HER2). Initial studies in yeast comparing mRNA *versus* protein levels have suggested a correlation of ~50% between mRNA and protein levels. In humans, global transcriptomic and proteomic analyses have shown that an estimated 30%–60% of changes in protein levels can be explained by corresponding variations in mRNA [23, 24]. In addition, a recent proteogenomics investigation in colorectal cancer [25] has revealed that mRNA abundance does not reliably predict protein abundance differences between tumors. This emphasizes the importance to analyse the protein level, as gene expression data may not reflect the abundance of the protein effectors in tumors.

In the present study, sortilin protein was found in a higher proportion of IDC than ILC. IDC represent the majority of breast cancers (~80%) and are generally more aggressive than ILC [26]. Sortilin expression was also detected across the molecular subtypes of breast tumors (luminal A, luminal B, HER2+ and triple negative/basal) with no significant difference. Interestingly, triple negative breast cancers, which do not express oestrogen receptor, progesterone receptor and the tyrosine kinase receptor HER2, were found to be positive for sortilin in 59% of cases. At this stage, triple negative breast cancers are characterized by what they don't express and they are the only molecular subtype of breast cancers for which there is no targeted therapies [27, 28]. As a consequence, triple negative tumors have a particularly poor prognosis with a higher propensity to metastasize. Our data suggest that sortilin could potentially be targeted in breast cancer, particularly in the aggressive and difficult to treat triple negative tumors.

The increased level of sortilin protein in breast cancers, alongside the association with lymph node invasion, has prompted us to look at the impact of sortilin inhibition in breast cancer cells. Our data indicated that decreasing the level of sortilin diminished breast cancer cell adhesion, while having no effect on cell proliferation

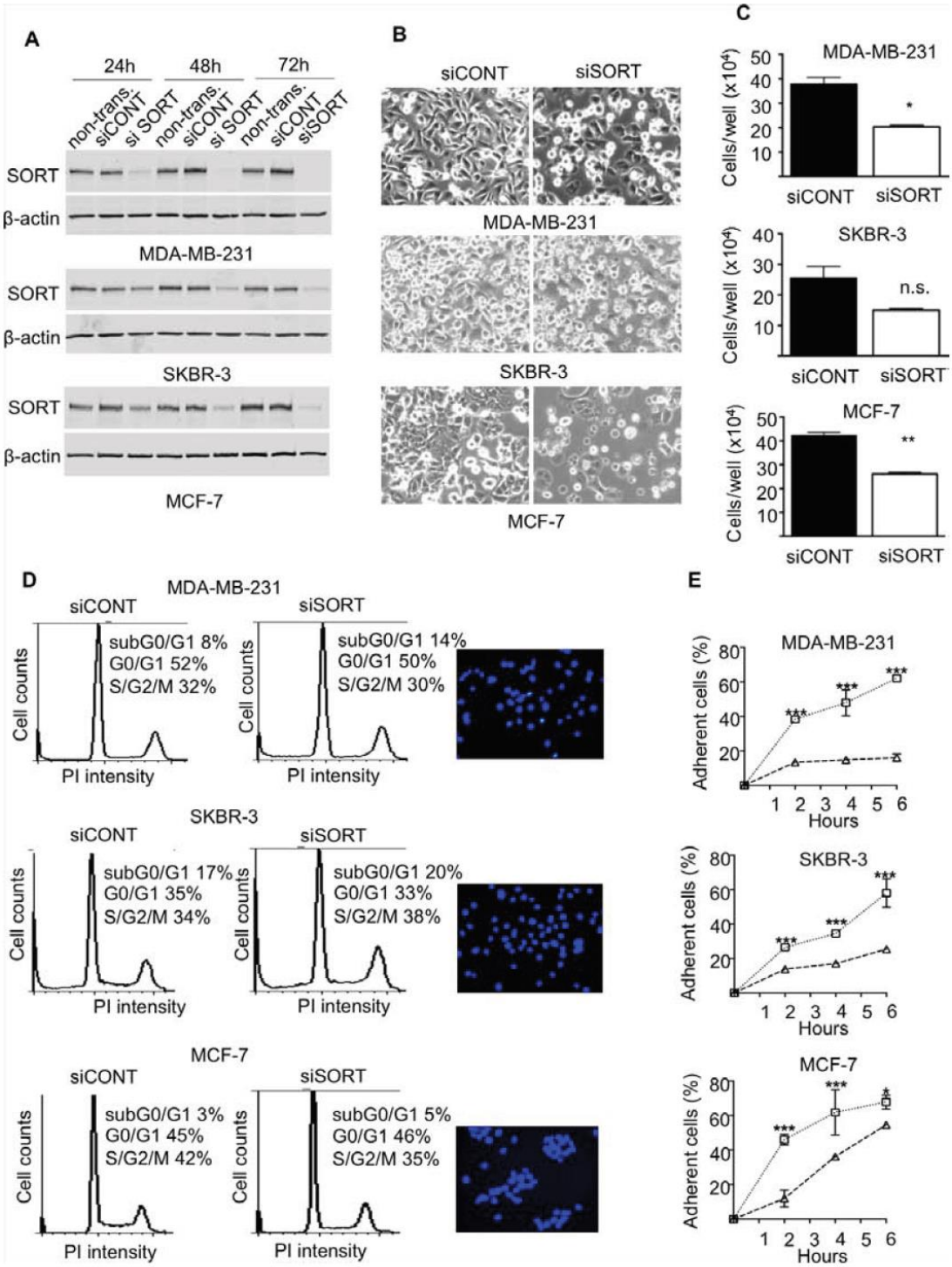

Figure 4: Impact of sortilin knockdown on proliferation, survival and adhesion of breast cancer cells. (A) SiRNA against Sortilin (siSORT) and universal negative control siRNA (siCONT) were transfected in MDA-MB-231, MCF-7 and SKBR-3 breast cancer cells, and the impact on the level of sortilin was measured by Western-blotting 24, 48 and 72 h after transfection. Non-transfected cells (non transf.) were also analyzed. **(B)** Microscopic observation of breast cancer cells 72 h after transfection with siSORT and siCONT. **(C)** Counting of breast cancer cells 72 h after transfection with siSORT versus siCONT. The histograms represent the mean number of cells per well. **(D)** Flow cytometry analysis of breast cancer cells 72 h after transfection with siSORT or siCONT. The percentage of cells in SG2M, G0/G1 and subG0/G1 is indicated. For each cell line, a picture of Hoechst staining observed in siSORT is shown. **(E)** Impact of siRNA against sortilin on breast cancer cell adhesion. Breast cancer cells were transfected with siRNA and were seeded in culture dishes. 48 h latter, number of attached cells was counted at the indicated times after seeding. Results are expressed, as percentage of adherent cells. For panel C and E, error bars represent SD. $*p < 0.05$, $**p < 0.01$, $***p < 0.001$, n.s. not significant, for the difference between siCONT and siSORT.

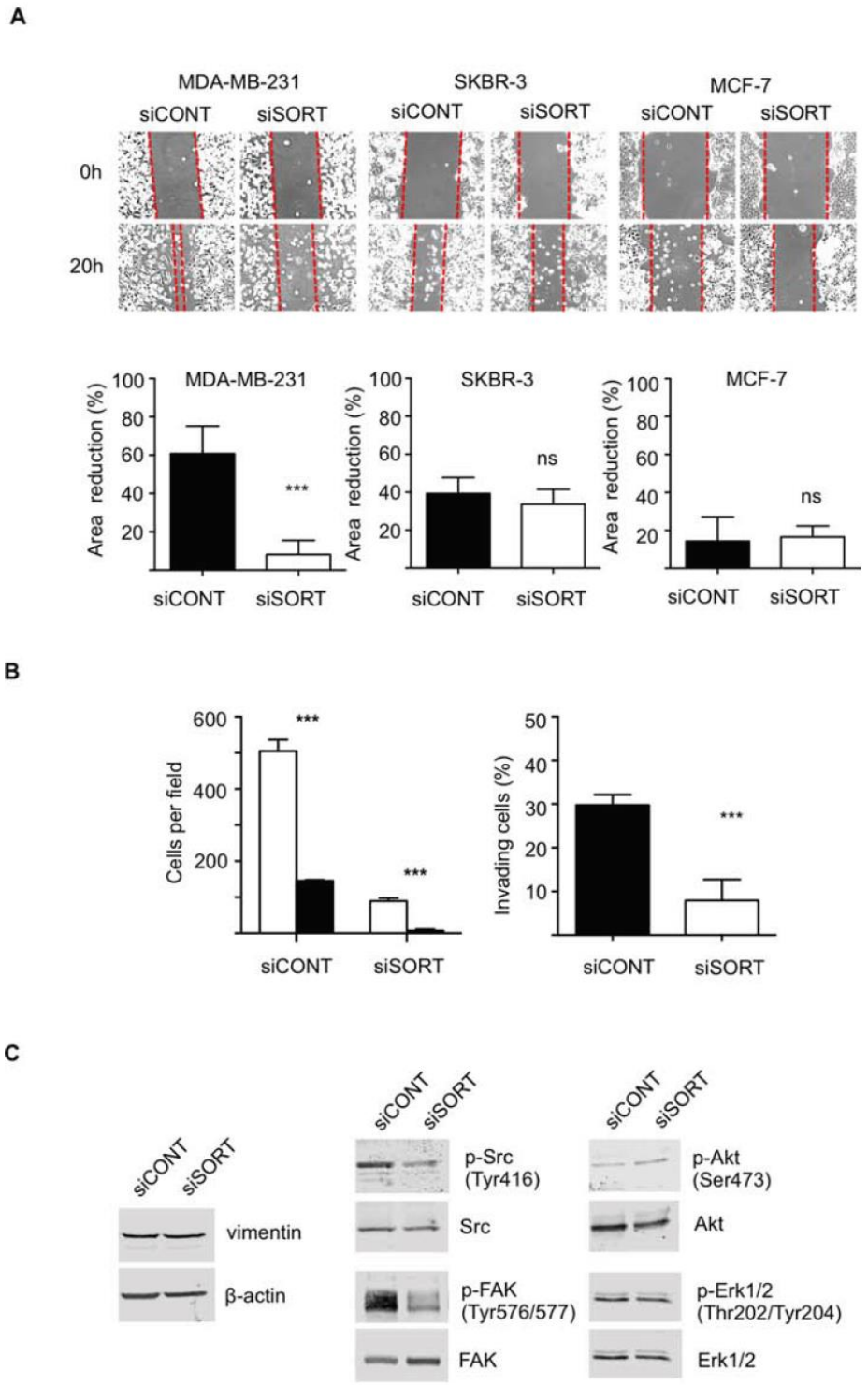

Figure 5: Impact of sortilin knockdown on migration and invasion of breast cancer cells. (A) Scratch assay. Breast cancer cells (MDA-MB-231, SKBR-3 and MCF-7) were transfected with siRNA against sortilin (siSORT) and universal negative control siRNA (siCONT). Scratching of the cell layer was performed 48 h after transfection and reduction in gap area was measured over 6 h. SiSORT inhibited migration only in MDA-MB-231 cells. **(B)** Transwell invasion assay of MDA-MB-231 cells. Transwell assays were set up 48 h after siRNA transfection and cells were allowed to invade for 48 h. To take under account a potential impact of cell adhesion on the assay, cells were counted on both sides of the Transwell filter. Left panel, white columns represent the number of cells on the upper side of the filter, and the black columns the number of cells on the down side. Right panel, the percentage of invading cells in siSORT *versus* siCONT is represented. **(C)** Western-blot detection of vimentin and activation of SRC, FAK, Akt and Erk1/2, 72 h after transfection with siSORT versus siCONT. Antibodies against vimentin, β-actin, SRC, phospho-SRC (Tyr416), FAK, phospho-FAK (Tyr576/577), Akt, phosphor-Akt (Ser473), Erk1/2, phosphor-Erk1/2 were used. For panel A and B, error bars represent SD. $*p < 0.05$, $**p < 0.01$, $***p < 0.001$, n.s. not significant, for the difference between siCONT and siSORT.

and survival. Interestingly, soluble forms of sortilin have already been implicated in cell adhesion. In the colorectal cancer cell line HT29, recent studies have shown that soluble sortilin can regulate FAK-dependent activation of the PI3 kinase pathway [29] and that soluble sortilin impairs cell to cell cohesion [30]. In breast cancer cells, we have not detected any soluble forms of sortilin (data not shown), and the molecular mechanism involved in the inhibition of cell adhesion/invasion remains to be determined. Our study also shows that sortilin is involved in breast cancer cell invasion as knockdown of sortilin in the highly invasive MDA-MB-231 cells was found to inhibit cell invasion. The process of cancer cell invasion requires not only cell migration, but also digestion of the extracellular matrix, and changes in cell adhesion are closely associated to the metastatic process [31]. Circulating cancer cells have to attach to the endothelial barrier to establish new tumoral niches and thus remodelling of cell adhesion and invasion is a hallmark of metastatic cells. The kinases SRC and FAK are generally involved in cancer cell adhesion and invasion, including in breast cancer cells [32]. Activation of SRC and FAK can be initiated by integrins and various tyrosine kinase receptors, and we show here that sortilin knockdown resulted in a decreased activation of these kinases. On the other hand, Akt and Erk1/2 were not affected, showing that sortilin inhibition has a targeted effect on cell invasion-related signaling. Further experiments are necessary to precisely define the cellular proteins directly targeted by sortilin in breast cancer cells. It has previously been shown that sortilin acts as a co-receptor for proNGF and is necessary to induce the activation of the tyrosine kinase receptor TrkA [17]. However, in the present study, proNGF was not added to the culture media and therefore, our data show that the impact of inhibiting sortilin on breast cancer cells goes beyond the regulation of proNGF activity. Although the molecular mechanism of action of sortilin in breast cancer cells, and in particular its direct interacting partners, remain to be elucidated, our data suggest sortilin, as a new potential therapeutic target in breast cancer.

In a broader perspective, it is worth noting that sortilin is also a nociceptor involved in the transmission of pain feeling by sensory neurons [33], and therefore, targeting sortilin in oncology could also inhibit cancer pain. To date, there is no available drug against sortilin, however the synthesis of a first small molecule potentially capable of inhibiting sortilin has recently been described [34] and further developments could lead to clinically relevant inhibitors [35]. As sortilin can induce neuronal apoptosis [6, 7], future sortilin inhibitors are anticipated to promote neuron survival and be of potential value for the treatment of neurodegenerative disease. Our study suggests that the inhibition of sortilin could also potentially be used in oncology to inhibit cancer cell invasion. In any case, the value of sortilin, as a potential target, in breast cancer and in other forms of cancer, warrants further consideration.

MATERIALS AND METHODS

Tumor microarrays

High-density tumor microarrays (TMA) of breast cancer biopsies and normal adjacent tissues were obtained from US Biomax Inc (Rockville, USA). These included 158 invasive ductal carcinomas, 159 invasive lobular carcinomas, and 53 normal adjacent tissues (TMAs Catalogue number BR1921 and BR1921a). Histopathological subtypes were reviewed by a pathologist (MMW). Clinical annotations included age, lymph node status, estrogen receptor (ER), progesterone receptor (PR) and human epidermal growth factor receptor 2 (HER2) status. This study was approved by the Human Research Ethics Committee of the University of Newcastle Australia.

Immunohistochemistry

After deparaffinization and rehydration, the TMAs were treated for immunohistochemistry as previously described [36]. Primary antibodies were rabbit polyclonal anti-sortilin (Cat ANT-009, Alomone Labs, Jerusalem, Israel) and non-immune rabbit IgG control (Alpha Diagnostic, San Antonio, USA) at 0.8 μg/mL. Sortilin labeling was scored by two independent observers including a pathologist, on a scale ranging from 0 to 3, as follows: 0 (no staining), 1 (low intensity staining), 2 (moderate staining), and 3 (strong staining).

Analysis of associations between sortilin expression and clinicopathological parameters

For the purpose of the analysis, because the labeling was homogeneous among sortilin positive cases, the scores were then grouped into two categories: sortilin negative (score 0) and sortilin positive (scores 1, 2, and 3). Simple unadjusted associations between sortilin and other pathological variables were performed using a chi-squared test. We used log-linear models to adjust the various bivariate associations for other potential confounders. The log linear models provided a Chi-squared test adjusted for all other variables; these included cancer type (lobular vs. ductal), lymph node involvement (yes/no), estrogen receptor positivity (yes/no), progesterone receptor positivity (yes/no), HER2+ (yes/no). The model was specified as a Poisson generalized linear model with a log-link function. Using hierarchical nesting of models we looked at all 3-way then 2-way interactions involving sortilin. Goodness of fit was tested using G2 Chi-squared statistics, as well as AIC and BIC. These models were fitted using SAS (SAS Institute, North Carolina, USA).

Cell culture

Breast cancer cells MCF-7, MDA-MB-231, SKBR-3, MDA-MB-468, MDA-MB-453, BT-474 were obtained from the American Type Culture Collection (ATCC, Manassas, USA). The brain metastatic 231-BR cell line was a generous gift from Dr Barbara Steeg (Bethesda, USA). HMEC (human mammary epithelial cells), as well as their derivatives (HME, HMLE, HMLER), were obtained from Dr Robert Weinberg (Boston, USA). Individual cell line authentication was performed after DNA extraction (Promega kit, catalogue number A1120) and using the GenePrint 10 PCR amplification kit (Promega catalogue number B9510). All cancer and non-tumorigenic cell lines were maintained in RPMI-1640 with 10% (v/v) fetal calf serum (FCS) (JRH Biosciences, St. Louis, USA) and 2 mM L-glutamine in a humidified incubator at 37°C with 5% (v/v) CO_2.

Transfection with siRNA

Cells were transfected with siRNA using lipofectamine RNAiMAX (Life Technologies) according to manufacturer's recommendations. Cells were seeded in 6-well plates and transfected 24 h later with siRNA against sortilin (siSORT CUCUGCUGUUAACACCACC[dT][dT] or a siRNA control sequence commercially available from Sigma (MISSION® siRNA Universal negative control #1). The efficiency of sortilin knockdown was assessed by Western-blotting using anti-sortilin antibody (ANT009, Alomone Labs, Israel). Actin detection (Cat antibody A2066, Sigma-Aldrich, St. Louis, USA) was used, as equiloading control.

Western-blotting

Western-blotting experiments were performed, as previously described [36], with anti-Sortilin (1:500 dilution; Cat ANT-009, Alomone Labs, Jerusalem, Israel) and mouse anti-β-actin (1:5000 dilution; Sigma-Aldrich, St. Louis, USA). Antibodies from Cell Signaling Technology (USA) were also used for SRC (cat 2100), phosphoSRC (Tyr416, cat 2101), FAK (cat 1009), phosphoFAK (Tyr576/577, cat 3281), Erk1/2 (cat 9107), phosphoErk1/2 (Thr202/Tyr204, cat 4370), Akt (cat 9272), phosphoAkt (Ser473, cat 9271), vimentin (cat 5741).

Quantitative reverse transcription-PCR (qRT-PCR)

Total RNA was isolated from breast cancer cell lines using the illustra RNAspin Mini RNA Isolation Kit (GE Healthcare Life Sciences, Little Chalfont, UK). Reverse transcription was performed with 1 μg of total RNA using the iScript cDNA Synthesis Kit (Bio-Rad Laboratories, Inc., Hercules, USA). Real-time PCR was performed using 2 μl 1/10 cDNA using iTaq Universal SYBR Green Supermix (Bio-Rad Laboratories, Inc., Hercules, USA). Sortilin Primers were Quantitect Primer Assay QT00073318 (Qiagen, Venlo, Netherlands). The PCR was carried out in a ABI7500 Real-Time PCR System (Applied Biosystems, Thermo Scientific, Waltham, USA) using the following conditions, 95°C for 10 minutes, 40 cycles of 95°C for 15 seconds and 60°C for 60 seconds followed by a continuous Melt curve from 65°C to 95°C. Data analysis was performed using the ABI7500 Real-Time Software (Applied Biosystems, Thermo Scientific, Waltham, USA). Relative expression was obtained using the $2^{-\Delta\Delta Ct}$ method.

Flow cytometry

Breast cancer cells (MDA-MB-231, SKBR-3, MCF-7) were collected by trypsinization after 72 h siRNA transfection, pooled with the saved growth media, and pelleted at 500 × g for 5 min. After PBS wash and counting, 10^6 cells were gently resuspended in 400 μL of ice-cold PBS followed by addition of 800 μL ice cold 100% (v/v) ethanol in order to achieve fixation in 66% (v/v) ice cold ethanol at 4°C overnight. On the day of cell cycle analysis, the fixed cell samples in ethanol were equilibrated to room temperature, gently re-suspended and pelleted at 500 × g for 5 min followed by a PBS wash. Labeling was performed by addition of 500 μL of FxCycle Propidium iodide/RNase staining solution (Life Technologies, USA) to each sample and incubation for 15–30 min at room temperature in the dark. Cell cycle analysis was performed with a BD FACSCanto flow cytometer (Becton Dickinson, Sydney, Australia) and the data was analyzed using the WEASEL software (WEHI, Melbourne, Australia). The percentage of cells in the different phases of the cell cycle (G0/G1, S, G2/M) as well as the subG0/G1 (indicative of cell death) was determined.

Hoechst staining

The proportion of cells in apoptosis was determined using Hoechst staining, as previously described [37].

Adhesion assay

Breast cancer cells were transfected with anti-sortilin or control siRNA as indicated above. After 48 h they were detached using trypsin free TrypLE dissociation solution (Invitrogen, Thermo Scientific, Waltham, USA), and seeded at 10^5 cells/mL in 12-well cell Corning culture plates (Corning, USA). After 2, 4, and 6 h, adherent cells were counted under a phase contrast microscope. Adherent cells appeared flat and attached, while non-adherent cells were round and mobile. Counting was performed in 5 random fields per culture dish. The assay was done in triplicate.

Migration assay

Breast cancer cells were seeded in 6-well plate (5×10^5 cells per well) and transfected with anti-sortilin

or control siRNA. After 48 h, the cell monolayer was scratched with a 200 µL pipette tip, rinsed three times with PBS and replaced with media containing 0.1% (v/v) FCS. The gap area that resulted from the scratch was monitored by taking pictures of three random areas using a phase contrast microscope (Zeiss) over 6 h post-scratch. Results are shown, as the percentage reduction of the gap area measured using ImageJ (NIH).

Invasion assay

Cell invasion assays were performed in 12-well Boyden microchambers (Transwell®) with 8 µm pore size membranes. Transwells were first coated with 100 µL of starvation medium with 0.1% (v/v) FCS plus 40 µg of rat-tail collagen I for 1 h at 37°C. Cell loading was done with 100,000 siRNA transfected cells (48 h after transfection) in 400 µL starvation medium with 0.1% (v/v) FCS in the upper chamber whereas 1.6 mL starvation medium with 0.1% (v/v) FCS was placed in the lower chamber. After 20 h of incubation, the Transwell filters were rinsed with PBS and cells at the upper surface of the membrane were gently scraped and removed for counting. Cells having invaded to the down side of the membrane were fixed and stained with 0.1% (w/v) crystal violet before counting (10 fields per membrane) through an inverted microscope.

Statistical analysis

In the cell growth, adhesion, migration and invasion assays, each condition was performed in triplicate and statistical analysis was conducted using GraphPad Prism 6. The results of cell growth, migration and invasion assays were compared using a *t*-test and cell adhesion over time was compared using repeated measure two-way ANOVA.

ACKNOWLEDGEMENTS

This work was supported by the University of Newcastle Australia, the Hunter Cancer Research Alliance, and the French National Institute of Health (INSERM). We thank Christopher Oldmeadow from the Clinical Research Design, IT, and Statistical Support (CReDITSS) Unit of the University of Newcastle. Helen Carpenter provided excellent technical assistance.

Author's contributions

SR carried out the immunohistochemistry and siRNA experiments. MW, who is an experienced pathologist, performed the grading and scoring of TMAs. SR duplicated grading and scoring. SK and JP have done the qRT-PCR and Western-blotting respectively. JP also formatted the Figures of the manuscript. SR and CCJ have performed the flow cytometry analysis. YD carried out some of the functional *in vitro* assay of cell growth, apoptosis and invasion. JA supervised the statistical analyses. HH, XDZ and MMW supervised the study. HH conceived the study and drafted the manuscript. All authors read and approved the final manuscript.

CONFLICT OF INTEREST

The authors declare no conflict of interest.

REFERENCES

1. Mancino M, Ametller E, Gascon P, Almendro V. The neuronal influence on tumor progression. Biochim Biophys Acta. 2011; 1816:105–118.
2. Mehlen P, Delloye-Bourgeois C, Chedotal A. Novel roles for Slits and netrins: axon guidance cues as anticancer targets? Nat Rev Cancer. 2011; 11:188–197.
3. Li ZJ, Cho CH. Neurotransmitters, more than meets the eye—neurotransmitters and their perspectives in cancer development and therapy. Eur J Pharmacol. 2011; 667:17–22.
4. Willnow TE, Petersen CM, Nykjaer A. VPS10P-domain receptors - regulators of neuronal viability and function. Nature reviews Neuroscience. 2008; 9:899–909.
5. Hermey G. The Vps10p-domain receptor family. Cell Mol Life Sci. 2009; 66:2677–2689.
6. Nykjaer A, Willnow TE. Sortilin: a receptor to regulate neuronal viability and function. Trends in neurosciences. 2012; 35:261–270.
7. Nykjaer A, Lee R, Teng KK, Jansen P, Madsen P, Nielsen MS, Jacobsen C, Kliemannel M, Schwarz E, Willnow TE, Hempstead BL, Petersen CM. Sortilin is essential for proNGF-induced neuronal cell death. Nature. 2004; 427:843–848.
8. Carlo AS, Gustafsen C, Mastrobuoni G, Nielsen MS, Burgert T, Hartl D, Rohe M, Nykjaer A, Herz J, Heeren J, Kempa S, Petersen CM, Willnow TE. The pro-neurotrophin receptor sortilin is a major neuronal apolipoprotein E receptor for catabolism of amyloid-beta peptide in the brain. J Neurosci. 2013; 33:358–370.
9. Nielsen MS, Jacobsen C, Olivecrona G, Gliemann J, Petersen CM. Sortilin/neurotensin receptor-3 binds and mediates degradation of lipoprotein lipase. J Biol Chem. 1999; 274:8832–8836.
10. Kiss M, Dallos A, Kormos B, Santha P, Dobozy A, Husz S, Kemeny L. Sortilin is expressed in cultured human keratinocytes and is regulated by cutaneous neuropeptides. J Invest Dermatol. 2010; 130:2553–2560.

11. Fauchais AL, Lalloue F, Lise MC, Boumediene A, Preud'homme JL, Vidal E, Jauberteau MO. Role of endogenous brain-derived neurotrophic factor and sortilin in B cell survival. J Immunol. 2008; 181:3027–3038.
12. Botta R, Lisi S, Pinchera A, Giorgi F, Marcocci C, Taddei AR, Fausto AM, Bernardini N, Ippolito C, Mattii L, Persani L, de Filippis T, Calebiro D, Madsen P, Petersen CM, Marino M. Sortilin is a putative postendocytic receptor of thyroglobulin. Endocrinology. 2009; 150:509–518.
13. Akil H, Perraud A, Melin C, Jauberteau MO, Mathonnet M. Fine-tuning roles of endogenous brain-derived neurotrophic factor, TrkB and sortilin in colorectal cancer cell survival. PloS one. 2011; 6:e25097.
14. Wilson CM, Naves T, Vincent F, Melloni B, Bonnaud F, Lalloue F, Jauberteau MO. Sortilin mediates the release and transfer of exosomes in concert with two tyrosine kinase receptors. J Cell Sci. 2014; 127:3983–3997.
15. Tanimoto R, Morcavallo A, Terraciano M, Xu SQ, Stefanello M, Buraschi S, Lu KG, Bagley DH, Gomella LG, Scotlandi K, Belfiore A, Iozzo RV, Morrione A. Sortilin regulates progranulin action in castration-resistant prostate cancer cells. Endocrinology. 2015:en20141590; 156:58–70.
16. Truzzi F, Marconi A, Lotti R, Dallaglio K, French LE, Hempstead BL, Pincelli C. Neurotrophins and their receptors stimulate melanoma cell proliferation and migration. J Invest Dermatol. 2008; 128:2031–2040.
17. Demont Y, Corbet C, Page A, Ataman-Onal Y, Choquet-Kastylevsky G, Fliniaux I, Le Bourhis X, Toillon RA, Bradshaw RA, Hondermarck H. Pro-nerve growth factor induces autocrine stimulation of breast cancer cell invasion through tropomyosin-related kinase A (TrkA) and sortilin protein. J Biol Chem. 2012; 287:1923–1931.
18. Elenbaas B, Spirio L, Koerner F, Fleming MD, Zimonjic DB, Donaher JL, Popescu NC, Hahn WC, Weinberg RA. Human breast cancer cells generated by oncogenic transformation of primary mammary epithelial cells. Genes Dev. 2001; 15:50–65.
19. Cerami E, Gao J, Dogrusoz U, Gross BE, Sumer SO, Aksoy BA, Jacobsen A, Byrne CJ, Heuer ML, Larsson E, Antipin Y, Reva B, Goldberg AP, Sander C, Schultz N. The cBio cancer genomics portal: an open platform for exploring multidimensional cancer genomics data. Cancer discovery. 2012; 2:401–404.
20. Cancer Genome Atlas N. Comprehensive molecular portraits of human breast tumours. Nature. 2012; 490:61–70.
21. Ringner M, Fredlund E, Hakkinen J, Borg A, Staaf J. GOBO: gene expression-based outcome for breast cancer online. PloS one. 2011; 6:e17911.
22. Gygi SP, Rochon Y, Franza BR, Aebersold R. Correlation between protein and mRNA abundance in yeast. Mol Cell Biol. 1999; 19:1720–1730.
23. Vogel C, Marcotte EM. Insights into the regulation of protein abundance from proteomic and transcriptomic analyses. Nature reviews Genetics. 2012; 13:227–232.
24. Li JJ, Bickel PJ, Biggin MD. System wide analyses have underestimated protein abundances and the importance of transcription in mammals. PeerJ. 2014; 2:e270.
25. Zhang B, Wang J, Wang X, Zhu J, Liu Q, Shi Z, Chambers MC, Zimmerman LJ, Shaddox KF, Kim S, Davies SR, Wang S, Wang P, Kinsinger CR, Rivers RC, Rodriguez H, et al. Proteogenomic characterization of human colon and rectal cancer. Nature. 2014; 513:382–387.
26. Weigelt B, Geyer FC, Reis-Filho JS. Histological types of breast cancer: how special are they? Molecular oncology. 2010; 4:192–208.
27. Metzger-Filho O, Tutt A, de Azambuja E, Saini KS, Viale G, Loi S, Bradbury I, Bliss JM, Azim HA, Jr., Ellis P, Di Leo A, Baselga J, Sotiriou C, Piccart-Gebhart M. Dissecting the heterogeneity of triple-negative breast cancer. J Clin Oncol. 2012; 30:1879–1887.
28. Duffy MJ, McGowan PM, Crown J. Targeted therapy for triple-negative breast cancer: where are we? Int J Cancer. 2012; 131:2471–2477.
29. Massa F, Devader C, Beraud-Dufour S, Brau F, Coppola T, Mazella J. Focal adhesion kinase dependent activation of the PI3 kinase pathway by the functional soluble form of neurotensin receptor-3 in HT29 cells. Int J Biochem Cell Biol. 2013; 45:952–959.
30. Massa F, Devader C, Lacas-Gervais S, Beraud-Dufour S, Coppola T, Mazella J. Impairement of HT29 Cancer Cells Cohesion by the Soluble Form of Neurotensin Receptor-3. Genes & cancer. 2014; 5:240–249.
31. Valastyan S, Weinberg RA. Tumor metastasis: molecular insights and evolving paradigms. Cell. 2011; 147:275–292.
32. Mitra SK, Schlaepfer DD. Integrin-regulated FAK-Src signaling in normal and cancer cells. Curr Opin Cell Biol. 2006; 18:516–523.
33. Lewin GR, Nykjaer A. Pro-neurotrophins, sortilin, and nociception. Eur J Neurosci. 2014; 39:363–374.
34. Andersen JL, Schroder TJ, Christensen S, Strandbygard D, Pallesen LT, Garcia-Alai MM, Lindberg S, Langgard M, Eskildsen JC, David L, Tagmose L, Simonsen KB, Maltas PJ, Ronn LC, de Jong IE, Malik IJ, et al. Identification of the first small-molecule ligand of the neuronal receptor sortilin and structure determination of the receptor-ligand

complex. Acta crystallographica Section, D, Biological crystallography. 2014; 70:451–460.

35. Longo FM, Massa SM. Small-molecule modulation of neurotrophin receptors: a strategy for the treatment of neurological disease. Nature reviews Drug discovery. 2013; 12:507–525.

36. Pundavela J, Demont Y, Jobling P, Lincz LF, Roselli S, Thorne RF, Bond D, Bradshaw RA, Walker MM, Hondermarck H. ProNGF Correlates with Gleason Score and Is a Potential Driver of Nerve Infiltration in Prostate Cancer. The American journal of pathology. 2014; 184:3156–3162.

37. Vanhecke E, Adriaenssens E, Verbeke S, Meignan S, Germain E, Berteaux N, Nurcombe V, Le Bourhis X, Hondermarck H. Brain-derived neurotrophic factor and neurotrophin-4/5 are expressed in breast cancer and can be targeted to inhibit tumor cell survival. Clin Cancer Res. 2011; 17:1741–1752.

This research was originally published in Molecular & Cellular Proteomics. Dun MD, Chalkley RJ, Faulkner S, Keene S, Avery-Kiejda KA, Scott RJ, et al., 'Proteotranscriptomic profiling of 231-BR breast cancer cells: Identification of potential biomarkers and therapeutic targets for brain metastasis'. Mol Cell Proteomics. 2015; 14:2316-2330. © the American Society for Biochemistry and Molecular Biology .

Research

Proteotranscriptomic Profiling of 231-BR Breast Cancer Cells: Identification of Potential Biomarkers and Therapeutic Targets for Brain Metastasis*[S]

Matthew D. Dun‡§‡‡, Robert J. Chalkley¶‡‡, Sam Faulkner‡§, Sheridan Keene‡§, Kelly A. Avery-Kiejda‡§, Rodney J. Scott‡§, Lasse G. Falkenby‖, Murray J. Cairns‡§, Martin R. Larsen‖, Ralph A. Bradshaw¶, and Hubert Hondermarck‡§**

Brain metastases are a devastating consequence of cancer and currently there are no specific biomarkers or therapeutic targets for risk prediction, diagnosis, and treatment. Here the proteome of the brain metastatic breast cancer cell line 231-BR has been compared with that of the parental cell line MDA-MB-231, which is also metastatic but has no organ selectivity. Using SILAC and nanoLC-MS/MS, 1957 proteins were identified in reciprocal labeling experiments and 1584 were quantified in the two cell lines. A total of 152 proteins were confidently determined to be up- or down-regulated by more than twofold in 231-BR. Of note, 112/152 proteins were decreased as compared with only 40/152 that were increased, suggesting that down-regulation of specific proteins is an important part of the mechanism underlying the ability of breast cancer cells to metastasize to the brain. When matched against transcriptomic data, 43% of individual protein changes were associated with corresponding changes in mRNA, indicating that the transcript level is a limited predictor of protein level. In addition, differential miRNA analyses showed that most miRNA changes in 231-BR were up- (36/45) as compared with down-regulations (9/45). Pathway analysis revealed that proteome changes were mostly related to cell signaling and cell cycle, metabolism and extracellular matrix remodeling. The major protein changes in 231-BR were confirmed by parallel reaction monitoring mass spectrometry and consisted in increases (by more than fivefold) in the matrix metalloproteinase-1, ephrin-B1, stomatin, myc target-1, and decreases (by more than 10-fold) in transglutaminase-2, the S100 calcium-binding protein A4, and L-plastin. The clinicopathological significance of these major proteomic changes to predict the occurrence of brain metastases, and their potential value as therapeutic targets, warrants further investigation. ***Molecular & Cellular Proteomics 14: 10.1074/mcp.M114.046110, 2316–2330, 2015.***

Brain metastases affect 10–20% of cancer patients with disseminated disease (1). Even small lesions can cause neurological disability, and the median survival time of patients with brain metastases is short, with about 80% mortality within one year of diagnosis. The molecular basis of cancer metastases to the brain remains unknown and with advances in the control of systemic disease, the incidence of brain metastases is increasing (1, 2). In the case of breast cancer, brain relapse typically occurs years after primary tumor excision, suggesting that disseminated breast cancer cells must first acquire specialized functions to invade and grow in this organ (3). Retrospective studies of breast cancer patients with brain metastases found that a young age at diagnosis, primary tumors that are estrogen receptor negative or overexpressing the human epidermal growth factor receptor 2 (HER2)[1] and/or epidermal growth factor receptor, and the

From the ‡School of Biomedical Sciences & Pharmacy and §Hunter Medical Research Institute, Faculty of Health and Medicine, University of Newcastle, Callaghan, New South Wales 2308, Australia¶Department of Pharmaceutical Chemistry, University of California San Francisco, California 94158; ‖Department of Biochemistry and Molecular Biology, University of Southern Denmark, Campusvej 55, DK-5230 Odense M, Denmark

Received November 3, 2014, and in revised form, May 28, 2015
Published, MCP Papers in Press, June 3, 2015, DOI 10.1074/mcp.M114.046110

Author contributions: M.D.D., R.J.C., R.A.B., and H.H. designed research; M.D.D., R.J.C., S.F., S.K., K.A., L.G.F., and M.R.L. performed research; L.G.F. and M.R.L. contributed new reagents or analytic tools; M.D.D., R.J.C., S.F., K.A., R.J.S., M.J.C., R.A.B., and H.H. analyzed data; R.A.B. and H.H. wrote the paper.

[1] The abbreviations used are: HER2, human epidermal growth factor receptor-2; EFNB1, ephrin-B1; ER, estrogen receptor; FOXO1, forkhead box protein O1; KDM5B, Lysine (K)-Specific Demethylase 5B; LC-MS/MS, liquid chromatography-tandem mass spectrometry; LCP1, lymphocyte cytosolic protein 1 (L-plastin); miRNA, microRNA; MMP1, matrix metalloproteinase-1; MYCT1, myc target-1; PGR, progesterone receptor; PRM, parallel reaction monitoring; S100A4, S100 calcium-binding protein A4; SILAC, stable isotope labeling of amino acids in cell culture; STOM, stomatin; SYVN1, synovial apoptosis inhibitor 1; TGF-β, transforming growth factor-β; TGM2, transglutaminase-2; TNF-α, tumor necrosis factor-α; TERM1, triggering receptor expressed on myeloid cells 1; UAP1, UDP-N-acetyl-glucosamine pyrophophorylase.

presence of lymph node or distant metastases were all associated with a higher risk of brain metastatic disease (4). However, at this stage there is no molecular marker, at the gene, mRNA or protein level that is clinically useful to predict, diagnose, or treat breast cancer-derived brain metastases (5). Therefore it is essential to better define the molecular basis for these phenomena and delineate predictive biomarkers and therapeutic targets for future innovative treatments.

In the present study, proteome changes associated to brain metastatic capabilities of breast cancer cells were explored. To that purpose, we have used the unique opportunity provided by the 231-BR/MDA-MB-231 cellular models. 231-BR cells (also named MDA-MB-231BR) have initially been established from the triple negative (no expression of estrogen receptor, progesterone receptor, and HER2) MDA-MB-231 cells, which are highly metastatic but have no organ specificity, being able to metastasize to many different sites. The brain metastatic 231-BR cell line has been derived from MDA-MB-231 cells after successive rounds of implantation, resection from the brain, and re-injection into mice, to produce a subline with selectivity for the brain as compared with other metastatic sites (6). 231-BR cells metastasize with 100% frequency to the brain and they have progressively emerged as an established preclinical model of brain metastatic breast cancer (2). For instance, they have been used to demonstrate that Her-2 overexpression increases the metastatic outgrowth of breast cancer cells in the brain (7), that the anti-HER2 drug lapatinib can inhibit the growth of brain metastatic cells (8), and that the blood–tumor barrier permeability determines drug efficacy in experimental brain metastases (9). They have also been used to analyze brain metastasis in magnetic resonance imaging (10) and to investigate brain damage induced by brain metastases (11).

Despite the considerable interest and use of 231-BR cells for studying the mechanisms underlying brain metastasis, the proteome of these cells has not been thoroughly explored. One study (12) has reported a 2D electrophoresis-based analysis, but no major proteome changes were identified. In the present report, stable isotope labeling of amino acids in culture (SILAC) and liquid chromatography (LC)-MS/MS tandem mass spectrometry was used to analyze the proteome of 231-BR *versus* MDA-MB-231 cells. Changes in the proteome were compared with those in the transcriptome (mRNA and miRNA), and several proteins and molecular pathways that may participate in the underlying basis of metastasis to the brain have been identified.

EXPERIMENTAL PROCEDURES

The workflow of this study is presented in Fig. 1. Institutional Ethics Committee approval was obtained from the University of Newcastle Australia.

Cell Culture and SILAC Labeling—Breast cancer cell lines 231-BR and parental MDA-MB-231 were a generous gift from Dr. Patricia S. Steeg (National Cancer Institute, Bethesda, MD). Both cell lines were routinely grown in DMEM supplemented with 2 mM L-glutamine and

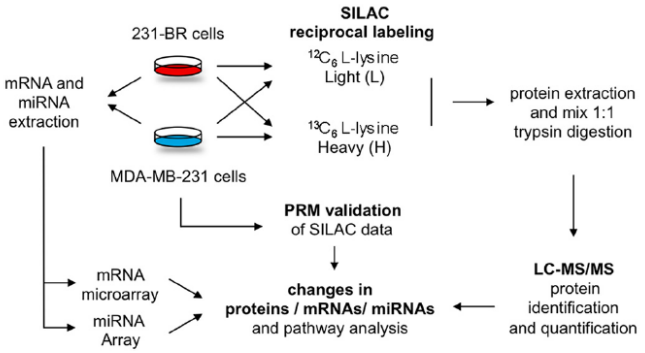

FIG. 1. **Experimental workflow.** Stable isotope labeling of amino acids in cell culture (SILAC) reciprocal labeling was performed on both the brain metastatic breast cancer cell line 231-BR and the parental cell line MDA-MB-231, which is also metastatic but has no organ selectivity. After extraction, mixing 1:1, and protein digestion with trypsin, LC-MS/MS analysis (using a Q-Exactive Plus from Thermo Fischer Scientific after liquid chromatography on a Nano-Acquity ultraperformance column from Waters) was used to identify and quantify reciprocally labeled proteins. Peptide sequence, protein identification, and quantification were obtained using Protein Prospector and the SwissProt database. Major protein changes observed in SILAC were validated in parallel reaction monitoring (PRM) from nonlabeled proteins. Protein pathway analysis was performed with Ingenuity Pathway Analysis software. In parallel to proteomics, a transcriptomic analysis was conducted. mRNA and miRNA were extracted from both cell lines (three biological replicates). GeneChip Exon arrays analysis and GeneChip miRNA arrays were used for analyzing the expression of mRNA and miRNA respectively.

10% fetal calf serum (Sigma-Aldrich, St. Louis, MO) in 75 cm^2 tissue culture flasks in a humidified incubator at 37 °C with 5% CO_2. 231-BR and MDA-MB-231 cells were reciprocally labeled using SILAC heavy $^{13}C_6$-lysine (Lys6) and L-arginine-HCl (Arg0), labels dissolved in SILAC RPMI 1640 medium without arginine and lysine and supplemented with 10% dialyzed fetal bovine serum (Pierce SILAC Protein Quantitation Kit, Rockford, IL). Light condition medium was supplemented with L-lysine 2HCl (Lys0) L-arginine HCl (Arg0). The concentrations of supplemented amino acids used were 50 mg/L. The cells were passaged seven times with intermediate splitting after 3 days and at a density of 5×10^5 cells/75-cm flask. Cells were counted and pelleted at 1×10^7 cells and snap frozen in liquid nitrogen. Reciprocal labeling provides a biological replicate, as two different sets of cell cultures are used for protein preparation before independent analyses by mass spectrometry. Specifically, there were two biological replicates for 231-BR cells ($^{13}C_6$ L-Lysine labeled-Heavy and $^{12}C_6$ L-Lysine labeled-Light), and two biological replicates for MDA-MB-231 ($^{13}C_6$ L-Lysine labeled-Heavy and $^{12}C_6$ L-Lysine labeled- Light). For mass spectrometric analyses ($^{13}C_6$ L-Lysine labeled-Heavy) 231-BR were analyzed *versus* ($^{12}C_6$ L-Lysine labeled-Light) MDA-MB-231), and ($^{12}C_6$ L-Lysine labeled-Light) 231-BR *versus* ($^{13}C_6$ L-Lysine labeled-Heavy) MDA-MB-231. The final results correspond to the mean of the two mass spectrometric analyses.

Protein Preparation for Mass Spectrometry—Membrane proteins were enriched from the soluble proteins of the SILAC heavy and light reciprocally labeled 231-BR and MDA-MB-231 cell pellets and unlabeled cell pellets for label-free parallel reaction monitoring (PRM) analysis (1×10^7 cells) by dissolving each cell pellet in 1 ml of ice-cold 0.1 M Na_2CO_3 supplemented with protease inhibitor (Roche Complete EDTA Free), sonicated for 2×20 s and incubated for 1 h at 4 °C. The homogenates were then centrifuged at $100,000 \times g$ for 90 min at 4 °C (13). The membrane pellets were redissolved in 500 mM triethylam-

monium bicarbonate and centrifuged at 14,000 × *g* for 30 min at 4 °C. These pellets were then briefly rinsed in 50 mM triethylammonium bicarbonate and stored on ice. Soluble proteins were concentrated (Microcon-10kDa Centrifugal Filter Unit, Millipore, Billerica, MA) and both the pellets and concentrated soluble proteins dissolved in urea buffer (6 M urea, 2 M thiourea) and reduced using 10 mM dithiotreitol (1 h, 56 °C), alkylated using 20 mM iodoacetamide (45 min, room temperature, in the dark), and subsequently digested with 0.05 activity units of Lys-C endoproteinase (Wako, Osaka, Japan) for 3 h at 37 °C. After Lys-C digestion, the solution was diluted below 0.75 M urea, 0.25 M thiourea, and digested with 2% w/w trypsin (Promega, Madison, WI) overnight at 37 °C. Each peptide sample was desalted using a modified StageTip microcolumn (14) consisting of a pipette tip with a C18 Empore disk plug packed with Poros Oligo R3 reversed phase material. Peptides were acidified (pH 2) using 10% trifluoroacetic acid (TFA) and loaded on the Oligo R3 microcolumn. The microcolumn was washed with 0.1% TFA, and the peptides were eluted sequentially with 50% acetonitrile, 0.1% TFA then 70% acetonitrile, 0.1% TFA. The eluents were lyophilized.

LC-MS/MS for SILAC Analyses—Mass spectrometry was performed using a Q-Exactive Plus (Thermo Fisher Scientific). Chromatography was performed using a NanoAcquity ultraperformance liquid chromatography system (Waters, Milford, MA) at a flow rate of 400 nl/min using a EASY-Spray PepMap C18 75 μm × 150 mm column (Thermo), with a 240-min gradient. Solvent A was water, 0.1% formic acid, and solvent B was acetonitrile, 0.1% formic acid; peptides were eluted by a gradient from 2 to 28% solvent B from 20 to 215 min, then 28 to 40% B over a further 5 mins, before returning to the starting conditions. After a precursor scan of intact peptides was measured in the Orbitrap by scanning from *m/z* 350–1500 (with a resolution of 70,000), the ten most intense multiply charged precursors were selected for higher energy collision-induced dissociation fragmentation with a normalized collision energy of 30.0, then measured in the Orbitrap at a resolution of 17,500. Automatic gain control targets were 3E6 ions for Orbitrap scans and 50,000 for MS/MS scans. Dynamic exclusion was employed for 15 s. SILAC labeling efficiency was determined using MS/MS spectra. The mean labeling efficiency between reciprocal experiments was calculated at 92%. The raw data has been uploaded to the MassIVE public repository: ftp://MSV000078911@massive.ucsd.edu.

Peptide and Protein Identification—Fragmentation data were converted to peak lists using an in-house script based on the Raw_Extract script in Xcalibur version 2.4 (Thermo Fisher Scientific), and the higher energy collision-induced dissociation data for each sample were searched using Protein Prospector version 5.10.15 (15) against all human entries in SwissProt (downloaded June 27, 2013, with a total of 20,265 entries), to which a randomized version of all entries had been concatenated. The following search parameters were used: mass tolerances in MS and MS/MS modes were 10 ppm and 20 ppm, respectively; trypsin was designated as the digestion enzyme, and up to two missed cleavages were allowed; S-carbamidomethylation of cysteine residues was designated as a fixed modification; variable modifications considered were protein N-terminal acetylation, N-terminal glutamine conversion to pyroglutamate, methionine oxidation and $^{13}C_6$-labeled lysine. Results from searches of membrane and soluble fractions were merged into a single results file using Search Compare. Results were thresholded at an estimated 1% false discovery rate (FDR) at the protein level (peptide-level FDR was around 0.1%) according to concatenated database search results (16). Annotated spectra can be viewed using MS-Viewer (http://prospector2.ucsf.edu/prospector/cgi-bin/msform.cgi?form = msviewer) (17) using the following search keys: Biological Repeat 1 - p2iuesahfg; Biological Repeat 2 (reciprocal labeling) - lzcne57i8x.

Protein Quantification Using SILAC—SILAC quantification measurements were extracted from the raw data by Search Compare in Protein Prospector. Search Compare averaged together MS scans from −10 s to +20 s from the time at which the MS/MS spectrum was acquired to produce measurements averaged over the elution of the peptide. Search Compare calculates a noise level in the averaged spectrum. Only peaks with a signal to noise of greater than 10 were used in quantification measurements. The raw data has been uploaded to the MassIVE public repository: ftp://MSV000078911@massive.ucsd.edu. If one of the SILAC pair is above this threshold and the other is below, then the ratio is reported with a > or < (see raw data for SILAC), indicating one value was below the noise level, so the ratio reported is a minimum estimate. The standard deviation of the log ratios for peptides matched to the same protein (where all ratios should be the same) was 0.11. The twofold threshold change employed as significant therefore corresponds to 2.74 (log(2)/0.11) standard deviations from the mean. Assuming a Gaussian distribution, this threshold would correspond to a 99.4% confidence threshold that a twofold difference is nonrandom. This corresponds to a 0.6% FDR. Furthermore it is necessary to emphasize here that multiple testing adjustment is not required in this study, as we are only testing one hypothesis; that protein x is changing in abundance in one cellular model. For these calculations the fact that one protein changes or not does not affect the probability of another protein changing.

PRM Mass Spectrometry—PRM was used to confirm the major protein changes in 231-BR *versus* MDA-MB-231 cells (proteins up-regulated by more than fivefold and down-regulated more than 10-fold) observed in the SILAC analyses. Peptides were extracted from 231-BR and MDA-MD-231 cells as described above (see Protein preparation for mass spectrometry) but from a different batch of cultured cells (biological replicate). These peptides were loaded on C18-containing stage tips prior to reversed phase chromatography on a SPE-LC (modified EASY-nLC 1000, Thermo, Odense, Denmark), as described in Falkenby et al. (77). Short gradients ranging from 4 to 35% in 5 min were used. In-house prepared 6 cm columns with pulled emitter and ReproSil-Pur 120 C18-AQ 3 μm material (Dr Maisch, Germany) were used in combination with a nano-ESI source (Proxeon, Odense, Denmark). PRM was performed using a Q Exactive mass spectrometer (Thermo Scientific, Bremen, Germany). Methods optimized for collision energy, charge state, and retention times for the most significantly regulated peptides were generated experimentally using two unique peptides of high intensity and confidence for each target protein. Targeted MS2 spectra were acquired using a PRM approach (18) at a resolution of 35,000, employing a high AGC target value of 3e6 ions and a maximum injection time of 100 ms. Scheduled acquisition in windows of up to 1 min was used to limit the number of concurrent targets to a maximum of four. The raw data has been uploaded to the MassIVE public repository: ftp://MSV000078911@massive.ucsd.edu. These data were analyzed using Skyline (MacCoss Lab, University of Washington) (19) where signal intensities for individual peptide sequences for each of the significantly altered proteins were quantified relative to each sample and normalized to heat shock 60kDa protein 1 (chaperonin, HSPD1) that was found to be homogeneously expressed in each cell type (peptides for HSPD1 were optimized and shown to be high intensity and confident transitions). Quantification was performed by measuring the extracted ion chromatogram for each transition for each peptide in triplicate LC MS/MS runs and results were compared between cell types using a Student's *t* test.

Exon-based Microarray Analysis of mRNA Expression—Isolation of RNA was performed from three biological replicates of 231-BR and MDA-MB-231 cells using the illustra RNAspin Mini Isolation Kit (GE Healthcare) according to the manufacturer's instructions (protocol 25–0500-70PC). The RNA concentration was measured using Nano-

photometer (Implen, Munchen, Germany) and the quality was determined using Agilent 2100 Bioanalyser (Agilent Technologies, Santa Clara, CA). Microarray analysis of mRNA expression was performed at the Australian Genome Research Facility (AGRF, Melbourne, Australia). Briefly, a total of 3 μg was labeled using the Affymetrix WT cDNA Amplification kit (Millenium Science, Mulgrave, Australia). The subsequent cRNA was cleaned using the Affymetrix GeneChip Sample Cleanup kit (Millenium Sciences). Upon cleaning of the cRNA, dUTP was incorporated into the second cycle of the first strand cDNA synthesis step. The presence of the dUTP was used to facilitate fragmentation using the APE1 and UDG enzymes that specifically recognized dUTP. The fragmented cDNA was quality checked using the Agilent Bioanalyser 2100 with the NanoChip protocol. The fragmented single stranded cDNA was end-labeled using terminal deoxynucleotidyl transferase and the WT Terminal Labeling kit (Millenium Sciences). A total of 5 μg of labeled cDNA for each of the three biological replicates of 231-BR *versus* MDA-MB-231 was then hybridized to the *HumanExon 1.0 ST Array* GeneChip (Millenium Sciences) by preparing a probe mixture (labeled cDNA at 0.025 μg/ul) that includes 1× hybridization buffer (100 mM MES, 1 mM NaCl, 20 mM EDTA, 0.01% Tween-20), 0.1 mg/ml herring sperm DNA, 0.5 mg/ml BSA, and 7% DMSO. A total hybridization volume of 220 μl was prepared for each sample and 200 μl loaded into a *HumanExon 1.0 ST Array* GeneChip. The chip was hybridized at 45 °C for 16 h in an oven with a rotating wheel at 60 rpm. After hybridization the chip was washed using the appropriate fluidics script in the Affymetrix Fluidics Station 450. Upon completion of the washing, the chips are then scanned using the Affymetrix GeneChip Scanner 3000. The scanner operating software, GCOS, converts the signal on the chip into a DAT file, which was used for generating the subsequent CEL file for analysis. The ratio of gene expression in 231-BR *versus* MDA-MB-231 cells was derived from Cel files, but is presented in terms of % of increase/decrease. The raw data has been uploaded to the MassIVE public repository: ftp://MSV000078911@massive.ucsd.edu. The data from each array was imported into Genespring GX v 12.1 (Agilent Technologies) as CEL files and robust multi-array analysis was used to log-transform, background-correct, quantile normalize, and summarize the probe features resulting in a set of expression signal intensities. The signal intensities were baseline transformed to the median signal intensity of all arrays. Unpaired moderated *t* tests were used to identify genes with significantly altered expression (>twofold, $p < 0.05$). To correct for false positive results, a Benjamini and Hochberg FDR of 5.0% was used for multiple testing.

MicroRNA Expression Profiling—Isolation of microRNA (miRNA) from three biological replicates of 231-BR and MDA-MB-231 cells was performed using the mirVana miRNA isolation kit (Life Technologies) according to the manufacturer's instructions (protocol 1560 M Rev. C). The RNA concentration was determined using a Nanophotometer (Implen) and the quality was determined using Agilent 2100 Bioanalyser (Agilent Technologies). Total RNA (1 μg) from each replicate was biotinylated using the FlashTag Biotin HSR kit (Genisphere, Hatfield, PA) in triplicate according to the manufacturers' instructions (protocol 877.888.3DNA). Labeled RNA was hybridized to GeneChip miRNA-2 arrays (Affymetrix, Santa Clara, CA) for 16 h before washing and staining the arrays using the GeneChip Hybridization (Affymetrix), Wash and Stain kit according to the manufacturers' instructions (protocol P/N 702731 Rev. 3). Arrays were scanned on a GeneChip® Scanner 3000 7G (Affymetrix). Analysis GeneChip miRNA-2 arrays contain 15,644 probe features representing 1105 unique human mature miRNAs, 1105 unique human pre-miRNAs and 2334 human snoRNA and scaRNAs (Affymetrix). The data from each array was imported into Genespring GX v 12.1 (Agilent Technologies) and robust multi-array analysis was used to log-transform, background-correct, quantile normalize, and summarize the probe features resulting in a set of expression signal intensities. The signal intensities were then baseline transformed to the median signal intensity of all arrays. Unpaired moderated *t* tests were used to identify miRNAs with significantly altered expression (>2-fold, $p < 0.05$). To correct for false positive results, a Benjamini and Hochberg FDR of 5.0% was used for multiple testing. Supervised hierarchical cluster analysis was performed on miRNAs that were found to be significantly different (>2 fold, $p < 0.05$, FDR<0.05). Similarity in the average expression patterns between miRNAs was measured by Euclidian's distance. The raw data has been uploaded to the MassIVE public repository: ftp://MSV000078911@massive.ucsd.edu. Biological targets of differentially expressed miRNAs were identified by searching for the presence of conserved eight-mer and seven-mer sites within genes that match the seed region of each miRNA. For miRNA families, conservation cutoffs were defined as described by Friedman *et al.* (20) as follows: broadly conserved (conserved across most vertebrates, usually to zebrafish); conserved (conserved across most mammals, but usually not beyond placental mammals), or poorly conserved (all others). For human miRNA, site conservation were defined by conserved branch length, with each site type having a different threshold for conservation: eight-mer > = 0.8; seven-mer-m8 > = 1.3; seven-mer-1A > = 1.6 as defined (20). The data were searched for miRNA potential targets using sRNA Target Base (starBase, http://starbase.sysu.edu.cn) (21), which integrates data from 21 Ago or TNRC6 CLIP-Seq sequence data sets with the target prediction programs Target Scan, Pictar and miRanda. The analysis was performed as previously described (22) and miRNA that were validated by all three target-prediction algorithms, and for which confidence is therefore high, have been selected.

Molecular Pathway Analysis—SILAC data was analyzed using Qiagen Ingenuity Pathway Analysis (IPA®, Qiagen Redwood city, CA, www.qiagen.com/ingenuity). Proteins showing differential regulation (at least twofold expression changes) were uploaded and networks were generated using data sets containing gene identifiers and their corresponding expression values. Networks of these focus genes were then algorithmically generated based on their connectivity using stringent human filter options describing molecules and relationships. Graphical networks depicting significant activation or inhibition of molecular pathways were generated. Pathways with a *p* value <0.05 were considered to be significantly regulated. The *p* value<0.05 was used to identify pathways in the study that might explain the changes of protein expression observed between 231-BR and MDA-MD-231 cells. It suggests a statistically significant link between proteins showing significant regulation and genes that are regulated by a known transcription regulator. It was calculated, as part of Ingenuity Pathway analysis process, using Fisher's Exact Test (significance of the association or contingency test).

RESULTS

Proteome Profiling of 231-BR versus MDA-MB-231 Cells—Using SILAC based LC-MS/MS analysis of 231-BR and MDA-MB-231 cells, 2266 and 2434 proteins, respectively, were identified in reciprocal labeling experiments. Together, 1957 proteins were reciprocally identified and 1584 were quantified in both experiments. A total of 152 proteins, representing 9.6% of all quantified proteins, were found to be regulated by at least twofold in 231-BR as compared with MDA-MB-231, with 40 up- and 112 down-regulations (Fig. 2*A*). The correlation plot of changes in protein quantification obtained in the two replicates of the SILAC analysis is presented (Fig. 2*B*). The Pearson coefficient of correlation (R square) was 0.66 ($p < 0.0001$), demonstrating the reliability of the list of regulated

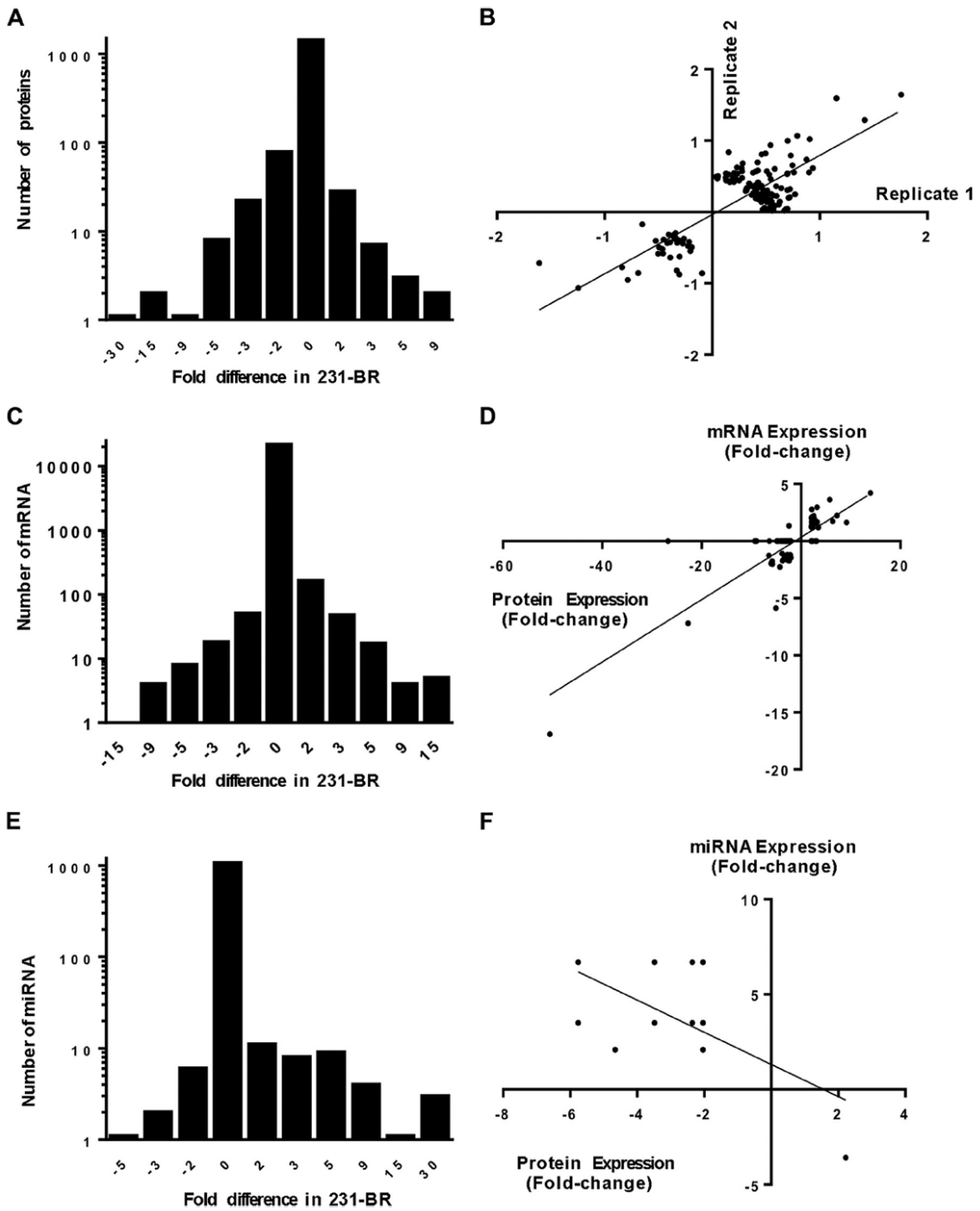

FIG. 2. **Distribution of protein, mRNA, miRNA changes in 231-BR compared with MDA-MB-231.** *A*, The level of 1584 proteins were compared between 231-BR and MDA-MB-231 cells and 152 were found regulated by more than twofold (112 decreased and 40 increased). The number of proteins (*y* axis) is in Log scale. *B*, Correlation plot between SILAC replicates. Changes in protein levels obtained in replicate 1 *versus* replicate 2 are presented. The x and y axes are in Log scale. The Pearson correlation coefficient (R square) was 0.66 ($p < 0.0001$). *C*, 22,011 mRNA were quantified in 231-BR *versus* and MDA-MB-231. Three hundred and six mRNA were significantly regulated by at least twofold (70 decreased and 226 increased). *D*, Correlation plot between protein and mRNA level changes. The mRNA change was plotted for the 152 protein changes in 231-BR. The Pearson correlation coefficient (R square) was 0.67 ($p < 0.0001$). *E*, 1105 miRNA were quantified in 231-BR *versus* MDA-MB-231 and 45 were found regulated by at least twofold. Nine miRNA were decreased and 36 increased in 231-BR cells. *F*, Correlation plot between miRNA and their predicted protein targets. The Pearson correlation coefficient (R square) was 0.37 ($p < 0.0459$).

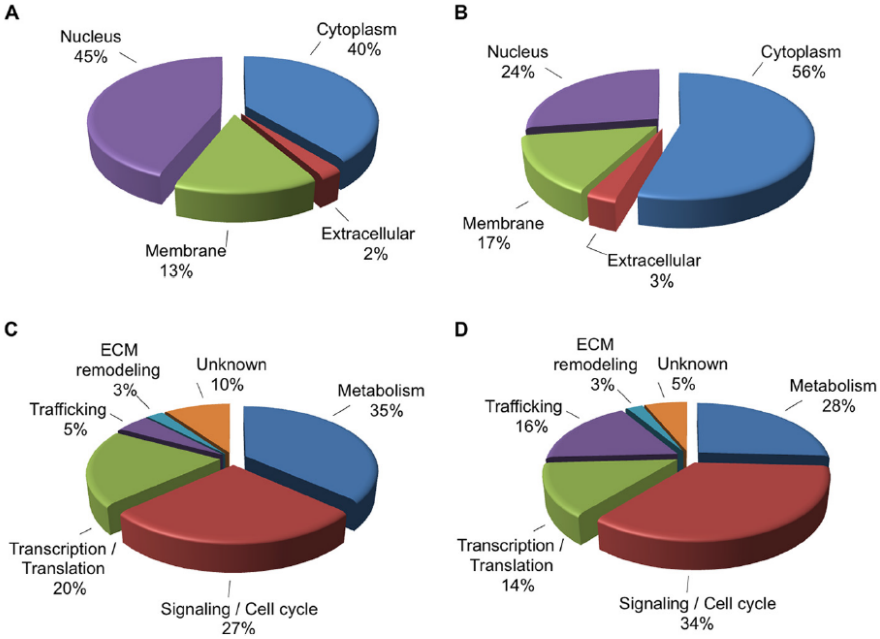

FIG. 3. **Distribution of proteins regulated in 231-BR cells (as compared with MDA-MB-231) in function of subcellular localization and ontology.** *A*, Subcellular localization of proteins showing increased expression by twofold or greater in 231-BR cells. *B*, Subcellular localization of proteins showing decreased expression by twofold or greater in 231-BR cells. *C*, Gene ontology of proteins identified showing increased expression by twofold or greater in 231-BR cells. *D*, Gene ontology analysis of proteins showing decreased expression by twofold or greater in 231-BR cells.

proteins. The characteristics (gene and protein name, accession number, number of unique peptides, protein fold changes, best peptide E-values, mRNA fold changes, and associated nominal *p* values) of the 152 proteins differentially regulated between 231-BR and MDA-MB-231 are shown in supplemental Table S1. For mRNA, test adjustments (Bonferroni, sidak, q-value) are in the raw data accessible on line (MassIVE public repository: ftp://MSV000078911@massive.ucsd.edu). Analysis of the localization (Fig. 3*A* and 3*B*) and function (Fig. 3*C* and 3*D*) of regulated proteins showed differences between up-regulated (Fig. 3*A* and 3*C*) and down-regulated (Fig. 3*B* and 3*D*) proteins. Statistical significances were calculated using Chi-square (two-tailed). The proportion of nuclear proteins was higher among up-regulated (45%) than down-regulated (24%) proteins ($p = 0.001$) and the proportion of cytoplasmic proteins was higher in the down-regulated proteins (56%) compared with the up-regulated proteins (40%) ($p = 0.023$). The proportion of membrane and extracellular proteins was not statistically different between up- and down-regulated proteins ($p > 0.05$). The proportion of different functional categories of regulated proteins was different among up- and down-regulated proteins (Fig. 3*C*–3*D*). The proportion of proteins involved in signaling and cell cycle was 27% in the up-regulated group and 34% in the down-regulated group ($p = 0.029$), whereas the proportion involved in intracellular trafficking was 5% in up-regulated proteins and 16% in down-regulated proteins ($p = 0.011$). The proportion of proteins involved in ECM remodeling, transcription/translation, metabolism, and proteins of unknown function was not statistically different between up- and down-regulated proteins ($p > 0.05$). The largest proteome changes in 231-BR were increases (by more than fivefold) in the matrix metalloproteinase MMP1, the growth factor ephrin-B1 (EFNB1), the membrane protein STOM, the *N*-acetyl-glucosamine pyrophophorylase UAP1, the target of Myc MYCT1, and decreases (by more than 10-fold) in the transglutaminase TGM2, the metastasis associated protein S100A4 and the actin cross-linker LCP1 (or L-plastin). The MS/MS spectra of the most up-regulated and down-regulated proteins, MMP1 and TGM2, respectively, are presented in Fig. 4. Figs. 4*B*, 4*C*, 4*E*, and 4*F* demonstrate the reproducible quantification results obtained between the reciprocal labeling experiments.

PRM Analysis of the Major Protein Changes in 231-BR versus MDA-MB-231—The major protein changes in 231-BR (increases by more than fivefold for MMP1, EFNB1, STOM1, UAP1, MYCT1 and decreases by more than 10-fold for TGM2, S100A4, and LCP1) were analyzed by label-free PRM mass spectrometry. The analysis was performed from a different set of cell cultures than for the SILAC analyses (biological replicate). Product ions of selected peptides were monitored in parallel using one injection over a full mass range. Two unique peptides for each protein were used for quantification. Each PRM experiment was performed in triplicate and normalized to control peptides revealed by SILAC based LC-MS/MS analysis to be expressed 1:1 (HSPD1, further confirmed to be expressed 1:1 by PRM). Peptide ratios for the label-free PRM quantification were generated in Skyline measuring the area

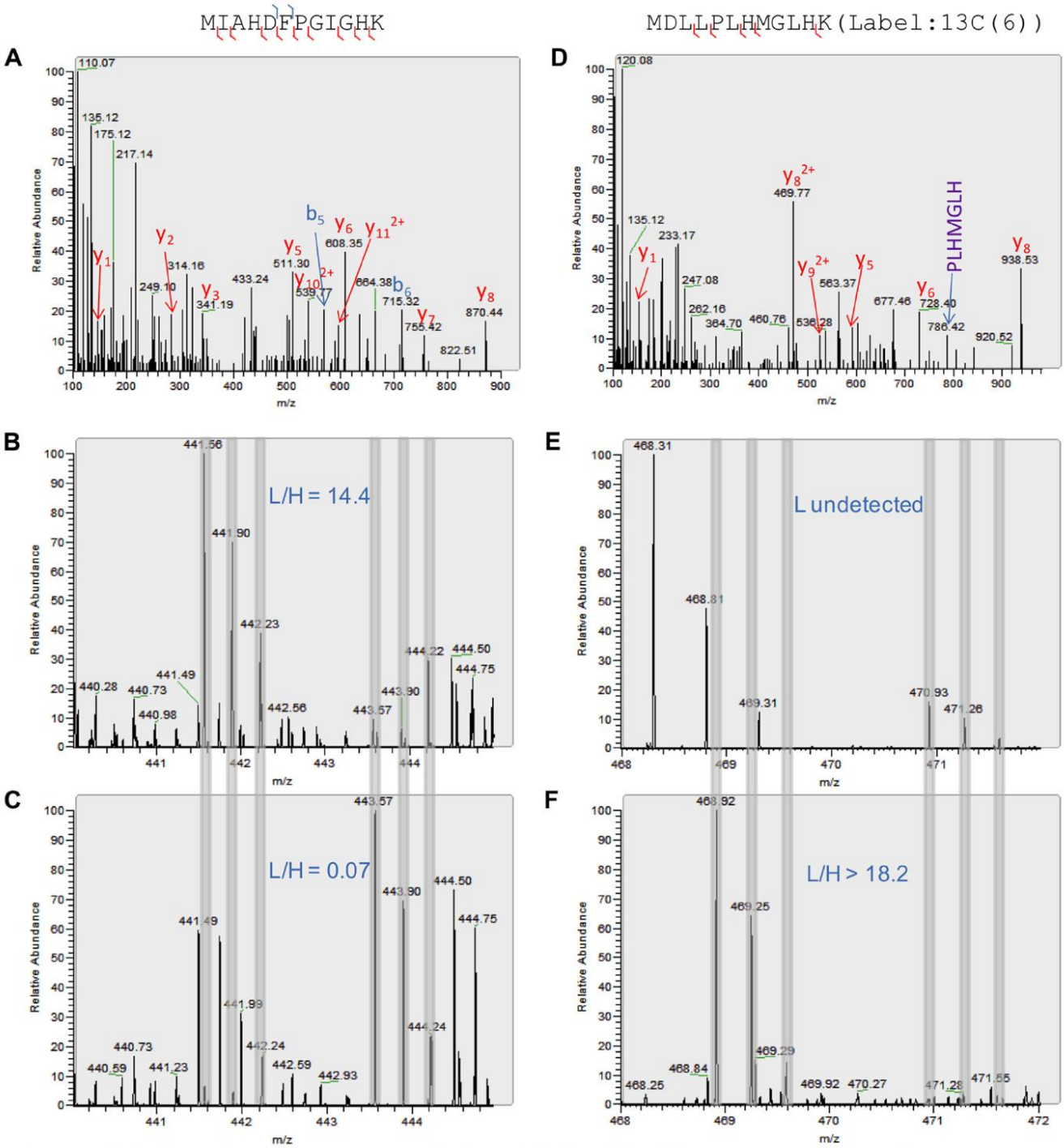

FIG. 4. **LC-MS/MS based identification and quantification of MMP1 and TGM2.** Matrix metalloproteinase-1 (MMP1) and transglutaminase-2 (TGM2) were differentially expressed between 231-BR and MDA-MB-231 cells. *A*, MS/MS spectrum of peptide MIAHDFPGIGHK from MMP1. *B*, Precursor intensity for this peptide in 231-BR cells is roughly 14-fold more intense than in the parent cell line, based on SILAC labeling; *C*, In the reciprocal labeling experiment, the heavy precursor is now significantly more intense. *D*, MS/MS spectrum of heavy-labeled peptide MDLLPLHMGLHK from TGM2. *E*, The light equivalent of this peptide was not detected in 231-BR sample; *F*, In the reciprocal labeling experiment signal for the 231-BR sample is in the noise level of the spectrum, indicating an at least 18-fold difference in expression level between cell lines.

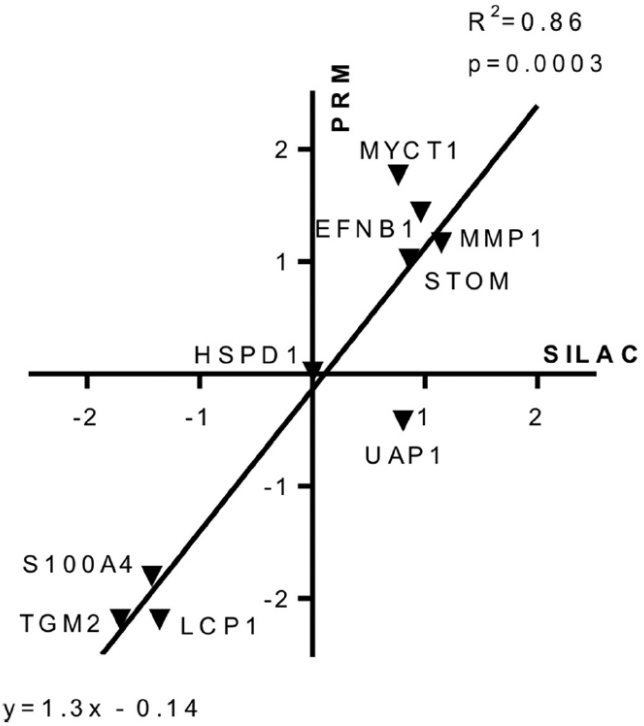

FIG. 5. **Correlation plot of PRM and SILAC quantification of protein changes in 231-BR *versus* MDA-MB-231 cells.** The eight proteins that were found most regulated in 231-BR compared with MDA-MB-231 cells using SILAC-based quantification were analyzed in a label-free quantification PRM experiment. The changes in protein levels were confirmed in seven out of eight cases (MMP1, EFNB1, STOM1, MYCT1, TGM2, LCP1, S100A4) in PRM. Only the change in UAP1 level was not confirmed in PRM. Data (from PRM and SILAC) for these proteins are plotted here. HSP1 was used as a control unregulated protein. The axes for SILAC and PRM represent the Log of mean ratios 231-BR/MDA-MB-231. The coefficient of linear regression (coefficient of determination, R square) between PRM and SILAC was 0.86 ($p < 0.0003$).

under the curve of three to eight transitions selected for each peptide (precursor ion/product ion). These were averaged for each protein and then compared with averaged reciprocal SILAC quantification values. All transition ions obtained for each of the nine analyzed proteins are presented (supplemental Table S2). The quantifications for each analyzed protein (using two peptides/protein) in 231-BR *versus* MDA-MB-231 are presented (supplemental Fig. S3). The results indicate that for 7/8 proteins analyzed, the PRM data validated the results obtained using SILAC. The increase in MMP1, EFNB1, STOM1, MYCT1 in 231-BR, as well as the decrease in TGM2, S100A4, and LCP1 were confirmed by PRM. The only change that was not confirmed by PRM was the increase in UAP1. As shown in supplemental Fig. S3, the two peptides used for UAP1 provided contradictory results in PRM as one showed no change whereas the other indicated decrease in 231-BR. In the SILAC analyses, UAP1 was characterized with only one peptide. Therefore, change in the UAP1 level in 231-BR could not be confirmed. A correlation curve was generated (Fig. 5) between protein changes observed by PRM and by SILAC. The coefficient of correlation (coefficient of determination, R-square) was 0.86 ($p < 0.0003$), indicating a high level of correspondence in the results obtained by the two methodological approaches.

Expression of mRNA in 231-BR versus MDA-MB-231 Cells—Changes in mRNA levels in 231-BR compared with MDA-MB-231 cells were analyzed in exon-based microarray analysis. A total of 296 changes in individual mRNA levels of at least twofold were observed in 231-BR (supplemental Table S4). This included 226 up-regulations and 70 down-regulations of individual mRNAs. The distribution of changes in mRNA is reported in Fig. 2*C* and the relative mRNA levels for each of the proteins regulated in the SILAC proteomics experiment are reported in supplemental Table S1. Overall, only 43% of the individual changes in protein expression were associated with corresponding changes in the transcript levels. The correlation plot of changes in proteins *versus* mRNA (Fig. 2*D*) indicated a Pearson correlation coefficient (R square) of 0.67 ($p < 0.0001$). This shows that alterations in mRNAs are limited predictors of changes in the corresponding proteins, suggesting post-transcriptional regulation. Noticeably, there was a significant difference between up- and down-regulated proteins in regard to changes in mRNA levels. In the case of up-regulated proteins, 65% had a corresponding increase in mRNA, but for down-regulated proteins a corresponding change in mRNA level was found in only 35% of cases. Therefore 65% of the up-regulated proteins could be related, at least in part, to increases in mRNA level, whereas only 35% of the down-regulated proteins were accompanied by a decrease in mRNA, further supporting post-transcriptional regulation as being particularly relevant to the down-regulation of individual proteins in 231-BR.

miRNA Expression in 231-BR versus MDA-MB-231 Cells—The level of 1105 unique mature miRNA, 1105 pre-miRNAs, and 2334 snoRNA and scaRNAs was analyzed in 231-BR and MDA-MB-231 cells using microarrays. A total of 45 miRNAs were found to be differentially regulated by at least twofold in 231-BR cells (supplemental Table S5), including nine down-regulations and 36 up-regulations (Fig. 2*E*). The higher proportion of miRNA that were increased matched the predominant down-regulation of protein levels observed in the SILAC proteomic results (supplemental Table S1), suggesting that miRNAs are involved in protein level changes, and in particular in the down-regulations. However, using prediction of miRNA targets, we were able to identify only six of the proteins regulated in 231-BR as potential targets of four regulated miRNA (supplemental Table S6). To be more specific, three increases in miRNA (miR-195, miR-182, miR-34a) potentially corresponded to down-regulation at the protein levels (for VAMP8, IGF2R, HDGF, ACTR2, ANLN), and 1 miRNA decrease (miR-424–5p) corresponded to up-regulation at the protein level (SLC4A7). Overall, five out of the 112 down-regulated proteins were targets of certain miRNAs, whereas it

TABLE I

Overview of proteome/mRNA/miRNA changes in 231-BR versus MDA-MB-231. + indicates up-regulation and - indicates down-regulation. FDR, false discovery rate. Cut-off values for significance were as follows. For proteins, >twofold, best E-value<2.5E-05, FDR = 0.6%. For mRNA, >twofold, $p < 0.05$, FDR = 5%. For miRNA, >twofold, $p < 0.05$, FDR = 5%

	Regulated in 231-BR		Total numbers quantified
	-	+	
Proteins	112	40	1,584
mRNA	70	226	22,011
miRNA	9	36	1,105

was 1/40 for up-regulated proteins; this was not statistically different ($p > 0.05$ using Chi-square two-tailed). Also, the correlation plot between changes in miRNA and their predicted protein targets (Fig. 2*F*) indicated a Pearson correlation coefficient (R square) of only 0.37 ($p < 0.0459$).

Integrated Overview of the Proteome/Transcriptome/miRNA Changes in 231-BR versus MDA-MB-231 Cells and Molecular Pathway Analysis—An overview of changes observed at the three expression levels (protein - mRNA - miRNA) is presented in Table I. Ingenuity pathway analysis revealed that most proteome changes in 231-BR (Fig. 6*A*) were related to cell death and survival, cell growth and differentiation, cellular movement, cell cycle and cell-to-cell interaction. In terms of prediction of upstream regulatory pathways, the pathways regulated by tumor necrosis factor α (TNF-α), extracellularly regulated kinases, the histone demethylase KDM5B (Lysine (K)-Specific Demethylase 5B), the estrogen receptor and the cyclin dependent kinase 1A (CDKN1A) were activated in 231-BR (Fig. 6*B*). Significantly inhibited pathways in 231-BR cells (Fig. 6*C*) were predicted to be related to transforming growth factor β (TGF-β), the E3 ubiquitin-protein ligase SYNVN1 (synovial apoptosis inhibitor 1 or synoviolin), the transcription factor FOXO1 (Forkhead box protein O1), the receptor TREM1 (triggering receptor expressed on myeloid cells 1), and the progesterone receptor. The TNF-α and TREM1 pathways were found with 5% FDR and $p < 0.05$, whereas all the other pathways were found with 1% FDR and $p < 0.01$ (Fig. 6*B* and 6*C*).

DISCUSSION

In this study, the differential protein/mRNA/miRNA content of a brain-colonizing breast cancer cell line (231-BR) was compared with the parental nonspecific metastatic cell line (MDA-MB-231), with the view of determining the molecular features that could account for the differing phenotypes of these cells. There has already been many studies comparing the proteome of metastatic *versus* nonmetastatic breast cancer cells (23–27); this study focused on a unique genetically homogenous cellular model to delineate proteome changes associated to a brain-seeking phenotype of breast cancer cells. The seed and soil theory of metastasis that was originally established in breast cancer by Paget in 1889 (28), described metastasis in terms of an interaction between a tumor cell and a local environment. This concept has been extended to other types of cancer and although it is constantly revisited (29), there is an agreement that adequate molecular determinants are necessary, on both the cancer cells and the target organ, to permit the establishment of metastases. The proteomic signature identified in this study provides a framework for a better understanding of the mechanisms triggering brain metastasis, and for delineating future biomarkers and therapeutic targets of clinical interest.

Overall Changes in Proteins versus mRNA and miRNA—Comparing changes in 231-BR at the protein *versus* the mRNA level indicates that only 43% of the individual protein changes were associated with concomitant changes in the respective mRNA. This confirms the already reported fact that the transcript level is a limited predictor of the protein level (30, 31). Currently, breast tumors are classified based on transcriptomics/gene expression into four main classes: luminal A, luminal B, HER2+, and triple negative; however, this classification is constantly being refined with the addition of new subclasses (32). The limited association between changes at the protein *versus* mRNA level that are reported herein points to the need to further explore the proteome of breast tumors, and ultimately define the proteogenomic profile of this disease. This study represents an exploratory step in this direction. Significantly, most of the proteome changes in 231-BR were decreases in individual protein levels (112/152), suggesting that down-regulation of specific proteins may be an important part of the mechanism underlying the ability of breast cancer cells to metastasize specifically to the brain. Alternatively, it is also possible that the proteins are down-regulated simply because they are no longer needed in brain metastasis and they have been selected against during the multiple cycles of injection and recovery from the mice. Interestingly, differential microRNA analyses indicated that most miRNA changes in 231-BR were up-regulations (36/45), suggesting that the trend toward protein down-regulation could be at least partially controlled by opposite changes in levels of regulatory miRNAs. However, target prediction of miRNA, using three different target prediction tools, identified only four regulated miRNA potentially corresponding to six regulated proteins. Together, these results suggest that changes in miRNAs are part of the molecular profile of brain metastatic breast cancer cells, but the correlation between specific up-regulated miRNAs, putative down-regulated protein targets and brain metastatic phenotype was not tested experimentally. Further functional investigation will be needed to clearly link specific changes in miRNA to changes in protein levels.

Pathway Activation/Inactivation—It is important to emphasize the predictive nature of pathway analysis. The pathways presented here indicate predicted activation and inhibition of

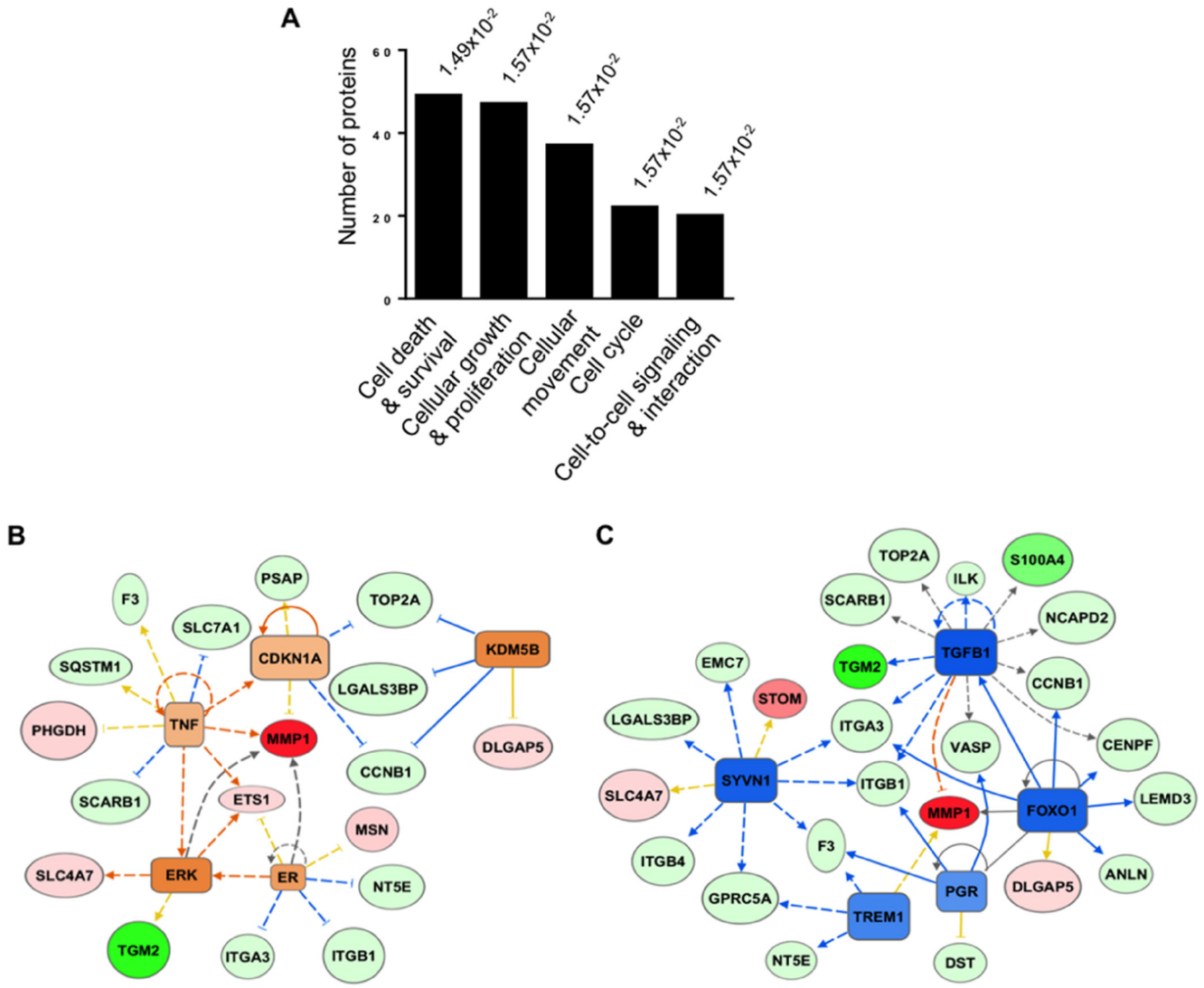

FIG. 6. **Protein pathways regulated in 231-BR.** Pathway analysis of proteins differentially regulated in 231-BR *versus* MB-MDA-231 was performed using Ingenuity Pathway Analysis. *A*, Protein pathways activated in 231-BR were found related to cell death and survival, protein synthesis, cell cycle, cell-to-cell interaction, and molecular transport (number of proteins for each pathway are indicated in ordinate, *p* values are indicated on top of each column). *B*, Predicted upstream pathways activated in 231-BR. The *p* values for activated pathways were CDKN1A, 4.1×10^{-5}; extracellularly regulated kinases, 2.9×10^{-3}; KDM5B, 7×10^{-3}; TNF-α, 4.3×10^{-2}; ER, 2.9×10^{-3}. *C*, Predicted upstream pathways inhibited in 231-BR. The *p* values obtained for inhibited pathways were TGF-β, $2. \times 10^{-6}$; SYVN1, 6.25×10^{-7}; FOXO1, 4.69×10^{-7}; TREM1, 3.73×10^{-2}; PGR, 9.44×10^{-3}. For *B* and *C*, the TNF-α and TREM1 pathways were found with 5% FDR and $p < 0.05$, whereas all the other pathways were found with 1% FDR and $p < 0.01$. Networks are presented in the centroid of connecting lines in bold font with rectangle icons. Blue fill indicates a significant inhibition in the 231-BR cells and B orange indicates significant activation. Proteins are represented by circle or oval icons with a green shading corresponding to a twofold or greater decreased expression, and a red shading correspond to a twofold or greater increased expression in the 231-BR cells. Intensity of each color represents the level of expression. Solid lines suggest direct interactions and dashed lines suggest indirect ones. Orange lines lead to activation and blue lines lead to inhibition. Yellow lines are for inconsistency in state (up or down) of downstream molecule and gray are for effect yet to be predicted. Protein names are reported in supplemental Table S1.

signaling networks based on the up- and down-regulations determined in the SILAC analysis. However it does not constitute a graphical representation of SILAC results and there is no direct evidence in our study for those hub proteins. However, as described below, the literature indicates that these hubs are expressed in breast cancer cells. Significantly inhibited pathways in 231-BR were those related to TGF-β, the E3 ubiquitin-protein ligase SYNVN1 and the transcription factor FOXO1, whereas the pathways associated to TNF-α, and the histone demethylase KDM5B were activated. TGF-β has been shown to be produced by both glial cells and neurons, and to participate in the development and maintenance of the brain

microenvironment mainly through its neuroprotective effect (33). TGF-β has also been shown to inhibit the anchorage-independent growth of 231-BR (6); therefore it is conceivable that the down-regulation of the TGF-β signaling pathway could be a way to escape growth inhibition by TGF-β normally present in the brain microenvironment. The pathway controlled by SYVN1 was also down-regulated in 231-BR. SYVN1 is involved in endoplasmic reticulum (ER)-associated degradation and removes unfolded proteins accumulated during ER stress by retrograde transport to the cytosol from the ER. This protein also uses the ubiquitin-proteasome system for additional degradation of unfolded proteins. The potential role of SYVN1 in carcinogenesis is, at this stage, limited to the targeting of the tumor suppressor p53 for ubiquitination (34) leading to its degradation in the cytoplasm, but it is unclear how this relates to brain metastasis. The third down-regulated pathway identified is related to the transcription factor FOXO1. Suppression of FOXO1 activity has recently been associated with increased tumorigenicity of breast cancer cells (35) and FOXO1 is involved in the control of E2F1 transcriptional specificity and apoptotic function (36). Therefore the down-regulation of FOXO1 is coherent with increased tumor aggressiveness and in return may also participate in the regulation of the TGF-β, MMP1, and SYVN1 pathways. In contrast to inhibited pathways, this study also points to the significant activation of pathways associated to TNF-α and the histone demethylase KDM5B. TNF-α is a major pro-inflammatory cytokine involved in growth, differentiation, and survival of many cell types. In breast cancer cells, TNF-α participates in the epithelial–mesenchymal transition phenotype (37) and its targeting, using blocking antibodies, suppresses breast cancer growth (38). Our study therefore emphasizes the value of targeting the TNF-α pathway in breast cancer. Similar to genetic alterations, epigenetic aberrations contribute significantly to tumor initiation and progression. The pathway related to the histone demethylase KDM5 was found to be increased in 231-BR cells. The KDM5 family of histone demethylases are capable of removing tri- and di-methyl groups from lysine 4 on histone H3, a modification that occurs at the start site of transcription in actively transcribed genes (39). Preclinical studies suggest that the inhibition of these enzymes can suppress tumorigenesis (40), and this study points to a possible involvement in brain metastasis. Interestingly, the pathways controlled by progesterone and estrogen receptors were found differentially regulated, despite the fact that 231-BR and MDA-MB-231 cells are triple negative breast cancer cells that do not express these receptors. However, the pathway analysis provides clues for alternate regulation. Indeed, the regulation of NT5E, ITGB1, and ITGA3, which can be controlled by ER, can also occur through the pathways mediated by TREM1 and TGF-β (as shown in Fig. 6*C*). Also, the regulation of ETS1 can be induced through the TNF-α pathway (as shown in Fig. 6*B*). Similarly, the up-regulation of F3 that can be controlled by PR can also be regulated through the TNF-α pathway (as shown in Fig. 6*B*). Each of these alternate potential effectors (TREM1, TGF-β, and TNF-α) has been identified previously in breast cancer cells (41–43).

Proteins Up-regulated in the Brain Metastatic 231-BR Cells—Of particular interest was the up-regulation (by ~14-fold) of the matrix metalloproteinase MMP1, which promotes collagen degradation. MMP1 overexpression has been associated with metastatic capacities of breast cancer cells by favoring extracellular matrix degradation and thus facilitating invasion and extravasation of cancer cells (44). Of note, MMP1 expression is under the control of the transcription factor ETS1 that was also found to be up-regulated (although to a lesser extent than MMP1) in 231-BR. MMP1 overexpression is associated with poor patient outcome (45) and in a mouse xenograft model it has been shown that MMP1 inhibition decreases local growth and brain metastasis of breast cancer cells (46). Therefore the results presented here confirm the involvement of MMP1 in brain metastasis by showing its increased protein level in 231-BR cells. A few recent studies have suggested that MMP1 plays an important role in the regulation of neuronal apoptosis and astrocyte proliferation (47), suggesting that MMP1 up-regulation in breast cancer cells could lead to a remodeling of brain extracellular matrix, making it favorable for their implantation into the brain microenvironment. In terms of therapeutic targeting, inhibitors of MMPs, despite considerable excitement during the last two decades, have failed to enter the clinic because of their unwanted musculoskeletal side effects (48, 49) and it is therefore unlikely that targeting MMP1 would be a viable therapeutic option for metastatic breast cancer. Interestingly, other enzymes involved in extracellular matrix remodeling were also found among the regulated proteins.

Another major change in 231-BR cells was the up-regulation (by ninefold) of ephrin-B1. Ephrins are plasma membrane-bound growth factors that act by stimulation of Eph tyrosine kinase receptors on juxtaposed cells, initiating multiple intracellular phosphorylation cascades (50). The ensuing signals are bidirectional as ephrins can also transduce signals (known as reverse signals) following their interaction with Eph receptors. The biological functions of ephrins range from cell growth, adhesion, and migration to axon guidance and angiogenesis, resulting in critical regulatory roles in embryonic development and carcinogenesis (50). Eph receptors require direct cell-to-cell interaction for activation and they are divided into EphA and EphB receptor classes, depending on their preferential binding affinity for ephrinA or ephrinB ligands. Eph receptors have been documented in cancer (51), but the ligands have not been thoroughly investigated and in particular there is limited data on ephrinB1. However, a recent study has shown that enhanced expression of ephrinB1 is associated with lymph node metastasis and poor prognosis in breast cancer (52). The authors did not propose a mechanism to explain the association between ephrinB1 and poor patient

survival, but another recent study has shown that ephrinB1 is a substrate for PTEN and interacts with the tyrosine kinase receptor HER2 (or ErbB2) (53). Interestingly, breast tumors overexpressing HER2 are prone to metastasize to the brain (7) and therefore an association of HER2 with ephrinB1 could be a driver of brain metastasis. In terms of therapeutic potential, ephrinB1 is expressed at the cell surface and could potentially be targeted. Although there are no inhibitors of ephrins in clinical use, a number of peptides and chemical compounds that target Eph receptors and inhibit ephrin binding or downstream kinase activation have been identified (56). These molecules show promise as probes to study Eph receptor/ephrin biology, as lead compounds for drug development and as targeting agents to deliver drugs or imaging agents to tumors. The data presented herein clearly support that the potential use of ephrin inhibitors against brain metastasis should be further considered.

Stomatin (STOM) and MYCT1 were also found to be strongly up-regulated (by at least fivefold) in 231-BR. Stomatin is an integral membrane protein, the absence of which is associated with a form of hemolytic anemia known as hereditary stomatocytosis. It is reported that stomatin regulates the gating of acid-sensing ion channels in mammalian neurons, but the function of stomatin is not fully understood (57). MYCT1 (or MTMC1) is a helix-loop-helix leucine zipper transcription factor, which is a direct target of c-Myc. Its overexpression recapitulates multiple c-Myc phenotypes, including cell transformation (61). Deregulation of c-Myc is a hallmark of many human cancers, as the c-Myc oncoprotein directly regulates the expression of >1500 genes controlled by RNA polymerases I, II, and III (62). Although a role for MYCT1 in brain metastasis has not been reported, this study suggests that it could be related to brain metastasis.

Proteins Down-regulated in 231-BR Cells—The most dramatically down-regulated protein was tissue transglutaminase TGM2, which was decreased by ~50-fold in 231-BR. Interestingly the mRNA of TGM2 was also strongly decreased (by ~16-fold), suggesting a regulation at the transcriptional level. TGM2 is a thiol enzyme that catalyzes a crosslinking reaction between a specific γ-glutamyl containing peptide substrate and either a ε-amino group from a peptide-bound Lys residue or a free primary amine (63). These reactions result in post-translational modifications of proteins that can alter their solubility, structure, and function. The γ-glutamyl- ε-lysine (isopeptide) bonds that can be catalyzed by TGM2 result in the formation of either an inter- or intra-isopeptide bond. Many intra- and extracellular proteins have been identified as TGM2 substrates (63). TGM2 acts at both intracellular and extracellular levels (49), as TGM2 is localized at the cell-surface, cytoplasmic, and nuclear levels. The intracellular substrates of TGM2 noticeably include the transcription factor NFkappaB, which is involved in breast cancer cell growth and survival (64). TGM2 activates NFkappaB by cross-linking and polymerizing the inhibitor of NFkappaB, IkappaB, leading to its proteasomal degradation (64). In addition, protein crosslinking is important for extracellular matrix stabilization and while at the cell surface TGM2 interacts with a variety of ECM proteins including integrins (65) and fibronectin (66). Cell surface TGM2 is involved in stabilizing tissues and in particular, lower TGM2 level leads to less cross-linked collagen (67) that can be more efficiently digested by metalloproteinases such as MMP1. Thus, the strong up-regulation of MMP1 in 231-BR and the down-regulation of TGM2 may synergistically contribute to destabilizing the brain microenvironment and facilitate metastatic implantation and growth.

Another strongly down-regulated protein (by 26-fold) was the calcium binding and metastasis-associated protein, S100A4. It is well documented that S100A4 is expressed in cancer cells and contributes to tumor cell motility and metastatic progression, as well as angiogenesis (68). An important characteristic feature of S100 proteins is their dual function, inside and outside the cell, which may explain how it is able to participate in a phenotype characteristic of cancer metastasis. However, the exact underlying mechanisms remain unresolved (69). It is not known in this study whether the change in S100A4 occurs at the intra- or extracellular level, or both, but the strong decrease in 231-BR suggests a relationship to the brain metastatic capability of breast cancer cells. In addition, LCP1 (or L-plastin) was found down-regulated by more than 20-fold. This protein is an actin filament cross-linker that has been shown to contribute to the fine-tuning of actin turnover in breast cancer cells, and its phosphorylation by PKC-delta has recently been shown to induce actin polymerization and tumor cell invasion (72). The expression of LCP1 enhances metastatic properties in both prostate cancer and melanoma cells (73) and this study indicates a potential link with brain metastasis as well.

CONCLUSION

This exploratory proteotranscriptomic study provides a knowledgebase for better understanding the molecular mechanisms leading to brain metastasis and for delineating future biomarkers and therapeutic targets of clinical interest. The primary purpose of the study was to identify proteins regulated in the human MDA-MB-231/231-BR model of brain metastasis, which is unique because of its syngeneic nature. The PRM analysis has been used as a further step to validate the more dramatic changes observed in SILAC. In this regard, the major up-regulated proteins (MMP1, EFNB1, STOM, MYCT1) certainly represent the most valuable candidates for further functional and clinical investigations by brain metastasis specialized groups. However, the limitation of using a single parent-descendent cell culture system dictates caution in the interpretation of the results and suggests that a conservative approach toward describing broad applications is appropriate. In future studies, xenografts may be used to examine the proteome in the context of animal model to see

if the cell line differences persist in the microenvironment. In addition, functional investigations will have to be conducted to evaluate the impact of the identified proteins in brain metastasis and to define the clinical relevance. For instance using shRNAi against the up-regulated proteins of interest (or conversely overexpressing a down-regulated protein) in 231-BR could be used in functional brain metastasis assays. However, there is no *in vitro* assay for brain metastasis, and *in vivo* animal models have to be used as previously reported (7, 8). At the clinical level, it would be valuable to correlate the expression of these proteins with the occurrence of brain metastases and the survival of breast cancer patients. However, most data available, like in the Tumor Cancer Genome Atlas (TCGA) (74), are at the gene/mRNA levels, and TCGA breast cancer does not record brain metastasis. In this context, proteogenomics, a globalized approach encompassing gene/mRNA/protein levels together (75), represents a promising perspective. A first proteogenomic analysis of colon cancer has recently been published (76) and the completion of the same kind of study in breast cancer would provide a powerful means to explore the functional and clinical involvement of the proteins we describe here. Finally, the clinical ramifications of this study may go beyond breast cancer. Brain metastases commonly arise from primary cancers of the lung and skin (melanoma), as well as at a lower frequency in patients with other cancer types (1) and the candidate biomarkers identified in this study could eventually be relevant for brain metastases in other types of cancer. However, it is impossible with only one cellular model to determine how generalizable the observations will be, and this hypothesis will have to be experimentally tested by investigating brain metastasis models in other cancers.

* This work was supported in part by the University of Newcastle Australia, the Hunter Cancer Research Alliance, the Biomedical Technology Research Centers Program of the USPHS National Institute of General Medical Sciences, 8P41GM103481, and NIH 1S10OD016229. We thank the Australian Genome Research Facility (AGRF) and the support it receives from the Commonwealth. LBF is a recipient of a PhD fellowship from Thermo Fisher Scientific (Dornierstrasse 4, 82110 Germering, Germany).

[S] This article contains supplemental material.

** To whom correspondence should be addressed: School of Biomedical Sciences & Pharmacy, Life Sciences Building (LS3-35), The University of Newcastle, Callaghan, NSW 2308, Australia. Tel.: +61 2492 18830; Fax: +61 2492 16903; E-mail: hubert.hondermarck@newcastle.edu.au.

‡‡ Contributed equally to the study.

REFERENCES

1. Nayak, L., Lee, E. Q., and Wen, P. Y. (2012) Epidemiology of brain metastases. *Curr. Oncol. Reports* **14,** 48–54
2. Eichler, A. F., Chung, E., Kodack, D. P., Loeffler, J. S., Fukumura, D., and Jain, R. K. (2011) The biology of brain metastases-translation to new therapies. *Nature Rev. Clin. Oncol.* **8,** 344–356
3. Seoane, J., and De Mattos-Arruda, L. (2014) Brain metastasis: New opportunities to tackle therapeutic resistance. *Mol. Oncol.* **8,** 1120–1131
4. Palmieri, D., Smith, Q. R., Lockman, P. R., Bronder, J., Gril, B., Chambers, A. F., Weil, R. J., and Steeg, P. S. (2006) Brain metastases of breast cancer. *Breast Disease* **26,** 139–147
5. Eckhardt, B. L., Francis, P. A., Parker, B. S., and Anderson, R. L. (2012) Strategies for the discovery and development of therapies for metastatic breast cancer. *Nat. Rev. Drug Discov.* **11,** 479–497
6. Yoneda, T., Williams, P. J., Hiraga, T., Niewolna, M., and Nishimura, R. (2001) A bone-seeking clone exhibits different biological properties from the MDA-MB-231 parental human breast cancer cells and a brain-seeking clone in vivo and in vitro. *J. Bone Miner. Res.* **16,** 1486–1495
7. Palmieri, D., Bronder, J. L., Herring, J. M., Yoneda, T., Weil, R. J., Stark, A. M., Kurek, R., Vega-Valle, E., Feigenbaum, L., Halverson, D., Vortmeyer, A. O., Steinberg, S. M., Aldape, K., and Steeg, P. S. (2007) Her-2 overexpression increases the metastatic outgrowth of breast cancer cells in the brain. *Cancer Res.* **67,** 4190–4198
8. Gril, B., Palmieri, D., Bronder, J. L., Herring, J. M., Vega-Valle, E., Feigenbaum, L., Liewehr, D. J., Steinberg, S. M., Merino, M. J., Rubin, S. D., and Steeg, P. S. (2008) Effect of lapatinib on the outgrowth of metastatic breast cancer cells to the brain. *J. Nat. Cancer Inst.* **100,** 1092–1103
9. Lockman, P. R., Mittapalli, R. K., Taskar, K. S., Rudraraju, V., Gril, B., Bohn, K. A., Adkins, C. E., Roberts, A., Thorsheim, H. R., Gaasch, J. A., Huang, S., Palmieri, D., Steeg, P. S., and Smith, Q. R. (2010) Heterogeneous blood-tumor barrier permeability determines drug efficacy in experimental brain metastases of breast cancer. *Clin. Cancer Res.* **16,** 5664–5678
10. Percy, D. B., Ribot, E. J., Chen, Y., McFadden, C., Simedrea, C., Steeg, P. S., Chambers, A. F., and Foster, P. J. (2011) In vivo characterization of changing blood-tumor barrier permeability in a mouse model of breast cancer metastasis: a complementary magnetic resonance imaging approach. *Invest. Radiol.* **46,** 718–725
11. Fitzgerald, D. P., Subramanian, P., Deshpande, M., Graves, C., Gordon, I., Qian, Y., Snitkovsky, Y., Liewehr, D. J., Steinberg, S. M., Paltan-Ortiz, J. D., Herman, M. M., Camphausen, K., Palmieri, D., Becerra, S. P., and Steeg, P. S. (2012) Opposing effects of pigment epithelium-derived factor on breast cancer cell versus neuronal survival: Implication for brain metastasis and metastasis-induced brain damage. *Cancer Res.* **72,** 144–153
12. Li, F., Glinskii, O. V., Zhou, J., Wilson, L. S., Barnes, S., Anthony, D. C., and Glinsky, V. V. (2011) Identification and analysis of signaling networks potentially involved in breast carcinoma metastasis to the brain. *PloS One* **6,** e21977
13. Fujiki, Y., Hubbard, A. L., Fowler, S., and Lazarow, P. B. (1982) Isolation of intracellular membranes by means of sodium carbonate treatment: Application to endoplasmic reticulum. *J. Cell Biol.* **93,** 97–102
14. Larsen, M. R., Cordwell, S. J., and Roepstorff, P. (2002) Graphite powder as an alternative or supplement to reversed-phase material for desalting and concentration of peptide mixtures prior to matrix-assisted laser desorption/ionization-mass spectrometry. *Proteomics* **2,** 1277–1287
15. Chalkley, R. J., Baker, P. R., Medzihradszky, K. F., Lynn, A. J., and Burlingame, A. L. (2008) In-depth analysis of tandem mass spectrometry data from disparate instrument types. *Mol. Cell. Proteomics* **7,** 2386–2398
16. Elias, J. E., and Gygi, S. P. (2007) Target-decoy search strategy for increased confidence in large-scale protein identifications by mass spectrometry. *Nat. Methods* **4,** 207–214
17. Baker, P. R., and Chalkley, R. J. (2014) MS-viewer: A web-based spectral viewer for proteomics results. *Mol. Cell. Proteomics* **13,** 1392–1396
18. Gallien, S., Duriez, E., Crone, C., Kellmann, M., Moehring, T., and Domon, B. (2012) Targeted proteomic quantification on quadrupole-orbitrap mass spectrometer. *Mol. Cell. Proteomics* **11,** 1709–1723
19. MacLean, B., Tomazela, D. M., Shulman, N., Chambers, M., Finney, G. L., Frewen, B., Kern, R., Tabb, D. L., Liebler, D. C., and MacCoss, M. J. (2010) Skyline: an open source document editor for creating and analyzing targeted proteomics experiments. *Bioinformatics* **26,** 966–968
20. Friedman, R. C., Farh, K. K., Burge, C. B., and Bartel, D. P. (2009) Most mammalian mRNAs are conserved targets of microRNAs. *Genome Res.* **19,** 92–105
21. Yang, J. H., Li, J. H., Shao, P., Zhou, H., Chen, Y. Q., and Qu, L. H. (2011) starBase: a database for exploring microRNA-mRNA interaction maps from Argonaute CLIP-Seq and Degradome-Seq data. *Nucleic Acids Res.* **39,** D202–D209
22. Avery-Kiejda, K. A., Braye, S. G., Mathe, A., Forbes, J. F., and Scott, R. J. (2014) Decreased expression of key tumour suppressor microRNAs is associated with lymph node metastases in triple negative breast cancer.

BMC Cancer **14,** 51
23. Terp, M. G., Lund, R. R., Jensen, O. N., Leth-Larsen, R., and Ditzel, H. J. (2012) Identification of markers associated with highly aggressive metastatic phenotypes using quantitative comparative proteomics. *Cancer Genomics Proteomics* **9,** 265–273
24. Leth-Larsen, R., Lund, R., Hansen, H. V., Laenkholm, A. V., Tarin, D., Jensen, O. N., and Ditzel, H. J. (2009) Metastasis-related plasma membrane proteins of human breast cancer cells identified by comparative quantitative mass spectrometry. *Mol. Cell. Proteomics* **8,** 1436–1449
25. Geiger, T., Madden, S. F., Gallagher, W. M., Cox, J., and Mann, M. (2012) Proteomic portrait of human breast cancer progression identifies novel prognostic markers. *Cancer Res.* **72,** 2428–2439
26. Ho, J., Kong, J. W., Choong, L. Y., Loh, M. C., Toy, W., Chong, P. K., Wong, C. H., Wong, C. Y., Shah, N., and Lim, Y. P. (2009) Novel breast cancer metastasis-associated proteins. *J. Proteome Res.* **8,** 583–594
27. Kulasingam, V., and Diamandis, E. P. (2007) Proteomics analysis of conditioned media from three breast cancer cell lines: a mine for biomarkers and therapeutic targets. *Mol. Cell. Proteomics* **6,** 1997–2011
28. Paget, S. (1989) The distribution of secondary growths in cancer of the breast. 1889. *Cancer Metastasis Rev.* **8,** 98–101
29. Pienta, K. J., Robertson, B. A., Coffey, D. S., and Taichman, R. S. (2013) The cancer diaspora: Metastasis beyond the seed and soil hypothesis. *Clin. Cancer Res.* **19,** 5849–5855
30. Gygi, S. P., Rochon, Y., Franza, B. R., and Aebersold, R. (1999) Correlation between protein and mRNA abundance in yeast. *Mol. Cell. Biol.* **19,** 1720–1730
31. Vogel, C., and Marcotte, E. M. (2012) Insights into the regulation of protein abundance from proteomic and transcriptomic analyses. *Nat. Rev. Genet.* **13,** 227–232
32. Dawson, S. J., Rueda, O. M., Aparicio, S., and Caldas, C. (2013) A new genome-driven integrated classification of breast cancer and its implications. *EMBO J.* **32,** 617–628
33. Rodriguez-Martinez, G., and Velasco, I. (2012) Activin and TGF-beta effects on brain development and neural stem cells. *CNS Neurol. Disord. Drug Targets* **11,** 844–855
34. Yamasaki, S., Yagishita, N., Sasaki, T., Nakazawa, M., Kato, Y., Yamadera, T., Bae, E., Toriyama, S., Ikeda, R., Zhang, L., Fujitani, K., Yoo, E., Tsuchimochi, K., Ohta, T., Araya, N., Fujita, H., Aratani, S., Eguchi, K., Komiya, S., Maruyama, I., Higashi, N., Sato, M., Senoo, H., Ochi, T., Yokoyama, S., Amano, T., Kim, J., Gay, S., Fukamizu, A., Nishioka, K., Tanaka, K., and Nakajima, T. (2007) Cytoplasmic destruction of p53 by the endoplasmic reticulum-resident ubiquitin ligase 'Synoviolin'. *EMBO J.* **26,** 113–122
35. Wang, X., Lin, C., Zhao, X., Liu, A., Zhu, J., Li, X., and Song, L. (2014) Acylglycerol kinase promotes cell proliferation and tumorigenicity in breast cancer via suppression of the FOXO1 transcription factor. *Mol. Cancer* **13,** 106
36. Shats, I., Gatza, M. L., Liu, B., Angus, S. P., You, L., and Nevins, J. R. (2013) FOXO transcription factors control E2F1 transcriptional specificity and apoptotic function. *Cancer Res.* **73,** 6056–6067
37. Asiedu, M. K., Ingle, J. N., Behrens, M. D., Radisky, D. C., and Knutson, K. L. (2011) TGFbeta/TNF(alpha)-mediated epithelial-mesenchymal transition generates breast cancer stem cells with a claudin-low phenotype. *Cancer Res.* **71,** 4707–4719
38. Yu, M., Zhou, X., Niu, L., Lin, G., Huang, J., Zhou, W., Gan, H., Wang, J., Jiang, X., Yin, B., and Li, Z. (2013) Targeting transmembrane TNF-alpha suppresses breast cancer growth. *Cancer Res.* **73,** 4061–4074
39. Blair, L. P., Cao, J., Zou, M. R., Sayegh, J., and Yan, Q. (2011) Epigenetic regulation by lysine demethylase 5 (KDM5) enzymes in cancer. *Cancers* **3,** 1383–1404
40. Rasmussen, P. B., and Staller, P. (2014) The KDM5 family of histone demethylases as targets in oncology drug discovery. *Epigenomics* **6,** 277–286
41. Simmons, K. M., Beaudin, S. G., Narvaez, C. J., and Welsh, J. (2015) Gene Signatures of 1,25-Dihydroxyvitamin D Exposure in Normal and Transformed Mammary Cells. *J. Cell. Biochem.* **116,** 1693–1711
42. Imamura, T., Hikita, A., and Inoue, Y. (2012) The roles of TGF-beta signaling in carcinogenesis and breast cancer metastasis. *Breast Cancer* **19,** 118–124
43. Yang, Y., Feng, R., Bi, S., and Xu, Y. (2011) TNF-alpha polymorphisms and breast cancer. *Breast Cancer Res. Treat.* **129,** 513–519
44. Hadler-Olsen, E., Winberg, J. O., and Uhlin-Hansen, L. (2013) Matrix metalloproteinases in cancer: Their value as diagnostic and prognostic markers and therapeutic targets. *Tumour Biol.* **34,** 2041–2051
45. McGowan, P. M., and Duffy, M. J. (2008) Matrix metalloproteinase expression and outcome in patients with breast cancer: Analysis of a published database. *Ann. Oncol.* **19,** 1566–1572
46. Liu, H., Kato, Y., Erzinger, S. A., Kiriakova, G. M., Qian, Y., Palmieri, D., Steeg, P. S., and Price, J. E. (2012) The role of MMP-1 in breast cancer growth and metastasis to the brain in a xenograft model. *BMC Cancer* **12,** 583
47. Zhou, Y., Cui, Z., Xia, X., Liu, C., Zhu, X., Cao, J., Wu, Y., Zhou, L., Ben, Z., Song, Y., Zhang, H., and Zhang, D. (2014) Matrix metalloproteinase-1 (MMP-1) expression in rat spinal cord injury model. *Cell. Mol. Neurobiol.* **34,** 1151–1163
48. Coussens, L. M., Fingleton, B., and Matrisian, L. M. (2002) Matrix metalloproteinase inhibitors and cancer: trials and tribulations. *Science* **295,** 2387–2392
49. Lia, N. G., Shib, Z. H., Tang, Y. P., and Duan, J. A. (2009) Selective matrix metalloproteinase inhibitors for cancer. *Curr. Med. Chem.* **16,** 3805–3827
50. Pasquale, E. B. (2008) Eph-ephrin bidirectional signaling in physiology and disease. *Cell* **133,** 38–52
51. Kaenel, P., Mosimann, M., and Andres, A. C. (2012) The multifaceted roles of Eph/ephrin signaling in breast cancer. *Cell Adhesion Migration* **6,** 138–147
52. Yin, H., Lu, C., Tang, Y., Wang, H., Wang, H., and Wang, J. (2013) Enhanced expression of EphrinB1 is associated with lymph node metastasis and poor prognosis in breast cancer. *Cancer Biomarkers* **13,** 261–267
53. Vermeer, P. D., Bell, M., Lee, K., Vermeer, D. W., Wieking, B. G., Bilal, E., Bhanot, G., Drapkin, R. I., Ganesan, S., Klingelhutz, A. J., Hendriks, W. J., and Lee, J. H. (2012) ErbB2, EphrinB1, Src kinase and PTPN13 signaling complex regulates MAP kinase signaling in human cancers. *PloS One* **7,** e30447
54. Yang, S., Li, Y., Gao, J., Zhang, T., Li, S., Luo, A., Chen, H., Ding, F., Wang, X., and Liu, Z. (2013) MicroRNA-34 suppresses breast cancer invasion and metastasis by directly targeting Fra-1. *Oncogene* **32,** 4294–4303
55. Lodygin, D., Tarasov, V., Epanchintsev, A., Berking, C., Knyazeva, T., Korner, H., Knyazev, P., Diebold, J., and Hermeking, H. (2008) Inactivation of miR-34a by aberrant CpG methylation in multiple types of cancer. *Cell Cycle* **7,** 2591–2600
56. Noberini, R., Lamberto, I., and Pasquale, E. B. (2012) Targeting Eph receptors with peptides and small molecules: progress and challenges. *Semin. Cell Dev. Biol.* **23,** 51–57
57. Lapatsina, L., Brand, J., Poole, K., Daumke, O., and Lewin, G. R. (2012) Stomatin-domain proteins. *Eur. J. Cell Biol.* **91,** 240–245
58. Mio, T., Yabe, T., Arisawa, M., and Yamada-Okabe, H. (1998) The eukaryotic UDP-N-acetylglucosamine pyrophosphorylases. Gene cloning, protein expression, and catalytic mechanism. *J. Biol. Chem.* **273,** 14392–14397
59. Yip, G. W., Smollich, M., and Gotte, M. (2006) Therapeutic value of glycosaminoglycans in cancer. *Mol. Cancer Ther.* **5,** 2139–2148
60. Bos, P. D., Zhang, X. H., Nadal, C., Shu, W., Gomis, R. R., Nguyen, D. X., Minn, A. J., van de Vijver, M. J., Gerald, W. L., Foekens, J. A., and Massague, J. (2009) Genes that mediate breast cancer metastasis to the brain. *Nature* **459,** 1005–1009
61. Rogulski, K. R., Cohen, D. E., Corcoran, D. L., Benos, P. V., and Prochownik, E. V. (2005) Deregulation of common genes by c-Myc and its direct target, MT-MC1. *Proc. Natl. Acad. Sci. U.S.A.* **102,** 18968–18973
62. Cohen, D. E., and Prochownik, E. V. (2006) A functional hierarchy for c-Myc target genes? Lessons from MT-MC1. *Cell Cycle* **5,** 392–393
63. Lai, T. S., and Greenberg, C. S. (2013) TGM2 and implications for human disease: Role of alternative splicing. *Frontiers Biosci.* **18,** 504–519
64. Brown, K. D. (2013) Transglutaminase 2 and NF-kappaB: An odd couple that shapes breast cancer phenotype. *Breast Cancer Res. Treat.* **137,** 329–336
65. Akimov, S. S., Krylov, D., Fleischman, L. F., and Belkin, A. M. (2000) Tissue transglutaminase is an integrin-binding adhesion coreceptor for fibronectin. *J. Cell Biol.* **148,** 825–838
66. Hang, J., Zemskov, E. A., Lorand, L., and Belkin, A. M. (2005) Identification of a novel recognition sequence for fibronectin within the NH2-terminal beta-sandwich domain of tissue transglutaminase. *J. Biol. Chem.* **280,**

23675–23683
67. Greenberg, C. S., Birckbichler, P. J., and Rice, R. H. (1991) Transglutaminases: multifunctional cross-linking enzymes that stabilize tissues. *FASEB J.* **5,** 3071–3077
68. Boye, K., and Maelandsmo, G. M. (2010) S100A4 and metastasis: A small actor playing many roles. *Am. J. Pathol.* **176,** 528–535
69. Mishra, S. K., Siddique, H. R., and Saleem, M. (2012) S100A4 calcium-binding protein is key player in tumor progression and metastasis: preclinical and clinical evidence. *Cancer Metastasis Rev.* **31,** 163–172
70. Kozlova, E. N., and Lukanidin, E. (2002) Mts1 protein expression in the central nervous system after injury. *Glia* **37,** 337–348
71. Dmytriyeva, O., Pankratova, S., Owczarek, S., Sonn, K., Soroka, V., Ridley, C. M., Marsolais, A., Lopez-Hoyos, M., Ambartsumian, N., Lukanidin, E., Bock, E., Berezin, V., and Kiryushko, D. (2012) The metastasis-promoting S100A4 protein confers neuroprotection in brain injury. *Nat. Commun.* **3,** 1197
72. Al Tanoury, Z., Schaffner-Reckinger, E., Halavatyi, A., Hoffmann, C., Moes, M., Hadzic, E., Catillon, M., Yatskou, M., and Friederich, E. (2010) Quantitative kinetic study of the actin-bundling protein L-plastin and of its impact on actin turn-over. *PloS One* **5,** e9210
73. Riplinger, S. M., Wabnitz, G. H., Kirchgessner, H., Jahraus, B., Lasitschka, F., Schulte, B., van der Pluijm, G., van der Horst, G., Hammerling, G. J., Nakchbandi, I., and Samstag, Y. (2014) Metastasis of prostate cancer and melanoma cells in a preclinical in vivo mouse model is enhanced by L-plastin expression and phosphorylation. *Mol. Cancer* **13,** 10
74. Cancer Genome Atlas Research Network, N., Weinstein, J. N., Collisson, E. A., Mills, G. B., Shaw, K. R., Ozenberger, B. A., Ellrott, K., Shmulevich, I., Sander, C., and Stuart, J. M. (2013) The Cancer Genome Atlas Pan-Cancer analysis project. *Nat. Genet.* **45,** 1113–1120
75. Faulkner, S., Dun, M. D., and Hondermarck, H. (2015) Proteogenomics: emergence and promise. *Cell Mol. Life Sci.* **72,** 953–957
76. Zhang, B., Wang, J., Wang, X., Zhu, J., Liu, Q., Shi, Z., Chambers, M. C., Zimmerman, L. J., Shaddox, K. F., Kim, S., Davies, S. R., Wang, S., Wang, P., Kinsinger, C. R., Rivers, R. C., Rodriguez, H., Townsend, R. R., Ellis, M. J., Carr, S. A., Tabb, D. L., Coffey, R. J., Slebos, R. J., Liebler, D. C., and Nci, C. (2014) Proteogenomic characterization of human colon and rectal cancer. *Nature* **513,** 382–387
77. Falkenby, L. G., Such-Sanmartín, G., Larsen, M. R., Vorm, O., Bache, N., Jensen, O. N. (2014) Integrated solid-phase extraction-capillary liquid chromatography (speLC) interfaced to ESI-MS/MS for fast characterization and quantification of protein and proteomes. *J Proteome Res.* **13,** 6169–6175

A.2 Co-authorship declaration

By signing below I confirm that ***Sam Faulkner*** *significantly contributed experimentally and intellectually to the publication entitled* ***Nerve fibers infiltrate the tumor microenvironment and are associated with nerve growth factor production and lymph node invasion in breast cancer*** *and endorse its inclusion as part of this thesis.*

Signature: *Date: 22/08/2017*

Jay Pundavela *dd/mm/yyyy*

Signature: *Date: 22/08/2017*

Severine Roselli *dd/mm/yyyy*

Signature: *Date: 21/08/2017*

John Attia *dd/mm/yyyy*

Signature: *Date: 21/08/2017*

Rodney J. Scott *dd/mm/yyyy*

Signature:

Date: 22/08/2017

Rick F. Thorne *dd/mm/yyyy*

Signature: *Date: 25/08/2017*

John F. Forbes *dd/mm/yyyy*

Signature: *Date: 21/08/2017*

Ralph A. Bradshaw *dd/mm/yyyy*

Signature:

`Marjorie M. Walker *Date: 21/08/2017*

dd/mm/yyyy

Signature: *Date: 22/08/2017*

dd/mm/yyyy

Phillip Jobling

Signature: *Date: 22/08/2017*

Hubert Hondermarck *dd/mm/yyyy*

Signature: Date: 9/10/2017

dd/mm/yyyy

Professor Robert Callister

Assistant Dean (Research Training)

A.3 List of prizes and awards

2017

Kellerman Award for Medical Biochemistry

University of Newcastle, Australia

2016

Margaret Taylor Travel Grant

Hunter Medical Research Institute (HMRI)

2016

Best Poster Presentation – ASMR Hunter Region Scientific Meeting

Awarded by the Australian Society for Medical Research

Hunter Medical Research Institute (HMRI)

Bibliography

1. Skaper SD. The neurotrophin family of neurotrophic factors: an overview. Methods in molecular biology. 2012; 846:1-12.

2. Shooter EM. Early days of the nerve growth factor proteins. Annual review of neuroscience. 2001; 24:601-629.

3. Bradshaw RA, Pundavela J, Biarc J, Chalkley RJ, Burlingame AL and Hondermarck H. NGF and ProNGF: Regulation of neuronal and neoplastic responses through receptor signaling. Advances in biological regulation. 2014.

4. West AE, Pruunsild P and Timmusk T. Neurotrophins: transcription and translation. Handbook of experimental pharmacology. 2014; 220:67-100.

5. Hondermarck H. Neurotrophins and their receptors in breast cancer. Cytokine Growth Factor Rev. 2012; 23(6):357-365.

6. Lee R, Kermani P, Teng KK and Hempstead BL. Regulation of cell survival by secreted proneurotrophins. Science. 2001; 294(5548):1945-1948.

7. Pang PT, Teng HK, Zaitsev E, Woo NT, Sakata K, Zhen S, Teng KK, Yung WH, Hempstead BL and Lu B. Cleavage of proBDNF by tPA/plasmin is essential for long-term hippocampal plasticity. Science. 2004; 306(5695):487-491.

8. Teng KK, Felice S, Kim T and Hempstead BL. Understanding proneurotrophin actions: Recent advances and challenges. Developmental neurobiology. 2010; 70(5):350-359.

9. Sun XL, Chen BY, Xia Y, Wang JJ and Chen LW. Functional switch from pro-neurotrophins to mature neurotrophins. Current protein & peptide science. 2013; 14(7):617-625.

10. Hempstead BL. Deciphering proneurotrophin actions. Handbook of experimental pharmacology. 2014; 220:17-32.

11. Nykjaer A, Lee R, Teng KK, Jansen P, Madsen P, Nielsen MS, Jacobsen C, Kliemannel M, Schwarz E, Willnow TE, Hempstead BL and Petersen CM. Sortilin is essential for proNGF-induced neuronal cell death. Nature. 2004; 427(6977):843-848.

12. Glerup S, Nykjaer A and Vaegter CB. Sortilins in neurotrophic factor signaling. Handbook of experimental pharmacology. 2014; 220:165-189.

13. Nykjaer A and Willnow TE. Sortilin: a receptor to regulate neuronal viability and function. Trends in neurosciences. 2012; 35(4):261-270.

14. Vaegter CB, Jansen P, Fjorback AW, Glerup S, Skeldal S, Kjolby M, Richner M, Erdmann B, Nyengaard JR, Tessarollo L, Lewin GR, Willnow TE, Chao MV and Nykjaer A. Sortilin associates with Trk receptors to enhance

anterograde transport and neurotrophin signaling. Nat Neurosci. 2011; 14(1):54-61.

15. Bradshaw RA, Pundavela J, Biarc J, Chalkley RJ, Burlingame AL and Hondermarck H. NGF and ProNGF: Regulation of neuronal and neoplastic responses through receptor signaling. Advances in biological regulation. 2015; 58:16-27.

16. Demont Y, Corbet C, Page A, Ataman-Onal Y, Choquet-Kastylevsky G, Fliniaux I, Le Bourhis X, Toillon RA, Bradshaw RA and Hondermarck H. Pro-nerve growth factor induces autocrine stimulation of breast cancer cell invasion through tropomyosin-related kinase A (TrkA) and sortilin protein. The Journal of biological chemistry. 2012; 287(3):1923-1931.

17. Schecterson LC and Bothwell M. Neurotrophin receptors: Old friends with new partners. Developmental neurobiology. 2010; 70(5):332-338.

18. Pezet S and McMahon SB. Neurotrophins: mediators and modulators of pain. Annual review of neuroscience. 2006; 29:507-538.

19. Wang W, Chen J and Guo X. The role of nerve growth factor and its receptors in tumorigenesis and cancer pain. Bioscience trends. 2014; 8(2):68-74.

20. Kumar V and Mahal BA. NGF - the TrkA to successful pain treatment. J Pain Res. 2012; 5:279-287.

21. Richards N and McMahon SB. Targeting novel peripheral mediators for the treatment of chronic pain. Br J Anaesth. 2013; 111(1):46-51.

22. Jobling P, Pundavela J, Oliveira SM, Roselli S, Walker MM and Hondermarck H. Nerve-Cancer Cell Cross-talk: A Novel Promoter of Tumor Progression. Cancer research. 2015; 75(9):1777-1781.

23. Harrington AW, Leiner B, Blechschmitt C, Arevalo JC, Lee R, Morl K, Meyer M, Hempstead BL, Yoon SO and Giehl KM. Secreted proNGF is a pathophysiological death-inducing ligand after adult CNS injury. Proceedings of the National Academy of Sciences of the United States of America. 2004; 101(16):6226-6230.

24. Al-Shawi R, Hafner A, Olsen J, Chun S, Raza S, Thrasivoulou C, Lovestone S, Killick R, Simons P and Cowen T. Neurotoxic and neurotrophic roles of proNGF and the receptor sortilin in the adult and ageing nervous system. Eur J Neurosci. 2008; 27(8):2103-2114.

25. Quistgaard EM, Madsen P, Groftehauge MK, Nissen P, Petersen CM and Thirup SS. Ligands bind to Sortilin in the tunnel of a ten-bladed beta-propeller domain. Nat Struct Mol Biol. 2009; 16(1):96-98.

26. Lewin GR and Nykjaer A. Pro-neurotrophins, sortilin, and nociception. The European journal of neuroscience. 2014; 39(3):363-374.

27. Pundavela J, Demont Y, Jobling P, Lincz LF, Roselli S, Thorne R, Bond D, Bradshaw RA, Walker MM and Hondermarck H. ProNGF Correlates with Gleason Score and Is a Potential Driver of Nerve Infiltration in Prostate Cancer. The American journal of pathology. 2014.

28. Fahnestock M, Yu G, Michalski B, Mathew S, Colquhoun A, Ross GM and Coughlin MD. The nerve growth factor precursor proNGF exhibits neurotrophic activity but is less active than mature nerve growth factor. J Neurochem. 2004; 89(3):581-592.

29. Masoudi R, Ioannou MS, Coughlin MD, Pagadala P, Neet KE, Clewes O, Allen SJ, Dawbarn D and Fahnestock M. Biological Activity of Nerve Growth Factor Precursor Is Dependent upon Relative Levels of Its Receptors. The Journal of biological chemistry. 2009; 284(27):18424-18433.

30. Beattie MS, Harrington AW, Lee R, Kim JY, Boyce SL, Longo FM, Bresnahan JC, Hempstead BL and Yoon SO. ProNGF induces p75-mediated death of oligodendrocytes following spinal cord injury. Neuron. 2002; 36(3):375-386.

31. Volosin M, Trotter C, Cragnolini A, Kenchappa RS, Light M, Hempstead BL, Carter BD and Friedman WJ. Induction of proneurotrophins and activation of p75NTR-mediated apoptosis via neurotrophin receptor-interacting factor in hippocampal neurons after seizures. The Journal of neuroscience : the official journal of the Society for Neuroscience. 2008; 28(39):9870-9879.

32. Howard L, Wyatt S, Nagappan G and Davies AM. ProNGF promotes neurite growth from a subset of NGF-dependent neurons by a p75NTR-dependent mechanism. Development. 2013; 140(10):2108-2117.

33. Buttigieg H, Kawaja MD and Fahnestock M. Neurotrophic activity of proNGF in vivo. Exp Neurol. 2007; 204(2):832-835.

34. Clewes O, Fahey MS, Tyler SJ, Watson JJ, Seok H, Catania C, Cho K, Dawbarn D and Allen SJ. Human ProNGF: biological effects and binding profiles at TrkA, P75NTR and sortilin. J Neurochem. 2008; 107(4):1124-1135.

35. Herrup K and Shooter EM. Properties of the beta nerve growth factor receptor of avian dorsal root ganglia. Proceedings of the National Academy of Sciences of the United States of America. 1973; 70(12):3884-3888.

36. Rodriguez-Tebar A, Dechant G and Barde YA. Binding of brain-derived neurotrophic factor to the nerve growth factor receptor. Neuron. 1990; 4(4):487-492.

37. Rodriguez-Tebar A, Dechant G, Gotz R and Barde YA. Binding of neurotrophin-3 to its neuronal receptors and interactions with nerve growth factor and brain-derived neurotrophic factor. Embo J. 1992; 11(3):917-922.

38. Squinto SP, Stitt TN, Aldrich TH, Davis S, Bianco SM, Radziejewski C, Glass DJ, Masiakowski P, Furth ME, Valenzuela DM and et al. trkB encodes a functional receptor for brain-derived neurotrophic factor and neurotrophin-3 but not nerve growth factor. Cell. 1991; 65(5):885-893.

39. Reichardt LF. Neurotrophin-regulated signalling pathways. Philosophical transactions of the Royal Society of London Series B, Biological sciences. 2006; 361(1473):1545-1564.

40. Pimenta AC, Dourado DF, Martins JM, Melo A, Dias Soeiro Cordeiro MN, Almeida RD, Morra G and Moreira IS. Dynamic structure of NGF and proNGF complexed with p75NTR: pro-peptide effect. Journal of chemical information and modeling. 2014; 54(7):2051-2067.

41. Aggarwal BB. Signalling pathways of the TNF superfamily: a double-edged sword. Nat Rev Immunol. 2003; 3(9):745-756.

42. Smith CA, Farrah T and Goodwin RG. The TNF receptor superfamily of cellular and viral proteins: activation, costimulation, and death. Cell. 1994; 76(6):959-962.

43. Yan H and Chao MV. Disruption of cysteine-rich repeats of the p75 nerve growth factor receptor leads to loss of ligand binding. The Journal of biological chemistry. 1991; 266(18):12099-12104.

44. Roux PP and Barker PA. Neurotrophin signaling through the p75 neurotrophin receptor. Prog Neurobiol. 2002; 67(3):203-233.

45. He XL and Garcia KC. Structure of nerve growth factor complexed with the shared neurotrophin receptor p75. Science. 2004; 304(5672):870-875.

46. Feng D, Kim T, Ozkan E, Light M, Torkin R, Teng KK, Hempstead BL and Garcia KC. Molecular and structural insight into proNGF engagement of p75NTR and sortilin. Journal of molecular biology. 2010; 396(4):967-984.

47. Hondermarck H, Demont Y and Bradshaw RA. (2015). The TrK Receptor Family. In: Wheeler DL and Yarden Y, eds. Receptor Tyrosine Kinases: Family and Subfamilies. (Cham: Springer International Publishing), pp. 777-820.

48. Hermey G, Keat SJ, Madsen P, Jacobsen C, Petersen CM and Gliemann J. Characterization of sorCS1, an alternatively spliced receptor with completely different cytoplasmic domains that mediate different trafficking in cells. The Journal of biological chemistry. 2003; 278(9):7390-7396.

49. Jacobsen L, Madsen P, Jacobsen C, Nielsen MS, Gliemann J and Petersen CM. Activation and functional characterization of the mosaic receptor SorLA/LR11. The Journal of biological chemistry. 2001; 276(25):22788-22796.

50. Mazella J, Zsurger N, Navarro V, Chabry J, Kaghad M, Caput D, Ferrara P, Vita N, Gully D, Maffrand JP and Vincent JP. The 100-kDa neurotensin

receptor is gp95/sortilin, a non-G-protein-coupled receptor. The Journal of biological chemistry. 1998; 273(41):26273-26276.

51. Teng HK, Teng KK, Lee R, Wright S, Tevar S, Almeida RD, Kermani P, Torkin R, Chen ZY, Lee FS, Kraemer RT, Nykjaer A and Hempstead BL. ProBDNF induces neuronal apoptosis via activation of a receptor complex of p75NTR and sortilin. The Journal of neuroscience : the official journal of the Society for Neuroscience. 2005; 25(22):5455-5463.

52. Wollscheid B, Bausch-Fluck D, Henderson C, O'Brien R, Bibel M, Schiess R, Aebersold R and Watts JD. Mass-spectrometric identification and relative quantification of N-linked cell surface glycoproteins. Nat Biotechnol. 2009; 27(4):378-386.

53. Lewandrowski U, Moebius J, Walter U and Sickmann A. Elucidation of N-glycosylation sites on human platelet proteins: a glycoproteomic approach. Mol Cell Proteomics. 2006; 5(2):226-233.

54. Munck Petersen C, Nielsen MS, Jacobsen C, Tauris J, Jacobsen L, Gliemann J, Moestrup SK and Madsen P. Propeptide cleavage conditions sortilin/neurotensin receptor-3 for ligand binding. Embo J. 1999; 18(3):595-604.

55. Kaplan DR, Hempstead BL, Martin-Zanca D, Chao MV and Parada LF. The trk proto-oncogene product: a signal transducing receptor for nerve growth factor. Science. 1991; 252(5005):554-558.

56. Kliemannel M, Golbik R, Rudolph R, Schwarz E and Lilie H. The pro-peptide of proNGF: structure formation and intramolecular association with NGF. Protein Sci. 2007; 16(3):411-419.

57. Paoletti F, Covaceuszach S, Konarev PV, Gonfloni S, Malerba F, Schwarz E, Svergun DI, Cattaneo A and Lamba D. Intrinsic structural disorder of mouse proNGF. Proteins. 2009; 75(4):990-1009.

58. Wiesmann C, Ultsch MH, Bass SH and de Vos AM. Crystal structure of nerve growth factor in complex with the ligand-binding domain of the TrkA receptor. Nature. 1999; 401(6749):184-188.

59. Wehrman T, He X, Raab B, Dukipatti A, Blau H and Garcia KC. Structural and mechanistic insights into nerve growth factor interactions with the TrkA and p75 receptors. Neuron. 2007; 53(1):25-38.

60. Levi-Montalcini R. Effects of mouse tumor transplantation on the nervous system. Annals of the New York Academy of Sciences. 1952; 55(2):330-344.

61. Halvorson KG, Kubota K, Sevcik MA, Lindsay TH, Sotillo JE, Ghilardi JR, Rosol TJ, Boustany L, Shelton DL and Mantyh PW. A blocking antibody to nerve growth factor attenuates skeletal pain induced by prostate tumor cells growing in bone. Cancer research. 2005; 65(20):9426-9435.

62. Bloom AP, Jimenez-Andrade JM, Taylor RN, Castaneda-Corral G, Kaczmarska MJ, Freeman KT, Coughlin KA, Ghilardi JR, Kuskowski MA and Mantyh PW. Breast cancer-induced bone remodeling, skeletal pain, and sprouting of sensory nerve fibers. The journal of pain : official journal of the American Pain Society. 2011; 12(6):698-711.

63. Descamps S, Lebourhis X, Delehedde M, Boilly B and Hondermarck H. Nerve growth factor is mitogenic for cancerous but not normal human breast epithelial cells. The Journal of biological chemistry. 1998; 273(27):16659-16662.

64. Descamps S, Toillon RA, Adriaenssens E, Pawlowski V, Cool SM, Nurcombe V, Le Bourhis X, Boilly B, Peyrat JP and Hondermarck H. Nerve growth factor stimulates proliferation and survival of human breast cancer cells through two distinct signaling pathways. The Journal of biological chemistry. 2001; 276(21):17864-17870.

65. El Yazidi-Belkoura I, Adriaenssens E, Dolle L, Descamps S and Hondermarck H. Tumor necrosis factor receptor-associated death domain protein is involved in the neurotrophin receptor-mediated antiapoptotic activity of nerve growth factor in breast cancer cells. The Journal of biological chemistry. 2003; 278(19):16952-16956.

66. Dolle L, El Yazidi-Belkoura I, Adriaenssens E, Nurcombe V and Hondermarck H. Nerve growth factor overexpression and autocrine loop in breast cancer cells. Oncogene. 2003; 22(36):5592-5601.

67. Adriaenssens E, Vanhecke E, Saule P, Mougel A, Page A, Romon R, Nurcombe V, Le Bourhis X and Hondermarck H. Nerve growth factor is a potential therapeutic target in breast cancer. Cancer research. 2008; 68(2):346-351.

68. Lagadec C, Meignan S, Adriaenssens E, Foveau B, Vanhecke E, Romon R, Toillon RA, Oxombre B, Hondermarck H and Le Bourhis X. TrkA overexpression enhances growth and metastasis of breast cancer cells. Oncogene. 2009; 28(18):1960-1970.

69. Zan H, Tat C, Qiu Z, Taylor JR, Guerrero JA, Shen T and Casali P. Rad52 competes with Ku70/Ku86 for binding to S-region DSB ends to modulate antibody class-switch DNA recombination. Nature communications. 2017; 8:14244.

70. Lagadec C, Romon R, Tastet C, Meignan S, Com E, Page A, Bidaux G, Hondermarck H and Le Bourhis X. Ku86 is important for TrkA overexpression-induced breast cancer cell invasion. Proteomics Clinical applications. 2010; 4(6-7):580-590.

71. Roselli S, Pundavela J, Demont Y, Faulkner S, Keene S, Attia J, Jiang CC, Zhang XD, Walker MM and Hondermarck H. Sortilin is associated with breast cancer aggressiveness and contributes to tumor cell adhesion and invasion. *Oncotarget*. 2015; 5.

72. Tomellini E, Touil Y, Lagadec C, Julien S, Ostyn P, Ziental-Gelus N, Meignan S, Lengrand J, Adriaenssens E, Polakowska R and Le Bourhis X. Nerve

growth factor and proNGF simultaneously promote symmetric self-renewal, quiescence, and epithelial to mesenchymal transition to enlarge the breast cancer stem cell compartment. Stem Cells. 2015; 33(2):342-353.

73. Jobling P, Pundavela J, Oliveira SM, Roselli S, Walker MM and Hondermarck H. Nerve-Cancer Cell Cross-talk: A Novel Promoter of Tumor Progression. Cancer research. 2015.

74. Romon R, Adriaenssens E, Lagadec C, Germain E, Hondermarck H and Le Bourhis X. Nerve growth factor promotes breast cancer angiogenesis by activating multiple pathways. Molecular cancer. 2010; 9:157.

75. Houtz J, Borden P, Ceasrine A, Minichiello L and Kuruvilla R. Neurotrophin Signaling Is Required for Glucose-Induced Insulin Secretion. Developmental cell. 2016; 39(3):329-345.

76. Zhu Z, Friess H, diMola FF, Zimmermann A, Graber HU, Korc M and Buchler MW. Nerve growth factor expression correlates with perineural invasion and pain in human pancreatic cancer. Journal of clinical oncology : official journal of the American Society of Clinical Oncology. 1999; 17(8):2419-2428.

77. Zhu Z, Kleeff J, Kayed H, Wang L, Korc M, Buchler MW and Friess H. Nerve growth factor and enhancement of proliferation, invasion, and tumorigenicity of pancreatic cancer cells. Mol Carcinog. 2002; 35(3):138-147.

78. Demir IE, Friess H and Ceyhan GO. Neural plasticity in pancreatitis and pancreatic cancer. Nat Rev Gastroenterol Hepatol. 2015; 12(11):649-659.

79. Demir IE, Boldis A, Pfitzinger PL, Teller S, Brunner E, Klose N, Kehl T, Maak M, Lesina M, Laschinger M, Janssen KP, Algul H, Friess H and Ceyhan GO. Investigation of Schwann cells at neoplastic cell sites before the onset of cancer invasion. Journal of the National Cancer Institute. 2014; 106(8).

80. Bapat AA, Munoz RM, Von Hoff DD and Han H. Blocking Nerve Growth Factor Signaling Reduces the Neural Invasion Potential of Pancreatic Cancer Cells. PloS one. 2016; 11(10):e0165586.

81. Lei Y, Tang L, Xie Y, Xianyu Y, Zhang L, Wang P, Hamada Y, Jiang K, Zheng W and Jiang X. Gold nanoclusters-assisted delivery of NGF siRNA for effective treatment of pancreatic cancer. Nature communications. 2017; 8:15130.

82. Wang ZY, Ding Y, Miki T, Warita K, Matsumoto Y, Takeuchi Y, Wang SJ, Feng JG, Liu W, Wang YD, Wang XL, Wang YH, Liu Y and Shan BE. Nerve growth factor and receptors are significantly affected by histamine stimulus through H1 receptor in pancreatic carcinoma cells. Molecular medicine reports. 2010; 3(1):103-109.

83. Devader C, Beraud-Dufour S, Coppola T and Mazella J. The anti-apoptotic role of neurotensin. Cells. 2013; 2(1):124-135.

84. Mijatovic T, Gailly P, Mathieu V, De Neve N, Yeaton P, Kiss R and Decaestecker C. Neurotensin is a versatile modulator of in vitro human pancreatic ductal adenocarcinoma cell (PDAC) migration. Cell Oncol. 2007; 29(4):315-326.
85. Pincelli C and Yaar M. Nerve growth factor: its significance in cutaneous biology. The journal of investigative dermatology Symposium proceedings / the Society for Investigative Dermatology, Inc [and] European Society for Dermatological Research. 1997; 2(1):31-36.

86. Marconi A, Panza MC, Bonnet-Duquennoy M, Lazou K, Kurfurst R, Truzzi F, Lotti R, De Santis G, Dumas M, Bonte F and Pincelli C. Expression and function of neurotrophins and their receptors in human melanocytes. Int J Cosmet Sci. 2006; 28(4):255-261.

87. Fabricant RN, De Larco JE and Todaro GJ. Nerve growth factor receptors on human melanoma cells in culture. Proceedings of the National Academy of Sciences of the United States of America. 1977; 74(2):565-569.

88. Sherwin SA, Sliski AH and Todaro GJ. Human melanoma cells have both nerve growth factor and nerve growth factor-specific receptors on their cell surfaces. Proceedings of the National Academy of Sciences of the United States of America. 1979; 76(3):1288-1292.

89. Iwamoto S, Burrows RC, Agoff SN, Piepkorn M, Bothwell M and Schmidt R. The p75 neurotrophin receptor, relative to other Schwann cell and melanoma markers, is abundantly Expressed in spindled melanomas. The American Journal of dermatopathology. 2001; 23(4):288-294.

90. Iwamoto S, Odland PB, Piepkorn M and Bothwell M. Evidence that the p75 neurotrophin receptor mediates perineural spread of desmoplastic melanoma. Journal of the American Academy of Dermatology. 1996; 35(5 Pt 1):725-731.

91. Huttenbach Y, Prieto VG and Reed JA. Desmoplastic and spindle cell melanomas express protein markers of the neural crest but not of later committed stages of Schwann cell differentiation. Journal of cutaneous pathology. 2002; 29(9):562-568.

92. Lazova R, Tantcheva-Poor I and Sigal AC. P75 nerve growth factor receptor staining is superior to S100 in identifying spindle cell and desmoplastic melanoma. Journal of the American Academy of Dermatology. 2010; 63(5):852-858.

93. Florenes VA, Maelandsmo GM, Holm R, Reich R, Lazarovici P and Davidson B. Expression of activated TrkA protein in melanocytic tumors: relationship to cell proliferation and clinical outcome. Am J Clin Pathol. 2004; 122(3):412-420.

94. Truzzi F, Marconi A and Pincelli C. Neurotrophins in healthy and diseased skin. Dermatoendocrinol. 2011; 3(1):32-36.

95. Truzzi F, Marconi A, Lotti R, Dallaglio K, French LE, Hempstead BL and Pincelli C. Neurotrophins and their receptors stimulate melanoma cell proliferation and migration. J Invest Dermatol. 2008; 128(8):2031-2040.

96. Shonukan O, Bagayogo I, McCrea P, Chao M and Hempstead B. Neurotrophin-induced melanoma cell migration is mediated through the actin-bundling protein fascin. Oncogene. 2003; 22(23):3616-3623.

97. Pasini L, Re A, Tebaldi T, Ricci G, Boi S, Adami V, Barbareschi M and Quattrone A. TrkA is amplified in malignant melanoma patients and induces an anti-proliferative response in cell lines. BMC cancer. 2015; 15:777.

98. Entschladen F, Palm D, Lang K, Drell TLt and Zaenker KS. Neoneurogenesis: tumors may initiate their own innervation by the release of neurotrophic factors in analogy to lymphangiogenesis and neoangiogenesis. Med Hypotheses. 2006; 67(1):33-35.

99. Delsite R and Djakiew D. Characterization of nerve growth factor precursor protein expression by human prostate stromal cells: a role in selective neurotrophin stimulation of prostate epithelial cell growth. Prostate. 1999; 41(1):39-48.

100. Du JJ, Dou KF, Peng SY, Qian BZ, Xiao HS, Liu F, Wang WZ, Guan WX, Gao ZQ, Liu YB and Han ZG. Expression of NGF family and their receptors in gastric carcinoma: a cDNA microarray study. World journal of gastroenterology : WJG. 2003; 9(7):1431-1434.

101. Ahluwalia A, Jones MK, Brzozowski T and Tarnawski AS. Nerve growth factor is critical requirement for in vitro angiogenesis in gastric endothelial cells. Am J Physiol Gastrointest Liver Physiol. 2016; 311(5):G981-G987.

102. Hayakawa Y, Sakitani K, Konishi M, Asfaha S, Niikura R, Tomita H, Renz BW, Tailor Y, Macchini M, Middelhoff M, Jiang Z, Tanaka T, Dubeykovskaya ZA, Kim W, Chen X, Urbanska AM, et al. Nerve Growth Factor Promotes Gastric Tumorigenesis through Aberrant Cholinergic Signaling. Cancer cell. 2017; 31(1):21-34.

103. Zhao Q, Yang Y, Liang X, Du G, Liu L, Lu L, Dong J, Han H and Zhang G. The clinicopathological significance of neurogenesis in breast cancer. BMC cancer. 2014; 14:484.

104. Huang D, Su S, Cui X, Shen X, Zeng Y, Wu W, Chen J, Chen F, He C, Liu J, Huang W, Liu Q, Su F, Song E and Ouyang N. Nerve fibers in breast cancer tissues indicate aggressive tumor progression. Medicine (Baltimore). 2014; 93(27):e172.

105. Verbeke S, Meignan S, Lagadec C, Germain E, Hondermarck H, Adriaenssens E and Le Bourhis X. Overexpression of p75(NTR) increases survival of breast cancer cells through p21(waf1). Cell Signal. 2010; 22(12):1864-1873.

106. Lim H, Devesa SS, Sosa JA, Check D and Kitahara CM. Trends in Thyroid Cancer Incidence and Mortality in the United States, 1974-2013. Jama. 2017; 317(13):1338-1348.

107. Ranganath R, Shah MA and Shah AR. Anaplastic thyroid cancer. Curr Opin Endocrinol Diabetes Obes. 2015; 22(5):387-391.

108. van der Laan BF, Freeman JL and Asa SL. Expression of growth factors and growth factor receptors in normal and tumorous human thyroid tissues. Thyroid. 1995; 5(1):67-73.

109. Pundavela J, Demont Y, Jobling P, Lincz LF, Roselli S, Thorne RF, Bond D, Bradshaw RA, Walker MM and Hondermarck H. ProNGF correlates with Gleason score and is a potential driver of nerve infiltration in prostate cancer. The American journal of pathology. 2014; 184(12):3156-3162.

110. Rocha AS, Risberg B, Magalhaes J, Trovisco V, de Castro IV, Lazarovici P, Soares P, Davidson B and Sobrinho-Simoes M. The p75 neurotrophin receptor is widely expressed in conventional papillary thyroid carcinoma. Hum Pathol. 2006; 37(5):562-568.

111. Bevan S, Pal T, Greenberg CR, Green H, Wixey J, Bignell G, Narod SA, Foulkes WD, Stratton MR and Houlston RS. A comprehensive analysis of MNG1, TCO1, fPTC, PTEN, TSHR, and TRKA in familial nonmedullary thyroid cancer: confirmation of linkage to TCO1. The Journal of clinical endocrinology and metabolism. 2001; 86(8):3701-3704.

112. Nucera C, Nehs MA, Mekel M, Zhang X, Hodin R, Lawler J, Nose V and Parangi S. A novel orthotopic mouse model of human anaplastic thyroid carcinoma. Thyroid. 2009; 19(10):1077-1084.

113. Champa D and Di Cristofano A. Modeling anaplastic thyroid carcinoma in the mouse. Horm Cancer. 2015; 6(1):37-44.

114. Magnon C, Hall SJ, Lin J, Xue X, Gerber L, Freedland SJ and Frenette PS. Autonomic nerve development contributes to prostate cancer progression. Science. 2013; 341(6142):1236361.

115. Zhao CM, Hayakawa Y, Kodama Y, Muthupalani S, Westphalen CB, Andersen GT, Flatberg A, Johannessen H, Friedman RA, Renz BW, Sandvik AK, Beisvag V, Tomita H, Hara A, Quante M, Li Z, et al. Denervation suppresses gastric tumorigenesis. Sci Transl Med. 2014; 6(250):250ra115.

116. Saloman JL, Albers KM, Li D, Hartman DJ, Crawford HC, Muha EA, Rhim AD and Davis BM. Ablation of sensory neurons in a genetic model of pancreatic ductal adenocarcinoma slows initiation and progression of cancer. Proceedings of the National Academy of Sciences of the United States of America. 2016; 113(11):3078-3083.

117. Peterson SC, Eberl M, Vagnozzi AN, Belkadi A, Veniaminova NA, Verhaegen ME, Bichakjian CK, Ward NL, Dlugosz AA and Wong SY. Basal cell carcinoma preferentially arises from stem cells within hair follicle and mechanosensory niches. Cell stem cell. 2015; 16(4):400-412.

118. Frick CG, Richtsfeld M, Sahani ND, Kaneki M, Blobner M and Martyn JA. Long-term effects of botulinum toxin on neuromuscular function. Anesthesiology. 2007; 106(6):1139-1146.

119. Ilkhchoui Y, Ghaly RF, Knezevic NN and Candido KD. Central nervous system toxicity after botulinum neurotoxin injection. Anesth Pain Med. 2013; 3(1):223-225.

120. Longo FM and Massa SM. Small-molecule modulation of neurotrophin receptors: a strategy for the treatment of neurological disease. Nature reviews Drug discovery. 2013; 12(7):507-525.